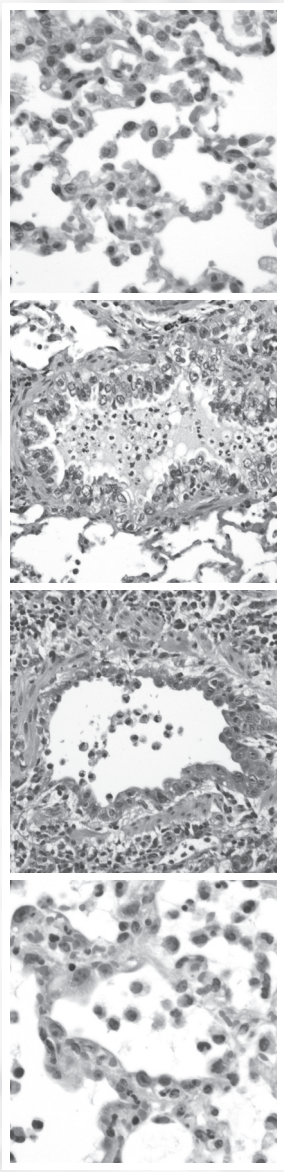

EXPERIMENTAL SARS AND INFLUENZA:
SIMILAR DISEASE, DIFFERENT PATHWAYS

Judith van den Brand

EXPERIMENTAL SARS AND INFLUENZA: SIMILAR DISEASE, DIFFERENT PATHWAYS

Cover

Front: Lung tissue of ferrets 4 days after infection with SARS coronavirus (SARS-CoV) or pandemic H1N1 influenza virus (pH1N1). From top to bottom: alveoli of a ferret infected with SARS-CoV, bronchiole of a ferret infected with SARS-CoV, bronchiole of a ferret infected with pH1N1, and alveoli of a ferret infected with pH1N1. (Hematoxylin and eosin staining)

Back: Presence of SARS-CoV antigen (brown-red staining) in the cytoplasm of a ciliated bronchial epithelial cell of a cat 4 days after infection with SARS-CoV. (Immunohistochemistry with hematoxylin counterstain)

ISBN: 978-94-90320-00-3, Erasmus MC Virologie
Lay-out: W. Schoneveld, www.wenziD.nl
Print: Optima Grafische Communicatie

EXPERIMENTAL SARS AND INFLUENZA: SIMILAR DISEASE, DIFFERENT PATHWAYS

Experimentele SARS en influenza:
vergelijkbare ziekte, verschillende mechanismen

PROEFSCHRIFT

Ter verkrijging van de graad van doctor aan de
Erasmus Universiteit Rotterdam
op gezag van de
rector magnificus

Prof.dr. H.G. Smidt

en volgens besluit van het College voor Promoties.
De openbare verdediging zal plaatsvinden op

donderdag 17 januari 2013 om 13.30 uur
door

Judith Maria Anthonia van den Brand
geboren te 's-Gravenhage

PROMOTIECOMMISSIE

Promotoren:	Prof.dr. T. Kuiken
	Prof.dr. A.D.M.E. Osterhaus
Overige leden:	Prof.dr. G.F. Rimmelzwaan
	Prof.dr. P.J.M. Rottier
	Dr. G. Gabriel
Co-promotor:	Dr. B.L. Haagmans

The research described in this thesis was conducted at the Department of Viroscience, Erasmus MC, Rotterdam, at Viroclinics Biosciences BV, Rotterdam, and at NVI, de Bilt, The Netherlands with financial support of the Virgo consortium, an Innovative Cluster installed by the Netherlands Genomics Initiative and of the Dutch Government (grant BSIK 03012), NIH (grant HL080621-01A1), DISSECT (European grant SP22-CT-2004-511060), NIAID-NIH (contract HHSN266200700010C), EU FP6 FLUVAC (044407), EU FP7 EMPERIE (project 223498), FP7 ADITEC (project 280873), TI Pharma (grant T4-214).

Financial support for printing of this thesis by the following companies and foundations is gratefully acknowledged:
Novartis Vaccines and Diagnostics
Star-Oddi (www.star-oddi.com)
Viroclinics Biosciences BV
J.E. Jurriaanse Stichting
Dako Benelux

CONTENTS

CHAPTER 1

GENERAL INTRODUCTION

Partly based on:
T Kuiken, JMA van den Brand, D van Riel, M Pantin-Jackwood, and DE Swayne
Comparative Pathology of Select Agent Influenza A Virus Infections.
Veterinary Pathology (2010) 47(5):893-914

OVERALL INTRODUCTION

In humans, viral infections causing respiratory disease have been known for many years. Every now and then such viruses may cause epidemics involving large groups of people or even pandemics with spread across the world. At the end of last century and at the beginning of this century zoonotic viruses emerged that were of serious risk for the human population: severe acute respiratory syndrome (SARS) caused by SARS coronavirus (CoV), highly pathogenic avian influenza (HPAI) virus H5N1, and pandemic influenza virus A(H1N1)pdm09 (pH1N1). Both SARS-CoV and influenza A viruses cause respiratory disease that may lead to severe and even fatal cases of pneumonia. The course and outcome of the infections is related to their pathogenesis, which can be explored by describing and comparing pathology, virology, and genomics. Understanding the pathogenesis of SARS and influenza is valuable for development of therapeutic and preventive strategies. Since the pathology of acute human fatal cases in SARS and influenza is rarely described, there is a need for animal models to provide information about the early stage of the disease. Also, pathological description of human cases with uncomplicated viral pneumonia is sparse because patients have multiple therapeutic interventions and secondary co-infections that may alter the pathology. Interestingly, the pathology of SARS-CoV and influenza virus infections has similar features; however, there are also differences in disease outcome. This thesis focusses on the pathology of SARS-CoV and influenza A virus infections in experimental animals. The pathology of these virus infections in animals is compared to that in humans and is related to the pathogenesis. The animal species that are used in this thesis to study the pathology of SARS-CoV infection are; cynomolgus macaques, African Green monkeys, ferrets, and cats. The pathology of influenza virus infection was studied in cynomolgus macaques, ferrets, and cats. Additionally, temporal and spatial dynamics for the pathology of different influenza virus infections in ferrets is described in a time course experiment. Finally, the effect of vaccination on the pathology is studied in ferrets and cynomolgus macaques for SARS-CoV infection and in ferrets for pH1N1 infection.

SARS CORONAVIRUS

Background

In November 2002, there was an unusual epidemic of severe pneumonia of unknown cause in Guangdong province in southern China with a high transmission rate to healthcare workers.[1]. The epidemic spread rapidly across the world by travelers resulting in a pandemic that peaked in the first half of 2003 and was stopped by July 2003. A total number of 8 096 probable cases were reported by the World Health Organization (WHO) which resulted in 774 deaths, a fatality rate of almost 9.6%.[2] In late 2003 and early 2004 this disease re-emerged at a small scale with rare cases in south China due to wild animal trading activities.[3,4] A novel coronavirus was proven to be the cause of the disease by fulfilling Koch's postulates.[5-7]

Coronaviruses are enveloped, positive-stranded RNA viruses of the family Coronaviridae, which can infect a variety of animal species and humans, and are predominantly associated with respiratory and enteric disease.[8] Coronavirus particles are enveloped with petal-shaped spike proteins (S-proteins) on the surface that display a typical crown-like ("corona") appearance in electron microscopy.[9]

SARS is a zoonotic disease and bats are believed to be the reservoir host of this virus.[10] Masked palm civet cats and raccoon dogs, which are kept and sold at so-called Chinese wet-markets (markets selling live poultry, fish and exotic animals for human consumption), have provided transmission of

the virus to humans.[11,12] In 2005, horseshoe bats were identified as a natural reservoir for a group of coronaviruses closely related to SARS-CoV with approximately 88 to 92% homology by genome sequences.[10,13] SARS is spread by close person-to-person contact through droplet transmission or excretions,[14] as was demonstrated in a hospital where virus spread due to over-crowding and poor ventilation,[15] and later also by airborne transmission in a private residential complex in Hong Kong.[16]

Clinical disease

SARS in humans is predominantly a respiratory disease that has an acute onset and is clinically characterized by fever, cough, myalgia and dyspnea. The clinical course of SARS generally follows a typical pattern:[17] phase 1 in the 1st week (viral replication) is associated with increasing viral load with fever and myalgia, and phase 2 in week 2 (immunopathological injury) is associated with decreasing viral load with recurrence of fever, diarrhea, hypoxemia and radiological progression of pneumonia.[17] Most cases of severe acute respiratory distress syndrome are seen in week 3. The estimated mean incubation period is 4.6 days and the mean time from onset to death in fatal cases is 23.7 days.[18] Apart from pneumonia, diarrhea is seen in many patients.[19,20]

In laboratory analyses lymphopenia, low-grade disseminated intravascular coagulation, and elevated lactate dehydrogenase and creatinine kinase are often seen.[21,22] A low absolute neutrophil count in the serum on presentation along with poor clinical responses to antibiotic treatment may raise the suspicion for SARS.[23,24] In the acute phase of SARS there is a lymphopenia with a rapid decrease of CD4 and CD8 T-cells associated with an adverse outcome.[22,25]

Several risk factors are related to the progression to severe and even fatal disease after infection with SARS-CoV in humans. One of the most important risk factors is high age; the estimated fatality rate is 43% in patients of 60 years and older, while it is 6.8% or less in younger patients.[26] Other risk factors are also associated with pre-existing co-morbidities (including cardiovascular disease, cerebrovascular disease, cancer, diabetes mellitus, chronic renal failure, chronic liver disease chronic obstructive pulmonary disease and asthma) and pregnancy. Additionally, male sex was associated with increased risk of fatality, however, the reason for this remains unclear.[27] Furthermore, poor outcomes are associated with high neutrophil counts, atypical presenting symptoms, and elevated lactate dehydrogenase on admission.[18,26,28-30]

Pathology of SARS in humans

Gross pathology of the respiratory tract demonstrates a varying degree of consolidation, edema, hemorrhage, congestion, and pleural effusion in the thoracic cavity.[31-33] The lungs often are three to four times heavier than normal lungs.[34] Histopathology of SARS is characterized by diffuse alveolar damage (DAD). The stage of DAD is related to the duration of the illness and may be divided into an acute or exudative phase, a proliferative or organizing phase, and a fibrotic phase. Patients in the initial 10 days of the disease demonstrate an acute phase with necrosis of alveolar epithelial cells, severe alveolar edema, fibrin exudation, hyaline membrane formation, hemorrhage, and infiltrates with inflammatory cells such as monocytes or macrophages, lymphocytes and less neutrophils in the alveolar wall and lumina.[31,32,35,36] There is necrosis and desquamation of the bronchiolar and bronchial epithelium with infiltrates of monocytes, lymphocytes and neutrophils in the bronchial wall and fibrin deposition.[32,37] In the organizing phase, after 10 to 14 days, there is less epithelial damage with interstitial and alveolar fibrosis, bronchiolitis obliterans organizing pneumonia, and

regeneration that is characterized by type II pneumocyte hyperplasia.[36-39] Large multinucleated cells composed of macrophages or pneumocytes are frequently observed and atypical enlarged pneumocytes with large nuclei, amphophillic granular cytoplasm, and prominent nucleoli are seen.[31,33,37] Other features are hemophagocytosis, squamous metaplasia,[31] and fibrin thrombi in vessels.[32]

Extra-respiratory changes are present that differ in severity of the pathology and vary with the duration of illness. The lymphoid system demonstrates hemophagocytic syndrome, and lymphoid depletion or necrosis in lymph nodes and white pulp of the spleen.[32,34] Hemophagocytic syndrome is characterized by phagocytosis by macrophages of erythrocytes, leukocytes, platelets, and their precursors in bone marrow and other tissues. This syndrome has been associated with a variety of viral, bacterial, fungal, and parasitic infections, as well as collagen-vascular diseases and malignancies.[40] The pathology in other organs is characterized by acute tubular necrosis in the kidneys, edema and degeneration of neurons in the central nervous system, myofiber necrosis and atrophy in skeletal muscles, necrosis and infiltration of lymphocytes and monocytes in the adrenal gland, destruction of follicular epithelial cells in the thyroid gland, germ cell destruction in the testes, and edema and atrophy of myocardial fibers in the heart.[20,32,34,41-44]

Pathogenesis

SARS-CoV enters the body via the respiratory system by droplet transmission and interacts with cellular receptors via the surface S-protein to infect target cells.[9] Several receptors have been found to bind to the S-protein: metallopeptidase angiotensin-converting enzyme 2 (ACE2), C-type lectin DC-SIGN expressed on dendritic cells (DC), and human CD209L (or liver/lymph node specific (L)-SIGN).[45-47] Binding of the S-protein to the functional receptor ACE2 on the target cell leads to fusion. SARS-CoV infection of ACE2 expressing cells seems to be dependent on the proteolytic enzyme cathepsin L.[48,49] ACE2 in humans is present in type I and II pneumocytes, small intestinal enterocytes, brush border of proximal tubular cells of the kidneys, endothelial cells of small and large arteries and veins, and arterial smooth muscle cells.[50]

The main target cells for the virus to infect are the epithelial cells of the respiratory tract, which are the first cells the virus encounters after entering the body. The sites of viral replication correspond with the presence of ACE2, the main functional receptor for the SARS-CoV. Immunohistochemistry (IHC) and in situ hybridization (ISH) studies demonstrate virus antigen or viral nucleic acid in alveolar, bronchiolar, bronchial and tracheal epithelial cells, alveolar macrophages, and multinucleated cells.[36,51] Co-staining for cytokeratin and surfactant shows that the infected cells were mostly pneumocytes, predominantly type II pneumocytes.[36] Type II pneumocytes secrete surfactant that is involved in reduction of the surface tension and integrity of the alveolar lumen, and are important in tissue restitution and differentiation into type I pneumocytes. In extra-respiratory tissues SARS-CoV RNA was detected in small and large intestine, lymph nodes, spleen, liver, heart, kidney, skeletal muscle, adrenal gland and cerebrum,[52,53] suggesting that SARS has extra-pulmonary dissemination leading to virus excretion in respiratory secretions, stools, urine and possibly sweat.[20,52,53]

After attachment to and infection of the host cells, there is damage of those cells and surrounding cells with attraction of inflammatory cells. In the early stage, the severe edema, fibrin deposits and hemorrhage, as is seen in the histopathology of human cases, is most likely due to the necrosis of epithelial cells with loss of epithelial lining and damage to blood vessels resulting in vascular leakage. Necrosis or apoptosis of infected cells is induced by cytolysis due to virus replication, and by cytokines that regulate apoptosis or necrosis.[5,54] In the later stage and even after elimination

of the virus, inflammatory cells are attracted by chemokines and cytokines and enter the damaged tissue. The inflammatory cells consist mainly of monocytes and macrophages, and less lymphocytes and neutrophils. These stimulated inflammatory cells may subsequently induce the secretion of additional cytokines and enhance the inflammation.[55] Additionally, the lymphopenia in many SARS patients suggests that the cytotoxic T-cell response, which is a major specific defense against viral infection, is diminished leading to more replication of the virus.

Next to damage due to virus replication, the severe pulmonary damage may be attributed to an excessive host immune response with the production of proinflammatory cytokines as is demonstrated in cytokine and chemokine profiles.[19,31,56,57] Chemokines and cytokines are soluble proteins that have a key function in the innate immune system by attracting and activating inflammatory cells and by inducing other inflammatory responses. In SARS patients the results of cytokine and chemokine measurements are difficult to interpret due to many confounding factors. However, the levels of both cytokines and chemokines in the blood are elevated: interleukin (IL)-1, IL-6, IL-8, IL-12, interferon (IFN) gamma, monocyte chemotractant protein (MCP)-1 (or CC-motif ligand 2, CCL2), monokine induced by IFN gamma (MIG), IFN-inducible protein (IP-10, or chemokine C-X-C motif ligand 10, CXCL10), and transforming growth factor beta(TGF-β).[56-61] Elevated levels of IP-10, MIG and IL-8 during the first week and after the onset of fever and elevation of MIG during the second week are associated with poor disease outcome.[60] Despite decreasing viral loads in the second week of the disease, the condition of many patients deteriorated with increased levels of several cytokines.[31]

Several genetic factors of both the virus and the host are known to modify the susceptibility and immune response to SARS-CoV infection. Genetic analyses of SARS-CoV demonstrate that genetic variation in the spike gene of SARS-CoV isolates from civet-cats causes increased transmission and affinity of the virus for both civet and human ACE2 receptors.[62,63] Genetic analyses of the host demonstrate that species-to-species variation in the sequence of the ACE2-gene affects the efficiency by which the virus can enter the cells.[64] Additionally, certain human-leucocyte-antigen class (HLA) haplotypes are associated with a higher susceptibility to SARS-CoV infection.[65,66] In contrast, L-SIGN homozygote individuals have a lower susceptibility to SARS-CoV infection.[67] Also in the protection against SARS-CoV infection there may be a genetic factor involved; genotypes producing low concentrations of mannose-binding lectine – a collectin in the serum that is able to bind the glycosylated S-protein – were associated with increased risk of developing SARS.[65]

Animal models for SARS in humans

Many different animal species are found to be susceptible to SARS-CoV and subsequently demonstrate viral replication and disease: non-human primates, cats, ferrets, mice, pigs, chickens, hamsters, guinea pigs, and rats.[63,68-72] Experimental SARS-CoV infection in each of these species has been performed for a variety of purposes, and resemble the clinical and pathological of SARS in humans to a variable degree. Mice and hamsters have been used in studies for pathogenesis and screening for vaccines and antiviral drugs.[73,74] Young mice show viral replication that is not accompanied by substantial inflammation in the lungs; in contrast, old BALB/c mice develop clinical illness with weight loss and histopathological changes characterized by pneumonitis and bronchiolitis.[72,74] Non-human primates like cynomolgus macaques, African green monkeys and rhesus macaques, have been used to evaluate treatment and for pathogenesis studies.[7,75-80] The presence and extent of clinical illness and histopathological changes are not consistent. Histopathology show DAD with

resembling features as in humans but with a multifocal distribution rather than the more diffuse distribution in humans, and with a less severe pathology often without syncytia and hyaline membranes.[19,76] Cats and ferrets have been used to evaluate the pathogenesis, while ferrets also have been used for vaccination studies.[69,81] Cats demonstrate no clinical signs while ferrets become lethargic and even die.[69] The pathology of SARS-CoV infection in cats and ferrets resembles that in humans, albeit a variable outcome with less severe lesions and without the specific features that are seen in humans.

There are several factors that may influence the course of the infection in animal models for SARS-CoV. The age of the animals has an important influence as was seen in young and aged mice.[63] Additionally, the virus strain used for the infection can cause a variable outcome; for example clinical disease was seen in macaques infected with HK39 but not in macaques infected with Urbani.[7,75] Another discriminate is the route of inoculation. Different inoculation routes are used; intranasal, intratracheal, intravenous, conjunctival and oral. Intranasal, intravenous, or oral inoculation appears to cause a milder disease than intratracheal inoculation.[7,72,75] Although different animal species are susceptible to SARS-CoV infection, no animal model has been established in which all aspects of the severe human disease are accurately replicated.

INFLUENZA A VIRUS

Background

Influenza was first described as epidemics of acute, rapidly spreading catarrhal fevers in humans and the first epidemic was most probably described by Hippocrates in 412 B.C.[82,83] These epidemics of influenza, or more recently termed pandemics, have occurred throughout the last 2500 years of history. Today, human influenza occurs yearly as seasonal influenza, mainly in the winter months of temperate climates; every several years as interpandemic epidemics; and, sporadically at average of 35 year intervals, as the most severe influenza, i.e., pandemics. Seasonal influenza and interpandemic epidemics occur as a result of mutations in influenza viruses that are circulating in the human population (antigenic drift). In contrast, influenza pandemics occur as a result of introduction of an animal influenza virus or a human-animal influenza reassortant virus in which the surface glycoprotein hemagglutinin, with or without other virus proteins, differs substantially from those circulating in the human population (antigenic shift).[83]

Since 1900, there have been four pandemics of human influenza: 1918 H1N1 'Spanish' influenza, 1957 H2N2 'Asian' influenza, 1968 H3N2 'Hong Kong' influenza and the 2009 H1N1 'Mexican' influenza.[83,84] Of these, the 1918 'Spanish' influenza pandemic was the worst, causing acute illness in 25-30% of world population, and death of nearly 50 million people.[85-87] Most of the fatalities occurred among 15-34 year-olds, with primary acute interstitial pneumonia, pulmonary hemorrhage and pulmonary edema, often with secondary bacterial pneumonia.[85,87]

Influenza is caused by negative-sense, single-stranded segmented RNA viruses of the family *Orthomyxoviridae*.[83] Influenza A virus infections occur in both mammals and birds and are further classified, based on surface glycoproteins, into 17 hemagglutinin (HA) (H1-17) and 9 neuraminidase (NA) (N1-9) subtypes.[88,89] Most HA and NA subtypes have been reported in avian species, but the subtypes reported in mammals are more restricted in their host range, with stable lineages including endemic human, porcine and equine influenza viruses of the H1N1 (humans and pigs), H3N2 (humans and pigs), and H3N8 (horses and dogs) subtypes, and rare occurrence of other avian

influenza (AI) subtypes that spill over from birds to mammals. The natural reservoir for all influenza viruses are aquatic birds where replication occurs in the intestinal tract, thus facilitating fecal-oral transmission among avian species.[90] In aquatic birds the infection with influenza viruses are asymptomatic whereas in poultry they may lead to severe disease and mortality. Avian influenza virus can be of high or low pathogenicity (HPAI or LPAI) based on the pathogenicity for chickens. During infection human influenza viruses use host trypsin-like proteases that are limited to the respiratory tract to cleave HA, while LPAI viruses replicate in both respiratory and digestive tract of birds.[91] HPAI viruses use a wide range of proteases allowing replication outside the respiratory tract.[92]

HPAI virus H5N1 (H5N1) initially was present in poultry, but in 1997 crossed the species barrier and infected humans in China.[93] H5N1 continues to circulate among poultry in many countries in Asia, Africa, and Europe, and occasionally spreads to humans with often fatal consequences. H5N1 is the first avian influenza virus to cause significant numbers of human infections and deaths, i.e., 604 infections with 357 fatalities since January 2004.[88,94] The H5N1 human infections with accompanying 60% case fatality rate raise concerns for HPAI viruses, through mutation and/or reassortment, becoming the next human pandemic virus.[95]

In the beginning of April 2009, a novel H1N1 influenza A virus (pH1N1) was identified as the cause of acute respiratory disease of humans in Mexico.[96] This virus was a complex reassortant influenza A virus, which had not been previously reported in animals, but had gene segments related to North American classic H1N1 swine viruses (hemagglutinin, nucleoprotein, and non-structural gene segments), North American avian viruses (polymerase A and B2 genes), human influenza A virus (polymerase B1 genes) and Eurasian H1N1 swine viruses (neuraminidase and matrix genes).[96] On 1 August 2010 at the end of the pandemic, more than 214 countries had reported laboratory confirmed cases of this pH1N1, including at least 18,449 deaths.[97]

Clinical disease

Seasonal influenza virus infections vary in the severity of the symptoms including fever, headache, sore throat, cough, runny nose, muscle ache, fatigue and sometimes diarrhea.[98] The acute symptoms and fever can persist for 7 to 10 days. Like in seasonal influenza virus, pH1N1 infection usually causes uncomplicated influenza. Fatal outcome of pH1N1 was seen in 0.5% of cases, usually associated with severe pneumonia and respiratory failure. Neuromuscular and cardiac complications were unusual.[99] Patients affected with H5N1 present fever, cough, shortness of breath, diarrhea and rarely neurologic symptoms. The average incubation period is 2 to 5 days. In fatal cases, death occurs approximately 9 days after the beginning of the disease, but sometimes as early as 2 days after the onset of symptoms.

Laboratory analyses for H5N1 reveal leucopenia and lymphopenia that are more often seen with severe and fatal cases and that is more severe than for pH1N1 and seasonal influenza.[100] Increased levels of lactate dehydrogenase are also associated with more severe and even fatal disease.[101] Other abnormalities in the blood are: thrombocytopenia, and elevated levels of aminotransferases and creatinine phosphokinase, hypoalbuminaemia, and changes indicative for disseminated intravascular coagulopathy.[102]

The highest case fatality rate for seasonal influenza virus is seen in the very young and elderly, and in patients with underlying chronic illness. In contrast to seasonal influenza, severe disease from pH1N1 virus infection is concentrated in older children and young adults, with fewer cases reported

in patients older than 60 years.[103] Most complications occurred among previously healthy individuals, with risk factors such as obesity, respiratory or cardiac disease, diabetes mellitus, and pregnancy. For H5N1 most fatal cases are seen in patients between 10 and 19 years old without pre-existing morbidity.[104]

Pathology of influenza in humans

Uncomplicated influenza is a mild inflammation of the upper respiratory tract that consists mainly of rhinitis, paranasal sinusitis, pharyngitis, and laryngitis. Histopathology demonstrates diffuse, superficial, necrotizing tracheo-bronchitis, characterized by desquamation of epithelial cells, edema and hyperemia in the lamina propria, and infiltration with lymphocytes and histiocytes. The inflammation is short-lasting: epithelial regeneration is already visible within 2 days after onset of symptoms.[105]

Viral pneumonia is a complication of influenza virus infection. Gross pathology of the lungs shows extensive consolidation with varying degree of hemorrhage. Histopathology caused by influenza virus infection of the alveoli consists of DAD both acute in the exudative phase (for patients dying in the first 2 weeks), and chronic organizing phase (for patients dying in the third week or later).[106] In the acute stage, DAD is characterized by necrosis of alveolar epithelium and flooding of the alveolar lumina by edema fluid, mixed with variable proportions of fibrin, erythrocytes, alveolar macrophages, and neutrophils. Some alveoli are lined by hyaline membranes. The alveolar septa are widened due to hyperemia, edema, and infiltration by mainly neutrophils, macrophages and activated lymphocytes. Alveolar capillaries and small pulmonary blood vessels may contain fibrin thrombi. At the chronic stage of DAD, there is type II pneumocyte hyperplasia, interstitial fibrosis of alveolar septa and interstitium with hyaline and paucicellular appearance without bronchiolitis obliterans organizing pneumonia-like appearance, and infiltration by predominantly lymphocytes and plasma cells. Other features are desquamation of epithelium into alveolar lumina, hemorrhage, bronchiolitis, and alveolar macrophages that display hemophagocytosis in the alveolar lumina.[107] Influenza viral pneumonia often occurs together with, or is followed by, bacterial pneumonia. Pathology of pH1N1 in human fatal cases when compared to H5N1 human cases showed similar DAD. However, pH1N1 fatal cases showed more inflammation in nose, trachea, bronchi and bronchioles, a feature that was also seen in fatal cases of seasonal influenza.[108,109]

H5N1 virus infection has also been associated with extra-respiratory disease. In the lymphoreticular system there was marked histiocytic hyperplasia and reactive hemophagocytic syndrome. Other organs displayed: atrophic white pulp in the spleen, centrilobular necrosis in the liver, acute tubular necrosis in the kidney, necrosis of skeletal muscle fibers, and necrosis in the brain with microglial nodules.[110-113] Infection with pH1N1 rarely demonstrates neuromuscular and cardiac complications.[99] Infection with seasonal influenza virus primarily infects and causes disease in the respiratory tract and is associated—albeit to a lesser extent—with disease in extra-respiratory organs. These include influenza-associated acute encephalopathy,[114] myocarditis,[115] and myopathy.[116]

Pathogenesis

Like in SARS-CoV infection, the route of entry is via droplet transmission into the respiratory system. Attachment of the viral hemagglutinin to its host cell receptor is the first step in influenza virus replication following transmission. The receptor on the surface of the host cell is a sialic acid (SA)-terminated glycan. Human-adapted influenza viruses prefer binding by an α-2,6 SA linkage that is

present throughout the human respiratory epithelium, while avian influenza viruses prefer binding by an α-2,3 SA linkage that is abundantly present in the respiratory and intestinal tract of aquatic birds.[117,118] Because different influenza viruses use different sialic acids as their receptor, and because the expression of sialic acids differs both across the respiratory tract and across species, this step influences both pattern of disease in the respiratory tract and host range of virus infection.

H5N1 infection in humans often results in extra-respiratory complications. In general, there are two explanations for the pathogenesis of these extra-respiratory complications.[119] The first is that influenza virus spreads via blood to these tissues and replicates there. However, viremia from human influenza virus infection appears to be rare after onset of symptoms and, if it occurs, is not sustained for long periods.[120] Proof of replication of human influenza virus in extra-respiratory tissues comes from direct immunofluorescence, IHC, or ISH in the tissue concerned. However, such reports are rare and further confirmation of the ability of human influenza virus to replicate in extra-respiratory human tissues in vivo is needed. Distribution of virus by infected immune cells such as macrophages and lymphocytes may be another way of spread through the blood.[121,122] The second explanation for the pathogenesis of extra-respiratory complications is suggested by the link between acute respiratory distress syndrome (ARDS) and multiple organ dysfunction syndrome (MODS).[123] ARDS, which has multiple causes including influenza virus infection, commonly progresses to MODS, most commonly involving the hepatic, renal, central nervous, gastrointestinal, hematologic, and cardiac systems. The pathogenesis of MODS has not been elucidated, but may involve the microcirculation and mitochondrial metabolism, as well as the release of cytokines into the circulation.

The pathology of uncomplicated influenza in humans corresponds to the pattern of virus attachment which is measured by virus histochemistry.[124-126] Based on those studies, the primary targets of seasonal influenza virus are bronchial, tracheal and nasal epithelial cells and in the alveoli type I pneumocytes.[125] This corresponds with the few in vivo descriptions of the target cells of human influenza virus in fatal pneumonia: virus antigen expression is seen in URT epithelial cells and alveolar epithelial cells, alveolar macrophages, and interstitial macrophages.[127-130] H5N1 in the human respiratory tract attaches predominantly to non-ciliated epithelial cells. Attachment is rare in the upper respiratory tract and trachea, and increases progressively towards the bronchioles.[124,126] Within the terminal bronchioles, H5N1 virus attaches preferentially to non-ciliated cuboidal epithelial cells, and within the alveoli, to type II pneumocytes and alveolar macrophages.

After attachment, the virus can infect the cell; evidence for the presence of virus is demonstrated by IHC and ISH, often in association with lesions.[131] In the respiratory tract, H5N1 virus antigen and viral RNA expression are seen in type II pneumocytes and ciliated and non-ciliated tracheal epithelial cells by IHC and ISH, respectively.[131] pH1N1 antigen is predominantly expressed in type II pneumocytes, and less in type I pneumocytes and intra-alveolar macrophages, and in airway epithelium.[132] Seasonal influenza virus antigen was seen in bronchial epithelial cells and submucosal gland epithelial cells.[108] In extra-respiratory tract tissues, H5N1 virus antigen was demonstrated in brain, intestine, liver, lymph nodes, placenta, and fetal lung.[131]

The severe damage to type I and type II pneumocytes allows fluid to flood into and accumulate in the alveolar lumina. This has severe consequences for the gas exchange function of the respiratory tract, resulting in severe, and in some cases fatal, respiratory dysfunction as is also seen in SARS-CoV infection.[133] Damage to the alveolar epithelium is in part due to the direct cytolytic effect of

virus infection. The cytolytic effect could be due to necrosis or apoptosis as a result of replication of the virus. There are clear indications that active virus replication and higher viral loads are correlated to a negative disease outcome.[134] Additionally, apoptosis may be induced by up-regulation of certain chemokines and cytokines.[135]

Like in SARS, fatal infection with H5N1 is associated with hypercytokinemia.[134,135] Chemokines and cytokines such as IP-10, MIG, MCP-1, IL-8, IL-10, IL-6, IL-1α and β, and IFN-gamma are elevated in the serum of patients infected with H5N1 and are particularly high in fatal cases. The cytokine levels correlate with the pharyngeal viral load suggesting that the increased levels may reflect the viral replication.[134] Cytokine levels are not only elevated in the serum but also high expression of tumor necrosis factor-α (TNF-α) is detected in the lungs of fatal cases of H5N1 infection.[110]

Influenza viruses change over time due to antigenic shift and drift. Avian influenza viruses are known to infect humans and pigs and are endemic among poultry without overt disease. When such avian viruses combine gene segments and surface proteins from human or porcine influenza viruses due to reassortment they may have altered receptor binding properties leading to enhanced ability to infect and spread among humans. The immune response of infected humans provides specific antibodies to protect the host against disease by a second infection, by vaccination against the subtype, or by cross-reactive antibodies against other subtypes. The latter response explains the relatively low mortality in older pH1N1 patients due to cross-reactive antibodies acquired during previous influenza infection. The differences in disease after infection with various subtypes indicate the importance of virus specific genetic factors in the course of the disease.

Animal Models for Influenza in Humans

Animal models help both to better understand influenza in humans and to develop medical countermeasures against this disease. Forms of influenza in humans for which animal models have been developed include uncomplicated influenza, influenza pneumonia, influenza-associated bacterial sepsis, influenza-associated neurologic disease, influenza in immunocompromised hosts, and virus transmission.[136] Specific goals for which animal models are designed are to determine transmissibility of different viruses, virulence of different viruses, pathogenesis of viral infection, and efficacy of vaccines or antiviral drugs.

Important variables in animal models for influenza are route of inoculation and experimental animal species. Routes of inoculation include exposure to infected animals, exposure to aerosolized viruses, endotracheal or endobronchial instillation, or intranasal instillation.[137] Experimental animal species used include laboratory mouse,[138] domestic ferret,[138] Syrian hamster,[139] chinchilla,[140] domestic horse,[141] laboratory rat,[142] domestic dog, [143] domestic cat,[144] cotton rat,[145] domestic pig,[146] guinea pig,[147] and non-human primates (e.g., squirrel monkeys, cynomolgus macaque, and rhesus macaque).[148-150] Experimental animal species used in this thesis are cynomolgus macaques, ferrets, and cats.

Cynomolgus macaques have been used for pathogenesis studies and vaccination studies.[151] Ferrets have been used to model uncomplicated upper respiratory tract infection, to model viral pneumonia, and to model influenza virus transmission among humans.[152-154] Cats have been used to model systemic disease after infection with H5N1 influenza and to investigate the pathogenesis of H5N1.[144] The pathology of H5N1 virus infection in macaques, ferrets and cats resembles the clinical signs, virus replication and associated lesions in the respiratory tract, followed by death as is seen

in humans. However, there are differences between different animal species and humans infected with influenza virus: cats inoculated with H5N1 show systemic virus replication and associated lesions and macaques inoculated with seasonal influenza virus macaques show mild or no disease. Therefore, the animal model used for severe disease in humans needs proper monitoring all aspects of the model including animal species, inoculation route, and inoculum dose.

PREVENTION AGAINST SARS AND INFLUENZA

Newly emerging infectious diseases that cause outbreaks and serious disease among humans, ask for a fast development of effective therapeutical drugs and preventive vaccines. Although SARS-CoV appears to be eradicated from the human population, viruses similar to the epidemic strain of SARS-CoV are currently circulating in bats.[155-157] Many different candidate vaccines against disease from SARS-CoV infection have been tested with variable outcomes, with so far no suitable vaccine against SARS-CoV. For SARS in humans there are no animal models that completely reflect the human disease. However, animal models can help in the development of vaccines.

Animal models may be used for the development of new antiviral drugs and more efficacious vaccines against influenza virus infection. Problems include the need for high antigen dose, limited production capacity, long production time, poor immunogenicity of adjuvants, and limited cross-protective immunity, both intra-subtypic and inter-subtypic. Again, suitable animal models are required for the evaluation of the efficacy and safety of novel influenza vaccines.[158] To study influenza in humans there are well-established models in different experimental animal species. Still, there is room for improvement of these models in different ways. First, it is important to better characterize the pathology of influenza in humans so that it is possible to determine whether the models used are accurate reflections of the situation in humans. Second, currently used animal models of influenza would benefit from better characterization of pathogenesis and pathology. There is a need for better understanding of the temporal progression of pulmonary lesions, by time course experiments, so that the timing of sacrifice for pathological examination is based on pathological as well as on virological and clinical criteria. Also, there is a need for better integration of histopathological, cytokine, and micro-array data in order to gain a more complete understanding of the pathogenesis of influenza virus infection. Third, research using animal models of influenza would profit from standardization of the most commonly used models to allow comparison of results from different experiments. Procedures to standardize would include method of anesthesia, route of inoculation, viral dose of inoculum, volume of inoculum, day of sacrifice, and a semi-quantitative grading system for scoring pulmonary lesions. Fourth, exposure to aerosol as a route of inoculation of experimental animals needs to be developed as an alternative, more natural, route of inoculation.

In this thesis the pathology of SARS-CoV and influenza virus infection is described to elucidate the pathogenesis of these viruses. A time course experiment for influenza viruses in ferrets is performed to provide information about the change over time of the lesions associated with the infection. Additionally, an improved model for seasonal influenza in ferrets is developed. Finally, vaccines against SARS-CoV and pH1N1 are tested for their efficacy and effect on lesions associated with virus infection.

OUTLINE OF THIS THESIS

Newly emerging zoonotic infectious diseases are a constant threat for human society as was seen by infection of humans with SARS coronavirus, highly pathogenic avian influenza virus H5N1, and pandemic H1N1 influenza virus. There is an urgent need to provide early recognition of the involved pathogen followed by suitable prevention and therapeutical measures. To elucidate the pathogenesis of SARS coronavirus and influenza virus infections, the pathology of these infections is compared by using different animal models.

Chapter 2 describes the pathology and vaccine development of SARS coronavirus in different laboratory animal species. SARS coronavirus infection is described in African green monkeys, cynomolgus macaques (chapter 2.1), ferrets, and cats (chapter 2.2). Preventive measures against severe disease caused by SARS coronavirus are assessed by means of vaccination with inactivated vaccine (chapter 2.3) or recombinant spike protein (chapter 2.4) in ferrets and macaques, and the pathology of challenge virus infection in immunized animals is compared to that in non-immunized animals.

Chapter 3 describes the pathology of and vaccine development for different influenza viruses in different laboratory animal species. Influenza virus infection is described in cynomolgus macaques (chapter 3.1), ferrets (chapter 3.2, 3.4, 3.5 and 3.6), and cats (chapter 3.3). A good model for pneumonia from seasonal human influenza virus infection is developed by modifying the ferret model (chapter 3.4). The dynamics of influenza virus infection over time and location in the respiratory tract is described in ferrets infected by different influenza viruses (chapter 3.5). Preventive measures against severe disease caused by pH1N1 are assessed by vaccination with MF59 adjuvanted seasonal and pandemic influenza vaccines in ferrets (chapter 3.6).

Chapter 4 concludes with summarizing the results of the performed experiments, comparing this to the human situation, and discussing the differences and similarities between the pathology and the pathogenesis of SARS coronavirus and influenza virus infection in humans and laboratory animals.

CHAPTER 2

SARS CORONAVIRUS INFECTION IN ANIMAL MODELS

2.1

Distinct SARS coronavirus-induced acute lung injury pathways in two different non-human primate species

Journal of Virology (2011) 85(9): 4234-4245

SL Smits,[1] JMA van den Brand,[1] A de Lang,[1] LME Leijten,[1] WF van IJcken,[2]
G van Amerongen,[1] ADME Osterhaus,[1] AC Andeweg,[1] BL Haagmans,[1]

Department of Virology, Erasmus Medical Center, Rotterdam, The Netherlands [1]
Center for Biomics, Erasmus Medical Center, Rotterdam, The Netherlands [2]

ABSTRACT

Acute lung injury (ALI) and acute respiratory distress syndrome (ARDS), caused by influenza A virus H5N1 and severe acute respiratory syndrome coronavirus (SARS-CoV), supposedly depend on activation of the oxidative-stress machinery that couples to innate immunity, resulting in a strong pro-inflammatory host response. Inflammatory cytokines, such as interleukin 1β (IL-1β), IL-8 and IL-6, play a major role in mediating and amplifying ALI/ARDS by stimulating chemotaxis and activation of neutrophils. To obtain further insight into the pathogenesis of SARS-CoV-associated ALI, we compared SARS-CoV infection in two different non-human primate species, cynomolgus macaques and African green monkeys. Viral titers in the upper and lower respiratory tract were not significantly different in SARS-CoV-infected macaques and African green monkeys. Inflammatory cytokines that play a major role in mediating and amplifying ALI/ARDS or have neutrophil chemoattractant activity, such as IL-6, IL-8, CXCL1, and CXCL2, were, however, induced only in macaques. In contrast, other pro-inflammatory cytokines and chemokines, including osteopontin and CCL3, were up-regulated in the lungs of African green monkeys to a significantly greater extent than in macaques. Because African green monkeys developed more severe ALI than macaques, with hyaline membrane formation, some of these differentially expressed pro-inflammatory genes may be critically involved in development of the observed pathological changes. Induction of distinct pro-inflammatory genes after SARS-CoV infection in different non-human primate species needs to be taken into account when analysing outcomes of intervention strategies in these species.

INTRODUCTION

Acute lung injury (ALI) and acute respiratory distress syndrome (ARDS), major causes of respiratory failure with high morbidity and mortality, are observed under multiple pathogenic conditions, among which are sepsis, gastric acid aspiration, and infections with influenza A virus H5N1 and severe acute respiratory syndrome coronavirus (SARS-CoV).[133,159] Increased permeability of the alveolar-capillary barrier, resulting in pulmonary edema, hypoxia, and influx of neutrophils observed under these conditions, may be followed by a fibroproliferative phase with alveolar hyaline membranes and various degrees of interstitial fibrosis that may ultimately progress or resolve.[160] The onset of severe lung injury supposedly depends on activation of the oxidative-stress machinery that is coupled with innate immunity and activates transcription factors, such as NF-κB, resulting in a pro-inflammatory host response.[159] As similar ARDS symptoms, triggered by different stimuli, can be observed in multiple species, a common ARDS "injury pathway" has been proposed.[159] Inflammatory cytokines, such as interleukin 1β (IL1β), IL8 and IL6, play a major role in this pathway, mediating and amplifying ALI/ARDS by stimulating chemotaxis and activation of neutrophils.[133,160]

SARS-CoV infection in humans causes lower respiratory tract disease, and 20 to 30% of patients develop severe inflammation of the lung, characterised by ARDS.[17,161] Children younger than 12 years of age are relatively unaffected by the disease,[162-164] whereas elderly patients have a poor prognosis, with mortality rates of up to ~50%.[17,161] The pulmonary damage is thought to be caused by a disproportionate immune response, with elevated levels of cytokines such as CXCL10, CCL2, IL-6, IL-8, IL-1β, and gamma interferon (IFN-γ).[56-58,60,165-167]

Although a wide range of animals can be infected with SARS-CoV, among them rodents (mice and hamsters), carnivores (ferrets and cats), and non-human primates (macaques and African green monkeys), none of the current animal models has fully reproduced all features of SARS.[168,169] SARS-CoV-infected adult mice show no clinical signs of disease, although viral titers peak early after infection and reach relatively high levels in the respiratory tract, and the infection results in mild inflammatory changes in the respiratory tract. Aged mice and mice infected with certain adapted SARS-CoV variants do show signs of clinical disease and significant pathological changes in the lungs, which correlate with higher virus titers and/or a stronger host response, with differential expression of IL-6, CCL3, CXCL10, IL-1β, and tumor necrosis factor alpha (TNF-α).[63,169-171] SARS-CoV infection of non-human primates results in multiple foci of diffuse alveolar damage (DAD), with flooding of the alveoli with edema fluid and influx of macrophages, neutrophils, and lymphocytes and extensive loss of epithelium from alveolar and bronchial walls.[7,168,172] Analysis of gene signatures in SARS-CoV-infected macaques revealed induction of a strong innate immune response characterized by the induction of antiviral signaling pathways and the stimulation of various pro-inflammatory cytokine genes, including IL-1β, CCL2, IL-6, IL-8, and CXCL10.[173,174] Aged macaques develop more severe pathology upon SARS-CoV infection than young adult macaques, which could be explained by stronger innate host responses with an increase in differential expression of genes associated with inflammation, including IL8.[174] These data are in line with previous observations in ALI/ARDS caused by multiple non-viral pathogenic conditions.[133,160]

Despite intensive studies of the pathogenesis of SARS-CoV, the molecular mechanisms of virus-induced acute lung injury are still largely uncharacterized. Aging is a predisposing factor for severe SARS-CoV-associated disease, and young adults show only mild symptoms and pathology upon infection. Previous studies in SARS-CoV infected young adult African green monkeys revealed a more severe course of the infection than in young adult macaques.[75] To determine which pathogenic pathways operate in these two related non-human primate host species upon SARS-CoV infection, comparative host genomic analyses of SARS-CoV-infected young adult African green monkeys and macaques were performed. The observed commonalities and differences provide new insights into SARS-CoV pathogenesis and virus-induced acute lung injury.

MATERIALS AND METHODS

Animal studies

Approval for animal experiments was obtained from the Institutional Animal Welfare Committee. Four cynomolgus macaques (*Macaca fascicularis*) and 4 African green monkeys (*Chlorocebus aethiops*), 3 to 5 years old with active temperature transponders in the peritoneal cavity, were inoculated with 5 x 10^6 50% tissue culture infective doses ($TCID_{50}$) of SARS-CoV strain HKU39849 suspended in 5 ml phosphate-buffered saline (PBS). Four milliliters was applied intratracheally, 0.5 ml intranasally, and 0.25 ml on each conjunctiva, as described previously.[6,7,172-174] The four SARS-CoV-infected young adult cynomolgus macaques have been described previously.[174] For reverse transcriptase (RT)-PCR and immunohistochemistry, data from previously SARS-CoV-infected aged cynomolgus macaques were used.[174] Two young adult macaques and African green monkeys (age range, 3 to 9 years old) were mock (PBS) infected. Animals were checked daily for clinical signs. Just before infection and at days 2 and 4 post infection, animals were anesthetized with ketamine and oral, nasal, and rectal swabs were taken and placed in 1 ml Dulbecco's modified Eagle's medium supplemented with 100 IU penicillin/ml and 100 μg of streptomycin/ml

(virus transport medium). The swabs were frozen at -70°C until RT-PCR analysis was performed. The animals were euthanized 4 days after infection by exsanguination under ketamine anesthesia.

Necropsies were performed according to a standard protocol. For semiquantitative assessment of gross pathology, the percentage of affected lung tissue from each lung lobe was determined at necropsy and recorded on a schematic diagram of the lung, and the area of affected lung tissue was subsequently calculated (gross pathology score). One lung from each monkey was inflated with 10% neutral-buffered formalin by intrabronchial intubation and suspended in 10% neutral-buffered formalin overnight. Samples were collected in a standard manner (from the cranial, medial, and caudal parts of the lung), embedded in paraffin, cut at 3 μm, and used for titration (see below) immunohistochemistry (see below) or stained with hematoxylin and eosin (HE). The lung, liver, spleen, kidney, intestine, trachea, and tracheobronchial lymph node HE sections were examined by light microscopy.

For semiquantitative assessment of SARS-CoV infection-associated inflammation in the lung, two HE-stained slides per animal (cranial and caudal lobes) were examined for inflammatory foci by light microscopy using a 10x objective. Each focus was scored for size (1, smaller than or equal to area of 10x objective; 2, larger than area of 10x objective and smaller than or equal to area of 2.5x objective; 3, larger than area of 2.5x objective) and degree of inflammation (1, low density of inflammatory cells; 2, intermediate density of inflammatory cells; 3, high density of inflammatory cells). The cumulative scores for the inflammatory foci provided the total score per animal. Sections were examined without knowledge of the identity of the animals.

Three lung tissue samples (one from the cranial part of the lung, one from the medial part and one from the caudal part) were homogenized in 2 ml virus transport medium, using Polytron PT2100 tissue grinders (Kinematica). After low-speed centrifugation, the homogenates were frozen at -70 °C until they were inoculated on Vero E6 cell cultures in 10-fold serial dilutions. The identity of the isolated virus was confirmed as SARS-CoV by RT-PCR of the supernatant.[172]

Immunohistochemistry

Serial 3-μm lung sections were stained using mouse anti-SARS nucleocapsid IgG2a (clone Ncap4; Imgenex; 1:1 600), mouse anti-osteopontin (clone AKm2A1; Santa Cruz), rabbit anti-ACE2 (angiotensin 1-converting enzyme 2) (ab15348; Abcam), or isotype control antibodies (clones 11711 and 20102; R&D), according to standard protocols.[7,172] Quantitative assessment of SARS-CoV antigen expression in the lungs was performed as described previously.[172] For phenotyping (to confirm cell types), we used a destaining-restaining technique.[175] Briefly, the red precipitate (aminoethylcarbazole [AEC]) used for visualization of osteopontin antigen staining was dissolved in graded 100% to 70% alcohols. To detach the primary antibody and red immunohistochemistry signals, slides were soaked in eluting buffer (5ml 0.1 M HCl, 95 ml 0.1 M NaCl containing 1 M glycine) for 2 hours. The sections were treated for two 5-min intervals by heating them in citric acid buffer, pH 6.0, to denature any undetached primary antibody. The slides were then incubated with mouse anti-human CD68 (clone KP1; DAKO) 1/200 in PBS/0.1% bovine serum albumin (BSA) for 1 hour at room temperature. After being washed, the sections were incubated with horseradish peroxidase-labeled goat-anti-mouse IgG1 (Southern Biotech) 1/100 in PBS/0.1% BSA for 1 hour at room temperature. Peroxidase activity was revealed by incubating slides in 3,3'-diaminobenzidine-tetrachlorhydrate (DAB) (Sigma) for 3 to 5 minutes, resulting in a brown precipitate, followed by counterstaining with hematoxylin.

RNA-extraction and quantitative RT-PCR

RNA from 200 µl of swabs was isolated with the Magnapure LC total nucleic acid isolation kit (Roche) external lysis protocol and eluted in 100 µl. SARS-CoV RNA was quantified on the ABI prism 7700, with use of the Taqman Reverse Transcription Reagents and Taqman PCR Core Reagent kit (Applied Biosystems), using 20 µl isolated RNA, 1x Taqman buffer, 5.5 mM $MgCl_2$, 1.2 mM deoxynucleoside triphosphates (dNTPs), 0.25 U Amplitaq gold DNA polymerase, 0.25 U Multiscribe reverse transcriptase, 0.4 U RNAse-inhibitor, with 200 nM primers, and 100 nM probe specific for the SARS-CoV nucleocapsid protein gene.[173,174] The amplification parameters were 30 min at 48ºC, 10 min at 95ºC, and 40 cycles of 15 s at 95ºC, and 1 min at 60ºC. RNA dilutions isolated from a SARS-CoV stock were used as a standard. Average results (± SEM) for macaque (n = 4) and African green monkey (n = 4) groups were expressed as SARS-CoV equivalents per ml swab medium.

Lung tissue samples (0.3 to 0.5 g) were taken for RT-PCR and microarray analysis in RNA-later (Ambion, Inc.). RNA was isolated from homogenized post mortem tissue samples using Trizol Reagent (Invitrogen) and the RNeasy mini kit (Qiagen). cDNA synthesis was performed with ~1 µg total RNA and Superscript III RT (Invitrogen) with oligo(dT), according to the manufacturer's instructions. Semiquantitative RT-PCR was performed as described previously to detect SARS-CoV mRNA and to validate cellular gene expression changes as detected with microarrays of SPP1, CCL3, and CCL20 (Applied Biosystems; Hs00167093_m1; Rh02788104_gH ; Rh02788116_m1), and IL-8, IL-6, and IFN-β.[173] Differences in gene expression are represented as the fold change in gene expression relative to a calibrator and normalized to a reference, using the $2^{-\Delta\Delta Ct}$ method.[176] GAPDH (glyceraldehydes-3-phosphate dehydrogenase) was used as an endogenous control to normalize quantification of the target gene. The samples from the mock-infected macaques or African green monkeys were used as a calibrator. Average results (± SEM) for groups were expressed as the fold change compared to PBS-infected animals.[176]

Statistical analysis

Data (RT-PCR, gross pathology and histology scores for SARS-CoV-infected animals) were compared using Student's t-test. Differences were considered significant at $P < 0.05$.

RNA labeling, microarray hybridization, scanning and data preprocessing

Pooled total RNA (2.4 µg) from one to three separate lung pieces per animal, with substantial SARS-CoV replication (> 10^5 fold change), was labeled using the One-Cycle Target Labeling Assay (Affymetrix) and hybridized onto Affymetrix GeneChip Rhesus Macaque Genome Arrays (Affymetrix) according to the manufacturer's recommendations. Image analysis was performed using Gene Chip Operating Software (Affymetrix). Microarray Suite version 5.0 software (Affymetrix) was used to generate .dat and .cel files for each experiment. Data were normalized using a variance stabilization algorithm (VSN).[177] Transformed probe values were summarized into one value per probe set by the median polish method.[178] Primary data are available at http://www.virgo.nl in accordance with proposed minimum information about a microarray experiment (MIAME) standards.

Microarray data analysis

Principal component analysis (PCA) was performed on a single normalized data set, including all

African green monkey and cynomolgus macaque samples. For PCA, 1 147 probe sets were included that deviated ≥ 1.5-fold from the geometrical mean (absolute values) for at least one of the samples. Differentially expressed mRNA transcripts were identified using LIMMA (version 2.12.0).[179] Correction for multiple testing was achieved by requiring a false discovery rate (FDR) of 0.05, calculated with the Benjamini-Hochberg procedure.[180] To understand the gene functions and the biological processes represented in the data and to obtain differentially expressed molecular and cellular functions, Ingenuity Pathways Knowledge Base (http://www.ingenuity.com/) was used. Heat maps of pro-inflammatory pathways were generated using complete linkage and Euclidian distance in Spotfire DecisionSite for Functional Genomics version 9.1 (http://www.spotfire.com/) and Ingenuity Pathways Knowledge Base (http://www.ingenuity.com/), using log (base 2)-transformed expression values, with minimum and maximum values of the color range of –4 and 4, respectively.

RESULTS

Clinical signs and gross pathology in SARS-CoV-infected African green monkeys

Cynomolgus macaques develop pathology upon SARS-CoV infection, and the severity is associated with aging.[174] In this study, we compared SARS-CoV infection in two related non-human primate host species, young adult cynomolgus macaques and African green monkeys, focussing on the latter. Four young adult African green monkeys were infected with SARS-CoV HKU39849, and as a control, two were PBS-infected. During the 4-day experiment, all animals remained free of clinical symptoms. Their body temperatures, measured by transponders in the peritoneal cavity, demonstrated a rhythmic pattern, with temperatures fluctuating between 35°C at night and 39°C during the day, prior to infection (Figure 1A). Between days 1 and 2 after SARS-CoV infection, an increase in body temperatures was recorded during the night in all animals. In addition, some African green monkeys showed an increase in body temperature up to 40°C during the first two days after SARS-CoV infection (Figure 1A). Even at days 3 and 4 post infection, elevated temperatures were still observed in some African green monkeys. At gross necropsy, four days post infection (dpi), the lungs of African green monkeys, showed (multi)focal pulmonary consolidation (Figure 1B-C). The consolidated lung tissue was gray-red, firm, level, and less buoyant than normal. Strikingly, one animal had severe lesions, with up to 30% of total lung tissue affected (Figure 1B). Four young adult cynomolgus macaques infected with SARS-CoV HKU39849 and two PBS-infected cynomolgus macaques were used for comparative analyses.[174] In contrast to infected African green monkeys, no increase in body temperature of up to 40°C during the first two days after SARS-CoV infection was observed in macaques.[174] Between days 1 and 2 after SARS-CoV infection, an increase in body temperatures was recorded during the night in three out of four animals.[174] Temperatures returned to normal from day 3 post infection onwards.[174] The lungs of young adult macaques showed small, patchy, macroscopic lesions (Figure 1C).[174]

Histopathology in SARS-CoV-infected African green monkeys

The lesions in the lungs of African green monkeys consisted of acute exudative DAD characterized by thickened alveolar septa with infiltration of moderate numbers of neutrophils and macrophages, lymphocytes and plasma cells, and necrosis with karyolysis, karyorrhexis, and loss of cellular detail (Figure 2A). Multifocally, moderate hypertrophy and hyperplasia of type II pneumocytes

was observed (Figure 2A-B). A variable amount of eosinophilic proteinaceous fluid (edema and exudate) with fibrin and eosinophilic hyaline membrane formation (Figure 2A-C), few syncytia, moderate numbers of foamy alveolar macrophages, neutrophils, and erythrocytes (hemorrhage) were seen in alveolar lumina. Mild necrosis, hypertrophy and hyperplasia of bronchiolar epithelium were encountered (Figure 2A). Peribronchiolar, peribronchial, and perivascular infiltrations of moderate numbers of lymphocytes, plasma cells, macrophages, and neutrophils with mild to moderate edema were seen (Figure 2A). There was a mild to moderate proliferation of the bronchus-associated lymphoid tissue (BALT), with focal nodular lymphocytic proliferation with formation of follicles with additional exocytosis of neutrophils in the tracheal epithelium (Figure 2A). A mild multifocal lymphoplasmacytic tracheo-bronchoadenitis, characterized by a multifocal mild infiltration of lymphocytes, macrophages, plasma cells, and neutrophils in and surrounding the bronchial seromucous glands with mild necrosis of the epithelium, was observed in all African

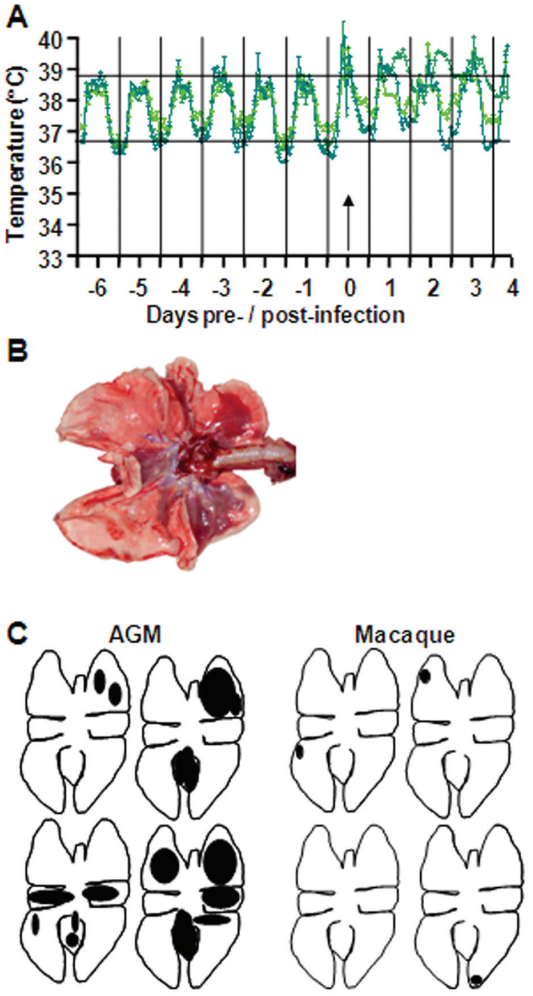

Figure 1. *African green monkeys (AGM) are more prone to develop SARS-CoV-associated disease than young adult macaques. (A) Fluctuations in body temperatures measured by transponders in the peritoneal cavity in three out of four SARS-CoV-infected AGM. Temperatures are shown from day 6 prior to infection until four days post infection. The arrow indicates day zero, when animals were infected. The black horizontal lines mark the average range of temperature fluctuations prior to infection. (B) Macroscopic appearance of lung tissue of SARS-CoV infected AGM at day 4 post infection, with dark-red consolidation. (C) Schematic diagrams of the lungs showing gross pathology lesions of SARS-CoV-infected young adults AGM and macaques.*

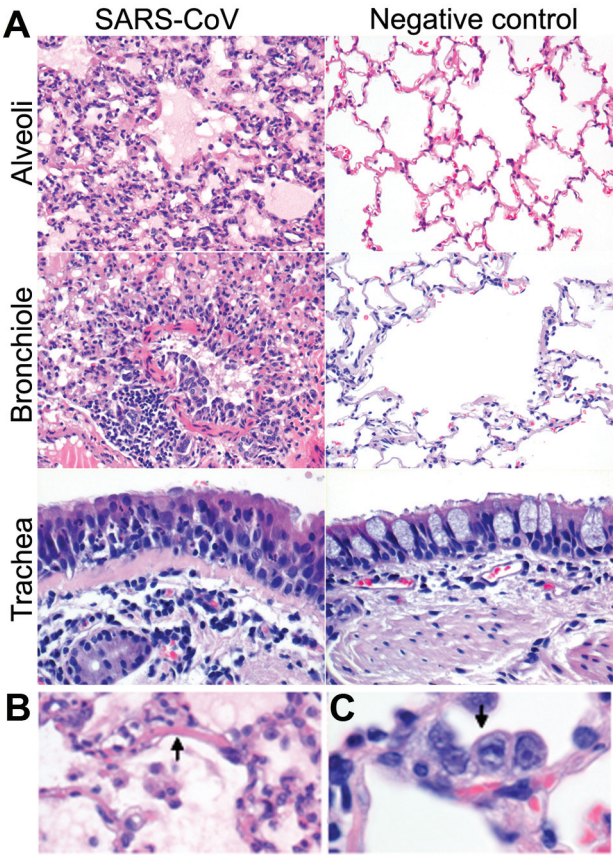

Figure 2. *Histologic analyses of lungs from SARS-CoV-infected African green monkeys (AGM). (A) Alveoli of PBS-infected (right) and SARS-CoV infected (left) AGM showing diffuse alveolar damage, characterized by distension of alveolar walls with influx of inflammatory cells, necrosis, type II pneumocyte hyperplasia, intra-alveolar edema and hyaline membrane formation. The bronchioles of PBS-infected (right) and SARS-CoV infected (left) AGM show infiltration of inflammatory cells, intraluminal edema fluid, and hypertrophy and hyperplasia of bronchiolar epithelium. The trachea of PBS-infected (right) and SARS-CoV infected (right) AGM with multifocal lymphoplasmacytic tracheo-bronchoadenitis with infiltration of inflammatory cells surrounding the bronchial seromucous glands in the SARS-CoV infected group. (B and C) Lesions of SARS-CoV infected AGM are shown in more detail, with hyaline membrane formation (B) and type II pneumocyte hyperplasia (C). HE, x20 and x40.*

green monkeys (Figure 2A). Two animals showed evidence of multifocal mild lymphoplasmacytic pleuritis consisting of a mild multifocal distention of the pleura with infiltration of few lymphocytes, plasma cells, macrophages, neutrophils, and mild edema. The lymphoid organs were activated, with proliferation of the tracheobronchial lymph node and spleen, characterized by increased numbers of neutrophils and histiocytes, and distinct germinal centers in the lymphoid follicles. No significant lesions were seen in other tissues examined or in the tissues of negative-control animals. The histopathologic lesions in the respiratory tract of SARS-CoV-infected cynomolgus macaques were largely similar in character as described for the African green monkeys.[174] However, hyaline membrane formation was not observed, and the lesions in macaques were significantly less severe and extensive than those in African green monkeys (Figure 3A), which corroborated the gross pathology scores (Figure 3B).

Virus replication and tropism in SARS-CoV-infected African green monkeys

SARS-CoV mRNA levels were detected in throat (Figure 4A), and nasal (Figure 4B) swabs of African green monkeys on 2 and 4 dpi and in rectal swabs on 4 dpi (data not shown). In addition, virus replication in the lungs was demonstrated by RT-PCR and titration, and

immunohistochemistry revealed SARS-CoV antigen expression in the lungs of African green monkeys, within or directly adjacent to areas with lesions (Figure 4C and D). In alveoli of African green monkeys, cells that resembled type I and type II pneumocytes and rarely alveolar macrophages expressed SARS-CoV antigen (Figure 5A). SARS-CoV antigen was not detected in bronchioles or bronchi but was observed in ciliated epithelial cells in the trachea of two African green monkeys (Figure 5A). The differences in the percentage of SARS-CoV infected cells in the lungs or virus titers in the throat, nose and lungs of African green monkeys and macaques were not statistically significant (Figure 4). SARS-CoV, however, was not detected in ciliated epithelial cells in the trachea on 4 dpi in young adult macaques (Figure 5A) or in rectal swabs. In both PBS-infected African green monkeys and macaques, we could show ACE2 expression, which is the receptor for SARS-CoV, in cells morphologically resembling type II epithelial cells (Figure 5B). Significant differences between ACE2 expression in African green monkeys and macaques could not be observed. Overall, African green monkeys displayed more severe pathology than macaques upon infection with SARS-CoV, which correlated with a broader range of cell types infected at 4 dpi, but not with the extent of virus replication.

Host response to SARS-CoV in African green monkeys and macaques

To understand why SARS-CoV-infection in African green monkeys results in more severe pathology than in young adult macaques, we generated genome-wide mRNA expression profiles from lung tissue with substantial SARS-CoV replication (Figure 6A). Principal-component analysis was

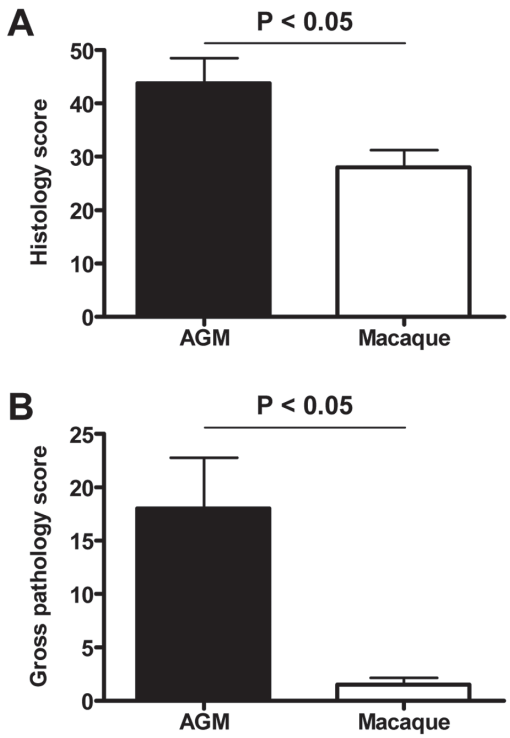

Figure 3. *African green monkeys display more severe pathology than macaques. (A) Histology scores of the lungs of African Green Monkey (AGM) and macaque groups were determined and averaged (plus SEM). (B) Gross pathology scores of AGM and macaque groups were determined by visual inspection of the lungs during necropsy and averaged (plus SEM).*

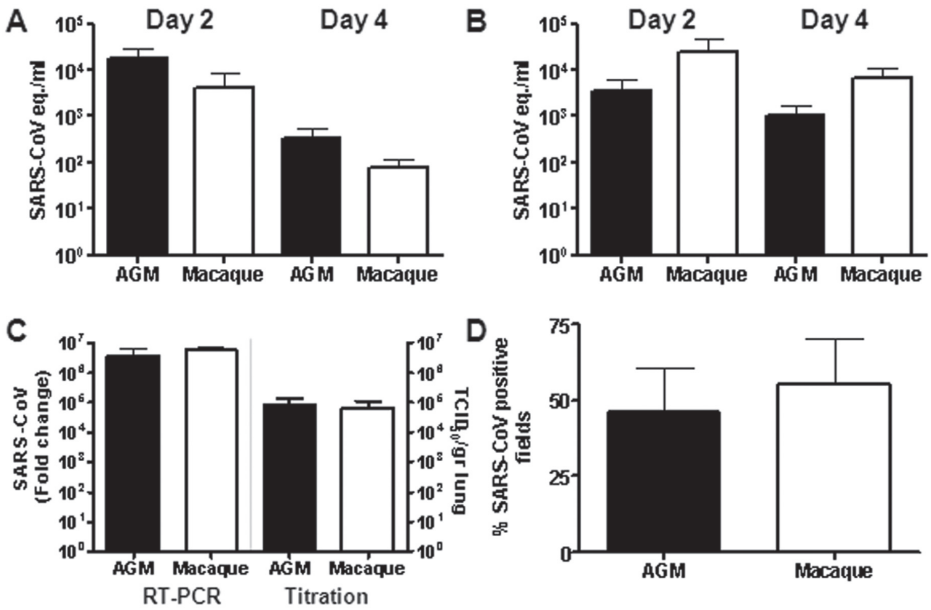

Figure 4. *Viral replication levels in the respiratory tract of SARS-CoV-infected African green monkeys (AGM) and macaques. (A and B) SARS-CoV replication in the throats (A) and noses (B) of SARS-CoV-infected AGM (black bars) and macaques (white bars) at day 2 and 4 post infection as determined by real-time RT-PCR. Viral RNA levels are displayed as $TCID_{50}$ equivalents (eq.)/ml swab medium (plus SEM). (C) Average fold change in SARS-CoV mRNA levels (plus SEM) in the lungs of African green monkeys and macaques compared to PBS-infected animals as determined by real-time RT-PCR and depicted on a log scale. In addition, SARS-CoV titration of lung homogenates is shown in $TCID_{50}$ per gram lung tissue. (D) Quantitative assessment of SARS-CoV infected cells in the lungs of African green monkeys and macaques depicted as a percentage of SARS-CoV-positive fields (plus SEM).*

performed on a single normalized data set of African green monkey samples, together with macaque samples. This unsupervised method clearly separated SARS-CoV-infected lung mRNA expression profiles from PBS control expression profiles for both species. In addition, the infected and uninfected expression profiles of the two species also separated well. Species- and infection-related expression profile differences coincided with principal component 1 and 2, respectively (Figure 6B). These results show that species-associated mRNA expression profile differences are maintained upon SARS-CoV infection, suggesting that African green monkeys and macaques respond differently to SARS-CoV infection.

To analyze the host response to infection in African green monkeys and macaques in more detail, mRNA transcripts differentially expressed between infected and uninfected lung samples were identified using the ANOVA-like method LIMMA[179] for both species separately. To obtain a maximum view of infection-induced host response differences between African green monkeys and macaques, the microarray data for the two species were normalized separately. Infected African green monkeys expressed 556 gene transcripts differentially from PBS-infected animals. These differentially expressed genes were analyzed within the context of molecular pathways, using a functional analysis approach of biologically related genes (Ingenuity). The most significantly regulated molecular/cellular functions in African green monkeys compared to PBS-infected animals

were associated with a pro-inflammatory response and included cellular growth and proliferation, cell death, cell movement, and cell-to-cell signalling (Figure 7A). Upon analysis of the gene transcripts within the context of biological pathways using Ingenuity Knowledge Base, the top gene interaction network in African green monkeys showed a strong antiviral response with differentially expressed type I interferon-stimulated genes and genes associated with the induction of type I interferons (Figure 7B), including ISG15, ISG20, DDX58, DHX58, IFI/IFITs, MX1, MX2, IRF7, IRF9, OAS1 and OAS2. In addition, this network contained NF-κB (Figure 7B), a transcription factor implicated in pro-inflammatory host responses and development of ALI/ARDS.[159,181,182] Differential expression of genes associated with acute lung injury, inflammation, and/or hypoxia signalling in African green monkeys included C3AR1, CEBPD, CCL2, CCL3, IL1RN, TIMP1, CDKN1A, SPARC, VEGFA, SPP1, CSF1, CSF3R, CD86, KIT, CCL8, CXCL10, PML, SP100, and SOD2. Some of these genes are also upregulated in SARS patient sera or in patients with ARDS.[60,133] Young adult SARS-CoV-infected macaques expressed 475 gene transcripts differentially from PBS-infected animals. These genes were associated with the same molecular/cellular functions as observed in African green monkeys, with similar numbers of differentially expressed genes per function (Figure 7A). Analysis of the gene transcripts in the context of biological pathways revealed differential expression of genes in both antiviral and pro-inflammatory responses (Figure 7C). These data suggest that both African green monkeys and macaques display similar types of responses upon infection, with strong induction of antiviral and pro-inflammatory pathways, which has been described for SARS-CoV-infected cynomolgus macaques previously but based on regulation of a different array of individual genes within the antiviral and pro-inflammatory pathways.[173,174]

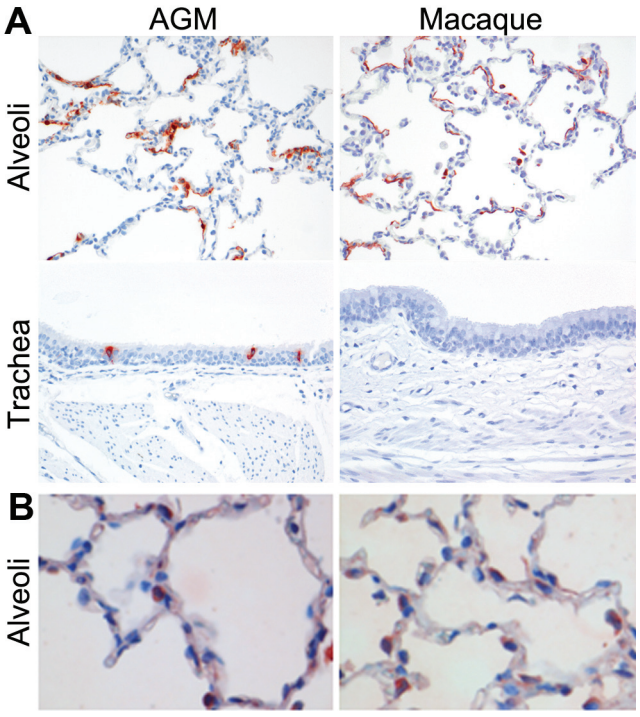

Figure 5. *Lungs of African green monkeys and cynomolgus macaques showing SARS-CoV (A) and ACE2 (B) antigen expression in the alveoli and/or trachea from SARS-CoV and PBS-infected animals, respectively. Immunoperoxidase counterstained with hematoxylin, x20.*

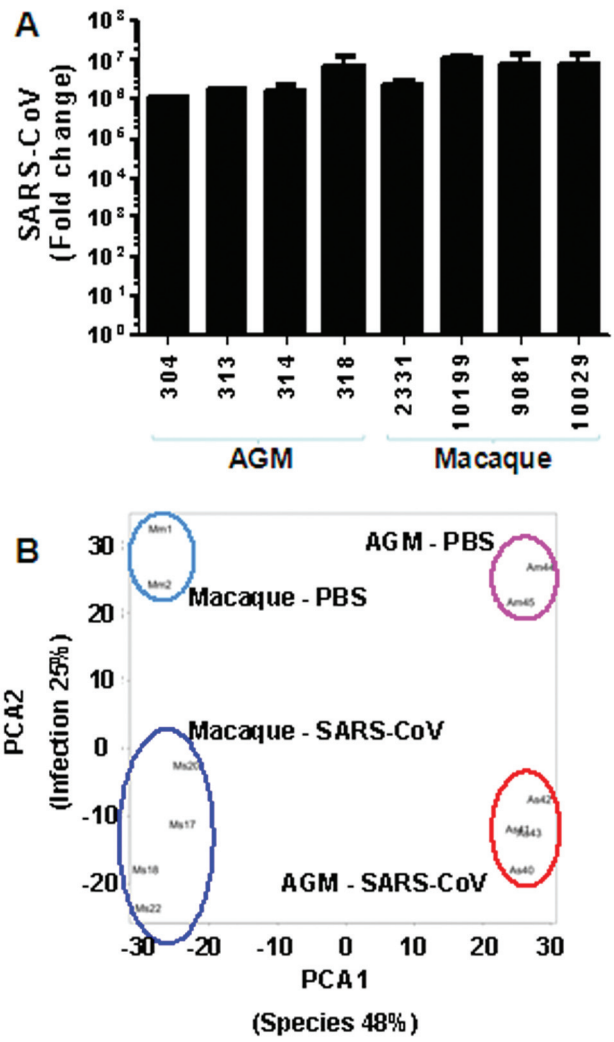

Figure 6. *Global gene expression profiles of individual African green monkeys (AGM) and macaques. (A) Average fold change in SARS-CoV mRNA levels (plus SEM in the lungs of AGM and macaques compared to PBS-infected animals as determined by real-time RT-PCR and depicted on a log scale. (B) PCA of transciptional profiling data. Each combination of letters and numbers (Am44, Am45, Mm1, Mm2, Am40, Am41, Am42, Am43, Mm17, Mm18, Mm20, Mm22) represents an individual PBS- or SARS-CoV-infected animal plotted in two dimensions using their projections onto the first two principal components, species and infection. The colored circles represent the groups of PBS-infected and SARS-CoV-infected AGM and macaques. The first two principle components account for 48% and 25% of variation in the data, respectively.*

As the principal component analysis suggested that the host response to SARS-CoV infection was different in African green monkeys and macaques, the gene expression profiles of SARS-CoV-infected African green monkeys and macaques ($n = 4$) were directly compared using LIMMA (8 samples normalized in a single set). A total of 1 607 gene transcripts were differentially expressed. Upon analysis of these 1 607 gene transcripts within the context of biological processes and pathways using Ingenuity Pathways Knowledge Base, this subset of genes showed indications of an innate host response to viral infection. Among the top significantly differentially regulated ($P < 0.005$) functional categories were inflammatory disease, cell movement, and cell-to-cell signalling and interaction, which included genes like CCL20, CXCL1, CXCL2, DEFB1, IL1RL1, IL1RN, MMP7, MMP9, IL-8, SERPINE1, SPP1, TFPI2, and VCAM1, which were either up- or downregulated depending on the gene (Figure 8A to C), indicating that they are upregulated either

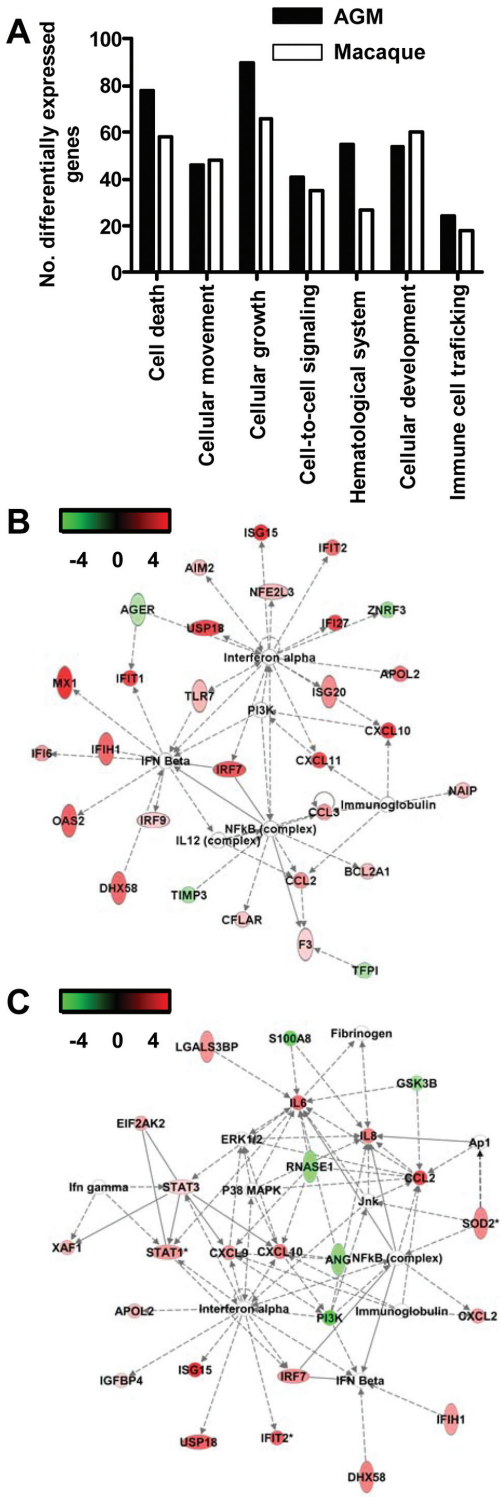

Figure 7. *Innate host response to SARS-CoV infection in African green monkeys (AGM). (A) Numbers of differentially expressed genes in AGM and macaques with functions in, for example, cellular growth and proliferation, cell movement, cell death, or cell-to-cell signaling and interaction obtained from Ingenuity Pathways Knowledge Base. (B) AGM present a "top" network, with genes involved in the antiviral response and pro-inflammatory response. A network is a group of biologically related genes that is derived from known relationships present in the Ingenuity Pathways Knowledge Base. The diagram represents the interactions, both direct (solid lines) and indirect (dashed lines), between differentially expressed genes and gene products identified on day 4 post infection in AGM. Red indicates upregulated genes, whereas downregulated genes are depicted in green. (C) Macaques also present a "top" network with genes involved in the antiviral response and pro-inflammatory response. The diagram represents the interactions, both direct (solid lines) and indirect (dashed lines), between differentially expressed genes and gene products identified on day 4 post infection in macaques. Red indicates upregulated genes, whereas downregulated genes are depicted in green.*

in African green monkeys or macaques. These data suggest that both host species and SARS-CoV infection are factors involved in determining transcription of cellular genes and that significant differences exist in the pro-inflammatory host response to SARS-CoV infection, corresponding to the host species.

In order to understand the host responses in the context of host species, we directly compared lung samples from PBS-infected African green monkeys ($n = 2$) and macaques ($n = 2$). LIMMA analysis revealed that 2 198 gene transcripts were differentially expressed (change, ≥ 2-fold; $P < 0.05$), with categories such as inflammatory disease, cell death, cell movement, and cellular growth and proliferation among the top significantly differentially regulated functions ($P < 0.005$). Of the 2 198 differentially expressed genes, 917 were also differentially expressed in the direct comparison of SARS-CoV-infected African green monkeys and macaques, but they did not include genes for cytokines/chemokines, such as CCL20, CCL3, and SPP1. Our data indicate that significant differences exist in the basal gene expression levels of African green monkeys and macaques, which may partly explain why differences in pathology were observed after SARS-CoV infection.

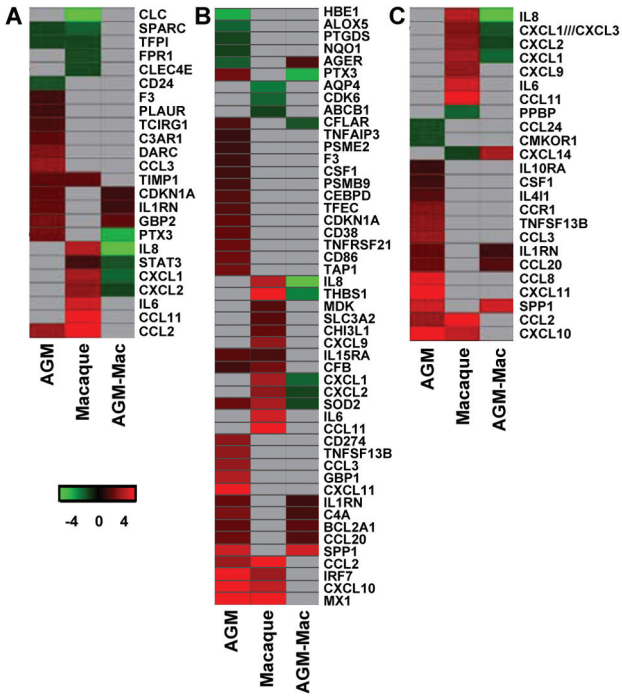

Figure 8. *Innate host responses to SARS-CoV infection in African green monkeys (AGM) and macaques. (A to C) Gene expression profiles showing differentially expressed genes involved in development of ARDS (A), NF-κB target genes (B), and cytokines/chemokines (C) of AGM and macaques compared to their PBS controls and from the direct contrast of SARS-CoV-infected AGM and macaques (AGM-Mac). Gene sets were obtained from Ingenuity Pathways Knowledge Base and changed ≥ 2-fold (absolute) in at least one of AGM or macaque groups as compared to their respective PBS-infected controls. The data presented are error-weighted fold change averages for four animals per group. The genes shown in red were upregulated, those in green downregulated, and those in gray were not significantly differentially expressed in infected animals relative to PBS-infected animals (log [base 2]-transformed expression values; the minimum and maximum values of the color range were –4 and 4).*

To obtain more insight in the differences in the host responses to SARS-CoV infection of African green monkeys and macaques, mRNA expression profiles for specific molecular pathways of infected animals of both species were compared to their PBS controls but also directly against each other. Heat maps were generated for differentially regulated genes involved in ARDS (Figure 8A), NF-κB signaling (Figure 8B), and cytokine/chemokine signaling (Figure 8C), which indicated that the host responses to infection with respect to these pathways in African green monkeys and macaques are different. Surprisingly, inflammatory cytokines that play a major role in mediating and amplifying ALI/ARDS or have neutrophil chemoattractant activity, such as IL-6, IL-8, CXCL1, and CXCL2,[133,181,183] were differentially expressed in macaques, but not in African green monkeys (Figure 8C). Taqman analysis confirmed that IL-6 and IL-8, key players in ALI/ARDS, were differentially expressed at significantly lower levels in African green monkeys than in young adult

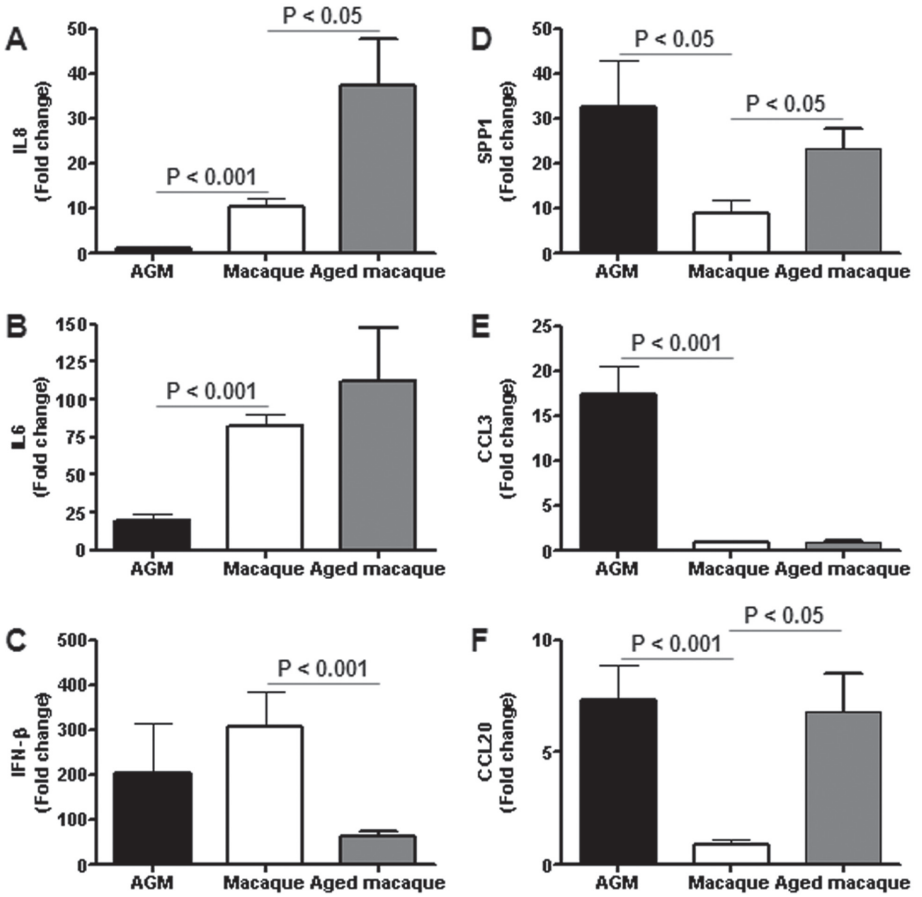

Figure 9. *Quantitative RT-PCR confirmation of cytokine/chemokine mRNA levels. Quantitative RT-PCR for IL-8 (A), IL-6 (B), IFN-β (C), SPP1 (D), CCL3 (E), and CCL20 (F) was performed on one to three separate lung samples per animal with substantial virus replication. The data presented are error-weighted (plus SEM) averages of the fold change in SARS-CoV-infected African green monkeys and macaques as compared to their respective PBS-infected controls.*

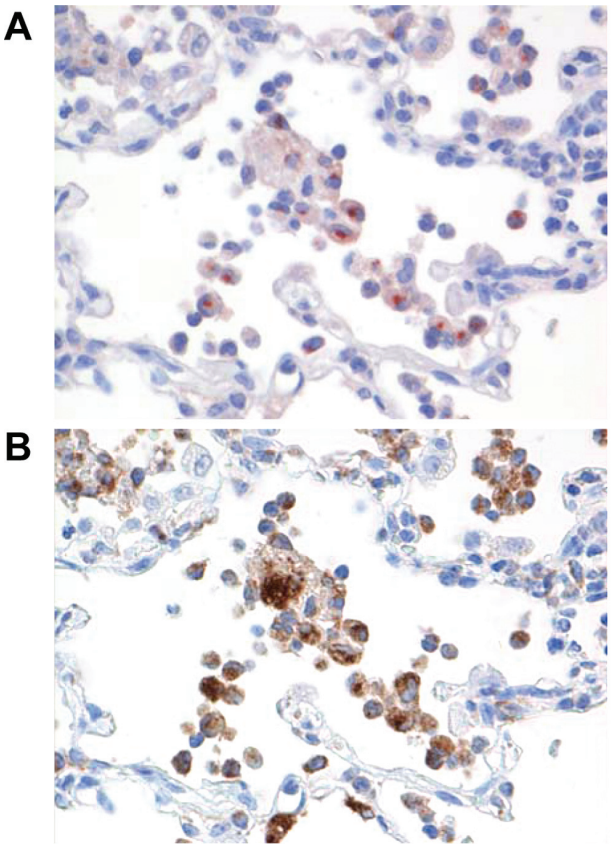

Figure 10. *Osteopontin expression in macrophages in SARS-CoV-infected African green monkeys. The same lung sections of SARS-CoV-infected African green monkeys were stained for expression of osteopontin (A) or CD68 (B), a marker for macrophages. Immunoperoxidase counterstained with hematoxylin, x20.*

macaques (Figure 9A and B), in contrast to the IFN-β levels, which were not significantly different (Figure 9C). Moreover, in the direct comparison of the microarray data of SARS-CoV-infected African green monkeys with macaques, IL-8, CXCL1, and CXCL2 were also differentially expressed (Figure 8A to C). These observations suggest that classical pathways known to be involved in development of ALI/ARDS are differently regulated in these two non-human primate species. From previous studies, we know that in aged cynomolgus macaques, IL-8 gene expression is further upregulated (Figure 9A)[174] and correlated with significantly more severe pathology. Because African green monkeys showed even more pathology than young adult macaques, other pathogenic pathways besides the induction of genes such as IL-6 and IL-8 are most likely involved in the observed pathological changes.[159,174]

Interestingly, CCL3, SPP1, and CCL20 were induced strongly in African green monkeys, but not in young adult macaques (Figure 8A to C and 9D to F). This observation was corroborated by the direct comparison of SARS-CoV-infected African green monkeys with macaques, which showed that CCL20 and SPP1 were differentially expressed (Figure 8B-C). It is notable that both these genes were also statistically significantly upregulated in aged macaques compared to young adult macaques (Figure 9D-F).[174] CCL3 is involved in the acute inflammatory state in the recruitment and activation of polymorphonuclear leukocytes, whereas CCL20 is strongly chemotactic for lymphocytes but

Table 1. Gene accession numbers

Symbol	Accession number
ABCB1	NM_001032887
AGER	XM_001114900
ALOX5	XM_001102354
AQP4	XM_001086526
BCL2A1	XM_001109281
C3AR1	XR_013068
C4A	XM_001119226
CCL11	NM_001032874
CCL2	NM_001032821
CCL20	AF449274.1
CCL24	XM_001109757
CCL3	AF457195.1
CCL8	NM_001032851
CCR1	NP_001286
CD24	XM_001090225
CD274	NP_054862
CD38	XR_012961
CD86	XM_001111935
CDK6	NP_001138778
CDKN1A	XM_001116894
CEBPD	XR_013007
CFB	XM_001113705
CFLAR	XM_001096860
CHI3L1	XM_001103739
CLC	XM_001087874
CLEC4E	XM_001118423
CSF1	NP_000748
CXCL1	NP_001502
CXCL1 /// CXCL3	AF449280.1
CXCL10	NP_001556
CXCL11	NP_005400
CXCL14	XM_001088271
CXCL2	NP_002080
CXCL9	NP_002407
DARC	XM_001117200
F3	XM_001104233
FPR1	NP_001180235
GBP1	XM_001085311
GBP2	NP_004111
HBE1	NM_001164428
IL10RA	XM_001092736
IL15RA	NM_001079517
IL1RN	XM_001091493
IL4I1	XM_001115731
IL6	NM_001042733
IL8	NP_000575
IRF7	NM_001136100
CMKOR1	XM_001083694
MDK	XR_012413
MX1	NM_001079693
NQO1	NP_000894
PLAUR	XM_001106634
PPBP	XM_001102705
PSMB9	XR_011310
PSME2	XM_001112445
PTGDS	XR_011937
PTX3	XM_001103515
SLC3A2	XR_011769
SOD2	NP_000627
SPARC	NP_003109
SPP1	XM_001093307
STAT3	NP_003141
TAP1	XM_001115506
TCIRG1	XM_001103418
TFEC	XM_001101140
TFPI	XR_014703
THBS1	XM_001093770
TIMP1	NM_001032939
TNFAIP3	XM_001096105
TNFRSF21	NP_055267
TNFSF13B	XM_001082119

weakly attracts neutrophils. Osteopontin, encoded by SPP1, has been implicated in a broad range of disease processes, including chronic obstructive pulmonary disease, asthma, multiple sclerosis, rheumatoid arthritis, and cardiovascular disease.[184,185] Osteopontin has both matrix protein-like and cytokine-like properties and is expressed by different cell types of the immune system.[184,185] To determine which cell types are responsible for the osteopontin expression, immunohistochemical detection of the protein was performed on lung sections of SARS-CoV-infected African green monkeys (Figure 10). SARS-CoV-infected African green monkeys showed marked staining of osteopontin in the alveoli in areas with lesions. Strong expression of osteopontin was observed in infiltrating cells, and staining with an antibody directed against CD68 indicated that the infiltrating cells that expressed osteopontin were mainly macrophages (Figure 9). Similar staining was performed on the lungs of young adult and aged macaques, also showing that mainly macrophages were stained for osteopontin expression (data not shown). The immunohistochemistry data, however, do not allow a quantification of the amounts of osteopontin expression in the different species.

DISCUSSION

The acute onset of severe lung injury supposedly depends on activation of the oxidative-stress machinery that is coupled with innate immunity and activates transcription factors, resulting in a pro-inflammatory host response.[159] Pro-inflammatory cytokines, such as IL-1β, IL-8, CXCL2, and IL-6, play a major role in mediating and amplifying ALI/ARDS by stimulating chemotaxis and activation of neutrophils.[133,160,181] Our previous studies with regard to SARS-CoV-associated ALI/ARDS in young adult and aged macaques are in line with these observations. The acute phase of SARS is characterized by infiltration of inflammatory cells, edema, the formation of hyaline membranes, and proliferation characterized by type II pneumocyte hyperplasia.[168,174] In addition, severe pathology in macaques was associated with an increased expression of pro-inflammatory cytokines, including CXCL10, CCL2, IL-6, and IL-8, which was also observed in human SARS cases.[56-58,60,165-167,174] Although great advances have been made in understanding ALI/ARDS disease processes, the different molecular mechanisms that control the outcome are still poorly understood. By comparing and contrasting SARS-CoV infection in different but related host species (African green monkeys and cynomolgus macaques), we can now further delineate host factors involved in disease outcome.

The nature of acute lung injury observed after SARS-CoV infection in young adult African green monkeys is in general similar to the pathology observed after SARS-CoV infection in young adult macaques.[174] Moreover, virus replication levels were not significantly different between the two species. SARS-CoV-infected African green monkeys, however, developed more severe pathology with hyaline membranes, than young adult macaques, for which hyaline membranes were not observed.[174] African green monkeys seem to be the only animal species that shows relatively severe pathology when infected with SARS-CoV infection as young adult. These data are in line with previous observations in SARS-CoV-infected African green monkeys.[75] Comparative gene expression analyses in African green monkeys and macaques upon SARS-CoV infection revealed that both antiviral and pro-inflammatory pathways are strongly induced upon infection. However, many individual genes within these pathways are differently induced by African green monkeys and macaques. To our surprise, inflammatory cytokines that play a major role in mediating and

amplifying ALI/ARDS or have neutrophil chemoattractant activity, such as IL-8, IL-6, CXCL1, and CXCL2,[133,181,183] were upregulated in young adult macaques, but not in African green monkeys. Aged macaques display an even stronger pro-inflammatory host response to infection than young adult macaques, with significantly increased expression of inflammatory genes, among which IL-8, suggesting that exacerbated expression of pro-inflammatory cytokines may result in development of severe pathology.[174] Thus, the host response in African green monkeys upon SARS-CoV infection is not similar to the host response in young adult or aged macaques.

Although induction of classical pro-inflammatory mediators, such as IL-8 and IL-6, known to be involved in development of ALI/ARDS, was not observed, other pro-inflammatory cytokines and chemokines, including SPP1, CCL20, and CCL3, were up-regulated to a significantly larger extent in African green monkeys than in young adult macaques. Previous studies revealed that CCL3 plays a critical role in promoting lung inflammation and fibrosis, that significantly elevated levels of CCL3 were observed in mice infected with highly pathogenic influenza A virus as compared to mice infected with low pathogenic virus, and that CCL3 has been associated with fatal outcomes in human H5N1 influenza A virus infections.[134,186-188] Osteopontin is involved in the development of various inflammatory diseases, including multiple sclerosis, rheumatoid arthritis, and atherosclerosis.[184,189-192] Moreover, osteopontin has been recognized as a key cytokine involved in immune cell recruitment and type 1 (Th1) cytokine expression, and it plays a role in development of lung fibrosis.[184,193,194] In addition, osteopontin regulates infiltration and activation of fibroblasts, considered the main mediators of tissue fibrosis.[195] Both in murine lung fibrosis and idiopathic pulmonary fibrosis, osteopontin is among the most prominently expressed cytokines,[184] and osteopontin is strongly expressed by alveolar macrophages in the lungs of acute respiratory distress syndrome patients.[196] This observation was underscored by our finding that osteopontin was mainly expressed in infiltrating macrophages in SARS-CoV-infected African green monkeys. The SPP1 promoter is responsive to many agents, including cytokines, growth factors, hormones and angiotensin II.[184,197] The latter is of interest as angiotensin II is a component of the renin-angiotensin system and promotes disease pathogenesis, induces lung edema and impairs lung function.[198] ACE2, the SARS-CoV receptor, cleaves angiotensin II and is a negative regulator of the system. In mice, it was shown that recombinant SARS-CoV spike protein downregulates ACE2 expression and thereby promotes lung injury.[199] These data provide a potential link between SARS-CoV infection, SPP1 gene expression, and lung injury. Given the fact that both SPP1 and CCL20 genes were up-regulated in aged SARS-CoV-infected macaques,[174] activation of these genes does not seem to be restricted *per se* to African green monkeys and may be involved in the exacerbated SARS-CoV disease in aged macaques.

Several recent studies have provided evidence for a critical role of macrophages in SARS. Depletion of alveolar macrophages before inoculation with a mouse-adapted version of SARS-CoV results in enhanced T-cell responses and protection of BALB/c mice from lethal infection.[200,201] Moreover, SARS-CoV-infected STAT1-/- mice exhibited dysregulation of T-cell and macrophage differentiation, leading to development of alternatively activated macrophages that mediate a pro-fibrotic environment, suggesting that macrophage dysregulation causes formation of pre-fibrotic lesions in the lungs of SARS-CoV-infected mice.[202] Based on our comparative analysis of SARS-CoV-associated acute lung injury in African green monkeys and macaques, we hypothesize that what is viewed as ARDS, consisting of infiltration of inflammatory cells, edema, the formation of hyaline membranes, and type II pneumocyte hyperplasia, may be caused by regulation of the transcription

of a different array of pro-inflammatory genes. Besides a common ARDS "injury pathway" with neutrophil influx and expression of IL-1β, IL-8, and IL-6, other pathways that can amplify ARDS may exist.[159] Possibly, a prominent influx of macrophages expressing pro-inflammatory cytokines, such as osteopontin, may play a role in development of ALI/ARDS as well. In this respect it is notable that an influx of neutrophils and macrophages was observed in SARS-CoV-infected aged macaques on 4 dpi,[188] whereas it seemed that mainly macrophages were infiltrating in the lungs in African green monkeys.

The fact that closely related non-human primates show intrinsic differences in the host response to virus infection is not unprecedented. African green monkeys infected with simian immunodeficiency virus (SIV) do not develop chronic immune activation and AIDS, in contrast to humans infected with human immunodeficiency virus or macaques infected with SIV.[203-206] The non-pathogenic SIV infections differ from pathogenic infections by their benign clinical course, maintenance of peripheral CD4+ T-cell counts at normal levels, absence of chronic immune activation by controlling levels of type I interferon, and preservation of normal levels of mucosal T helper type 17 cells.[203-206] One may speculate that the evolutionary adaptations in the innate immune system that allow co-existence of primate lentiviruses with the host without causing AIDS, also result in a different host response to other acute viral infections, such as observed for SARS-CoV infection in African green monkeys. Alternatively, both in macaques and African green monkeys, SARS-CoV antigen was detected in tracheal and bronchiolar epithelial cells early on days 1 or 2 post infection (reference 32 and our own unpublished observations). African green monkeys, however, may display more severe pathology than macaques upon infection with SARS-CoV as a consequence of the broader range of cell types infected at day 4 post infection. Studies in mice revealed that differences in tropism are associated with outcome of the SARS-CoV infection.[63]

Our studies provide evidence that the use of (closely) related host species reveals valuable insights in virus-host interactions.[207] If our assumption that different injury pathways can lead to development of ALI/ARDS is correct, it is important to realize that interventions that ameliorate pathology by modulating the host response in one host species may be ineffective in another species. Osteopontin induction by mediators of acute inflammation, such as TNF-α, IL-1β, angiotensin II, and NF-ϰB,[197] may be sensitive to the inhibitory action of type I IFN[208] and partly explain why type I interferon treatment of aged SARS-CoV-infected macaques resulted in mitigation of pathology.[174] Ultimately, these studies need to be extended to the human host in order to identify markers of host susceptibility and severity of disease that enable the rational design of multipotent biological response modifiers to combat ALI/ARDS induced by different agents.

Acknowledgements

We thank R. Dias d'Ullois, M.A. Bijl, and F. Zaaraoui-Boutahar for technical assistance.

CHAPTER 2

SARS CORONAVIRUS INFECTION IN ANIMAL MODELS

2.2

Pathology of experimental SARS coronavirus infection in cats and ferrets

Veterinary Pathology (2008) 45:551-562

JMA van den Brand, BL Haagmans, LME Leijten, D van Riel,
BEE Martina, ADME Osterhaus, and T Kuiken

Department of Virology, Erasmus Medical Center, Rotterdam, The Netherlands

ABSTRACT

The pathology of severe acute respiratory syndrome-coronavirus (SARS-CoV) infection in cats and ferrets is poorly described and the distribution of angiotensin-converting enzyme 2 (ACE2), a receptor for SARS-CoV, in the respiratory tracts of these species is unknown. We observed SARS-CoV antigen expression and lesions in the respiratory tracts of 4 cats and 4 ferrets at 4 days post inoculation and ACE2 expression in the respiratory tracts of 3 cats and 3 ferrets without infection. All infected cats and ferrets had diffuse alveolar damage associated with SARS-CoV antigen expression. A novel SARS-CoV-associated lesion was tracheo-bronchoadenitis in cats. SARS-CoV antigen expression occurred mainly in type I and II pneumocytes and serous cells of tracheo-bronchial submucosal glands of cats and in type II pneumocytes of ferrets. ACE2 expression occurred mainly in type I and II pneumocytes, tracheo-bronchial goblet cells, serous epithelial cells of tracheo-bronchial submucosal glands in cats, and type II pneumocytes and serous epithelial cells of tracheo-bronchial submucosal glands in ferrets. In conclusion, the pathology of SARS-CoV infection in cats and ferrets resembles that in humans except that syncytia and hyaline membranes were not observed. The identification of tracheo-bronchoadenitis in cats has potential implications for SARS pathogenesis and SARS-CoV excretion. Finally, these results show the importance of ACE2 expression for SARS-CoV infection *in vivo*: whereas ACE2 expression in type I and II pneumocytes in cats corresponded to SARS-CoV antigen expression in both cell types, expression of both ACE2 and SARS-CoV antigen in ferrets was limited mainly to type II pneumocytes.

INTRODUCTION

Severe acute respiratory syndrome (SARS) emerged in the human population in November 2002 and spread rapidly across Asia, Europe, and North America in subsequent months.[14] Although the causative virus, SARS-coronavirus (SARS-CoV),[5-7,19] was eradicated from the human population by July 2003, its progenitors are likely still present in animal reservoirs[10] and could again cross the species barrier into humans. In total, SARS caused 774 deaths out of more than 8 000 people with confirmed infection. Because the pathogenesis of SARS in humans is poorly understood, it is difficult to develop preventive and therapeutic strategies against this disease.[14]

The primary lesion of SARS in humans is diffuse alveolar damage (DAD), indicating injury to the alveolar septa.[31,32,37,209,210] This lesion corresponds in part to the cell types in the respiratory tract in which SARS-CoV antigen has been detected: alveolar epithelial cells (primarily type II pneumocytes), bronchial epithelial cells, and alveolar macrophages.[14,36,52,211,212] Cases of longer duration (more than 10 days) demonstrated features of organizing-phase or late stage DAD.[37,210]

Angiotensin-converting enzyme 2 (ACE2) has been identified as a receptor for the attachment to and uptake of SARS-CoV in host cells.[45] The distribution of ACE2 in human tissues corresponds largely to the cell types in which SARS-CoV replication has been observed: in addition to type II pneumocytes and bronchial epithelial cells, ACE2 expression has been observed in type I pneumocytes and endothelial cells as well as smooth muscle cells of blood vessels, but not alveolar macrophages.[51,213]

Since the appearance of SARS, several animal models have been developed for SARS-CoV infection in humans: SARS-CoV infection in macaques,[6] marmosets,[214] mice,[171,215] golden Syrian ham-

sters,[216] rats,[217] cats and ferrets.[69] Subbarao and Roberts reviewed the advantages and disadvantages of the above animal models.[169] The limitations of rodents such as hamsters and young inbred mice are that they do not show illness[169] and their lung structure differs from that of the human lung;[218] the limitations of non-human primates are availability, cost, and housing.[169] SARS-CoV infections in cats and ferrets do not show these limitations and may therefore be valuable as animal models.

Previous experiments showed that domestic cats and ferrets were susceptible to SARS-CoV infection and that they were able to transmit the virus efficiently to previously uninfected sentinel animals that were housed with them.[69] The acute pulmonary lesions seen in those species were reported to be similar to those in humans and macaques, but were not described.[69,219] Chronic lesions in ferrets euthanized at 23 days after infection were bronchial and bronchiolar hyperplasia as well as peribronchiolar and perivascular lymphocytic cuffing.[220,221] However, the pathology and viral distribution in cats and ferrets with acute SARS-CoV infection are poorly understood.

Our goal was to describe the pathology of acute SARS-CoV infection in cats and ferrets and to determine the expression of ACE2 in the respiratory tracts of these species. Therefore, we experimentally infected cats and ferrets with SARS-CoV and examined respiratory tract tissues at 4 days post inoculation (dpi) by histopathology, immunohistochemistry, and immunofluorescence.

MATERIALS AND METHODS

Virus preparation

Strain HKU 39849 of SARS-CoV was passaged 4 times on Vero 118 cells cultured in Iscove's Modified Dulbeco's Medium (Bio Whitaker, Walkersville, MD, USA). After centrifugation at 270 g for 5 min, 1 ml samples were made from the supernatant and from the pelleted cells, which were resuspended in 5 ml medium. The titer of this virus stock was 1 x 10^6 median tissue culture infectious dose ($TCID_{50}$) per ml. All cell cultures were done under biosafety level 3 conditions.

Experimental protocol

The experiments were performed under biosafety level 3 conditions at the Erasmus MC in Rotterdam under an animal study protocol approved by the Institutional Animal Welfare Committee. Specified pathogen-free cats and ferrets were purchased from commercial breeders (Harlan, Indianapolis, IN, USA and Schimmel, Uddel, The Netherlands, respectively), maintained in standard housing and provided with commercial food pellets and water *ad libitum* until the start of the experiment. Before infection, they were examined clinically and determined to be healthy by a registered veterinarian and were placed in negative-pressurized glove boxes. Four cats and 4 ferrets were inoculated intratracheally in 1-5 seconds under ketamine anesthesia with 10^6 $TCID_{50}$ of SARS-CoV. The animals were checked daily for clinical signs. At 4 dpi they were euthanized by exsanguination under ketamine anesthesia. Three cats and 3 ferrets were not inoculated and were used as negative controls.

Pathologic examination

The animals were necropsied according to a standard protocol by opening the thoracic and abdominal cavities and the skull and examining all major organs, including the brain. Samples were collected for histologic examination and were stored in 10% neutral-buffered formalin (lungs after inflation

with formalin), embedded in paraffin, sectioned at 4 µm, and stained with hematoxylin and eosin (HE) for examination by light microscopy. Selected lung sections also were stained with periodic acid Schiff (PAS) for detection of mucoid substances. The following tissues were examined by light microscopy: lung (cranial, middle, and caudal lobes of one lung), liver, spleen, kidney, trachea, urinary bladder, mesenteric lymph node, stomach (ferrets only), pancreas, duodenum, jejunum, ileum, and tracheo-bronchial lymph node. Semiquantitative assessment of SARS-CoV infection-associated inflammation in the lung was performed as reported earlier:[172] each slide was examined for inflammatory foci at 10x objective, and each focus was scored for size (1: smaller or equal than area of 10x objective, 2: larger than area of 10x objective and smaller than area of 2x objective, 3: larger than area of 2x objective) and severity of inflammation (1: mild, 2: moderate, 3: marked). Slides were examined without knowledge of the identity of the animals. The cumulative scores for the inflammatory foci provided the total score per animal.

Immunohistochemistry

Immunohistochemical examination on all tissues as examined by using light microscopy was performed as reported previously,[7] except that mouse anti-SARS-nucleocapsid IgG2a (clone Ncap4, Imgenex, San Diego, CA, USA) (0.3 µg/ml) and goat anti-mouse IgG2a (SouthernBiotech, Birmingham, AL, USA) were used as primary and secondary antibodies, respectively. Omission of the primary antibody or replacement of the primary antibody by an irrelevant mouse IgG2a antibody (clone 20102, R&D, Abingdon, UK) (0.3 µg/ml) were included as negative controls in each staining. The same tissues as mentioned above from non-infected cats and ferrets were used as negative controls. Lung sections from an experimentally inoculated ferret euthanized on 1 dpi were used as positive controls. Semiquantitative assessment of SARS-CoV antigen expression was performed as reported earlier:[172] 25 arbitrarily chosen 20x objective fields of lung parenchyma in each lung section were examined by using light microscopy for the presence of SARS-CoV antigen expression, without the knowledge of the identity of the animals. The cumulative scores for each animal were expressed as number of positive fields per 100 fields.

For double staining of SARS-CoV antigen and PAS positive material, staining for SARS-CoV antigen was performed as described above with the following modifications. Antigen retrieval was performed at 100 °C for 15 min with citric acid buffer, pH 6.0. Sections were cooled for 20 min on ice in the same buffer. To allow double staining, mouse anti-SARS-nucleocapsid IgG1 (Ncap17, Imgenex) (1.25 µg/ml) and biotin-labeled goat anti-mouse IgG1 (SouthernBiotech) were used as primary and secondary antibodies, respectively. After incubation with the secondary antibody, the labeled biotin was coupled to avidin-biotin-HRP complexes (DAKO, Heverlee, Belgium) for 1 hour at room temperature. Peroxidase activity was revealed by incubating slides in 3,3'–diamino-benzidine-tetrachlorhydrate (DAB) (Sigma, St Louis, MO, USA) for 3 to 5 min, resulting in a brown precipitate. After washing in PBS, slides were stained with PAS according to standard methods.

For detection of ACE2, tissue sections were pre-treated as described above and incubated with a rabbit polyclonal antibody to ACE-2 (Abcam, Cambridge, UK) (5 µg/ml) or rabbit IgG control (R&D) (5 µg/ml) in PBS/0.1% body surface aera (BSA) for 1 hour at room temperature. After washing with PBS, sections were incubated with HRP-labeled goat-anti-rabbit IgG (DAKO) in PBS/0.1% BSA for 1 hour at room temperature. Peroxidase activity was revealed by incubating slides in 3-amino-9-ethylcarbazole (AEC) (Sigma) for 10 min and counterstaining with hematoxylin.

To identify the ACE2 expression at the time of infection, we used the 3 non-infected cats and 3 non-infected ferrets, since spike protein binding during SARS-CoV infection results in down regulation of ACE2 expression.[199] For comparison of ACE2 expression and histological architecture of the tracheal submucosal glands among cats, ferrets and humans, archival human tracheal tissues of 3 individuals, without histologic lesions or evidence of respiratory tract infection at the time of death, also were stained with PAS and tested for ACE2 expression.

Immunofluorescence

For double staining of SARS-CoV antigen and keratin, 3-µm-thick, formalin-fixed, paraffin-embedded tissue sections were pre-treated as described above. Autofluorescence in the sections was blocked by incubation with 0.3 M glycine for 10 min. Sections were washed with PBS/0.05% Tween 20 and incubated with mouse IgG1 against human pankeratin AE1/AE3 (Neomarkers, Fremont, CA, USA) (8 µg/ml) for 1 hour at room temperature in the dark. After washing with PBS, sections were incubated with mouse IgG1 against SARS-CoV (clone Ncap17, Imgenex) (1.25 µg/ml) for 1 hour at room temperature in the dark. The pankeratin antibody was labeled with Zenon Alexa Fluor 488 Mouse IgG1 labeling kit (cat no. Z25090, Molecular Probes, Invitrogen, Breda, The Netherlands), according to the manufacturer's protocol. The SARS-CoV antibody was labeled by using a Zenon Alexa Fluor 594 Mouse IgG1 labeling kit (cat no. Z25007, Molecular Probes). The slides were mounted by using Vectashield, Hard Set with 4,6-diamidino-2-phenylindole (DAPI) (Vector, Burlingame, CA, USA).

Statistical analysis

One-way analysis of variance was used for comparing the scores of pulmonary lesions and viral antigen expression. Differences were considered significant at $P < 0.05$.

RESULTS

Clinical findings

The cats showed no clinical signs such as lethargy or dyspnea. The ferrets, however, became lethargic from 2 dpi onward, and one of these ferrets (No. 3) died at 4 dpi.

Gross examination

All 4 cats had multifocal pulmonary consolidation characterized by red, firm, level areas of approximately 1 cm in diameter in the cranial and medial lobes. Cat No. 4 had multifocal consolidation in all lung lobes. All 4 ferrets also had multifocal pulmonary consolidation similar to that in the cats, except that the foci were smaller, ranging from 0.1 to 1 cm in diameter, and were localized mainly in the caudal lobes. Ferret No. 2 also had dark red and enlarged mesenteric lymph nodes, and ferret No. 3 had a dark red, friable liver and a mottled, red-and-pink spleen. Other organs of the cats and ferrets showed no significant lesions.

Histology

The primary damage from SARS-CoV infection was seen in the respiratory tract in both cats and ferrets and was comparable in character and severity. In the cats, histologic lesions were seen in the lung, tracheo-bronchial submucosal glands, spleen, tracheo-bronchial and mesenteric lymph nodes,

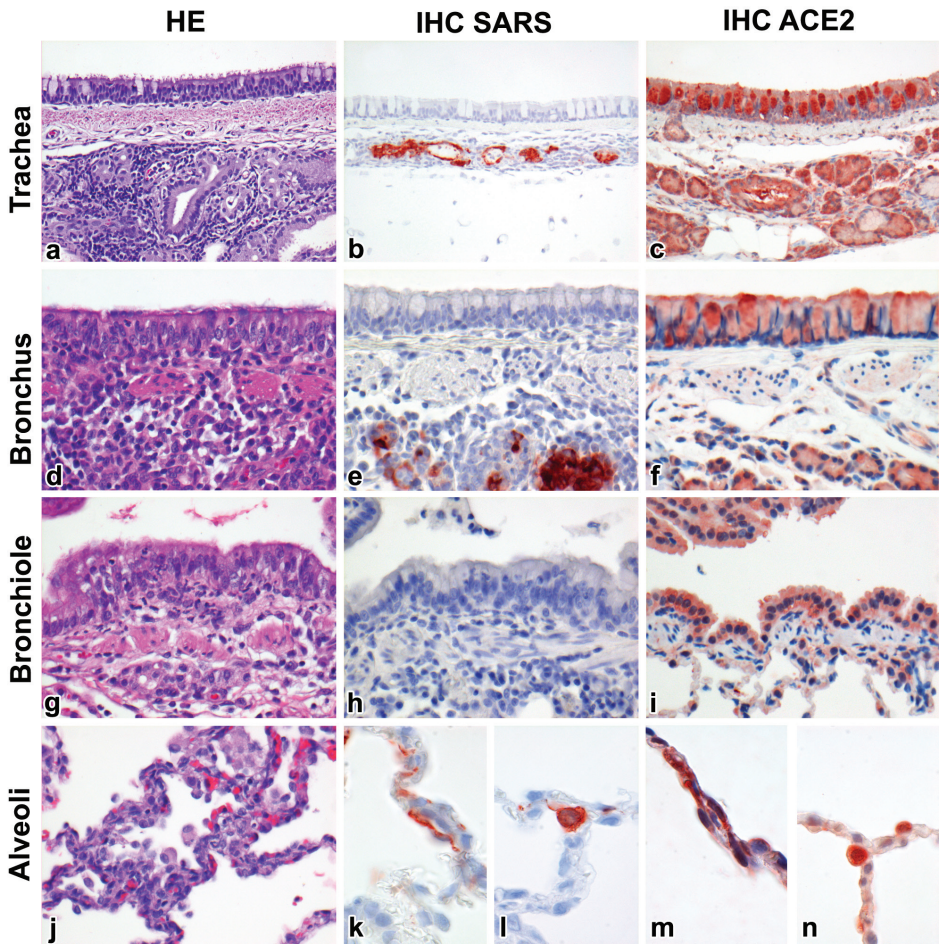

Figure 1. *Respiratory tract; histologic (HE) and immunohistochemical staining for SARS-CoV antigen and ACE2 (IHC) in SARS-CoV infected cats and control cats. Detailed descriptions can be found in the text. (a) Trachea cat. Moderate lymphoplasmacytic tracheoadenitis. (b) Trachea cat. SARS-CoV antigen expression in epithelial cells of submucosal glands. Immunoperoxidase with hematoxylin counterstain (IHC). (c) Trachea control cat. ACE2 expression in epithelial cells of mucosa and submucosal glands. (d) Bronchus cat. Moderate lymphoplasmacytic bronchoadenitis. (e) Bronchus cat. SARS-CoV antigen expression in epithelial cells of submucosal glands. (f) Bronchus control cat. ACE2 expression in epithelial cells of mucosa and submucosal glands. (g) Bronchiole cat. Mild lymphoplasmacytic and neutrophilic bronchiolitis. (h) Bronchiole cat. Lack of SARS-CoV antigen expression. (i) Bronchiole control cat. ACE2 expression in epithelial cells of mucosa. (j) Alveoli cat. Mild DAD. (k,l) Alveoli cat. SARS-CoV antigen expression in type I (k) and II (l) pneumocytes. (m,n) Alveoli control cat. ACE2 expression in type I (m) and II (n) pneumocytes.*

and Peyer's patches. In the lung, all cats had multifocal, mild to moderate, exudative DAD characterized by cellular debris in the alveolar lumen and epithelial cells with karyorrhexis, karyopyknosis and loss of cellular detail (multifocal necrosis), sparse type II pneumocyte hyperplasia, and infiltration with few neutrophils in the alveolar septa (Figure 1). In the lumina of terminal bronchioles and adjacent alveoli, there were few alveolar macrophages and neutrophils (Figure 1). In the tracheo-bronchial submucosal glands, all cats had multifocal mild to moderate

tracheo-bronchoadenitis (Figures 1, 2 and 3). This was characterized by multifocal epithelial necrosis in submucosal glands and by infiltration with moderate numbers of plasma cells and lymphocytes and with few macrophages and neutrophils in surrounding connective tissue. With PAS staining, these submucosal glands displayed narrow, empty lumina, a high proportion of serous cells compared to mucous cells, and mild granular PAS staining in mucous cells (Figure 3), which was also seen in non-infected cats. In cats Nos. 1 and 3, the spleen had moderate lymphoid hyperplasia, while tracheo-bronchial and mesenteric lymph nodes and Peyer's patches had both mild to moderate lymphoid hyperplasia and moderate to marked sinusoidal histiocytosis. No significant lesions were seen in other tissues examined or in the tissues of negative control cats.

In the ferrets, histologic lesions were seen in the lung, liver, spleen, and tracheo-bronchial lymph nodes. In the lung, all ferrets had multifocal, mild to severe, subacute, exudative DAD, characterized by variable numbers of alveolar macrophages and neutrophils, mixed with proteinaceous exudate in alveolar and bronchiolar lumina (Figure 4). The alveolar septa were moderately thickened with infiltrating neutrophils, macrophages and multifocal moderate epithelial necrosis. There was multifocal hyperplasia and hypertrophy of type II pneumocytes and bronchiolar epithelial cells. There was hyperplasia of bronchus-associated lymphoid tissue, and additionally, ferret No. 3 had lymphoid aggregates around pulmonary blood vessels. Overall, the severity of pulmonary lesions in the ferrets and cats showed no significant differences ($F = 0.48$, $P = 0.51$) (Figure 5). In the liver, all ferrets had mild diffuse hepatic lipidosis, while ferret No. 3 also had mild diffuse hepatic congestion and hemorrhage. The spleen and tracheo-bronchial lymph nodes of all ferrets showed mild lymphoid hyperplasia. In contrast to the cats, no significant lesions were seen in the tracheo-

Table 1. Expression of ACE2 and SARS-CoV antigen in the respiratory tract of cats, ferrets and humans with SARS

		Tissues and cell types												
		Alveolus			Bronchiole		Bronchus			Trachea			Pulmonary blood vessel	
Species	Antigen	Type I pneumocyte	Type II pneumocyte	Alveolar macrophage	Ciliated epithelial cell	Non-ciliated epithelial cell	Ciliated epithelial cell	Goblet cell	Glandular epithelial cell	Ciliated epithelial cell	Goblet cell	Glandular epithelial cell	Endothelial cell	Smooth muscle cell
Cat	ACE2	+++	+++	+	++	++	++	+++	+++	++	+++	+++	++	++
	SARS-CoV	+++	+++	+	+	-	+	-	+++	+	-	+++	-	-
Ferret	ACE2	-	+++	+	++	++	++	-	+++	++	-	+++	++	++
	SARS-CoV	-	+++	+	-	-	-	-	-	-	-	-	-	-
Human	ACE2213	++	+++	+	++	++	++	-	+++	++	-	+++	++	++
	SARS-CoV[14,36,52]	-	+++	+	-	-	-	-	-	-	-	-	-	-

NOTE: Abundance of ACE2 or SARS-CoV antigen expression: +++ = abundant; ++ = occasional; + = rare; - = absent.

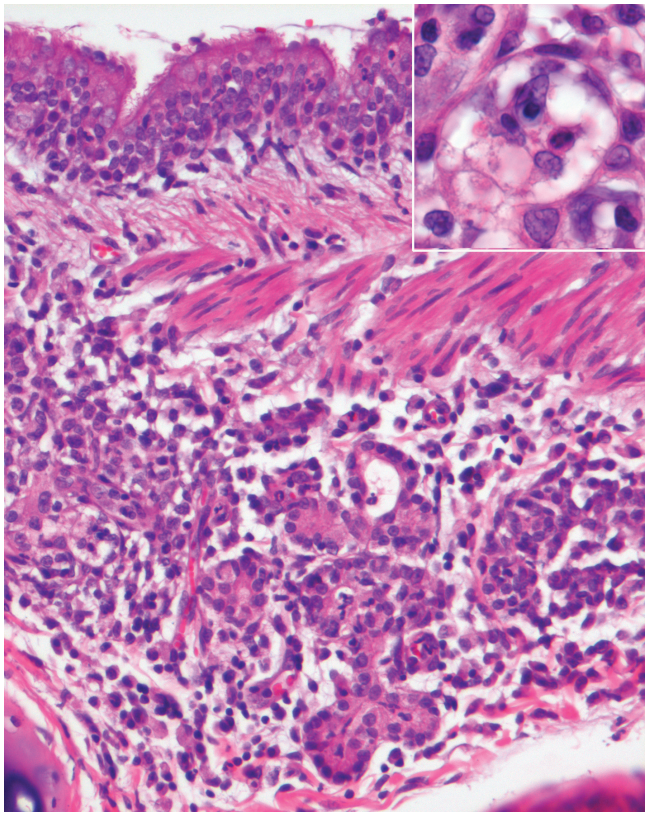

Figure 2. *Bronchus cat. Histologic staining of a bronchus in a cat infected with SARS-CoV. Moderate lymphoplasmacytic bronchoadenitis with mild necrosis of glandular epithelial cells. HE. Inset: Higher magnification of a submucosal gland with loss of epithelial cells.*

bronchial submucosal glands of the ferrets (Figure 3). PAS staining of these glands (in both infected and non-infected animals) showed wide lumina filled with PAS-positive material, a low proportion of serous cells compared to mucous cells, and intense, diffuse PAS-expression in mucous cells (Figure 3). No significant lesions were seen in other tissues examined or in the tissues of negative control ferrets.

In human tissues, the tracheal and bronchial submucosal glands had an almost equal mixture of serous and mucous cells. The lumina varied in size, and some were filled with large amounts of PAS-positive material.

SARS-CoV antigen expression

The cell types expressing SARS-CoV antigen, visible as diffuse red staining of the cytoplasm, differed between cats and ferrets (Table 1, Figures 1 and 4). In cats, SARS-CoV antigen expression was limited to the respiratory tract and the intestine. In the respiratory tract of all cats, SARS-CoV antigen expression was seen mainly in type I pneumocytes, type II pneumocytes, and serous cells of the tracheo-bronchial submucosal glands (Figure 1); occasionally in alveolar macrophages; and rarely in tracheal, bronchial, and (Cat No. 3 only) bronchiolar ciliated epithelial cells. The identity of SARS-CoV-antigen-positive type I and type II pneumocytes was based on their morphology (flat and cuboidal, respectively) and confirmed by double staining with pankeratin to exclude

macrophages (Figure 6). The identity of SARS-CoV-antigen-positive serous cells in the tracheobronchial submucosal glands was based on the central to paracentral round nucleus and finely granular cytoplasm. It was confirmed by double staining with PAS: serous cells showed no or only weak staining with PAS, in contrast to intense staining of mucous cells also present in these glands (Figure 3). In the other tissues, a few enterocytes in the ileum had expression of SARS-CoV antigen, but only in the intestine of cat No. 2.

In all ferrets, SARS-CoV antigen expression was limited to the respiratory tract, where it was seen mainly in type II pneumocytes (Figure 4), and rarely in type I pneumocytes and alveolar macrophages. Again, the identity of SARS-CoV-antigen-positive type I and type II pneumocytes was determined by their morphology and double staining with pankeratin (Figure 6). Neither ferrets nor cats had viral antigen expression in the other tissues. Virus antigen expression was present in positive tissue controls and absent in negative tissue as well as isotype and omission controls.

The expression of SARS-CoV antigen in the respiratory tract of both cats and ferrets was usually associated with the presence of histologic lesions. The level of SARS-CoV antigen expression in the lungs of ferrets and cats showed no significant differences ($F = 1.34$, $P = 0.29$) (Figure 5).

ACE2 expression

Expression of ACE2, visible as diffuse red staining of the cytoplasm and cell membrane, differed between the respiratory tract of cats and ferrets (Table 1, Figures 1 and 4). In cats, strong ACE2 expression was seen mainly in tracheal and bronchial goblet cells, serous epithelial cells of tracheobronchial submucosal glands, and type I and type II pneumocytes; moderate expression was seen in tracheal, bronchial, and bronchiolar ciliated cells, bronchiolar non-ciliated cells and mucous cells

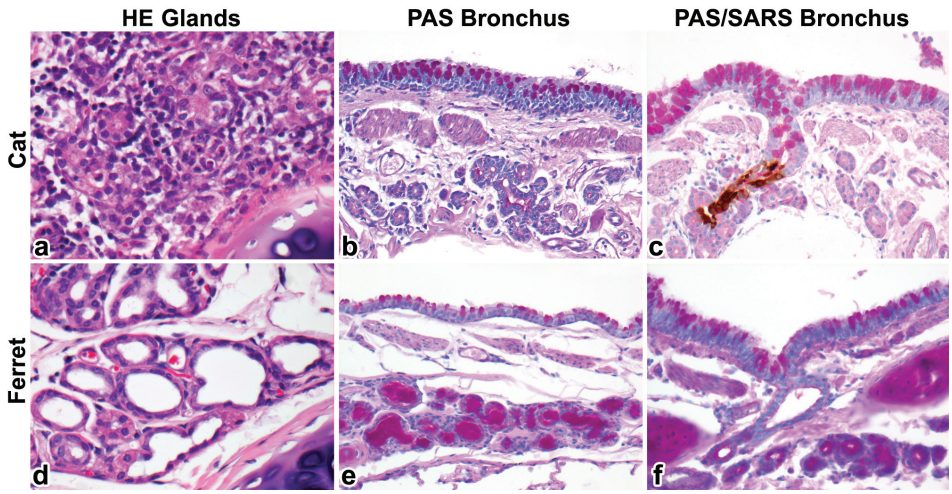

Figure 3. *Bronchus. Histologic (HE), histochemical (PAS) and immunohistochemical staining (SARS) of bronchi comparing cats and ferrets infected with SARS-CoV. (a) Cat. Moderate lymphoplasmacytic bronchoadenitis with mild necrosis of glandular epithelial cells. (b) Cat. Few PAS-positive cells in bronchial submucosal glands and scant mucus in acinar lumina. (c) Cat. SARS-CoV antigen expression in serous glandular epithelial cells. Double staining with PAS and immunoperoxidase. (d) Ferret. No lesions in bronchial submucosal glands. (e) Ferret. Many PAS-positive cells in bronchial submucosal glands and abundant mucus in acinar lumina. (f) Ferret. Lack of SARS-CoV antigen expression.*

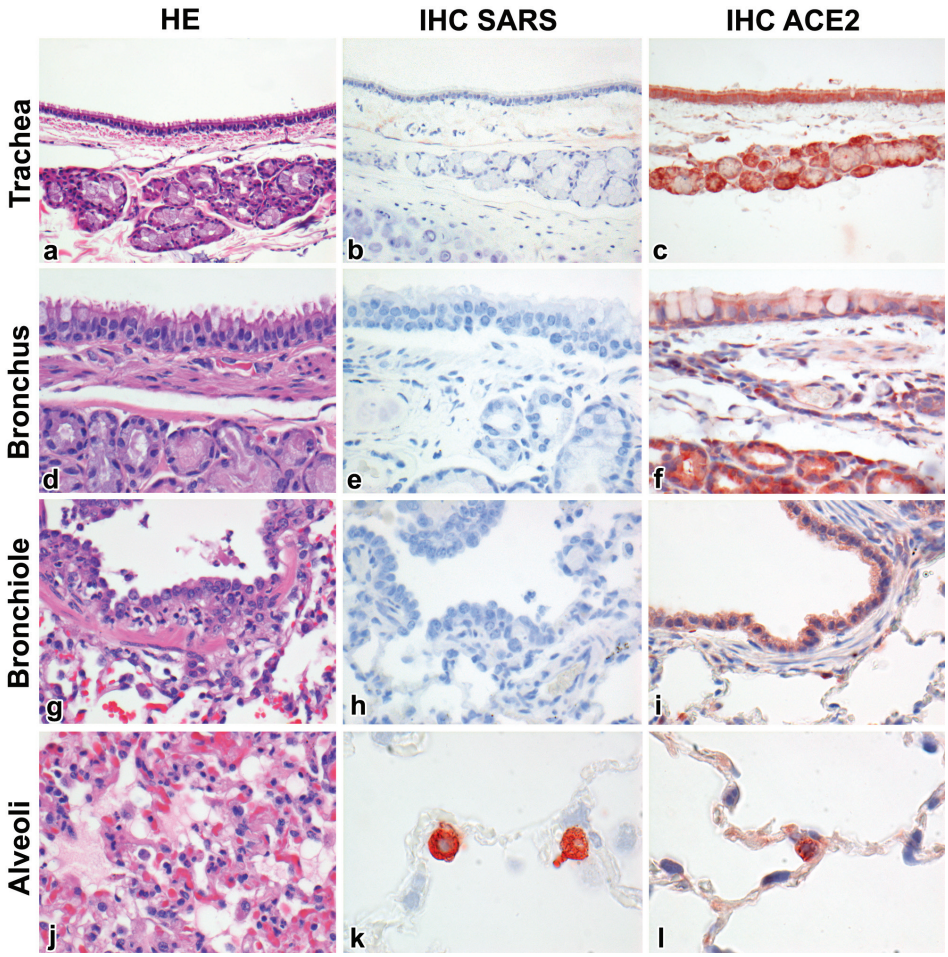

Figure 4. *Respiratory tract. Histologic (HE) and immunohistochemical staining for SARS-CoV antigen (IHC) and ACE2 in SARS-CoV-infected ferrets and control ferrets. Detailed descriptions can be found in the text. (a) Trachea ferret. No lesions. (b) Trachea ferret. Lack of SARS-CoV antigen expression. Immunoperoxidase with hematoxylin counterstain (IHC). (c) Trachea control ferret. ACE2 expression in epithelial cells of mucosa and submucosal glands. (d) Bronchus ferret. No lesions. (e) Bronchus ferret. Lack of SARS-CoV antigen expression. (f) Bronchus control ferret. ACE2 expression in epithelial cells of mucosa and submucosal glands. (g) Bronchiole ferret. Mild lymphoplasmacytic and neutrophilic bronchiolitis. (h) Bronchiole ferret. Lack SARS-CoV antigen expression. (i) Bronchiole control ferret. ACE2 expression in epithelial cells of mucosa. (j) Alveoli ferret. DAD with intraluminal protein. (k) Alveoli ferret. SARS-CoV antigen expression in type II pneumocytes. (l) Alveoli control ferret. ACE2 expression in type II pneumocytes.*

of the tracheo-bronchial submucosal glands (Figure 1); and weak expression was seen in alveolar macrophages. In addition, strong ACE2 expression was seen in endothelium and smooth muscle of pulmonary blood vessels. In ferrets, the pattern of ACE2 expression resembled that in cats, except that it was absent in type I pneumocytes and in tracheal and bronchial goblet cells (Figure 4). In human trachea, the ACE2 expression was stronger in serous cells than in mucous cells of mucosa and submucosal glands.

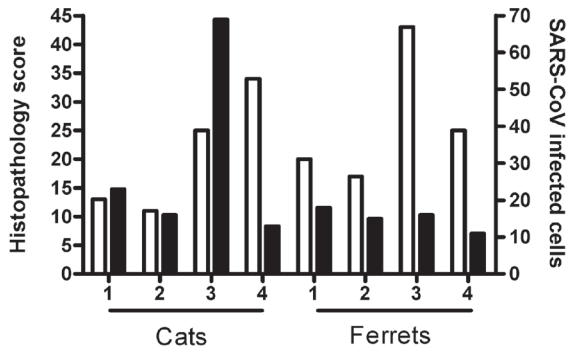

Figure 5. *Semi-quantitative scoring of histologic lesions (white bars) and SARS-CoV antigen expression (black bars) in the lung. These scores did not differ significantly between cats and ferrets.*

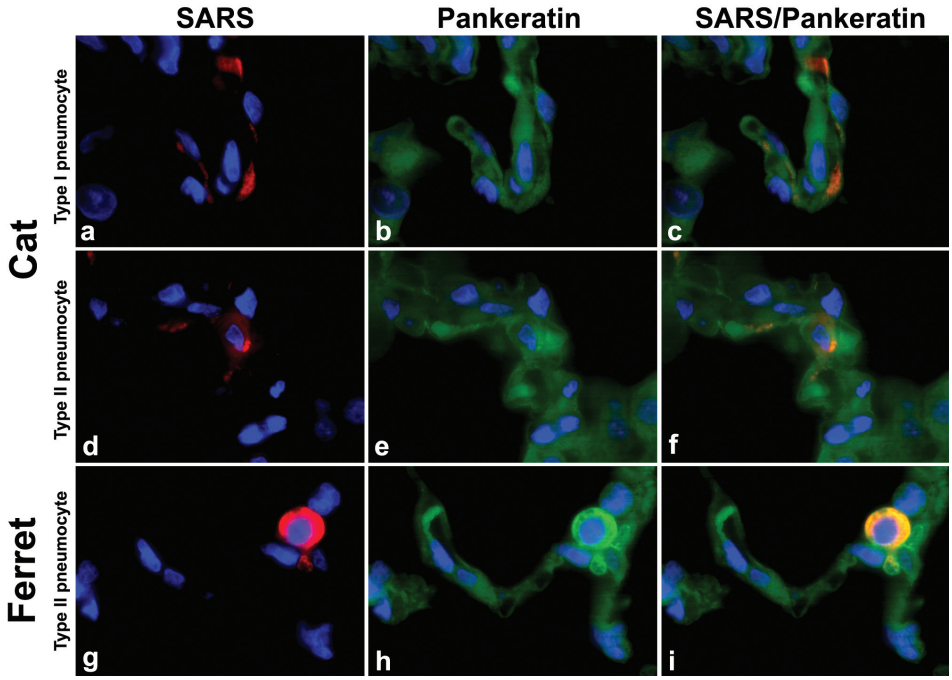

Figure 6. *Alveoli. Immunofluorescence double staining for SARS-CoV antigen and pankeratin in cats and ferrets infected with SARS-CoV antigen. (a) Cat. Type I pneumocyte with SARS-CoV antigen expression (red). (b) Cat. Type I pneumocyte with pankeratin expression (green). (c) Cat. Type I pneumocyte with co-localization of SARS-CoV antigen and pankeratin (orange). (d) Cat. Type II pneumocyte with SARS-CoV antigen expression (red). (e) Cat. Type II pneumocyte with pankeratin expression (green). (f) Cat. Type II pneumocyte with co-localization of SARS-CoV antigen and pankeratin (orange). (g) Ferret. Type II pneumocyte with SARS-CoV antigen expression (red). (h) Ferret. Type II pneumocyte with pankeratin expression (green). (i) Ferret. Type II pneumocyte with co-localization of SARS-CoV antigen and pankeratin (orange).*

DISCUSSION

The localization, character, and severity of respiratory tract lesions from acute SARS-CoV infection in cats and ferrets show both similarities to and differences from those in acute human cases.[32,34,36,37,210] First, the localization of the lesions in cats and ferrets is similar to that in humans: in all three species, the lesions affect mainly the alveoli and bronchioles. A clear difference is SARS-CoV-associated tracheo-bronchoadenitis, which we observed in cats, but has not been reported in humans. Second, the character of the lesions in alveoli and bronchioles of cats and ferrets shows some similarities to that of humans. In all three species, these lesions are characterized by necrosis and subsequent hyperplasia of alveolar and bronchiolar epithelium, infiltration by neutrophils, and increased numbers of alveolar macrophages. In humans and ferrets, proteinaceous exudate was seen in alveolar and bronchiolar lumina. A notable difference is the lack of syncytia in the pulmonary lesions of cats and ferrets, whereas this feature is considered characteristic for the disease in humans. Third, the severity of the lesions in cats and ferrets shows the most marked difference from that in humans. The pulmonary lesions in cats and ferrets are multifocal, in contrast to the more diffuse lesions in humans. Also, cats and ferrets lack fibrin exudation and hyaline membrane formation, both of which are features of severe damage to the alveolar septum, while these features are commonly reported for human SARS. However, these differences in severity are largely a reflection of the fact that pathologic reports of human SARS are generally limited to fatal cases, which only comprise about 10% of the total number of confirmed cases.[14] It is likely that many people who recovered from SARS had less severe respiratory tract lesions. Overall, this comparison suggests that SARS-CoV infections in cats and ferrets are suitable animal models to study the pathogenesis and pathology of human SARS in general. However, in their present form they do not replicate the lesions of fatal cases of human SARS. Adapting this virus to cats and ferrets might increase its pathogenicity as has been done for mice.[170]

Tracheo-bronchoadenitis caused by SARS-CoV infection is a novel finding, with potentially important implications for SARS pathogenesis and SARS-CoV excretion. Pathogenesis of SARS could be affected because the mucus produced by tracheo-bronchial submucosal glands is an important part of the mucociliary escalator that removes foreign material from the airways. Inflammation of these glands could reduce the efficiency of this defense system, thereby increasing the risk of lower respiratory tract infection by SARS-CoV and concurrent pathogens. Excretion of SARS-CoV might increase as a result of SARS-CoV infection of the tracheo-bronchial submucosal glands: virus secreted by these glands into the trachea and bronchi is more likely to be expectorated than virus produced lower in the respiratory tract.

The susceptibility of tracheo-bronchial submucosal glands to SARS-CoV infection shows clear host species differences, which may be relevant for human infection. Although the glands of both cats and ferrets expressed ACE2, only cat glands became infected and inflamed (Figures 1 and 2). One explanation may be that ferret glands lack a cofactor for SARS-CoV replication, as discussed above. Another explanation may be species differences in the histologic architecture of the tracheo-bronchial submucosal glands. The glands of ferrets had a higher proportion of mucous cells and more mucus in the acinar lumina than those of cats (Figure 3), and this may have inhibited the attachment of SARS-CoV to target cells. Therefore, we hypothesize that SARS-CoV infects mainly serous cells. To our knowledge, SARS-associated tracheo-bronchoadenitis has not been reported in humans. However, the expression of SARS-CoV antigen in the tracheal and bronchial submucosal

glands of fatal human cases[52] suggests that inflammation of these glands may be an as-yet-unreported feature of human SARS that requires further attention.

This study shows the importance of ACE2 expression for SARS-CoV infection *in vivo*. This is based on our observation that SARS-CoV antigen expression occurred only in ACE2-positive cells (Table 1, Figures 1 and 4). SARS-CoV S1 protein is reported to bind efficiently to both ferret and feline ACE2.[222,223] The importance of ACE2 expression is illustrated well by differences that we observed between cats and ferrets at the level of the alveoli: whereas cat type I pneumocytes abundantly expressed both ACE2 and SARS-CoV antigen, the absence of ACE2 expression in ferret type I pneumocytes corresponded with the absence of expression of SARS-CoV antigen (Figures 1 and 4). However, it must be realized that co-localization of ACE2 and SARS-CoV antigen expression is consistent with, but not proof of, a functional relationship. Also, several ACE2-positive cell types did not express SARS-CoV antigen (Table 1). Possible reasons for this could be that other receptors besides ACE2 are required for SARS-CoV attachment to the host cell, as is also described in humans.[46,224-226] For example, recent *in vitro* studies have shown that the presence of cathepsin L is required for productive SARS-CoV infection.[49,227] Alternatively, SARS-CoV may infect other cell types at an earlier or later stage of infection.

Alveolar macrophages in both cats and ferrets demonstrated weak expression of ACE2 and sparse expression of SARS-CoV antigen. This presence of SARS-CoV antigen indicates either virus infection of alveolar macrophages or, as is suggested for humans,[46,211] phagocytosis of viral antigen produced in other cells.

In conclusion, our study shows that SARS-CoV infections in cats and ferrets are suitable models for studying the pathology and pathogenesis of human SARS. We also have identified tracheobronchoadenitis in cats as a novel SARS-CoV-induced lesion, which could potentially occur in human SARS and affect the pathogenesis and virus excretion of this disease. Finally, we have shown *in vivo* that ACE2 expression is important for SARS-CoV infection and subsequent development of lesions in the respiratory tract.

Acknowledgments

We are grateful for the help of F. van der Panne with microphotographs and G. van Amerongen and R. Dias D'Ullois with animal experiments.

CHAPTER 2

SARS CORONAVIRUS INFECTION IN ANIMAL MODELS

2.3

Protective efficacy of MF59-adjuvanted SARS-CoV recombinant spike protein and inactivated whole virus vaccines in ferrets

Submitted

JMA van den Brand,[1] K Stadler,[2,5] BE Martina,[1] T Kuiken,[1] G van Amerongen,[1] ADME Osterhaus,[1,3] JB Ulmer,[4] and BL Haagmans[1]

Department of Virology, Erasmus Medical Center, Rotterdam, The Netherlands [1]
Novartis, Siena, Italy [2]
Viroclinics Biosciences BV, Rotterdam, The Netherlands [3]
Novartis Vaccines, Cambridge, MA 02139, USA [4]
Currently: Boehringer Ingelheim Vetmedica GmbH, 55216 Ingelheim am Rhein, Germany [5]

CHAPTER 2

SARS CORONAVIRUS INFECTION IN ANIMAL MODELS

2.4

SARS-CoV induces eosinophil infiltration in the lungs of macaques but not in those of ferrets immunized with an alum adjuvanted inactivated whole virus vaccine

In preparation

BL Haagmans,[1] JMA van den Brand,[1] F Boudet,[2] I Kusters,[2] TM Jourdier,[2] A de Lang,[1]
BEE Martina,[1] G van Amerongen,[1] T Kuiken,[1] JF Saluzzo,[2] ADME Osterhaus[1,3]

Department of Virology, Erasmus Medical Center, Rotterdam, The Netherlands [1]
Research Department Sanofi-Pasteur, Marcy-L'Etoile, France [2]
Viroclinics Biosciences BV, Rotterdam, The Netherlands [3]

CHAPTER 3

INFLUENZA VIRUS INFECTION IN ANIMAL MODELS

3.1

Pandemic 2009 H1N1 influenza virus causes diffuse alveolar damage in cynomolgus macaques

Veterinary Pathology (2010) 47(6): 1040-1047

S Herfst,[1,3] JMA van den Brand,[1,3] EJA Schrauwen,[1] E de Wit,[1,4] VJ Munster,[1,4]
G van Amerongen,[1] M Linster,[1] F Zaaraoui,[1] WFJ van Ijcken,[2] GF Rimmelzwaan,[1]
ADME Osterhaus,[1] RAM Fouchier,[1] AC Andeweg,[1] T Kuiken[1]

National Influenza Center and Department of Virology, Erasmus Medical Center, Rotterdam, [1]
The Netherlands
Erasmus Centre for Biomics, Rotterdam, The Netherlands [2]
These authors contributed equally to the results of this study [3]
Currently: Laboratory of Virology, Rocky Mountain Laboratories, [4]
National Institute of Allergy and Infectious Diseases, National Institutes of Health, Hamilton, Montana, USA

ABSTRACT

The pathogenesis of lower respiratory tract disease from the pandemic 2009 H1N1 (pH1N1) influenza A virus is poorly understood. Therefore, either pH1N1 virus or a seasonal human H1N1 influenza A virus was inoculated into cynomolgus macaques as a non-human primate model of influenza pneumonia, and virological, pathological, and microarray analyses were performed. Macaques in the pH1N1 group had virus-associated diffuse alveolar damage involving both type I and type II alveolar epithelial cells and affecting an average of 16% of the lung area. In comparison, macaques in the seasonal H1N1 group had milder pulmonary lesions. pH1N1 virus tended to be re-isolated from more locations in the respiratory tract and at higher titers than seasonal H1N1 virus. In contrast, differential expression of mRNA transcripts between pH1N1 and seasonal H1N1 groups did not show significant differences. The most up-regulated genes in pH1N1 lung samples with lesions belonged to the innate immune response and pro-inflammatory pathways and correlated with histopathological results. Our results demonstrate that the pH1N1 virus infects alveolar epithelial cells and causes diffuse alveolar damage in a non-human primate model. Its higher pathogenicity compared with a seasonal H1N1 virus may be explained in part by higher replication in the lower respiratory tract.

INTRODUCTION

The newly emerged influenza A virus of subtype H1N1 was declared pandemic as of June 11, 2009, and as of November 22 more than 622,482 confirmed cases had been reported world-wide (http://www.who.int/csr/don/2009_11_27a/en/index.html). The pandemic (H1N1) 2009 influenza virus (pH1N1 virus), probably originating from a swine reservoir,[96] has caused at least 7 826 confirmed deaths, mostly with a clinical diagnosis of atypical pneumonia or acute respiratory distress syndrome.[256] Influenza viruses may vary substantially in the human disease they cause.[106,125] The pathogenesis of pH1N1 virus infection in the human respiratory tract is largely unknown, as is the resultant damage compared with that caused by seasonal influenza viruses, which are well-adapted to their human host.

To establish a non-human primate model of influenza pneumonia, we inoculated either the pH1N1 virus or a seasonal human H1N1 influenza A virus (seasonal H1N1 virus) into cynomolgus macaques and performed virological, pathological, and microarray analyses. The cynomolgus macaque is a suitable species to model human pneumonia from infection by respiratory viruses, including HMPV,[257] SARS virus,[172] and influenza viruses.[148,258-260]

MATERIALS AND METHODS

Virus preparation

Influenza virus A/Netherlands/602/09 (pH1N1 virus) was isolated from a patient who had traveled from Mexico to the Netherlands and was the first laboratory-confirmed case of pH1N1 virus infection in the Netherlands. This virus was cultured from a nasopharyngeal swab in 11-day-old embryonated chicken eggs and subsequently passaged once in Madin-Darby Canine Kidney (MDCK) cells. The sequence of the virus that was used for inoculation of macaques was identical to that of the clinical isolate. This virus differs in 8 amino acid positions from influenza virus A/California/4/2009

(P100S, T214A and I338V in HA, I108V and V407I in NA, T373I in NP, P224S and M581L in PA; GISAID accession numbers EPI178246-250, EPI178467, EPI178290 and EPI178291). None of the differences map to known pathogenicity markers of influenza A virus. In fact, A/Netherlands/602/2009 is more representative (i.e., more consensus-like) than A/California/4/09; most amino acid changes in A/Netherlands/602/2009 compared with A/California/4/2009 were also found in the majority of sequenced strains in the database. The only unique sequence changes in A/Netherlands/602/2009 are I108V and V407I in neuraminidase, which can be considered conservative changes, not previously associated with virulence. Until now, the pH1N1 viruses have shown low genetic diversity and we consider the isolate used to be representative of the currently circulating pH1N1 virus. The seasonal H1N1 influenza virus A/Netherlands/26/07 (seasonal H1N1 virus) was isolated from a patient during the 2006-2007 influenza season and was subsequently passaged 3 times in MDCK cells.

Experimental protocol

Experiments were performed under biosafety level 3 conditions under an animal study protocol approved by the Institutional Animal Welfare Committee. Two weeks prior to infection, temperature loggers (DST micro-T ultra small temperature logger; Star-Oddi) that recorded the body temperature every 15 min, were placed in the peritoneal cavity of cynomolgus macaques under ketamine and domitor (medetomidine hydrochloride) anesthesia. Two groups of 4 macaques were inoculated with 1 x 10^7 median tissue culture infectious dose ($TCID_{50}$) of seasonal H1N1 virus or pH1N1 virus in 5 ml of phosphate buffered saline (PBS) (4 ml intra-tracheally and 1 ml intra-nasally) under ketamine and domitor anesthesia. Swabs were collected daily from macaques under ketamine anesthesia from nose and throat and placed in 1 ml of transport medium.[261] All macaques were euthanized 4 days after inoculation by exsanguination under ketamine anesthesia and were necropsied according to a standard protocol. Randomly collected lung tissue sections from 4 PBS (sham) inoculated age-matched cynomolgus macaques were used as control samples for below analyses.

Virus titration

Virus titers were determined in nose, throat and rectum swabs, and in the tissues collected during necropsy: nasal turbinate, tonsil, tracheobronchial lymph node, trachea, bronchus, lung, spleen, liver, kidney, jejunum, colon, duodenum, heart, eyelid, pancreas and brain. Tissue samples were weighed and subsequently homogenized with a FastPrep homogenizer (MP Biomedicals Europe, Illkirch, France) in 3 ml of transport medium. For lung, 4 samples of lung tissue collected from standard locations (cranioventral, craniodorsal, caudoventral and caudodorsal) in the right lung were pooled for each animal. Virus titrations were performed by end-point titration in MDCK cells. MDCK cells were inoculated with 10-fold serial dilutions of homogenized tissues, nose, throat, or rectum swabs. One hour after inoculation, cells were washed once with PBS and grown in 200 µl of infection media, consisting of EMEM (Lonza, Breda, The Netherlands) supplemented with 100 U/ml penicillin, 100 µg/ml streptomycin, 2 mM glutamine, 1.5mg/ml sodium bicarbonate (Cambrex), 10 mM Hepes (Lonza), non-essential amino acids (MP Biomedicals Europe) and 20 µg/ml trypsin (Cambrex). Three days after inoculation, the supernatants of infected cell cultures were tested for agglutinating activity using turkey erythrocytes as an indicator of infection of the cells. Infectious titers were calculated from 5 (homogenized tissues) or 4 (swabs) replicates by the method of Spearman-Karber.[262]

Histopathological examination and immunohistochemistry

Samples for histological examination were stored in 10% neutral-buffered formalin (lungs after inflation with formalin), embedded in paraffin, sectioned at 4 µm, and stained with hematoxylin and eosin (HE) for examination by light microscopy. Selected lung sections also were stained with periodic acid-Schiff (PAS) for detection of mucoid substances. The following tissues were examined by light microscopy: left lung (cranial, medial and caudal lobe), nose, nasal turbinates, nasal septum, larynx, trachea, bronchi, tracheobronchial lymph node, eyelid, tonsil, heart, liver, spleen, kidney, pancreas, duodenum, jejunum, colon, adrenal gland, and brain.

Semiquantitative assessment of influenza A virus-associated inflammation in the lung was performed as reported earlier.172 Briefly: each slide was examined for inflammatory foci at 10x objective, and each focus was scored for size and severity of inflammation in different areas of the lung. For the size of the inflammatory focus in the alveoli we used 1, smaller or equal than area of 10x objective; 2, larger than area of 10x objective and smaller than area of 2x objective; 3, larger than area of 2x objective. For the severity of inflammation we scored 1, mild (few inflammatory cells); 2, moderate (moderate numbers of inflammatory cells and/or mild necrosis and edema with erythrocytes); 3, marked (many inflammatory cells and/or necrosis and edema with inflammatory cells). Slides were examined without knowledge of the identity of the animals. The cumulative s cores for the inflammatory foci provided the total score per animal.

Sequential slides were used for detection of influenza A virus nucleoprotein in tissues as described before.[259] Endogenous peroxidase was blocked with 3% hydrogen peroxide. Lung sections from a domestic cat with experimental avian H5N1 influenza virus infection were used as positive controls. Semiquantitative assessment of influenza virus antigen expression in the lungs was performed as follows: for assessment of alveoli, 100 arbitrarily chosen 20x objective fields of lung parenchyma in all lung sections were examined by light microscopy for the presence of influenza virus antigen expression without the knowledge of the identity of the animals. The scores for each animal were presented as number of positive fields per 100 fields (%).

For detection of pankeratin in lung tissues of a pH1N1 infected macaque, 3-µm formalin-fixed, paraffin-embedded sections were deparaffinized and rehydrated to distilled water. Antigen retrieval was performed at 100°C for 15 minutes with citric acid buffer pH 6.0. Slides were cooled for 20 minutes on ice in the same solution. After washing with PBS endogenous peroxidase was blocked with 3% hydrogen peroxidase. The slides were briefly washed with 0.05% PBS Tween 20 and incubated with a mouse IgG1 antibody against human pankeratin AE1/AE3 (Neomarkers, Fremont, CA) (2 µg/ml) or mouse IgG1 isotypecontrol (R&D Systems Europe, Abingdon, UK) (2 µg/ml) in PBS/0,1% BSA for 1 hour at room temperature. After washing, sections were incubated with horseradish peroxidase labeled goat-anti-mouse IgG1 (Southern Biotech) (5 μg/ml) in PBS/0,1% BSA for 1 hour at room temperature. Horseradish peroxidase activity was revealed by incubating slides in 3-amino-9-ethylcarbazole (AEC) (Sigma) for 10 minutes, resulting in bright red precipitate, followed by counterstaining with hematoxylin.

Microarrays

One sample of lung tissue without macroscopically visible pathologic changes (non-lesional) and—if present—1 sample of lung tissue with macroscopically visible pathologic changes (lesional) were randomly selected from the right lung of each animal. Lesional lung samples for microarray were only available from 1 of 4 macaques infected with seasonal H1N1 virus because of the limited area

of lung affected. Also, 1 of 4 non-lesional lung samples from macaques infected with pH1N1 virus was not retained for analysis. Lung tissue samples were collected in RNAlater (Ambion), and total RNA was isolated and purified using Trizol Reagent (Invitrogen) and the RNEasy mini kit (Qiagen), respectively. RNA was subsequently labeled using the One-Cycle Target Labeling kit (Affymetrix) and hybridized onto Affymetrix GeneChip Rhesus Macaque Genome Arrays (Affymetrix), according to the manufacturer's recommendations. Image analysis was performed using Gene Chip Operating Software (Affymetrix). Data was preprocessed for background correction and normalized using variance stabilization.[177] Transformed probe values were summarized into 1 value per probe set by the median polish method (part of the Robust Multiarray Averaging [RMA] method). Probe set wise comparisons between the experimental conditions were performed by limma,[179] which is similar to analysis of variance. Correction for multiple testing was achieved by requiring a false discovery rate (FDR) of 0.05, calculated with the Benjamini-Hochberg procedure. Further downstream processing and interpretation of data including cluster analysis, visualization and pathway analysis was performed using Spotfire DecisionSite 9.1 for Functional Genomics (Spotfire Inc) and Ingenuity Pathways Knowledge Base (Ingenuity Inc). Hierarchical cluster analysis (single linkage) was performed with a set of transcripts identified as being differentially regulated in at least 1 of the 6 direct comparisons with a FDR ≤ 0.05 and 2log-fold change ≥ 1 threshold.

Statistical analysis

Data were compared using the Mann-Whitney test (affected lung area, histopathology score, percentage virus-infected cells, virus titers in different postmortem tissues). Differences were considered significant at $P < 0.05$.

RESULTS

Upon experimental inoculation with the pH1N1 virus, viral loads in throat swabs increased progressively in the pH1N1 group between 1 and 4 days post inoculation (dpi), when the mean titer was 2.8 log $TCID_{50}$ per ml (Figure 1A). In contrast, viral loads peaked on 2 dpi at a lower level of 1.6 log $TCID_{50}$ per ml in the seasonal H1N1 group. Virus was detected sporadically in nasal swabs of animals from both groups and could only be demonstrated in rectal swabs of 1 animal in each group at 4 dpi. The body temperature in the pH1N1 group peaked at 1 dpi and decreased in the following two days (Figure 1B). The body temperature in the seasonal H1N1 group followed a similar trend, but peaked at about 0.3 °C lower. One of the macaques from the pH1N1 group was lethargic at 4 dpi.

On necropsy at 4 dpi, the macaques in the pH1N1 group had focal or multifocal pulmonary consolidation and enlarged tracheobronchial lymph nodes. No lesions were seen in the extra-respiratory tissues. Histologically, pulmonary consolidation corresponded with diffuse alveolar damage (DAD) (Figures 2 and 3). This DAD was characterized by flooding of highly proteinaceous fluid into alveolar lumina (Figures 2 and 3) with rare PAS-positive hyaline membranes (Figure 3), necrosis of alveolar epithelial cells, and accumulation of many neutrophils and alveolar macrophages (Figures 2 and 3). Necrosis of alveolar epithelial cells was demonstrated by a partial loss of pankeratin-expressing pneumocytes. Other lesions were moderate bronchiolitis, characterized by epithelial necrosis and peribronchiolar infiltration with moderate numbers of macrophages and lymphocytes, and few plasma cells, neutrophils and eosinophils. There were mild bronchitis and

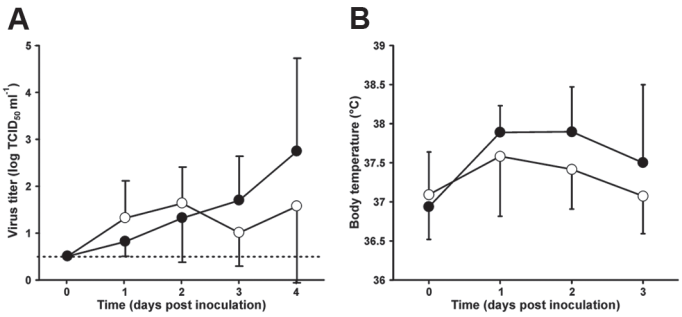

Figure 1. *(A) Pharyngeal viral loads (mean ± standard deviation) in the pH1N1 (black circles) (n = 4) and seasonal H1N1 groups (white circles) (n = 4). Horizontal dotted line indicates detection limit. (B) Body temperature (mean ± standard deviation) in the pH1N1 (black circles) and seasonal H1N1 groups (white circles).*

tracheitis, with epithelial necrosis and moderate numbers of neutrophils, macrophages and lymphocytes and a few plasma cells and eosinophils in the lamina propria and submucosa. In addition, there was a mild rhinitis, characterized by mild epithelial necrosis and a few neutrophils, macrophages and lymphocytes, and there were rare plasma cells and eosinophils in the lamina propria. The macaques in the seasonal H1N1 group had significantly fewer extensive pulmonary lesions than in the pH1N1 group (Figure 4). The alveoli had no flooding with edema fluid, only mild necrosis and fewer inflammatory cells. These inflammatory cells were a few neutrophils, macrophages, lymphocytes, and plasma cells that were located predominantly in the alveolar septa. Neither group had histological lesions in any of the extra-respiratory tissues.

By immunohistochemistry, all 4 macaques in the pH1N1 group expressed influenza virus antigen in alveolar epithelial cells, both type I pneumocytes (77 of 100 positive cells counted) and type II pneumocytes (23 of 100 positive cells counted), in or at the edges of the alveolar lesions (Figure 2). Except for a few epithelial cells in larynx and nasal septum of one macaque, influenza virus antigen expression was absent in other tissues in the pH1N1 group. There was no expression of influenza virus antigen in any tissues of the seasonal H1N1 group (Figure 2). Neither lesions nor expression of influenza virus antigen were observed in sham-inoculated macaque lungs (Figure 2). The macaques in the seasonal H1N1 group had significantly fewer severe pulmonary lesions (Figure 2), lacking edema fluid, with less necrosis and fewer inflammatory cells.

Virus was isolated from the respiratory tract and tonsils, whereas other tissues tested negative. In the pH1N1 group, virus was isolated from all 4 macaques, and positive tissues were nose, trachea, bronchus, lung, and tonsil. In the seasonal H1N1 group, virus was isolated from 2 of 4 macaques, and positive tissues were nose, lung, and tonsil. Viral titers, particularly in the lungs, tended to be higher in the pH1N1 group than in the seasonal H1N1 group (Figure 4).

Microarray analysis followed by hierarchical clustering of messenger RNA (mRNA) expression profiles revealed 3 clusters: samples of sham-infected lungs (controls), samples of lungs without lesions (non-lesional), and samples of lungs with lesions (lesional) (Figure 5). Cluster analysis did not separate samples of the pH1N1 and the seasonal H1N1 groups. Limma analysis179 identified almost 3,000 mRNA transcripts differentially expressed between pH1N1 lesional and control samples (FDR ≤ 0.05 and a 2log-fold change ≥ 1) and about 600—which largely overlapped—between non-lesional (both pH1N1 and seasonal H1N1) and control samples (Figure 6A). About 1,500 transcripts between lesional and non-lesional (both pH1N1 and seasonal H1N1) samples were differentially expressed, but only 3 between non-lesional samples of the pH1N1 and seasonal H1N1 groups (data not shown). Collectively, cluster and limma analyses showed that lung samples

with the same gross pathology exhibited virtually identical mRNA expression profiles, lesional samples differing significantly from non-lesional ones.

The top 35 upregulated genes in pH1N1 lesional samples mostly belonged to innate immune response and proinflammatory pathways (Figure 6B) and correlated with histopathology. For example, the high mRNA expression for CCL2, CCL3, CCL8, CXC10, IL8, and CXCL1—known chemoattractants for neutrophils and monocytes—corresponded with the abundance of these cell types in lesional samples (Figure 2). Pathway analysis (Ingenuity) of the differentially expressed genes showed profiles (Figure 7) similar to those observed previously in macaque influenza virus infections.[263]

DISCUSSION

We here show that the pH1N1 virus is found throughout the respiratory tract of macaques with a predilection for the lung, infecting alveolar epithelial cells and causing diffuse alveolar damage (Figure 2). Furthermore, we show by semi-quantitative analysis that pH1N1 virus causes significantly more severe pulmonary lesions than seasonal H1N1 virus in macaques (Figure 4). This corresponds with an earlier study where qualitatively more severe lung lesions were observed in macaques infected with an early U.S. isolate of pH1N1 virus, A/California/04/09, than in those infected with a recent human H1N1 virus.[264] Samples for microarray analysis were obtained at 1

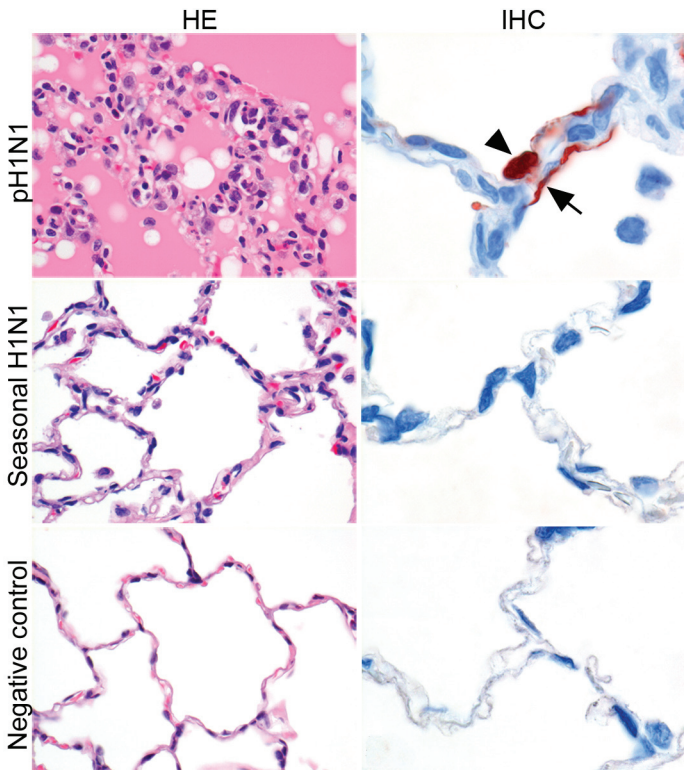

Figure 2. *Lung. Histologic and immunohistochemical staining for virus antigen in pH1N1- and seasonal H1N1-infected macaques and control macaques. First row: Alveoli of a macaque infected with pH1N1 show alveolar edema and infiltration by neutrophils and macrophages in alveolar lumina (HE) and influenza virus antigen expression in type I (arrow) and type II (arrow head) pneumocytes (IHC; Immunoperoxidase with hematoxylin counterstain). Second row: Alveoli of a macaque infected with seasonal H1N1 show no edema and fewer inflammatory cells and lack of influenza virus antigen. Third row: Alveoli of a negative control macaque.*

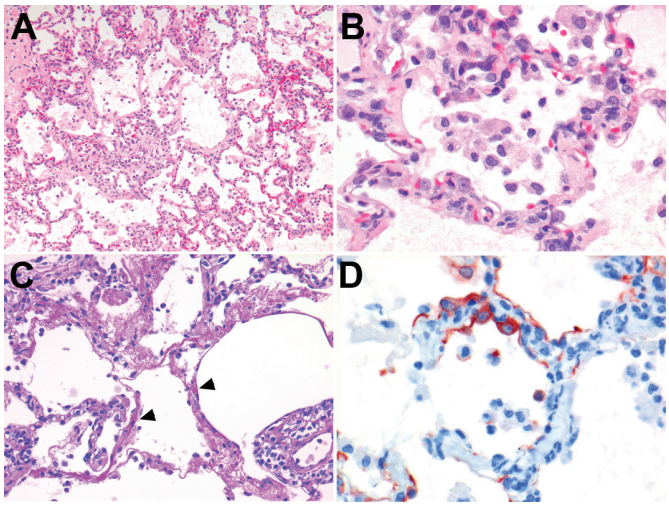

Figure 3. *(A) Lung of a macaque infected with pH1N1. Alveolar edema and accumulation of inflammatory cells. HE. (B) Lung of a macaque infected with pH1N1. Alveolar lumina with edema, fibrin, and accumulation of inflammatory cells, and alveolar septa with necrosis and infiltration of inflammatory cells. HE. (C) Lung of a macaque infected with pH1N1. PAS-positive hyaline membranes in the alveolar lumina (arrow heads). PAS. (D) Lung of a macaque infected with pH1N1. Loss of alveolar epithelium in a part of the alveolus, demonstrated by partial loss of pankeratin staining (red). Horseradish peroxidase with hematoxylin counterstain.*

time point post infection only and, unfortunately, lesional lung samples could only be collected from 1 animal inoculated with seasonal H1N1 virus and 3 animals with pH1N1 virus. Given this limitation, similar mRNA expression profiles between the more severely affected lungs in the pH1N1 virus infection and those in the seasonal H1N1 virus infection (Figure 5) do not suggest an intrinsically different molecular pathogenesis. Instead, the more severe pulmonary lesions are associated with more abundant virus in the lower respiratory tract by immunohistochemistry (Figure 4).

Diffuse alveolar damage, as observed in the macaques infected with the pH1N1 virus, is the pathological correlate of acute respiratory distress syndrome,[265] as diagnosed clinically in people who died with pH1N1 virus infection.[256] The character of the lesions and the cell types targeted in the alveoli of the macaques is qualitatively similar to those found at autopsy of people dying from rapidly progressive pneumonia during the influenza pandemics of 1918, 1957, and 1968.[106]

Interestingly, the predilection of the pH1N1 virus to infect type I pneumocytes of cynomolgus macaques corresponds more to the attachment pattern of avian influenza viruses than of human influenza viruses. In virus histochemistry studies, we found that avian influenza viruses attach mainly to type I pneumocytes in the macaque lung, whereas human influenza viruses show little or no attachment at all.[124,125,125] A possible explanation for this apparent discrepancy is given by a recent carbohydrate microarray study.[266] In this study, 2 pH1N1 viruses bound not only to the majority of α-2-6-linked sialyl sequences -"human-type" oligosaccharide receptors—but also to a considerable range of α-2-3-linked sialyl sequences—"avian-type" oligosaccharide receptors. This was in contrast to a seasonal human H1N1 virus, which bound exclusively to α-2-6-linked sialyl sequences. This suggests that pH1N1 virus is able to attach both to human-type and to avian-type oligosaccha-

ride receptors and may explain, at least in part, the higher virus replication and severity of lesions in macaque lungs than observed with seasonal H1N1 virus infection.

The pH1N1 virus causes milder clinical signs and lesions in cynomolgus macaques than either avian H5N1 virus[148,259] or 1918 H1N1 virus.[267] By histopathology, this was shown mainly by less extensive edema, inflammation, and necrosis in the lung parenchyma. These differences mirror those

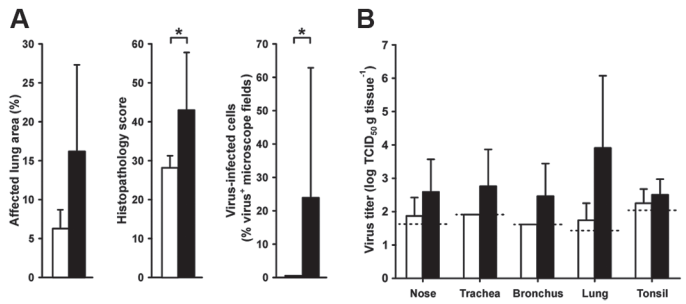

Figure 4. *(A) The percentage affected area, histological score, and virus-infected cells (mean ± standard deviation) in the lungs of the pH1N1 (black bars) and seasonal H1N1 groups (white bars). The histological score was based on the size and severity of inflammatory foci in different areas of the lung. Virus-infected cells were calculated as the percentage of microscope fields showing influenza virus antigen expression. * P = 0.04 and 0.03, respectively. (B) Viral loads in respiratory tract tissues of the pH1N1 (black bars) and seasonal H1N1 groups (white bars) (mean ± standard deviation). Horizontal dotted line indicates detection limit. This differs per tissue because of variation in sample weights.*

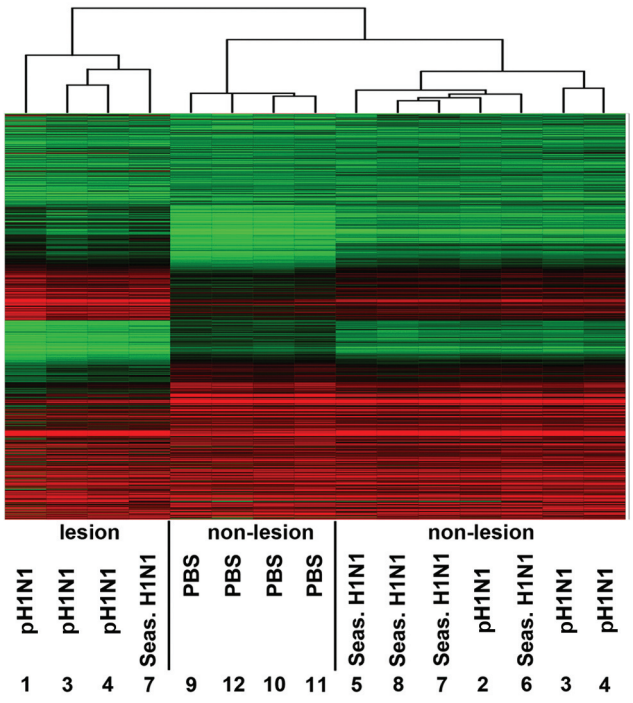

Figure 5. *Cluster analysis of gene expression profiles from lesional and nonlesional lung samples from macaques infected with pH1N1 virus or seasonal H1N1 virus. Hierarchical clustering of 15 gene expression profiles reveals 3 clusters. Normalized absolute hybridization signals ranged from 2^4 (green) to intermediate (2^8, black) and peaked at 2^{13} (red).*

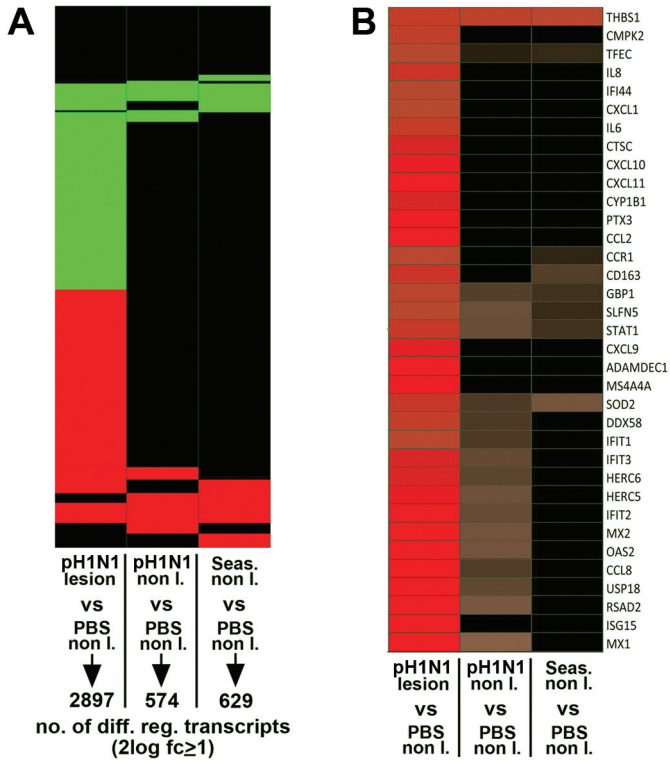

Figure 6. *(A) Limma analysis shows more up-regulated (red) or down-regulated (green) mRNA transcripts between pH1N1 lesional samples and control samples than between non-lesional (both pandemic and seasonal H1N1) samples and control samples. Transcripts that are not differentially regulated are represented in black. (B) The 35 most up-regulated genes in lesional samples of the pH1N1 group compared to control samples often belong to pathways of innate immune response and inflammation. Only a small proportion of these genes were up-regulated in non-lesional samples from the pH1N1 or seasonal H1N1 groups. Differential expression levels (2log) for these genes ranged from 0 (black) to 4.5 (red).*

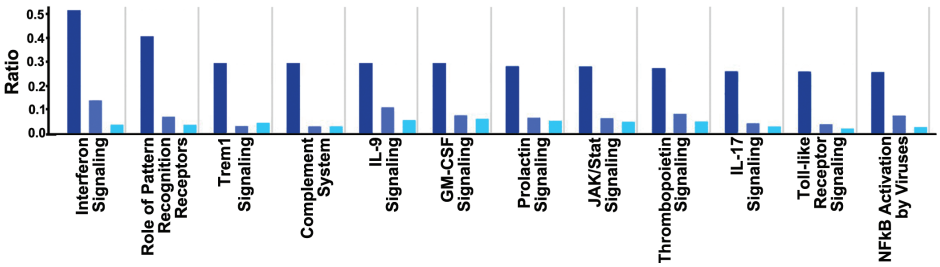

Figure 7. *Top 12 most significant (largest p value < 10^{-6}) and relevant differentially expressed molecular pathways for pH1N1 lesional samples (Ingenuity Pathways Knowledge Base). The y-axis depicts the fraction (ratio) of the genes assigned to a particular pathway that were differentially regulated (limma analysis, FDR ≤ 0.05, 2log-fold change ≥ 1). The dark, intermediate, and light blue bars refer to the comparative pathway analysis of pH1N1 lesional samples, pH1N1 non-lesional samples, and seasonal H1N1 non-lesional samples with control samples.*

of case fatality rates in humans from these respective infections.[268,269] Changes in the pathogenicity of the pH1N1 virus as it further adapts to its new human host need to be followed closely, because adaptation may involve increased or decreased pathogenicity. Increased pathogenicity may have occurred during the 1918-1919 influenza pandemic, when a first wave of mild disease was succeeded by one with higher disease impact and mortality.[270] Decreased pathogenicity may occur if the pH1N1 loses its ability to bind to α-2-3-linked sialosaccharides and therefore has less ability to infect the lower part of the respiratory tract.[266]

The absence of influenza virus antigen expression in the trachea and bronchi of the pH1N1 group contrasts with the results in ferrets infected with the same virus, where tracheal and bronchial epithelial cells showed abundant influenza virus antigen expression.[152] One possible explanation is differences in pattern of virus attachment between these 2 species: human influenza viruses attach more abundantly to tracheal and bronchial epithelium of ferrets than of macaques.[125] Another possible explanation is the different route of inoculation in the 2 experimental infections: intranasal in ferrets versus intratracheal in macaques.

The absence of influenza virus antigen expression in respiratory tract tissues of the seasonal H1N1 group is likely due to the lower virus titers that were present in the respiratory tract samples from animals inoculated with seasonal H1N1 virus, compared to the pH1N1 virus inoculated animals (Figure 4). The lack of virus antigen expression in tissues where virus was cultured may be due to the low quantity of viral antigen present that is below the detection limit of the immunohistochemical method. Recent pathogenesis studies in ferrets revealed comparable results in which pH1N1 virus could be detected in the trachea and lung 3 dpi, whereas no virus could be detected in these organs in animals that were inoculated with seasonal H1N1.[152]

We show here that the pH1N1 virus infects alveolar epithelial cells in a non-human primate model, resulting in diffuse alveolar damage that correlates with the clinical observations of acute respiratory distress syndrome in fatal human cases. Comparison with macaques infected by a seasonal human influenza virus, which is well adapted to its human host, shows that the newly emerged H1N1 virus causes more severe lung damage, which is associated with the presence of more virus in the lung parenchyma.

Acknowledgments

We thank T. Bestebroer, L. Leijten, M. Bijl, F. van der Panne, and P. van Run for assistance.

CHAPTER 3

INFLUENZA VIRUS INFECTION IN ANIMAL MODELS

3.2

Severity of pneumonia due to pandemic H1N1 Influenza Pneumonia in Ferrets is Intermediate between that due to Seasonal H1N1 Virus and Highly Pathogenic Avian Influenza H5N1 Virus

Journal of infectious disaeses (2010) 201: 993-999

JMA van den Brand,[1] KJ Stittelaar,[2] G van Amerongen,[1] GF Rimmelzwaan,[1,2] J Simon,[2] E de Wit,[1] V Munster,[1] T Bestebroer,[1] RAM Fouchier,[1] T Kuiken,[1] ADME Osterhaus[1,2]

Department of Virology, Erasmus Medical Centre, Rotterdam, The Netherlands [1]
Viroclinics Biosciences BV, Rotterdam, The Netherlands [2]

ABSTRACT

The newly emerged influenza A H1N1 virus (pH1N1 virus) is causing the first influenza pandemic of this century. Three influenza pandemics of the previous century caused variable mortality, which largely depended on the development of severe pneumonia. However, the ability of the pH1N1 virus to cause pneumonia is poorly understood. Therefore, the pH1N1 virus was inoculated intra-tracheally into ferrets. Its ability to cause pneumonia was compared with that of seasonal influenza H1N1 virus and highly pathogenic avian influenza (HPAI) H5N1 virus by clinical, virological, and pathological analyses. Our results showed that the pH1N1 virus causes pneumonia in ferrets intermediate in severity between that of seasonal H1N1 virus and HPAI H5N1 virus. The pH1N1 virus replicated well throughout the lower respiratory tract and more extensively than did both seasonal H1N1 virus (which replicated mainly in the bronchi) and HPAI H5N1 virus (which replicated mainly in the alveoli). High loads of pH1N1 virus in lung tissue were associated with diffuse alveolar damage and mortality. Therefore, the pH1N1 virus may be intrinsically more pathogenic for humans than is seasonal H1N1 virus.

INTRODUCTION

A new influenza A virus of the subtype H1N1 (pH1N1 virus) that first emerged in Mexico at the beginning of 2009 is the first pandemic human influenza virus of the 21st century. Studies have concluded that this virus probably originated from a domestic swine reservoir on the basis of its genetic signature.[96,271] On 11 June 2009, the World Health Organization declared phase 6 of the global pandemic alert level.[272] As of 25 August 2009, more than 182.166 cases, including 1799 deaths, in 177 countries have been officially reported.[256]

The main concerns about a new influenza pandemic are the disease burden and associated mortality it may cause. These are largely due to pneumonia resulting from extension of the viral infection to the lower respiratory tract. The initial lung damage may be complicated by concomitant or subsequent bacterial pneumonia, which has been shown to be a major cause of mortality during the Spanish flu in 1918, before the use of antibiotics.[273] In the current outbreak of pH1N1, bacterial co-infection was registered in only 20% of the cases investigated.[274] In contrast to the damage caused by the virus infection to the tracheo-bronchial epithelium in uncomplicated influenza, damage to the alveolar epithelium has severe consequences for the gas exchange function of the respiratory tract. It allows fluid from the alveolar capillaries to flood the alveolar lumina, causing severe, and in some cases fatal, respiratory dysfunction.[119]

On the basis of the observed relatively low case fatality rate in humans, it is assumed that the virulence of the pH1N1 virus is low. However, it is acknowledged that these Figures are uncertain because of too limited data.[275] Therefore, the potential of the pH1N1 virus to cause lower respiratory tract disease in humans is still poorly understood. In a previous publication, we used intranasal inoculation of influenza virus into ferrets mainly to model the transmission of the pH1N1 virus in humans.[152] Here, we use intra-tracheal inoculation of influenza virus into ferrets as a model of influenza pneumonia in humans. This intra-tracheal route of inoculation is an appropriate model of infection in humans, which is commonly thought to occur through inhalation of infectious droplets or airborne droplet nuclei.[276] We have used this route of inoculation successfully in previous studies involving both ferrets[277] and macaques[278] to model viral pneumonia. Our results showed that the

severity of pneumonia caused by the pH1N1 virus was intermediate between that caused by seasonal H1N1 virus and by HPAI H5N1 virus.

MATERIALS AND METHODS

Virus preparation

Three viruses were used: the pandemic (H1N1) 2009 influenza virus (A/Netherlands/602/2009), isolated from a specimen of a human patient who had recently visited Mexico; seasonal H1N1 influenza virus (A/Netherlands/26/2007), isolated from a patient during the 2006-2007 influenza season, and HPAI H5N1 virus (A/Indonesia/5/2005) as described earlier.[152]

Study design

For the survival study, groups of 3 ferrets (seasonal H1N1 virus) or 6 ferrets (pH1N1 and HPAI H5N1 viruses) with a temperature logger in the peritoneal cavity were inoculated intra-tracheally with each of these three viruses at each of the following doses in a 3-ml volume: 10^4, 10^6, and 10^8 median tissue culture infective dose ($TCID_{50}$). After inoculation, they were monitored daily for clinical signs until maximally 7 days post inoculation (dpi).[277] For the pneumonia study, groups of 3 ferrets (seasonal H1N1 virus) or 6 ferrets (pH1N1 and HPAI H5N1 viruses) were inoculated intra-tracheally with 10^6 $TCID_{50}$ and euthanized at 4 dpi or earlier when they were moribund before that time point. Necropsies were performed, and samples were obtained from both respiratory and extra-respiratory tissues for virological, pathological, and immunohistochemical analyses.

Ferrets

The experiments were performed under biosafety level 3 conditions at the Netherlands Vaccine Institute under an animal study protocol approved by the Institutional Animal Welfare Committee. Thirteen-month-old purpose-bred ferrets that were seronegative for antibody against circulating influenza viruses and Aleutian disease virus were maintained in standard housing and provided with commercial food pellets and water ad libitum until the start of the experiment. All ferrets were female (body weight, 815 to 1110 g) except for one male each in the pH1N1 virus and seasonal H1N1 virus groups of the pneumonia study (body weight, 1150 and 1290 g, respectively). Two weeks before infection, the animals were anesthetized using a cocktail of ketamine (Nimatek; Eurovet Animal Health BV) and domitor (Orion Pharma), and a temperature logger (data storage tag micro-T ultra small temperature logger; Star-Oddi) was placed in the peritoneal cavity. This device recorded the body temperature of the animals every 15 min.

Pathology

Three animals from every group were euthanized by exsanguination under ketamine anesthesia at 4 or 7 dpi, and necropsies were performed according to a standard protocol. The trachea was clamped off so that the lungs would not deflate upon opening the pleural cavity, which allowed visual estimation of the area of affected lung parenchyma. Samples for histological examination were stored in 10% neutral-buffered formalin (lungs after inflation with formalin), embedded in paraffin, sectioned at 4 μm, and stained with hematoxylin and eosin (HE) for examination by light microscopy. The following tissues were examined by light microscopy: left lung (cranial and caudal lobe), nasal turbinate, nasal septum, larynx, trachea, bronchus, tracheo-bronchial lymph node, eyelid, tonsil,

heart, liver, spleen, kidney, pancreas, duodenum, jejunum, colon, adrenal gland, and brain. Samples were obtained from the lungs in a standardized way, not guided by changes as seen in the gross pathology.

Semiquantitative assessment of influenza virus-associated inflammation in the lung was performed as reported elsewhere for the alveoli.[172] For the degree of inflammation in the bronchi and bronchioles, we used: (1) < 10% of the bronchial and bronchiolar epithelium inflamed, (2) 10%-50% of the bronchial and bronchiolar epithelium inflamed, and (3) > 50% of the bronchial and bronchiolar epithelium inflamed. For the severity of inflammation in the bronchi and bronchioles, we scored (1) peribronchial and peribronchiolar infiltrates, (2) mild necrosis and moderate numbers of inflammatory cells with scant exudates, and (3) marked necrosis and large numbers of inflammatory cells with abundant exudate. Microscopy slides were examined without knowledge of the identity of the animals. The cumulative scores for size and severity of inflammation provided the total score per animal.

Immunohistochemical analysis

For detection of influenza A virus antigen, tissues were stained with a primary antibody against the influenza A nucleoprotein as described elsewhere.[259] Semiquantitative assessment of influenza virus antigen expression in the lungs was performed as reported elsewhere for the alveoli.[172] For the bronchi and bronchioles, the percentage of positively staining bronchial and bronchiolar epithelium was estimated on every slide, and the average of the 4 slides was taken to provide the score per animal. For phenotyping of alveolar epithelial cells we used a destaining-restaining technique described elsewhere.[175]

Virology

Virus titers were determined by virus isolation in Madin-Darby canine kidney (MDCK) cells. Upon necropsy, samples of about 0.1 g of the cranial, median and caudal lobe of the right lung and of the accessory lobe from each animal were collected (total average weight of about 0.4-0.5 g/animal), pooled and homogenized with a FastPrep homogenizer (MP Biomedicals) in 3 ml transport medium. Quadruplicate 10-fold serial dilutions of these samples were cultured on MDCK cells.[279] Samples were obtained from the lungs in a standardized way, not guided by changes as seen in the gross pathology.

Statistical analysis

We used 1-way analysis of variance (ANOVA) and Tukey's multiple comparisons of means to compare body temperature, relative lung weight, lung virus titer, percentage of affected lung parenchyma, and histological and immunohistochemical scores at different levels of the lower respiratory tract for comparing the scores of pulmonary lesions and viral antigen expression. Differences were considered significant at $P < 0.05$.

RESULTS

The cumulative mortality rate of ferrets inoculated with the pH1N1 virus increased progressively from 0% at a dose of 104 TCID50 to 80% at a dose of 10^8 $TCID_{50}$ and was intermediate between the cumulative mortality rate with seasonal H1N1 virus and that for infection with HPAI H5N1 virus

(Figure 1). On the basis of these data, the estimated median lethal dose was about 10^4 $TCID_{50}$ for the HPAI H5N1 virus, about 10^7 $TCID_{50}$ for the pH1N1 virus, and > 10^8 $TCID_{50}$ for the seasonal H1N1 virus. Because the inoculation dose of 10^6 $TCID_{50}$ allowed the best discrimination in cumulative mortality rate between the 3 viruses, we performed additional comparative clinical, pathological, and virological studies on ferrets inoculated with this dose.

Clinical signs were observed in all ferrets inoculated with 10^6 $TCID_{50}$ of the pH1N1 virus from 1 dpi onwards; these signs included lethargy, loss of appetite, dyspnea, and raised body temperature (Figure 2A). In contrast, the seasonal H1N1 virus group showed no obvious clinical signs at any time point after inoculation. The body temperature in the pH1N1 virus group was significantly higher than that in the seasonal H1N1 virus group at 1 ($P = 0.02$) and 2 dpi ($P = 0.04$, Tukey test). The HPAI H5N1 virus group showed more severe clinical signs than did the pH1N1 virus group, and all ferrets died or were euthanized because of their moribund state by 3 dpi. The increase in body temperature of the HPAI H5N1 virus group was comparable to that in the pH1N1 virus group at 1 dpi; at later time points, it decreased due to the progressively moribund state of the ferrets. The mean loss in body weight ± standard deviation was 14% ± 5.3 % in the pH1N1 virus group and 8% ± 5.6 % in the seasonal H1N1 virus group at 4 dpi. Sneezing was not observed in any of the ferrets.

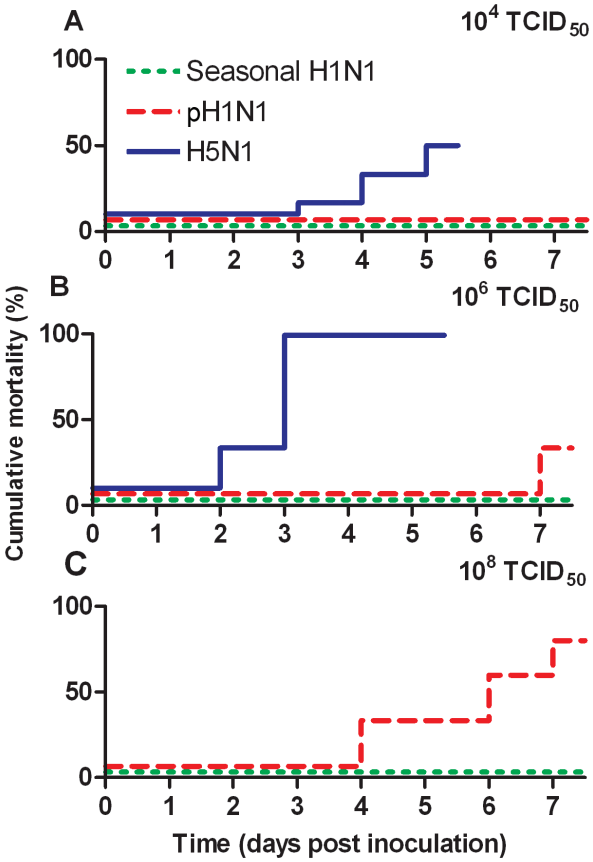

Figure 1. *Cumulative mortality rates of ferrets inoculated with different influenza viruses. Ferrets were intratracheally inoculated with seasonal H1N1 (n = 3), pH1N1 (n = 6) or HPAI H5N1 (n = 6) influenza viruses at a dose of 104 (A), 106 (B) or 108 (C) TCID50. Cumulative mortality for pH1N1 virus was intermediate between that for seasonal H1N1 virus and that for HPAI H5N1 virus.*

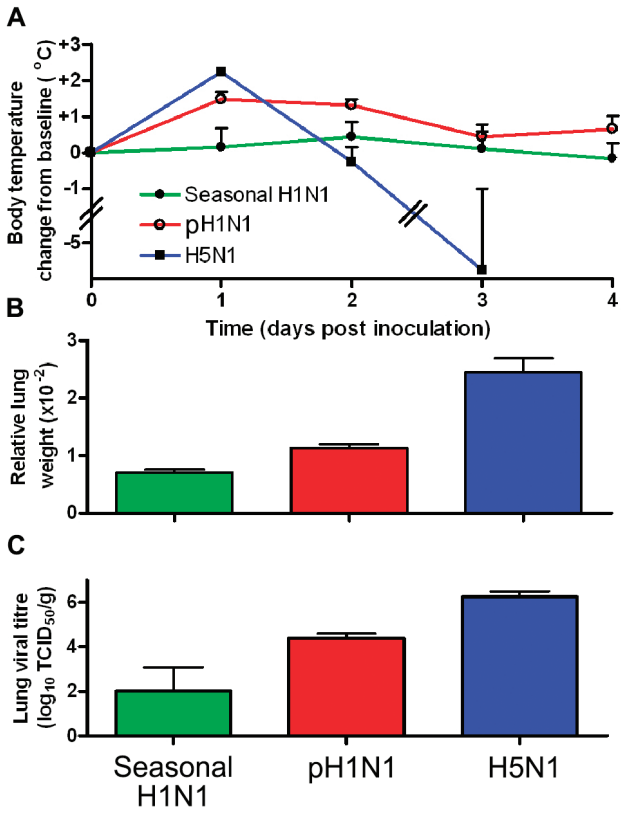

Figure 2. *Body temperatures, relative lung weights and lung viral titers of ferrets inoculated with different influenza viruses. The ferrets were intratracheally inoculated with seasonal H1N1 (n = 3), pH1N1 (n = 6) or HPAI H5N1 (n = 6) influenza viruses at a dose of 106 TCID50. The increase in body temperature (A), the relative lung weight (B), and the lung viral titer (C) of the pH1N1 virus group were intermediate between those of the seasonal H1N1 and the HPAI H5N1 virus groups.*

At necropsy on day 4 p.i., the relative lung weights (Figure 2B) and the lung virus titers (Figure 2C) of the pH1N1 virus group were intermediate between those of the seasonal H1N1 virus and those of the HPAI H5N1 virus group. The relative lung weights among the 3 virus groups were significantly different ($P = 0.001$, ANOVA, $F = 18.1$), with the relative lung weight of the HPAI H5N1 virus group significantly higher ($P = 0.006$, Tukey test) than that of the pH1N1 virus group. Lung virus titers among the 3 virus groups were significantly different ($P = 0.001$, ANOVA, $F = 17.4$), with lung viral titer of the pH1N1 virus group significantly higher ($P = 0.05$, Tukey test) than that of the seasonal H1N1 virus group.

All ferrets inoculated with the pH1N1 virus had multifocal or coalescing pulmonary lesions, which were dark red, raised, and firmer than normal (Figure 3). The percentage of lung parenchyma affected by this consolidation among the 3 virus groups was significantly different ($P = 0.0003$, ANOVA, $F = 42.5$). The percentage of affected lung parenchyma in the pH1N1 virus group (range: 20%-70%) was intermediate between that of the seasonal H1N1 virus group (range: 0%-10%; $P = 0.002$, Tukey test) and that of the HPAI H5N1 virus group (80%-100%; $P = 0.01$, Tukey test).

On histopathological examination, the alveoli of both the pH1N1 virus group and the HPAI H5N1 virus group showed diffuse alveolar damage (Figures 3 and 4A), whereas the alveoli of the seasonal H1N1 virus group did not. This lesion was characterized by flooding of alveolar lumina with alveolar macrophages, neutrophils, and erythrocytes, mixed with fibrin, edema fluid, and

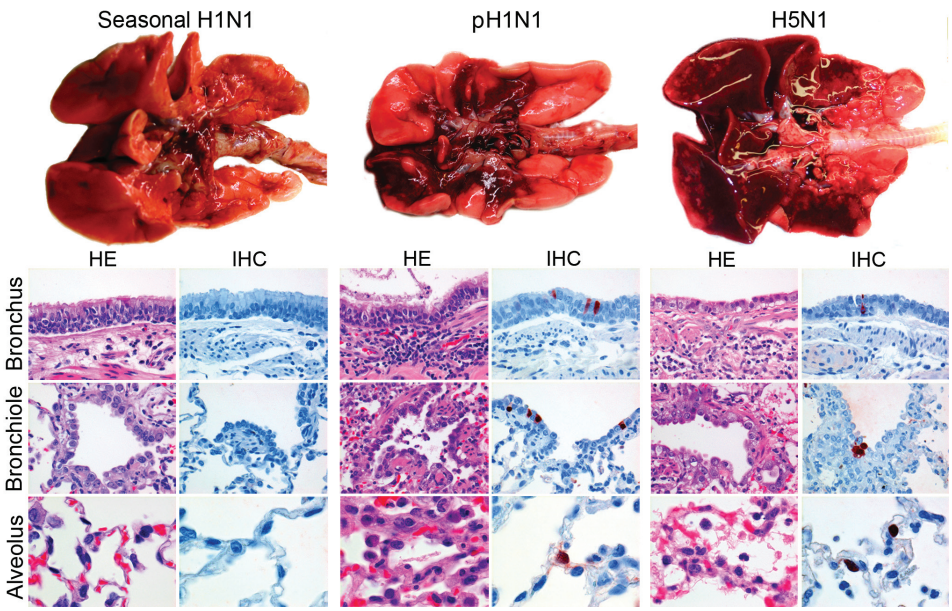

Figure 3. *Macroscopy, histopathology (HE) and immunohistochemistry (IHC) in the lungs of ferrets inoculated with different influenza viruses. The severity of macroscopic lung lesions (top row) in the pH1N1 virus group was intermediate between that in the seasonal H1N1 and the HPAI H5N1 virus groups. The pH1N1 virus group showed moderate influenza virus expression (IHC) in bronchi, bronchioles, and alveoli, associated with histological lesions (HE) characterized by inflammatory cell infiltrates and epithelial necrosis. In contrast, the seasonal H1N1 virus group showed minimal influenza virus expression and histological lesions. In the HPAI H5N1 virus group, there was more abundant influenza virus antigen expression in the alveoli associated with more severe histological lesions, but less abundant influenza virus antigen expression in the bronchi and bronchioles, associated with milder histological lesions. IHC with 3-amino-9-ethylcarbazole substrate and hematoxylin counterstain.*

cellular debris. The alveolar walls were thickened and had necrosis of the lining epithelium and multifocal type 2 pneumocyte hyperplasia. Qualitatively, the alveolar parenchyma of the pH1N1 virus group had more infiltration by inflammatory cells, whereas that of the HPAI H5N1 virus group had more necrosis and edema.

The bronchiolar epithelium of the pH1N1 virus group had multifocal necrosis with moderate infiltrates of neutrophils and multifocal peribronchiolar infiltration of moderate numbers of macrophages, lymphocytes and few neutrophils and plasma cells. In the bronchiolar lumina, there were moderate numbers of macrophages, neutrophils, and erythrocytes, mixed with fibrin, edema fluid, and cellular debris. Few bronchi had peribronchial infiltrates with moderate numbers of lymphocytes and macrophages, and few plasma cells; in the bronchial lumina were moderate amounts of cellular debris, fibrin, edema and few neutrophils. In the HPAI H5N1 and seasonal H1N1 virus groups, the bronchiolar and bronchial lesions were less severe overall than those in the pH1N1 virus group.

Quantitative histological scoring showed that the alveolar lesions in the pH1N1 virus group were intermediate in severity between those of the seasonal H1N1 virus group and those of the HPAI H5N1 virus group, and that the bronchiolar lesions in the pH1N1 virus group were the most severe of all three groups (Figure 5). The histological scores among the 3 virus groups differed significantly

for the alveoli ($P = 0.02$, ANOVA, $F = 6.6$), bronchioles ($P = 0.003$, ANOVA, $F = 11.7$), and bronchi ($P = 0.002$, ANOVA, $F = 14.2$). The HPAI H5N1 virus group had significantly higher histological alveolar scores than did the pH1N1 virus group ($P = 0.02$, Tukey test). The pH1N1 group had higher histological bronchiolar scores than did the HPAI H5N1 group ($P = 0.003$, Tukey test) and the seasonal H1N1 group ($P = 0.02$, Tukey test). Both the pH1N1 group ($P = 0.002$, Tukey test) and the seasonal H1N1 group ($P = 0.02$, Tukey test) had significantly higher histological bronchial scores than did the HPAI H5N1group.

On immunohistochemical analysis, influenza virus antigen expression was visible as diffuse-to-granular red staining, which usually was stronger in the nucleus than in the cytoplasm (Figure 3). Influenza virus antigen expression was closely associated with the presence of histological lesions at different levels of the lower respiratory tract. In the pH1N1 virus and HPAI H5N1 virus groups, influenza virus antigen expression was seen predominantly in type 1 and 2 pneumocytes (Figures 4B and C), alveolar macrophages, bronchiolar epithelial cells, and bronchial epithelial cells. In the seasonal H1N1 virus group, influenza virus antigen expression was seen in the same cell types, but was rare at any level of the lower respiratory tract. Quantitative scoring showed that influenza virus antigen expression in the pH1N1 virus group was high at all 3 levels of the lower respiratory tract (alveoli, bronchioles, and bronchi) (Figure 5). This contrasted to the influenza virus antigen expression in the HPAI H5N1 virus group, which was highest in alveoli, and lower in bronchioles and bronchi; and with that in the seasonal H1N1 virus group, which was most prominent in bronchi, but low at all 3 levels. The immunohistochemical scores among the 3 virus groups differed significantly for the alveoli ($P < 0.0001$, ANOVA, $F = 217$) and bronchi ($P = 0.01$, ANOVA, $F = 8.0$).

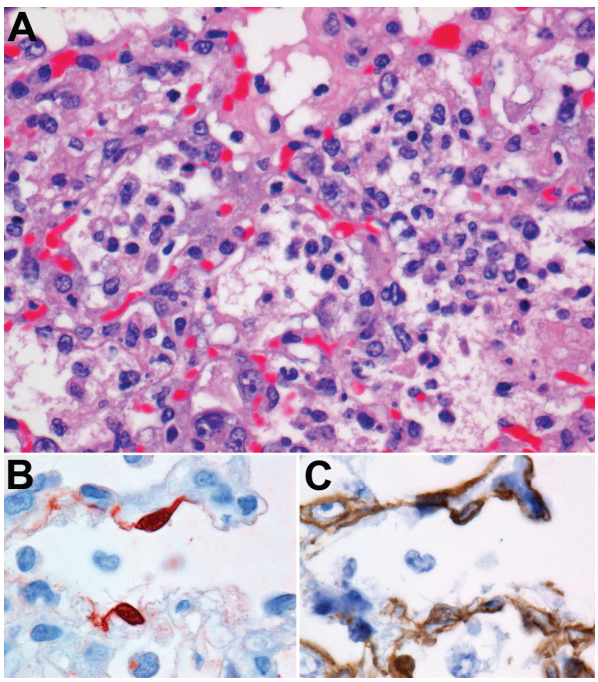

Figure 4. *Diffuse alveolar damage in a ferret inoculated with pH1N1 virus. (A) The alveolar architecture is obliterated by thickening of alveolar septa and flooding of alveolar lumina with alveolar macrophages, neutrophils, and erythrocytes, mixed with fibrin, edema fluid, and cellular debris. HE. (B) Influenza virus antigen expression in nucleus and cytoplasm of type 1 pneumocytes. IHC: Immunohistochemistry with 3-amino-9-ethylcarbazole substrate and hematoxylin counterstain. (C) Keratin expression in cytoplasm of identical cells that expressed influenza virus antigen (shown in panel B), confirming epithelial origin of infected cells. IHC.*

The pH1N1 virus group had significantly higher immunohistochemical scores than the seasonal H1N1 virus group for alveoli ($P < 0.00001$, Tukey test) and bronchi ($P = 0.01$, Tukey test), and significantly higher immunohistochemical bronchial scores than did the HPAI H5N1 virus group ($P = 0.03$, Tukey test). None of the ferrets in the seasonal H1N1 virus and pH1N1 virus groups had significant lesions or influenza virus antigen expression in extra-respiratory tissues, which is a hallmark of infection of ferrets with HPAI H5N1 virus A/Indonesia/5/2005.[280,281]

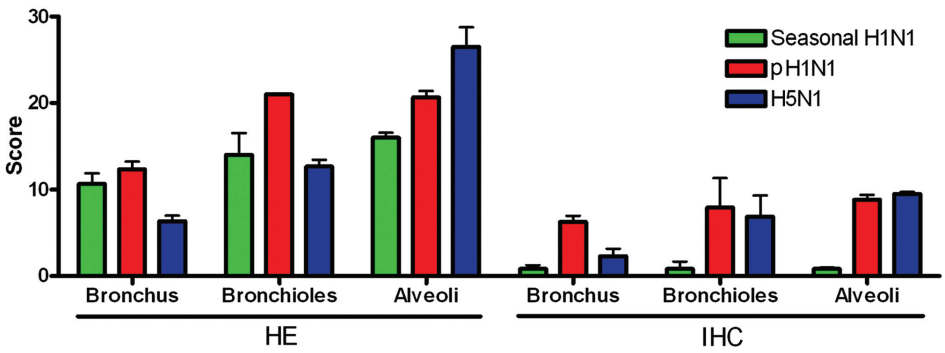

Figure 5. *Histological and immunohistochemical scoring in the lungs of ferrets inoculated with different influenza viruses. Histological scoring of samples stained with hematoxylin-eosin (HE) showed that the alveolar lesions in the pH1N1 virus group were intermediate in severity between those of the seasonal H1N1 virus group and the HPAI H5N1 virus group, and that the bronchiolar lesions in the pH1N1 virus group were the most severe of all 3 groups. Immunohistochemical (IHC) scoring showed that influenza virus antigen expression in the pH1N1 virus group was high in alveoli, bronchioles, and bronchi. In the HPAI H5N1 virus group, the scores were highest in alveoli, and lower in bronchioles and bronchi. In the seasonal H1N1 virus group, scores were low at all 3 levels.*

DISCUSSION

To cause a major pandemic, a newly emerging influenza virus needs to be not only efficiently transmissible among humans, but also must be able to cause severe pneumonia. The former has been demonstrated by epidemiological analysis of its spread in the human population, which provided R0 estimates in the range of 1.4-1.6, comparable with lower R0 estimates obtained from previous pandemics.[275] This was corroborated by our previous study, which showed ferret-to-ferret transmission of pH1N1 virus was equally efficient as that of a seasonal H1N1 virus upon intranasal inoculation.[152,282]

Here we show that the pH1N1 virus is not only efficiently transmissible but is also able to cause severe pneumonia in ferrets. With other factors held constant, the pH1N1 virus causes pneumonia that is intermediate in severity between that caused by seasonal H1N1 virus and that caused by HPAI H5N1 virus. The pH1N1 virus shares with HPAI H5N1 virus the ability to replicate well in epithelial cells in the lower respiratory tract and to cause diffuse alveolar damage. Our results correspond with those of Itoh et al.[264] who found that ferrets inoculated intranasally with pH1N1 influenza virus showed more severe bronchopneumonia than those inoculated with a recent seasonal H1N1 virus.

Because the pattern of influenza virus attachment to the lower respiratory tract is similar for ferrets and humans,[125] and because influenza-associated disease in ferrets resembles that in

humans,[283] a similar pattern of infection and associated disease by the pH1N1 virus may also be expected to occur in human's. This is corroborated by the clinical characterization of patients with confirmed fatal infection with pH1N1 virus, for whom acute respiratory distress syndrome was the most frequent diagnosis.[274]

The warning from this study—with the caveat that no animal model is able to capture all aspects of the human disease—is the intrinsic ability of the pH1N1 virus to cause more severe pneumonia than seasonal H1N1 virus. This fact needs to be taken into account in ongoing pandemic preparedness planning. Furthermore, regular evaluation of the severity of the pneumonia caused by the pH1N1 virus in this ferret model will provide valuable information about possible changes in virulence as this newly emerged virus further adapts to its human host.

Acknowledgments

We thank W. van Aert, R. Bodewes, R. Boom, C. van Hagen, R. van Lavieren, L. Leijten and P. van Run for technical assistance, A. Gomersbach and W. Vos for biotechnical assistance, F. van der Panne for figure preparation and R. Eijkemans for statistical analysis.

CHAPTER 3

INFLUENZA VIRUS INFECTION IN ANIMAL MODELS

3.3

Experimental Pandemic (H1N1) 2009 Virus Infection of Cats

Emerging infectious diseases (2010) 16(11): 1745-1747

JMA van den Brand,[1] KJ Stittelaar,[1,2] G van Amerongen,[1,2] M van de Bildt,[1]
LME Leijten,[1] T Kuiken,[1] and ADME Osterhaus,[1,2]

Department of Virology, Erasmus Medical Centre, Rotterdam, the Netherlands [1]
ViroClinics Biosciences BV, Rotterdam, the Netherlands [2]

ABSTRACT

To demonstrate that pandemic (H1N1) 2009 virus may cause respiratory disease in cats, we intratracheally infected cats. Diffuse alveolar damage developed. Seroconversion of sentinel cats indicated cat-to-cat virus transmission. Unlike in cats infected with highly pathogenic avian virus (H5N1), extrarespiratory lesions did not develop in cats infected with pandemic (H1N1) 2009 virus.

INTRODUCTION

Soon after pandemic (H1N1) 2009 virus (pH1N1) emerged in North America, infections in domestic cats were reported.[283,284] Infection with highly pathogenic avian influenza (HPAI) virus (H5N1) leads to severe and often fatal diffuse alveolar damage (DAD) and systemic virus spread in cats.[144,285,286] In contrast, seasonal human influenza viruses do not cause disease in cats.[287] To elucidate the pathogenesis of pH1N1 infection in cats, we studied 8 laboratory cats intratracheally infected with this virus.

MATERIALS AND METHODS

Pandemic (H1N1) 2009 virus (A/Netherlands/602/2009) was isolated from a 3-year-old girl from the Netherlands who had mild influenza after she visited Mexico in early 2009. Virus was cultured in embryonated chicken eggs and passaged once in Madin-Darby Canine Kidney (MDCK) cells.[152]

We used 2 groups (4 cats/group) of four 16-week-old, purpose-bred, specific pathogen free, European shorthair cats that were seronegative for hemagglutinin-inhibition (HI) antibodies against pandemic (H1N1) influenza 2009 virus and circulating seasonal influenza A viruses. These cats were intratracheally infected with a $10^{6.0}$ tissue culture infectious dose ($TCID_{50}$) of pH1N1. A third group of 3 sentinel cats were housed with these 2 infected groups (1 group with 1 and 1 group with 2) from 2 days post infection (dpi) onward. Serum samples were obtained on 0, 4, 7, and 21 dpi and stored at -20°C until tested for HI antibodies against pH1N1.[288]

All 11 cats were monitored daily for clinical signs, and body temperature was measured at 15-min intervals. Nasal, pharyngeal, and rectal swab specimens were obtained daily from all cats. After being anesthetized with ketamine, all cats were euthanized by exsanguination. Cats in groups 1 and 2 were euthanized at 4 dpi and 7 dpi, respectively. Sentinel cats were euthanized at 21 dpi. Experiments were performed under BioSafety Level 3 by using protocols approved by our Institutional Animal Welfare Committee.

Necropsies were performed according to a standard protocol. Lung, nasal turbinate, nasal septum, larynx, trachea, bronchus, tracheobronchial lymph node, nictitating membrane, tonsil, heart, liver, spleen, kidney, pancreas, duodenum, jejunum, colon, adrenal gland, brain, and olfactory bulb samples were obtained, were fixed in formalin, and processed to obtain sections for staining with hematoxylin and eosin (HE).

For detection of viral antigen, tissue sections were stained with viral nucleoprotein-specific antibody.[287] Alveolar epithelial cells were phenotyped by using a destaining-restaining technique.[175] After organ samples were weighed and stored at -80°C, pH1N1 virus was quantified by limiting dilution virus isolation in MDCK cells.[278]

RESULTS

Cats in groups 1 and 2 infected with pH1N1 showed mild-to-moderate clinical signs (lethargy, appetite loss, rapid and labored breathing, and protruding nictitating membrane) after 1 or 2 dpi onwards. Average body temperatures increased after 1 dpi, showed a maximum increase of ≈1.5°C by 2 dpi, and returned to baseline values within 4-5 dpi (Figure 1). Sentinel cats showed no clinical signs. Two cats in group 1 (2 pharyngeal samples) and 2 cats in group 1 and 1 cat in group 2 (1 pharyngeal sample) had low virus titers during 1-4 dpi (≤ $10^{1.8}$ $TCID_{50}$ /g). Nasal swab samples from all sentinel cats and pharyngeal and rectal swab specimens from 2 cats were virus positive by reverse transcription-PCR (cycle threshold ≥35) 2-6 days after first contact with infected cats. No virus was isolated from these swab specimens.

On 4 dpi, high virus titers were found in lungs, bronchi, and tracheas from4 infected cats ($10^{5.5-6.3}$, $10^{2.9-4.6}$ and $10^{3.1-3.8}$ $TCID_{50}$ /g, respectively). The tonsils from 2 cats, intestines from 1 cat, and the spleen from 1 cat also had high virus titers ($10^{3.0}$ and $10^{4.2}$, $10^{1.6}$, and $10^{1.6}$ $TCID_{50}$ /g, respectively). On 7 dpi, virus was detected in lung from 1 cat and trachea from 1 cat ($10^{3.0}$ and $10^{1.6}$ $TCID_{50}$ /g, respectively). Infectious virus ($10^{1.2-2.2}$ $TCID_{50}$ /g) was found in liver, intestine, brain, adrenal glands, and nictitating membranes of individual cats. The olfactory bulb of 1 cat was virus positive ($10^{3.0}$ $TCID_{50}$ /g). No other organs from any cats were virus positive (Table).

No serum HI antibodies (titer < 20) were found in group 1 cats on 4 dpi. All group 2 cats had serum HI antibodies (titers 30-120) on 7 dpi. One sentinel cat was seropositive on 15 dpi (titer 40); all cats were positive on 21 dpi (titer 80).

All infected cats showed multifocal or coalescing pulmonary consolidation, ranging from 30 to 50 % on 4 dpi and from 10 to 30 % on 7 dpi (Figure 2). All tracheobronchial lymph nodes were enlarged 3-5x. Palatine tonsils were enlarged ≈2x on 7 dpi. All sentinel cats showed mild multifocal consolidation; 5-10% of lung parenchyma was affected. Two cats had tracheo-bronchial lymph nodes enlarged 2-5x.

Histopathologic analysis (Figure 2) identified pulmonary consolidation indicative of DAD. Alveolar and bronchiolar lumina showed edema and contained variable numbers of macrophages, neutrophils, and erythrocytes mixed with fibrin and cellular debris. Alveolar walls were thickened and showed necrosis of lining epithelium and type II pneumocyte hyperplasia. Bronchiolar walls were moderately infiltrated by neutrophils and had multifocal epithelial necrosis and multifocal peribronchiolar moderate infiltration by macrophages and lymphocytes and few neutrophils and plasma cells. Bronchial lumina harbored few neutrophils and scant edema, fibrin, and cellular debris. There were few peribronchial infiltrates with a small number of lymphocytes, plasma cells, and macrophages. Lung lesions seen on 4 and 7 dpi were comparable except for more extensive type II pneumocyte hyperplasia on 7 dpi. Tracheobronchial lymph nodes and palatine tonsils had severe sinus histiocytosis and lymphocytolysis, and

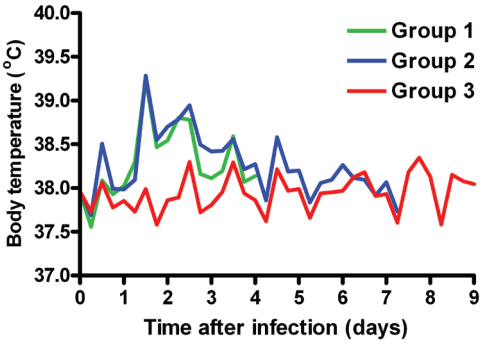

Figure 1. *Average body temperatures of 2 groups of cats experimentally infected with pandemic (H1N1) 2009 virus (groups 1 and 2) and sentinel cats (group 3).*

moderate infiltration by neutrophils. Histologic changes in lung parenchyma of all sentinel cats were consistent with chronic lesions resulting from those seen in the other cats. No lesions were seen in other organs of all cats.

Virus antigen expression was more prominent on 4 dpi than on 7 dpi and was closely associated with histologic lesions (Figure 2). Virus antigen expression was seen in many type II pneumocytes, few type I pneumocytes, alveolar macrophages, bronchiolar ciliated and non-ciliated epithelial cells, and rare bronchial ciliated epithelial cells. Type I and II pneumocytes were identified by double staining with cytokeratin. No virus antigen was observed in the sentinel cats.

Table 1. Immunohistochemic alanalysis and virus isolation on 4 and 7 dpi in respiratory and extra-respiratory tissues of cats intratracheally infected with pandemic (H1N1) 2009 virus

	No. positive[a]			
	IHC analysis		**Virus isolation[b]**	
Tissue	**4 dpi**	**7 dpi**	**4 dpi**	**7 dpi**
Respiratory				
Lung	4	3	4	1
Bronchus	2	0	4	0
Trachea	0	0	4	1
Nasal turbinates	0	0	2	0
Extra respiratory				
Liver	0	0	0	1
Intestine	0	0	1	1
Olfactory bulb	0	0	0	1
Brain	0	0	0	1
Spleen	0	0	1	0
Tonsil	0	0	2	0
Adrenal gland	0	0	0	2
Nictitating membrane	0	0	0	2

a Four cats were examined in each day. IHC, immunohistochemical; dpi, days post infection.
b No virus was isolated from the tracheobronchial lymph node, pancreas, heart, or kidney of any cats.

DISCUSSION

Intra-tracheal infection of domestic cats with pH1N1 resulted in mild-to-moderate clinical signs and virus replication throughout the respiratory tract, which caused DAD. The pathogenesis in the respiratory tract in cats was similar to that occurring in humans, macaques, and ferrets.[106,152,154,263] Seroconversion of sentinel cats indicated cat-to-cat transmission.

Unlike infection with seasonal human influenza viruses, infection with pH1N1 causes respiratory disease in cats. To compare infection of pH1N1 with HPAI virus (H5N1), we used our unpublished data for cats intratracheally inoculated with 105.0 TCID50 HPAI virus (H5N1) (A/Indonesia/5/2005) at 4 and 7 dpi[144] and for sham-infected cats. Histopathologic and immunohistochemical findings in lungs of cats infected with these viruses coincided, which indicated

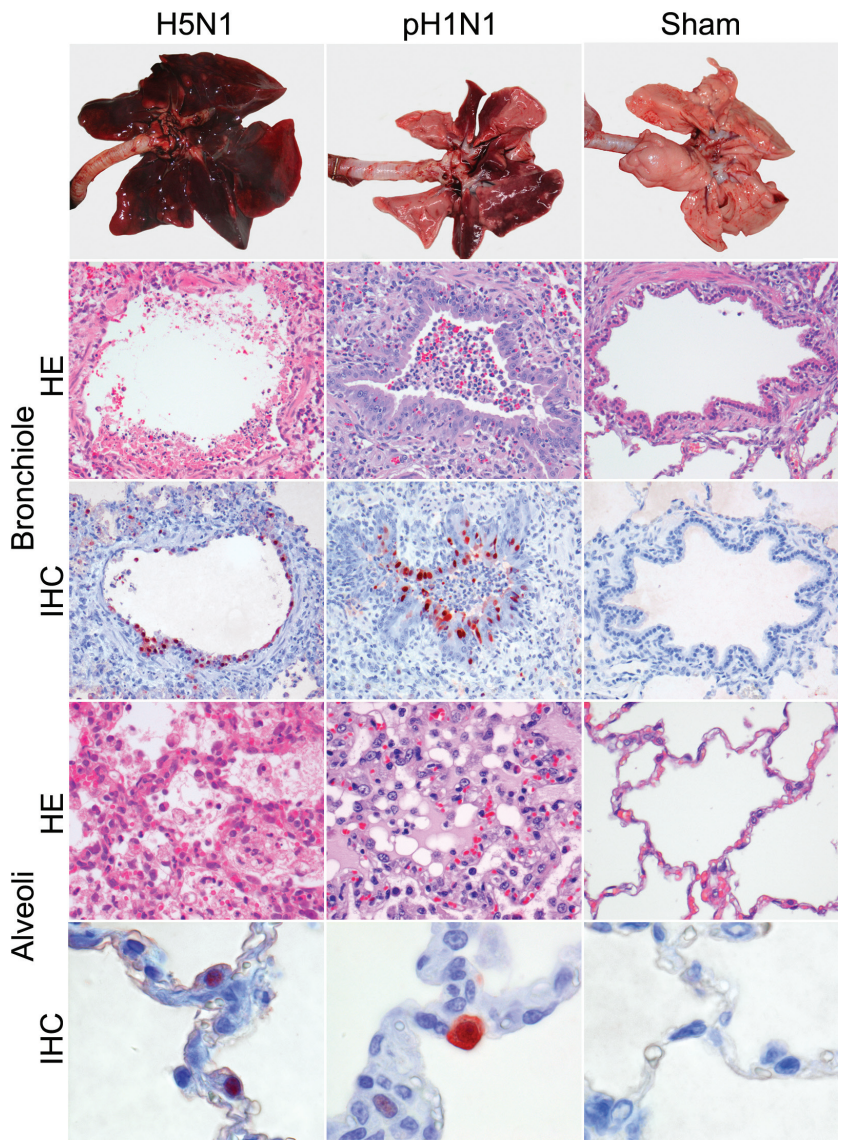

Figure 2. *Macroscopic, histopathologic and immunohistochemical analysis on day 4 of lungs of cats infected with highly pathogenenic avian influenza (HPAI) virus (H5N1), pandemic (H1N1) 2009 virus (pH1N1) or phosphate-buffered saline (PBS: Sham). Macroscopic analysis of lungs (top row) in cats infected with HPAI virus (H5N1) demonstrated multifocal or coalescing consolidation characterized by dark-red, firm, slightly raised areas. Multifocal consolidation occurred in the group infected with pH1N1. The sham-infected group had no lesions. Lesions of cats infected with HPAI virus (H5N1) (first column) showed severe epithelial necrosis in the bronchioles and alveoli (hematoxylin an eosin stain: HE) with intraluminal edema and inflammatory cell infiltrates, and associated influenza virus antigen expression (immunohistochemical stain with 3-amino-9-ethylcarbazole subtrate and hematocylin counterstain: IHC) in bronchiolar and type II alveolar epithelial cells. The group infected with pH1N1 (second column) had lesions characterized by inflammatory cell infiltrates in bronchioles and alveoli (HE) associated with influenza virus antigen expression in bronchiolar epithelial cells and type II alveolar epithelial cells (IHC). The group inoculated with PBS (third column) showed no lesions (HE) or expression of influenza virus antigen (IHC). Original magnification, bronchiole x200, alveoli HE x400, and alveoli IHC x1000.*

a similar pathogenetic process and increased severity in cats infected with HPAI virus (H5N1). However, in contrast to HPAI virus (H5N1), pH1N1 does not cause extrapulmonary lesions in infected cats. Our data show that pH1N1 may cause respiratory disease in cats and that human-to-cat transmission is the most likely route of infection.

Acknowledgements

We thank P. van Run, R. Verbeek, and L. de Waal for technical assistance; W. Vos for biotechnical assistance; and F. van der Panne for preparing the figures.

CHAPTER 3

INFLUENZA VIRUS INFECTION IN ANIMAL MODELS

3.4

Modification of the ferret model for pneumonia from seasonal human influenza A virus infection

Veterinary Pathology (2012) 49(3): 562-568

JMA van den Brand,[1] KJ Stittelaar,[2] LME Leijten,[1] G van Amerongen,[1,2]
JH Simon,[2] ADME Osterhaus,[1] T. Kuiken[1]

Department of Virology, Erasmus Medical Centre, Rotterdam, The Netherlands [1]
Viroclinics Biosciences BV, Rotterdam, The Netherlands [2]

ABSTRACT

The primary complication of seasonal influenza in humans is viral pneumonia. A conventional animal model - intranasal inoculation of ferrets with 10^6 median tissue culture infectious dose ($TCID_{50}$) of virus - results in disease that is neither consistent nor comparable with severe viral pneumonia in humans. Therefore, we modified the experimental procedures by increasing the $TCID_{50}$ to 10^9 and by inoculating via the intratracheal route, testing these procedures with H1N1 strains (A/Bilthoven/3075/1978 and A/Netherlands/26/2007) and H3N2 strains (A/Bilthoven/16190/1968 and A/Netherlands/177/2008) of seasonal influenza virus. The ferrets of all groups (n = 3 per virus strain) had clinical signs, increased body temperature, virus excretion from day 1, loss of body weight, and increased relative lung weight at 4 days post inoculation. All ferrets had severe pulmonary consolidation, and histological examination revealed moderate to severe necrotizing broncho-interstitial pneumonia with severe edema, necrosis of alveolar epithelium, inflammatory infiltrates in alveolar septa and lumina, epithelial regeneration, and perivascular and peribronchiolar inflammatory infiltrates. The lesions were associated with the presence of influenza virus antigen in respiratory epithelium by immunohistochemistry. Although all 4 virus strains caused pulmonary lesions of comparable severity, virus isolation in the lungs, trachea, nasal concha, and tonsils showed higher mean virus titers in the H1/07 and H3/68 groups than in the H1/78 and H3/08 groups. In conclusion, above H1N1 and H3N2 strains cause severe pneumonia in ferrets by use of the modified experimental procedures and provide a good model for pneumonia caused by seasonal influenza A virus infection in humans.

INTRODUCTION

Seasonal human influenza viruses cause viral pneumonia as a primary complication in the elderly, immunosuppressed, and very young.[290] In currently used animal models, seasonal influenza virus infection does not consistently cause viral pneumonia.[152,291,292] Therefore, it is difficult to study the pathogenesis of this complication or evaluate preventive or therapeutic measures against it.

Ferrets are commonly used as experimental animals to study the pathogenesis of human influenza and test vaccines and antivirals against influenza virus infection. Ferrets and humans have similarities in their respiratory tract and in their interaction with human influenza viruses. Ferrets have similar lung physiology and airway morphology as humans.[283] Human influenza viruses show a similar pattern of attachment to ferret respiratory tract epithelium.[125] Both species are susceptible to infection with human influenza viruses.[119,283] Both develop similar disease: usually upper respiratory tract disease, which is mild, and occasionally pneumonia, which is more severe or even fatal.119,283 That human influenza virus infection usually causes only mild disease in ferrets is a drawback if one wishes to have an animal model for severe influenza viral pneumonia.

Outcome of experimental influenza virus infection can be modified in different ways, including route of administration, viral dose, and virus strain. Intranasal inoculation of ferrets with seasonal human H1N1 influenza virus causes rhinitis without involvement of the lower respiratory tract,[152] while intratracheal inoculation of the same virus strain causes broncho-interstitial pneumonia.[292] Increasing the dose of viral inoculum from 10^4 to 10^8 mean tissue culture infectious dose ($TCID_{50}$) results in a higher mortality rate.[292] Influenza virus strains differ in pathogenicity. For example, the

strain of H1N1 virus that emerged in 2009 and caused a human pandemic causes more severe disease in different species of experimental mammals than the strain of H1N1 virus that has been circulating for decades in the human population.[264,292,293]

Making use of the above knowledge, we adapted the experimental procedures with the objective of establishing a model of human seasonal influenza virus infection that consistently induces pneumonia in ferrets. In this model, we used an intratracheal route of inoculation and a high viral dose of 10^9 $TCID_{50}$. We tested these modified experimental procedures for subtypes H1N1 and H3N2 and for both recent and older strains of these subtypes.

MATERIALS AND METHODS

Study design

We chose for intratracheal inoculation because this method delivers the viral inoculum closer to the site of pneumonia than intranasal inoculation. Also, we have shown previously that intratracheal inoculation more consistently induces pneumonia in ferrets than intranasal inoculation, both for seasonal H1N1 influenza virus[292] and for highly pathogenic avian H5N1 influenza virus.[294]

We chose for an inoculum dose of 10^9 $TCID_{50}$ on the basis of a previous study, where we had used doses ranging from 10^4 to 10^8 $TCID_{50}$ to inoculate ferrets intratracheally with seasonal H1N1 influenza virus.[292] Because even ferrets inoculated with a dose of 10^8 $TCID_{50}$ did not show mortality by 7 days postinoculation (dpi), we chose for a 10X higher dose, 10^9 $TCID_{50}$, which is the highest dose practical for most virus strains by use of current laboratory techniques.

We chose for an H1N1 virus strain (H1/07) and an H3N2 virus strain (H3/08) as representative for humans seasonal influenza viruses circulating most recently in the human population. For contrast, we chose an H3N2 virus strain (H3/68) that had been isolated soon after this subtype had been introduced into the human population in 1967 and an H1N1 virus strain (H1/78) that had been isolated soon after this subtype had been re-introduced into the human population in 1977. We considered that the older viruses might be more pathogenic in ferrets because they had not had as much time to adapt to replication in the mammalian host as more recent viruses.

For each virus (4 groups), a group of 3 ferrets was inoculated intratracheally with 10^9 $TCID_{50}$ in a 3-ml volume under anesthesia with ketamine (Nimatek, Eurovet Animal Health BV, Bladel, the Netherlands) and medetomidine hydrochloride (Domitor, Orion Pharma, Espoo, Finland). From 0 to 4 dpi, ferrets were monitored daily for clinical signs, and under ketamine/medetomidine hydrochloride anesthesia, body weight was measured and pharyngeal swabs were collected.[277] At 4 dpi, necropsies were performed, and samples were taken from respiratory and extra-respiratory tissues for virologic, pathologic, and immunohistochemical analyses. The experiments were performed under an animal study protocol approved by the Institutional Animal Welfare Committee and performed compliant with national and European legislation. All experiments were performed under biosafety level 3 conditions at the Netherlands Vaccine Institute.

Virus preparation

Four seasonal influenza viruses were isolated from patients during different influenza seasons: H1N1 strains A/Bilthoven/3075/1978 (H1/78) and A/Netherlands/26/2007 (H1/07) and H3N2 strains A/Bilthoven/16190/1968 (H3/68) and A/Netherlands/177/2008 (H3/08). The isolates were passaged 3 times in Madin-Darby Canine Kidney (MDCK) cells and titrated according to standard methods.

Subsequently, the viruses were purified and concentrated about 20-fold using sucrose gradient centrifugation, reaching an infectious virus titer of 1 x 10^9 $TCID_{50}$ per ml.[277,279]

Ferrets

Twelve 8-month-old purpose-bred female ferrets–seronegative for antibodies against circulating influenza viruses H1N1, H3N2, pandemic (H1N1) 2009 and Aleutian disease virus–were maintained in standard housing, and provided with commercial food pellets and water ad libitum until the start of the experiment. All ferrets were female (body weight, 690-1010 g). Two weeks prior to infection, the animals were anesthetized with ketamine and medetomidine hydrochloride, and a temperature logger (DST micro-T Ultra Small Temperature Logger, Star-Oddi, Reykjavik, Iceland) was placed in the peritoneal cavity. This device recorded the body temperature of the animals every 15 min. Changes in body temperature were calculated by subtracting the mean day and night temperature measured on 2 successive days in the period before the challenge from the mean day and night temperatures post infection. For the relative lung weight of control ferrets the lungs of 22 non-infected female ferrets were weight, expressed as a percentage of the total body weight.

Pathology

The animals were euthanized by exsanguination under ketamine anesthesia on 4 dpi and necropsied according to a standard protocol. The trachea was clamped off so that the lungs would not deflate upon opening the pleural cavity, thereby allowing visual estimation of the area of affected lung parenchyma. Samples for histologic examination were stored in 10% neutral buffered formalin (lungs after inflation with formalin), embedded in paraffin, sectioned at 4 μm, and stained with hematoxylin and eosin (HE) for examination by light microscopy. The following tissues were examined by light microscopy: left lung (four slides with either cranial or caudal lobe with longitudinal or cross section), nasal turbinate, nasal septum, larynx, trachea, bronchus, tracheo-bronchial lymph node, eyelid, tonsil, heart, liver, spleen, kidney, and brain.

Semiquantitative assessment of influenza virus-associated inflammation in the lung was performed as reported earlier:[295] For the extent of alveolitis and alveolar damage: 0, 0%; 1, 1-25%; 2, 25-50%; 3, > 50 %. For the severity of alveolitis, bronchiolitis, bronchitis, and tracheitis: 0, no inflammatory cells; 1, few inflammatory cells; 2, moderate numbers of inflammatory cells; 3, many inflammatory cells. For the presence of alveolar edema, alveolar hemorrhage, and type II pneumocyte hyperplasia: 0, no; 1, yes. For the extent of peribronchial, peribronchiolar, and perivascular infiltrates: 0, none; 1, 1-2 cells thick; 2, 3-10 cells thick; 3, more than 10 cells thick. Slides were examined without knowledge of the identity of the animals. The cumulative scores for size and severity of inflammation of all slides provided the total score per animal. As a control animal for histopathology and immunohistochemistry, a ferret was sham inoculated with phosphate buffered saline and euthanized at 4 dpi.

Immunohistochemistry

For detection of influenza A virus antigen, tissues were stained with a primary antibody against the influenza A nucleoprotein as described previously.[259] Alternatively, binding of the primary antibody was detected using a peroxidase labeled goat-anti-mouse IgG2a (Southern Biotech, Birmingham, AL). Peroxidase activity was revealed using 3-amino-9-ethylcarbazole (AEC) (Sigma, St Louis, MO, USA), resulting in a bright red precipitate. In each staining procedure an isotype control was

included as a negative control, and a lung section from an experimentally influenza-inoculated cat (H5N1) was used as positive control.

Semiquantitative assessment of influenza virus antigen expression in the lungs was performed as reported earlier:[295] for the alveoli, 25 arbitrarily chosen fields (20x objective) of lung parenchyma from 4 lung sections were examined by light microscopy for the presence of influenza virus nucleoprotein, without the knowledge of the identity of the animals. The cumulative scores for each animal were presented as number of positive fields per 100 fields. For the bronchi and bronchioles, the percentage of positively staining bronchial and bronchiolar epithelium was estimated on every slide and the average of the 4 slides provided the score per animal: 0, 0%; 1, 1-25%; 2, 25-50%; 3, > 50 %.

Virology

After collection on 0, 1, 2, 3 and 4 dpi, pharyngeal swabs were stored at -70°C in the same medium as that used for the processing of the lung samples. Quadruplicate 10-fold serial dilutions of lung and swab supernatants were used to determine the virus titers in confluent layers of MDCK cells as described previously.[279]

Samples of all lobes of the right lung and the accessory lobe, nasal concha, trachea, tonsil, tracheobronchial lymph node, spleen, brain, third eyelid, liver, kidney, and heart from all animals were collected on 4 dpi and stored at -70°C until further processing. The samples were weighed and subsequently homogenized with a FastPrep-24 (MP Biomedicals, Eindhoven, The Netherlands) in Hank's balanced salt solution containing 0.5% lactalbumin, 10% glycerol, 200 U/ml of penicillin, 200 µg/ml of streptomycin, 100 U/ml of polymyxin B sulfate, 250 µg/ml of gentamycin, and 50 U/ml of nystatin (ICN Pharmaceuticals, Zoetermeer, The Netherlands) and centrifuged briefly before dilution.

Statistical analysis

The one-way analyses (ANOVA) test for multiple comparisons was used to assess differences between the virus groups for: body weight, relative lung weight, percentage affected lung tissue, histologic scores, immunohistochemical scores, and viral load. A post-test was performed only when $P < 0.05$ (independent t test). Differences were considered significant when $P < 0.05$.

RESULTS

Clinical findings

The ferrets became lethargic at 2 dpi with loss of appetite, mild dyspnea, and raised body temperature (Figure 1). Sneezing was not observed in any of the ferrets. The body temperature profile after inoculation of the ferrets was similar in the different groups with an increase in body temperature starting 4 hours after inoculation until 1 dpi with a temperature increase up to 2 ˚C from the baseline. The differences in body temperature and body weight loss among groups (Table 1) were not statistically significant.

Gross pathology

At necropsy on 4 dpi, all ferrets had multifocal or coalescing pulmonary consolidation, with dark red, raised, and firm areas. The median percentage of lung tissue affected was 40% in all groups

(Table 1). The relative lung weights of all ferrets were similar with only small differences between the groups. The differences in percentage in lung tissue affected and relative lung weight among groups were not statistically significant.

Table 1. Ferrets with different recent and old seasonal human influenza viruses

Group	Virus	Weight loss (%)		Affected lung tissue (%)		Relative lung weight [b] (%)	
		Median	Range	Median	Range	Median	Range
1	H1N1 78	11	8-15	40	30-50	1.2	1.2-2.0
2	H1N1 07	7	6-8	40	40-40	1.2	0.9-1.3
3	H3N2 68	14	5-16	40	30-40	1.3	1.0-1.3
4	H3N2 08	9	7-19	40	40-50	1.3	1.1-1.3

[a] Per group, n = 3; 4 dpi.
[b] The relative lung weight is expressed as a percentage of the total body weight. The median relative lung weight of control ferrets was 0.6, with a range of 0.5-0.8.

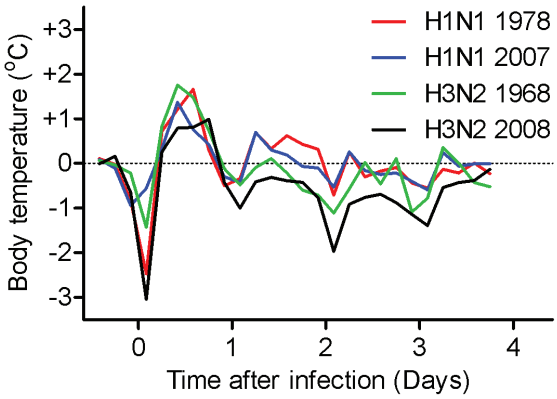

Figure 1. *Changes in body temperature from the baseline in ferrets infected with recent and old H1N1 and H3N2 seasonal human influenza viruses at 4 dpi.*

Histopathology

By histopathology (Figure 2), all groups showed a multifocal to diffuse, moderate to severe necrotizing broncho-interstitial pneumonia. This lesion was characterized by flooding of alveolar lumina with edema fluid, fibrin, and cellular debris mixed with alveolar macrophages, neutrophils, and erythrocytes (Figure 2). The alveolar walls were thickened and had necrosis of the lining epithelium and multifocal type II pneumocyte hyperplasia. The bronchiolar walls had multifocal epithelial necrosis with moderate infiltrates of neutrophils and peribronchiolar multifocal infiltration of moderate numbers of macrophages, lymphocytes, and few neutrophils and plasma cells. In the bronchiolar lumina, there were moderate numbers of macrophages, neutrophils, and erythrocytes, mixed with fibrin, edema fluid, and cellular debris (Figure 2). Histopathologic changes in the bronchi were similar but less severe (Figure 2). Multifocally, there was moderate lymphocytic and suppurative tracheo-bronchoadenitis, tracheitis, and rhinitis. In the other organs, there were no significant changes.

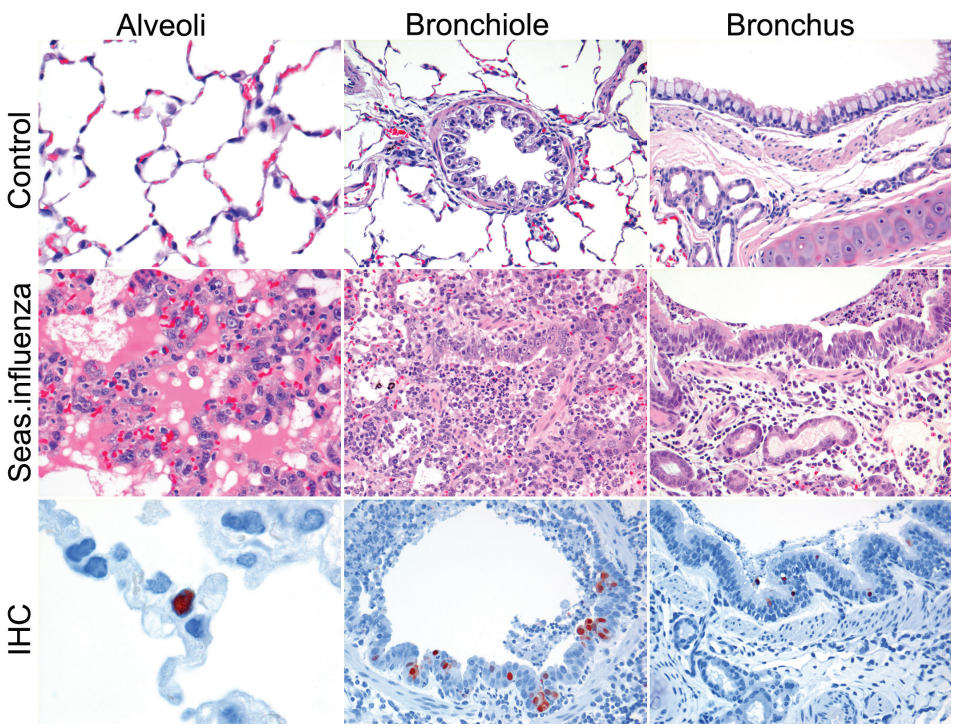

Figure 2. *Histology (HE) and immunohistochemistry (IHC) in the lungs of ferrets inoculated with different seasonal influenza viruses. Top row: uninfected control ferret. No lesions. Middle row: representative slide of a ferret infected with seasonal human influenza virus. Alveoli; in the alveolar lumina there is flooding with edema fluid, fibrin, and cellular debris mixed with alveolar macrophages, neutrophils, and erythrocytes. Bronchiole; representative slide of a ferret infected with seasonal human influenza virus. There is multifocal epithelial necrosis with moderate infiltrates of neutrophils, and in the bronchiolar lumen there are moderate numbers of macrophages, neutrophils, and erythrocytes, mixed with fibrin, edema fluid, and cellular debris. Bronchus; representative slide of a ferret infected with seasonal human influenza virus. In the bronchial lumen there are moderate numbers of neutrophils mixed with fibrin, edema fluid, and cellular debris. Bottom row: representative slide of a ferret infected with seasonal human influenza virus. Alveoli; IHC demonstrated expression of influenza virus antigen in a type II pneumocyte. Bronchiole; representative slide of a ferret infected with seasonal human influenza virus. IHC demonstrated expression of influenza virus antigen in bronchiolar epithelial cells. Bronchus; representative slide of a ferret infected with seasonal human influenza virus. IHC demonstrated expression of influenza virus antigen in bronchial epithelial cells.*

Semi-quantitative histological scoring of the respiratory tract showed that the alveolar, bronchiolar, and bronchial lesions were comparable among the viruses (Figure 3A), except for the bronchi where the scores were significantly higher in the H3/68 group when compared to the H1/78 (P = 0.049) and the H3/08 (P = 0.043) group. The differences in histologic scoring of the alveoli and bronchioles were not statistically significant.

Immunohistochemistry

By immunohistochemistry, influenza virus antigen expression was visible as diffuse to granular red staining, which usually was stronger in the nucleus than in the cytoplasm. Influenza virus antigen expression was closely associated with the presence of histologic lesions at different levels of the

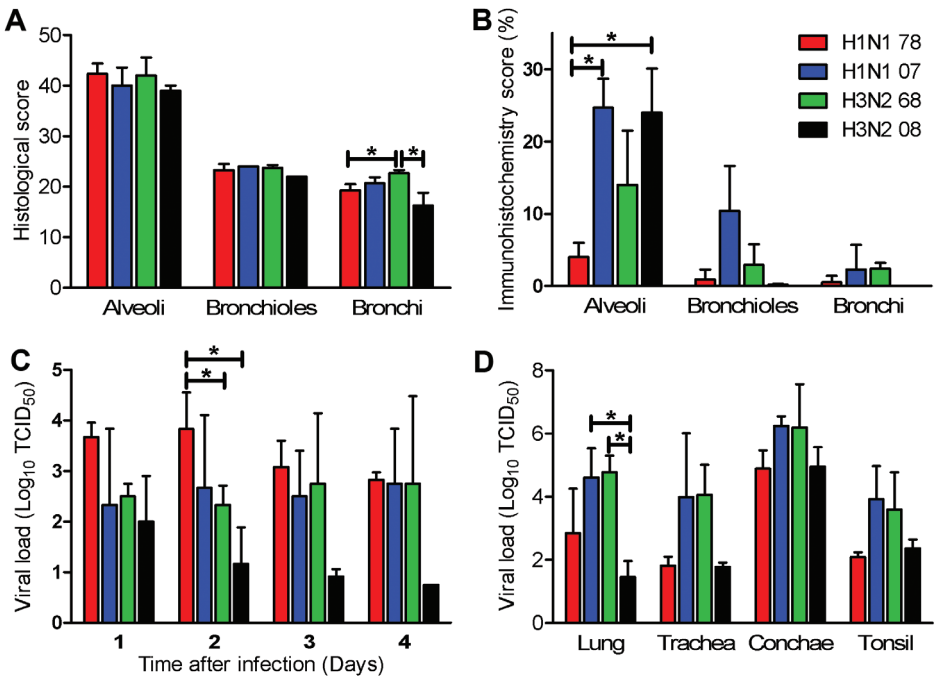

Figure 3. *(A) Histologic scoring of the lungs of ferrets infected with recent and old H1N1 and H3N2 seasonal human influenza viruses. Asterisks indicate that values differ significantly between the groups (P = 0.049 and P = 0.043, respectively). (B) Immunohistochemical scores of influenza-antigen-expressing cells in the lungs of ferrets infected with recent and old H1N1 and H3N2 seasonal human influenza viruses. Asterisks indicate that values differ significantly between the groups (P = 0.021 and P = 0.005, respectively). (C) The viral load of pharyngeal swabs taken from ferrets infected with recent and old seasonal human influenza viruses from 1 to 4 dpi. The limits of detection of the assay were assigned a value of 0.75 TCID50/gram tissue. Asterisks indicate that values differ significantly between the groups (P = 0.049 and P = 0.011, respectively). (D) The viral load of respiratory tissues from ferrets infected with recent and old seasonal human influenza viruses at 4 dpi. The limits of detection of the assay were assigned a value of 0.75 $TCID_{50}$/gram tissue. Asterisks indicate that values differ significantly between the groups (P = 0.013 and P = 0.001, respectively).*

lower respiratory tract. Influenza virus antigen expression was seen predominantly in type I and II pneumocytes, alveolar macrophages, bronchiolar epithelial cells, and bronchial epithelial cells (Figures 8-10). In the nose, variable numbers of epithelial cells expressed viral antigen that was more present in the H1/07 and H3/08 groups.

Semi-quantitative scoring showed that, in the alveoli, the expression of viral antigen was significantly higher in the H1/07 group ($P = 0.005$) and the H3/08 group ($P = 0.021$) than in the H1/78 group (Figure 3B). In the bronchioles and bronchi, the differences were not statistically different. None of the ferrets had influenza virus antigen expression in extra-respiratory tissues.

Virology

In the pharyngeal swabs of all ferrets there was excretion of virus up to 4 dpi, except for H3/08 with excretion up to 3 dpi. During the 4 days there was not a clear peak in virus excretion (Figure 3C). Virus excretion was significantly higher in the H1/78 group when compared to the H3/68 ($P = 0.049$) and H3/08 ($P = 0.011$) groups. At 4 dpi, in the lungs, the virus titers were significantly

higher in the H1/07 and H3/68 groups when compared to the groups infected with H3/08 (respectively, $P = 0.013$ and 0.001) (Figure 3D). The differences in virus titers between the other tissues and groups were not statistically significant. In the bronchial lymph nodes, the virus titer was below the detection limit of 0.75 $TCID_{50}$ per gram tissue. In non-respiratory organs, 1 ferret inoculated with H1/07 virus had virus in the heart ($10^{1.6}$ $TCID_{50}$/g tissue) and 7 animals had virus in the brain: 2 animals in both the H1/07 and H1/78 and all animals in the H3/68 group (range, $10^{1.0}$-$10^{2.1}$ $TCID_{50}$/g tissue). No virus was detected in other tissues.

DISCUSSION

In this study, we show that our experimental procedure of using a seasonal influenza virus inoculum of 10^9 $TCID_{50}$ via the intratracheal route consistently causes a moderate to severe pneumonia in ferrets. Co-localization of histologic lesions with virus antigen expression confirms that the lesions are caused by influenza virus infection. The histologic character of the lesions in the ferrets – necrotizing broncho-interstitial pneumonia – are comparable to the diffuse alveolar damage seen in human fatal cases of pneumonia from seasonal human influenza virus infection.[296] Therefore, this is a suitable animal model for pneumonia caused by seasonal influenza in humans. In the meantime, seasonal H1N1 has been replaced by pandemic (H1N1) 2009. Previously we have shown that pandemic (H1N1) 2009 caused a more severe pneumonia in ferrets than seasonal H1N1 influenza virus, but not as severe as highly pathogenic avian influenza virus H5N1.[15]

In the present experiment, virus antigen expression was detected in the alveolar epithelial cells as well as the bronchiolar and bronchial epithelial cells. In human cases of seasonal influenza infection, there was rarely virus antigen expression found in the alveolar epithelial cells.[109] Possible explanations for this difference in antigen expression between humans and ferrets include the direct intratracheal inoculation route[292,297] with the high doses of virus in the ferrets, the later stage of disease at which the lung sample usually is taken in humans,[119] the naïve immune status for influenza in ferrets when compared to humans, and a possible difference in tropism.

Our results did not show a difference in the severity of the lesions of H1/78 compared to H1/07 or H3/68 compared to H3/08. This means that this pneumonia model functions as well for recent and for older strains of seasonal influenza viruses. The high dose of the inocula seems to overcome the differences in disease outcomes among different subtypes of the virus, which is visible in lower doses as demonstrated by Svitek et al.[291]

The viral titers in the brain of few ferrets, albeit low, did not correlate with the results of histopathology and immunohistochemistry. Although we did find a slightly increased number of lymphocytes in the meninges and choroid plexus of few ferrets, there was no viral antigen expression by immunohistochemistry as a demonstration of virus-infected cells. Therefore, we cannot confirm virus replication in the brain. One explanation of the presence of virus in the brain could be that it is present in the sample (e.g. in the blood or cerebro-spinal fluid) and not replicating in the neuronal tissue. Another explanation is that virus isolation is more sensitive than immunohistochemistry.

In conclusion, we here demonstrate an animal model for pneumonia from seasonal influenza A virus infection in humans. Regardless of the virus strain used, the results of clinical, pathologic, and virologic analyses were consistent and comparable. This model appears to be suitable for both recent and older strains of H1N1 and H3N2 subtypes and should be useful to test vaccines and antiviral agents against pneumonia from these virus infections.

Acknowledgements

We thank C. van Hagen, R. van Lavieren, L. Leijten, P. van Run, and T. Bestebroer for technical assistance, A. Gomersbach and W. Vos for biotechnical assistance, D. van de Vijver and L. Reperant for statistical assistance and F. van der Panne for figure preparation.

CHAPTER 3

INFLUENZA VIRUS INFECTION IN ANIMAL MODELS

3.5

Comparison of temporal and spatial dynamics of seasonal H3N2, pandemic H1N1 and highly pathogenic avian influenza H5N1 virus infections in ferrets

PloS ONE (2012) 7(8): e42343

JMA van den Brand,[1] KJ Stittelaar,[2] G van Amerongen,[1] L Reperant,[1] L de Waal,[2]
ADME Osterhaus,[1,2] T Kuiken[1]

Department of Virology, Erasmus Medical Centre, Rotterdam, The Netherlands [1]
Viroclinics Biosciences BV, Rotterdam, The Netherlands [2]

ABSTRACT

Humans may be infected by different influenza A viruses—seasonal, pandemic, and zoonotic—which differ in presentation from mild upper respiratory tract disease to severe and sometimes fatal pneumonia with extra-respiratory spread. Differences in spatial and temporal dynamics of these infections are poorly understood. Therefore, we inoculated ferrets with seasonal H3N2, pandemic H1N1 (pH1N1), and highly pathogenic avian H5N1 influenza virus and performed detailed virological and pathological analyses at time points from 0.5 to 14 days post inoculation (dpi), as well as describing clinical signs and hematological parameters. H3N2 infection was restricted to the nose and peaked at 1 dpi. pH1N1 infection also peaked at 1 dpi, but occurred at similar levels throughout the respiratory tract. H5N1 infection occurred predominantly in the alveoli, where it peaked for a longer period, from 1 to 3 dpi. The associated lesions followed the same spatial distribution as virus infection, but their severity peaked between 1 and 6 days later. Neutrophil and monocyte counts in peripheral blood correlated with inflammatory cell influx in the alveoli. Of the different parameters used to measure lower respiratory tract disease, relative lung weight and affected lung tissue allowed the best quantitative distinction between the virus groups. There was extra-respiratory spread to more tissues—including the central nervous system—for H5N1 infection than for pH1N1 infection, and to none for H3N2 infection. This study shows that seasonal, pandemic, and zoonotic influenza viruses differ strongly in the spatial and temporal dynamics of infection in the respiratory tract and extra-respiratory tissues of ferrets.

INTRODUCTION

Humans may be infected with different categories of influenza A virus—seasonal, pandemic, and zoonotic—each with their own epidemiology and pathogenesis. Seasonal influenza viruses cause annual epidemics during autumn and winter in temperate regions. They predominantly cause upper respiratory tract disease with rare extension to the lower respiratory tract, resulting in severe and even fatal pneumonia.[119] Pandemic influenza viruses, like the pandemic H1N1 (pH1N1) virus in 2009, cause sporadic pandemics with variable mortality. In fatal cases of pH1N1 infection, virus antigen expression occurred throughout the respiratory tract and was associated with both upper and lower respiratory tract disease.[109] Zoonotic influenza viruses, such as highly pathogenic avian influenza (HPAI) H5N1 virus, are sporadically transmitted from poultry and other animals to humans, but do not transmit efficiently from human to human.[106] Human infection with HPAI H5N1 virus involves primarily the lower respiratory tract, resulting in diffuse alveolar damage (DAD) and a fatality rate of almost 60% in confirmed cases.[298]

The pathogenesis of both human and avian influenza virus infections in ferrets resembles that in humans.[297] In part, this is because the distribution of receptors for human and avian influenza viruses in the respiratory tract of ferrets is similar to that in humans.[125] Therefore, the ferret is often used in animal models to study the pathogenesis of different influenza virus strains and to evaluate the efficacy of vaccines and antiviral agents against influenza.[277,283,295,299] In these studies, it is critical to collect respiratory tract samples for virological, pathological, and molecular analyses at both the appropriate time point after infection and the appropriate location along the respiratory tract. This is because influenza virus infection is a highly dynamic process, both temporally and spatially.

We recently compared the pathogenesis of infections with seasonal human H1N1, pH1N1, and HPAI H5N1 virus in ferrets.[295] Our results showed that, at 4 days post inoculation (dpi), pH1N1 caused pneumonia intermediate in severity between that caused by seasonal H1N1 and HPAI H5N1. This was associated with virus replication throughout the lower respiratory tract for pH1N1, while seasonal H1N1 replicated mainly in the bronchi, and HPAI H5N1 replicated mainly in the alveoli. However, the location of virus replication and extent and severity of associated pathological changes were recorded at a single time point. Other experiments have used multiple time points (usually 1, 3, 5, and 14 dpi) to study the dynamics of influenza virus infection in the ferret respiratory tract;[281,299-304] however, these experiments often lacked detailed pathological or virological analyses of samples collected along the full length of the respiratory tract on all time points.

The goal of our study was to describe and compare the temporal and spatial dynamics of different influenza virus infections and associated pathology in the respiratory tract of the ferret. To this end, we inoculated ferrets with either seasonal human H3N2, pH1N1, or HPAI H5N1 virus, and performed detailed virological and pathological analyses at time points from 0.5 to 14 dpi, as well as measuring virus excretion, clinical signs, and hematological parameters. Additionally, we compared the results of histopathological analyses with digital microscopical scoring of tissue sections.

METHODS

Ethics statement

Animals were housed and experiments were conducted in strict compliance with European guidelines (EU directive on animal testing 86/609/EEC) and Dutch legislation (Experiments on Animals Act, 1997). The protocol was approved by the independent animal experimentation ethical review committee of the Netherlands Vaccine Institute (permit number 200900201) and was performed under animal biosafety level 3 conditions. Animal welfare was observed on a daily basis, and all animal handling was performed under light anesthesia using a mixture of ketamine and medetomidine to minimize animal suffering. After handling atipamezole was administered to antagonize the effect of medetomidine.

Virus preparation

Three viruses were used: seasonal H3N2 virus (A/Netherlands/177/2008), isolated from a patient during the 2008 influenza season;[305] pandemic (H1N1) 2009 virus (pH1N1) (A/Netherlands/602/2009), isolated from a specimen of a human patient who had recently visited Mexico during the pandemic in 2009;[152] and HPAI H5N1 virus (A/Indonesia/5/2005) as described earlier.[152] The H3N2 virus was chosen as a representative from a recent seasonal H3N2 influenza epidemic. Like virtually all recent H3N2 viruses the present virus exhibits the oseltamivir-sensitive neuraminidase-associated agglutination of turkey erythrocytes.[306] The pH1N1 virus which had been initially isolated in embryonated chicken eggs was chosen as a representative virus from the 2009 pandemic because it has been used in previous experiments by others[264] and ourselves.[152,292,307] The H5N1 virus was chosen as a representative of Clade 2 (subclade 1.3.2) of HPAI H5N1 virus, and has been used in several previous experiments.[292,308] The different isolates were passaged three times in Madin-Darby Canine Kidney (MDCK) cells and titrated according to standard methods. Subsequently, the viruses were clarified and reached an infectious virus titer of 1 x $10^{7.4}$ median tissue culture infectious dose (TCID50) per ml for H3N2 virus, and 1 x $10^{7.8}$ $TCID_{50}$ for both pH1N1 and H5N1 virus.[277,279]

The inoculum for the control group was prepared as follows: MDCK cells were grown up to a monolayer of 80 to 90 % in two 75 cm2 flasks (A and B). Virus medium (EMEM supplemented with HEPES, Sodium bicarbonate, BSA fraction V, L-glutamin, penicillin, streptomycin, trypsin and amphothericin-B) was added and the cells were incubated for 2 days at 37˚C. To mimic cellular damage in MDCK cells during virus infection when preparing the virus stock we aimed to reach a cytopathic effect (CPE) of 75%. Therefore, the cells in bottle B were collected by disrupting the monolayer with 3 mm glass beads (VWR, Amsterdam, The Netherlands), sonication (3 times 20 seconds in melting ice) and freezing at -80˚C, leading to lysis of all cells. The cells in bottle A were not damaged and the final inoculum consisted for 25% of the supernatant of bottle A and for 75% of the supernatant of bottle B.

Study design

For every virus and the sham inoculated group, 7 groups (5 groups for H5N1) of four ferrets were inoculated under anesthesia with ketamine (4-8 mg/kg; Nimatek, Eurovet Animal Health B.V., Bladel, The Netherlands) and medetomidine hydrochloride (0.1 mg/kg; Domitor, Orion Pharma, Espoo, Finland) with each of these three viruses with 10^6 $TCID_{50}$ in a 3-ml volume intra-tracheally and in a 0.3-ml volume intranasally evenly divided over the two nostrils. Intratracheal and intranasal inoculation was performed to ensure that the inocula would reach both the lower and the upper respiratory tract.[292,308] After inoculation, the ferrets received atipamezole hydrochloride (0.5 mg/kg Antisedan; Orion Pharma, Espoo Finland) and were monitored daily for clinical signs until maximally 14 dpi.[277] The animals were predestined to be sacrificed at 12 hours (0.5 day), 1, 2, 3, 4, 7 and 14 dpi (for H5N1 not at 7 and 14 dpi) in order to avoid any bias that could follow from clinical observation, or earlier when they were moribund before the selected time point of euthanasia (H5N1 only). The animals were euthanized by exsanguination after anesthesia with ketamine. At euthanasia, body weight was measured, nose, throat and rectal swabs were collected, blood was taken, and samples were taken from both respiratory and extra-respiratory tissues for virological, pathological, and immunohistochemical analyses.

The inoculum used for the sham control group induced comparable body weight loss, affected lung tissue, histological scores, digital scoring, and leucocyte counts as the H3N2 group. As an extra comparison, we therefore used non-inoculated healthy ferrets with the same age and background as the other ferrets as negative control animals to score and compare the above parameters.

Ferrets

Ferrets were used in this experiment since they resemble disease in humans when infected with influenza A viruses.[283,297] Hundred-and-four eleven-month-old purpose-bred ferrets, seronegative for antibodies against circulating influenza viruses H1N1 (A/Brisbane/059/2007), H3N2 (A/Uruguay/716/2007), and B: B/Brisbane/60/2008), and pH1N1 (A/Netherlands/602/2009), H5N1 (A/Indonesia/02/2005) and Aleutian disease virus, were maintained in standard housing, and provided with commercial food pellets and water. All ferrets were male (body weight: 1 302 to 2 150 g). Approximately three to four weeks prior to infection, the animals were anesthetized with ketamine and medetomidine hydrochloride, and a temperature logger (DST micro-T ultra small temperature logger; Star-Oddi, Reykjavik, Iceland) was placed in the peritoneal cavity. This device recorded the body temperature of the animals every 10 min. Effect of virus infection on

body temperature was based on changes in the daily average of the maximum body temperatures of the ferrets per virus group.

Clinical scores in all groups were assessed every day. Activity status was scored as follows: 0, alert and playful; 1, alert and playful only when stimulated; 2, alert but not playful when stimulated; 3, neither alert nor playful when stimulated. For diarrhea, sneezing, nasal and conjunctival discharge, inappetence and dyspnea we scored: 0, not present; 1, present.[281] Inappetence was measured by the amount of food that was still present in the cages at the time of feeding. As a control we also assessed the amount of food that was present in the stomach and intestine of the animals on the day of necropsy. Dyspnea was characterized by open-mouth breathing with exaggerated abdominal movement. Additionally, we used four eleven-month-old purpose-bred ferrets, seronegative for antibodies against circulating influenza viruses H1N1 (A/Brisbane/059/2007), H3N2 (A/Uruguay/716/2007), and B: B/Brisbane/60/2008), and pH1N1 (A/Netherlands/602/2009), H5N1 (A/Indonesia/02/2005) and Aleutian disease virus. The four ferrets were euthanized immediately by the same method as described above and necropsied to provide control data of non-inoculated ferrets, and blood was taken blood for hematologic analyses and respiratory tract tissues for histopathological scoring.

Pathology

For every virus four animals per time point were euthanized by exsanguination under ketamine/medetomidine anesthesia at 12 hours (0.5 day), 1, 2, 3, 4, 7 or 14 dpi and were necropsied according to a standard protocol. The trachea was clamped off to prevent the lungs from deflating upon opening the thoracic cavity, allowing visual estimation of the area of affected lung parenchyma. The lungs were weighed and the relative lung weight was calculated by the following formula: (lung weight on day of death/ body weight on day of death)*100, and presented as percentage. The following tissues were collected for histological examination: left lung, left nasal concha, nasal septum, larynx, trachea, bronchus, tracheo-bronchial lymph node, left tonsil, heart, liver, spleen, kidney, pancreas, duodenum, jejunum, colon, adrenal gland, left olfactory bulb and left brain (cerebrum and cerebellum). Lung samples were taken in a standardized way, not guided by changes as seen in the gross pathology. Tissues were stored in 10 % neutral-buffered formalin (lungs after careful inflation with formalin), embedded in paraffin, sectioned at 4 μm, and stained with hematoxylin and eosin (HE) for examination by light microscopy.

Semiquantitative assessment of influenza virus-associated inflammation in the lung (four slides with longitudinal section or cross-section of cranial or caudal lobes per animal) was performed on every slide as reported earlier:[295] for the extent of alveolitis and alveolar damage we used: 0,0 %; 1, 1-25 %; 2, 25-50 %; 3, > 50 %. For the severity of alveolitis, bronchiolitis, bronchitis, and tracheitis we scored: 0, no inflammatory cells; 1, few inflammatory cells; 2, moderate numbers of inflammatory cells; 3, many inflammatory cells. For the presence of alveolar edema, alveolar hemorrhage, and type II pneumocyte hyperplasia we scored: 0, no; 1, yes. Finally, for the extent of peribronchial, peribronchiolar, and perivascular infiltrates we scored: 0, none; 1, one to two cells thick; 2, three to ten cells thick; 3, more than ten cells thick. Slides were examined without knowledge of the treatment allocation of the animals. The cumulative scores for size and severity of inflammation of all slides provided the total score per animal.

To assess the number of neutrophils and alveolar macrophages in the alveolar lumina and the number of neutrophils in the alveolar walls, we counted them in 5 arbitrarily chosen 100x objective

fields per HE-stained slide, with a total of 20 fields per animal. Neutrophils were identified on the basis of their size (approximately 12 to 15 μm in diameter) and the morphology of their nucleus (heterochromatic and segmented, with 3 to 5 lobes joined by thin strands). Neutrophils in the alveolar walls were counted when present in small capillaries, but were excluded if present in larger blood vessels. Pulmonary alveolar macrophages were identified on the basis of their morphology and location: large, oval to round cells with a distinct cell border, foamy cytoplasm and large, oval to bean-shaped nucleus, located in the alveolar lumen separate from the alveolar wall.[309]

Immunohistochemistry

For detection of influenza A virus antigen, tissues were stained with a primary antibody against the influenza A nucleoprotein as described previously.[305] In each staining procedure, an isotype control was included as a negative control and a lung section from a cat infected experimentally with H5N1 was used as positive control.[310]

Semiquantitative assessment of influenza virus antigen expression in the lungs was performed as reported earlier:[292] for the alveoli, twenty-five arbitrarily chosen, 20x objective, fields of lung parenchyma of four lung sections were examined by light microscopy for the presence of influenza virus nucleoprotein, without the knowledge of the identity of the animals. The cumulative scores for each animal were presented as number of positive fields per 100 fields. For the nose, trachea, bronchi and bronchioles, the percentage of positively staining epithelium was estimated on every slide and the average of the four slides was taken to provide the score per animal: 0, 0 %; 1, 1-25 %; 2, 25-50 %; 3, > 50 %.

For computerized scoring of slides we used the cross-section of the left caudal lung of all animals to make a digital scan using the NanoZoomer with accompanying software (NanoZoomer Digital Pathology and NDP.scan and NDP.view, Hamamatsu, Higashi-ku, Hamamatsu City, Japan). Of every scan, 20 pictures of the alveoli were made in a randomized order with the 20x objective. From every picture, we calculated: the quantity of tissue (visualized in blue staining) and the quantity of red staining consistent with virus antigen expression using Zeiss KS 400 version 3.0 image analysing system (Carl Zeiss Vision GmbH, Eching, Germany). The images were 1024 X 768 pixels with 0.455 μm per pixel. The percentage of air-containing space present in the pulmonary tissue was calculated as 100% minus the total percentage of pulmonary tissue (blue staining) that was present in the pictures. The quantity of virus replication was calculated either as the percentage of antigen expression (red staining) relative to quantity of tissue (blue staining), or as the number of times red staining was detected in a picture.

Virology

After collection on day 0 and the day of euthanasia, nose, pharyngeal and rectal swabs were collected in virus transport medium (EMEM containing bovine serum albumin (fraction V), penicillin, streptomycin, amphothericin-B, L-glutamine, sodium bicarbonate and Hepes), aliquotted and stored at -70°C. Upon necropsy, samples were collected from the following tissues: nasal concha, trachea, bronchus, tracheo-bronchial lymph node, tonsil, heart, liver, spleen, kidney, pancreas, duodenum, jejunum, colon, adrenal gland, olfactory bulb and brain. Specifically from the lungs, sections of the cranial, median and caudal lobe of the right lung and of the accessory lobe from each animal were collected and pooled (total average weight of about 0.4-0.5 g/animal); lung samples were taken in a standardized way, not guided by changes as seen in the gross pathology. Tissue samples were

homogenized with a FastPrep-24 (MP Biomedicals, Eindhoven, The Netherlands) in influenza infection medium (EMEM containing bovine serum albumin (fraction V), penicillin, streptomycin, amphothericin-B, L-glutamine, sodiumbicarbonate, Hepes and trypsin) and centrifuged briefly before titration. Quadruplicate 10-fold serial dilutions of tissue and swab supernatants were used to determine the virus titers in confluent layers of MDCK cells as described previously.[279]

Hematologic analyses

On day 0 and the day of euthanasia (0.5, 1, 2, 3, 4, 7 or 14 dpi or when an animal was sacrificed due to a moribund state) blood was collected from the euthanized animals. Total leucocyte counts were determined in blood collected in EDTA Vacutainer tubes (Vacuette, Greiner Bio-One GmbH, Kremsmünster, Austria) using an automated hematology analyser Sysmex pocH-100i (Sysmex Europe GMBH, Norderstedt, Germany). Thin blood films were prepared from EDTA blood and stained with May-Grünwald-Giemsa (Merck, Darmstadt, Germany). Differential cell counts were obtained by counting 100 cells per slide, and the numbers of lymphocytes, mononuclear cells, blastocytes, rod-shaped neutrophils, segmented neutrophils, eosinophils, basophils and normoblasts were calculated by multiplying these percentages by the leucocyte counts obtained for the same sample. By using the total leucocyte counts we calculated the absolute number of different leucocytes in 10^9/L.

Statistical analysis

The non-parametric Mann-Whitney test was used to compare several parameters of the different virus infection per day for; percentage of affected lung tissue, relative lung weight, extent and severity of alveolitis and alveolar damage, percentage of air containing space in pulmonary tissue, virus titers in lung tissue, antigen expression in the alveoli by immunohistochemistry, percentage of antigen expression in the alveoli by digital scoring, and number of antigen expression counts in the alveoli by digital scoring. The outcomes were considered significant when $P < 0.05$.

Generalized linear models (GLM) were used to determine the most appropriate predictors of viral excretion for each virus, based on viral production and damage in the respiratory tract. These models were used to determine the linear equations of the form $y=\sum(a_i x_i + b_i)$ that best fit the data, where y is viral excretion, x_i is a predictor, and ai and b_i are the predictor and intercept coefficients, respectively. Viral excretion was measured as the sum of nasal swab and pharyngeal swab viral titers. Predictors initially included in the models were measures of viral production and measures of damage in upper (nose and trachea) and deeper regions of the respiratory tract (bronchi, bronchioles and alveoli), as well as all two-ways interactions. Measures of viral production for each region were calculated as the product of the viral titers and immunohistochemistry scores in the respective regions. This was done to take into account the fact that virus isolated in a particular region of the respiratory tract may not be produced locally. Measures of damage for each region were calculated as the sum of the severity scores in the respective regions. The severity scores were used because they were similarly assessed in all regions of the respiratory tract. Only predictors or interactions of predictors with $P < 0.05$ were retained in the final GLM.

RESULTS

Seasonal H3N2

Clinical data and gross pathology

The survival rate was 100 % in all groups. Clinical signs (Table 1, p 160) were mild with sneezing from 2 to 14 dpi and nasal discharge from 2 to 3 dpi, as shown by increased licking on the nose. Nasal and pharyngeal swabs revealed excretion of virus from 0.5 to 4 dpi with a peak on 1 dpi in the nasal swabs (Figure 1A and B). The mean body temperature was slightly raised on 2 dpi (Figure 1C) and the mean body weight loss was around 10 % (Figure 1D). On gross pathology, a few dark red and raised areas were seen in the lungs of some animals and were consistent with mild pulmonary consolidation. Estimated areas of lung affected ranged from 0 to 10 % (Figure 2A) between 0.5 and 14 dpi. The relative lung weight was comparable to that of non-infected ferrets (Figure 2B). There was a mild splenomegaly from 0.5 to 14 dpi (data not shown). The trachea-bronchial lymph nodes were slightly enlarged between 0.5 and 4 dpi, with a peak on 2 dpi (Table 1, p 160).

Histopathology and virus antigen expression

By histopathology, there was a mild to severe multifocal rhinitis with necrosis of the epithelium and mild multifocal tracheitis. In the lungs, there was a mild multifocal bronchitis and bronchiolitis with intra-epithelial neutrophils, mild peribronchiolar and perivascular cuffing, mild broncho-adenitis, and mild multifocal alveolitis with mild intra-epithelial infiltration of neutrophils with mild epithelial necrosis and mild edema in the alveolar lumina. By immunohistochemistry, influenza virus antigen expression was visible as diffuse to granular red staining, which usually was stronger in the nucleus than in the cytoplasm (Figures 3 to 8). Antigen expression in the nose was present from 0.5 to 4 dpi, while no antigen expression was seen in the tracheal, bronchial, bronchiolar, and tracheo-bronchial glandular epithelium at any time point, and little antigen expression in few type II pneumocytes in the alveoli. Changes in the histological lesions and antigen expression over time are described in the supporting information (Supporting information S1, p 155).

Semiquantitative histological scoring (Table 2, p 162) showed that the extent and severity of the alveolar lesions were comparable for all days of sampling with no obvious changes. No expression of virus antigen was seen in extra-respiratory tissues on any days. By digital scoring, there was on average 63 to 73 % of air in the pulmonary tissue (Table 3, p 164). Additionally, the percentage of antigen-expressing tissue and counts of virus antigen expression were absent and negligible, respectively (Table 3, p 164).

Virology of tissues

Comparable with the pattern of antigen expression in the respiratory tissues, high virus titers were seen in the nasal concha from 0.5 to 4 dpi with a peak on 1 dpi (Figure 3). Low virus titers were present in the trachea, bronchi, lungs, tracheo-bronchial lymph nodes and tonsil (Figure 3 and Table, p 166). All other tissues did not contain replication competent virus.

Hematology and comparison of leucocytes in blood and alveolar lumina

Total leucocyte counts after infection were slightly increased on all days except for 14 dpi compared to those in negative control animals (Table 5 , p 168). In blood, there was a slight increase in the number of mononuclear cells on 1 dpi and of neutrophils on 2 dpi, followed by a mild decrease up to 4 dpi after which again a small increase of both was observed (Figure 9). In the alveolar lumina,

the number of mononuclear cells was only slightly increased on 2 dpi (Figure 8).

Generalized linear model of viral excretion

We used generalized linear models (GLM) to define possible predictors of viral excretion, based on viral production and damage scores in upper (nose and trachea) and deeper regions of the respiratory tract (bronchi, bronchioles and alveoli). These models were used to determine significant linear relationships between these scores and viral excretion (as measured by viral titers in nose and throat swabs; see methods). The final GLM predicting excretion of H3N2 included only viral production in the upper regions of the respiratory tract as a significant predictor (LR $\chi^2 = 16.8$, df = 1, $P < 0.0001$). Excretion of H3N2 was a positive linear function of viral production in the upper regions (Table 6, p 170). As such, viral excretion of H3N2 could be directly estimated based on viral production scores in the nose and trachea, strongly suggesting that these regions were the main sources of excreted virus.

Pandemic H1N1

Clinical data and gross pathology

The survival rate was 100 %. Clinical signs per group were observed from 2 to 14 dpi (Table 1, p 160). The activity status varied over the different time points with the highest score (status 3) seen in one animal between 5 and 8 dpi. Dyspnea was seen only in this animal. Inappetence, sneezing and nasal discharge was seen in all animals. Virus excretion was shown in nasal and pharyngeal swabs with a peak on 1 dpi and higher values in the nasal swabs (Figure 1A). The virus titers for the pharyngeal swabs were comparable to those of the animals inoculated with H3N2 (Figure 1B). An increase in body temperature was seen with a peak on 1 dpi (Figure 1C). The mean body weight loss was up to 15 % on 7 dpi (Figure 1D). By gross pathology, multifocal pulmonary consolidation was seen on 0.5 dpi with grey-red raised, and slightly firmer than normal areas. On 1 dpi, the percentage of affected lung tissue was increased (Figure 2A). On 2 dpi the lesions were dark red and firmer with increased relative lung weight. On 14 dpi the percentage of affected lung tissue decreased again (Figure 2A). The relative lung weight was increased from 1 to 7 dpi and decreased on 14 dpi (Figure 2B). The trachea-bronchial lymph nodes were enlarged from 0.5 to 7 dpi, with a peak on 7 dpi (Table 2, p 162). There was a mild splenomegaly from 0.5 to 14 dpi (data not shown).

Histopathology and virus antigen expression

By histopathology, there was a mild to severe multifocal rhinitis with necrosis of the epithelium and mild to moderate multifocal tracheitis. In the lungs, there was a mild to severe multifocal bronchitis and bronchiolitis with intra-epithelial and intraluminal neutrophils, mild to severe necrosis of epithelium, mild to severe peribronchiolar and perivascular cuffing, mild to severe broncho-adenitis, and mild to severe multifocal alveolitis with infiltration of neutrophils in alveolar walls and lumina, mild to moderate epithelial necrosis and mild to moderate edema in the alveolar lumina with hypertrophy and hyperplasia of epithelium (Figures 10 and 11). The tracheo-bronchial lymph nodes and tonsils demonstrated lymphadenopathy, and in the palatine roof of two animals there was severe inflammation and necrosis of the sero-mucous glands.

Antigen expression in the nose was present from 0.5 to 7 dpi starting on 0.5 dpi in the respiratory epithelium and on 1 dpi in the olfactory epithelium. In the trachea there was antigen expression from 0.5 to 6 dpi and in the bronchi and bronchioles from 0.5 to 7 dpi with peak values on 1 dpi.

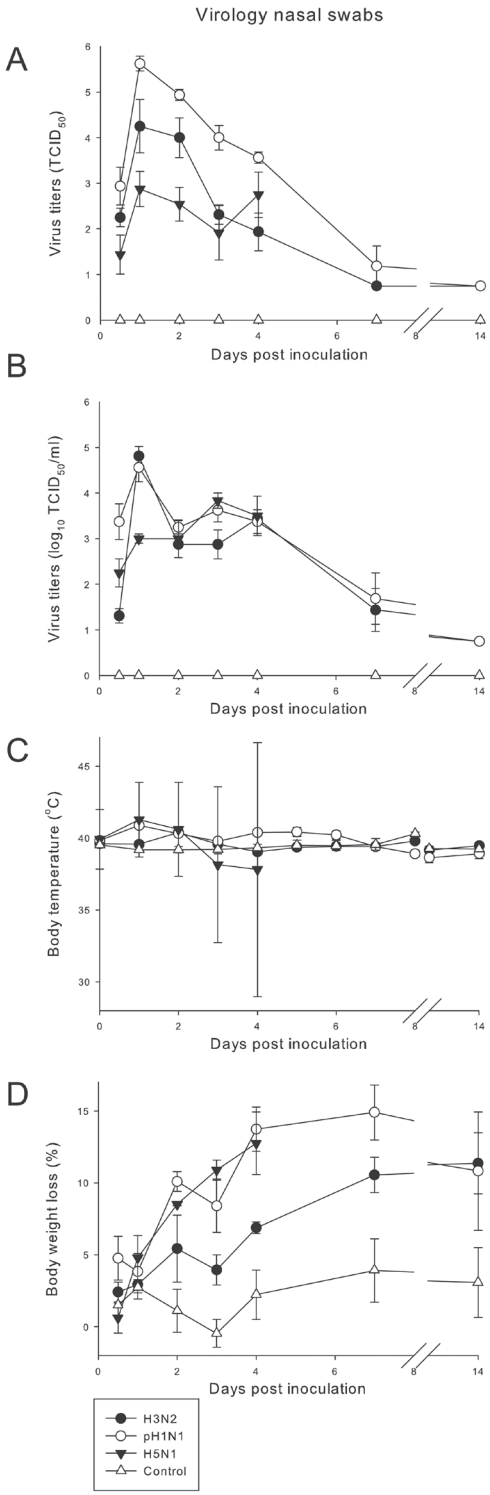

Figure 1. *Clinical data of ferrets inoculated with different influenza viruses. The data are depicted as median values and standard errors of the mean (SEM). (A) Virus titers in nasal swabs demonstrate highest titers for pH1N1, intermediate titers for H3N2 and lowest titers for H5N1. (B) Virus titers in pharyngeal swabs demonstrate initially comparable virus titers for pH1N1 and H3N2 and lower titers for H5N1, and on 4 dpi comparable titers for pH1N1 and H5N1 and lower titers for H3N2. (C) Body temperatures in ferrets inoculated with pH1N1 and H5N1 are higher than for H3N2 and the sham-inoculated group. The large SEM for H5N1 is due to the low body temperatures of moribund animals. (D) Body weight loss in animals inoculated with pH1N1 and H5N1 was comparable and higher when compared to H3N2.*

Bronchial glandular epithelial cells expressed virus antigen with often more expression in glandular cells than in bronchial epithelial cells. In the alveoli there was antigen expression in type II pneumocytes and less in type I pneumocytes and alveolar macrophages from 0.5 to 7 dpi with highest values on 1 dpi. The high values decreased after 1 dpi consistent with the severe damage of the epithelium. The tracheo-bronchial lymph nodes and tonsils did not express virus antigen while glandular epithelial cells in the palatine roof of two animals did express antigen on 7 dpi. There was no virus antigen expression in extra-respiratory tissues. Changes in the histological lesions and antigen expression over time are described in the supporting information (Supporting information S1, p 155).

Digital scoring demonstrated that the amount of air-containing tissue was comparable for all days with averages between 63 and 77 % (Table 3, p 164). When digital scoring for antigen expression was performed, antigen expression as well as the number of positive counts showed that virus antigen was clearly present on 0.5 dpi with peak scores on 1 dpi, albeit with high variation between the different animals (Table 3, p 164).

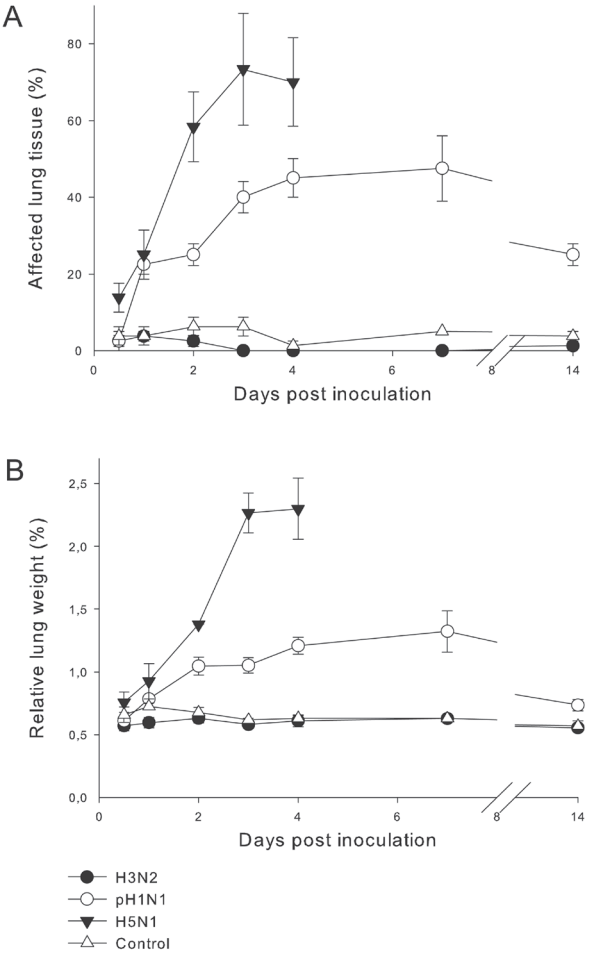

Figure 2. *Gross pathology of the lungs of ferrets inoculated with different influenza viruses. The data are depicted as median values and standard errors of the mean. (A) Percentages of affected lung tissue show highest values for H5N1, intermediate values for pH1N1 and lowest values for H3N2. (B) Percentages relative lung weight show highest values for H5N1, intermediate values for pH1N1 and lowest values for H3N2.*

Virology

In the respiratory tissues, the changes in virus titers over time showed a comparable pattern to that of viral antigen expression, with high virus titers from 0.5 to 4 dpi (Figure 3). In the extra-respiratory tissues, virus was isolated from the olfactory bulb, cerebellum, cerebrum, and heart (Table 4, p 166).

Hematology and comparison of leucocytes in blood and alveolar lumina

Total leucocyte counts showed higher values on all time points when compared to those from negative control animals (Table 5, p 168). On 1 dpi, there was an increase of neutrophils in the blood and in the alveoli. On 2 dpi, there was a severe decrease in the number of neutrophils in the alveoli, but the number of neutrophils in the blood remained high. The number of mononuclear cells in the alveoli increased during the first 3 days while the number of mononuclear cells in the blood decreased. On 14 dpi, the numbers of neutrophils and mononuclear cells were decreased in both the blood and the alveoli.

Generalized linear model of viral excretion

Similarly to H3N2, the final GLM predicting excretion of pH1N1 included only viral production in the upper regions of the respiratory tract (nose and trachea) as a significant predictor (LR $\chi^2 = 58.9$, df = 1, $P < 0.0001$). Excretion of pH1N1 was a positive linear function of viral production in the upper regions (Table 6, p 170).

H5N1

Clinical data and gross pathology

On 2.5 dpi, one animal died and one animal was euthanized because of its moribund state. On 3 dpi, another animal died. From 2 to 4 dpi all animals developed severe clinical signs characterized by decreased activity, dyspnea, and inappetance (Table 1, p 160). Two animals showed nervous signs, characterized by ataxia, drifting to the right, walking into a corner and aggression. Virus was excreted in nasal and pharyngeal swabs, with lower virus titers than the pH1N1 and H3N2 groups during the first 3 days for the nose and the first 2 days for the pharynx (Figures 1A and B). In contrast to what was seen in the other virus groups, the nasal swabs showed lower titers than the pharyngeal swabs. This indicated lower replication in the nose, as was also suggested by the low levels of virus antigen expression and low virus titers in the nose (Figure 3). The increase in body temperature showed a peak on 1 dpi. At later time points, the average temperature decreased below baseline values due to the progressively moribund state of most of the ferrets (Figure 1C). The body weight loss increased during time and was comparable to that of the pH1N1 group (Figure 1D). By gross pathology, there was multifocal pulmonary consolidation on 0.5 dpi with dark red, raised, and firmer than normal areas affecting an average of 13% of the lung tissue (Figure 2A). On 1 dpi, there was fluid in the bronchi and lung parenchyma, and the percentage of affected lung tissue was increased. On 2 dpi, the percentage of affected lung tissue had increased dramatically to almost 60% (Figure 2A). The relative lung weights were increased on all time points and were much higher than in the other virus groups (Figure 2B). Tracheo-bronchial lymph nodes were enlarged starting on 0.5 dpi, and up to two times the normal size on 4 dpi. There was a mild splenomegaly on all days (data not shown).

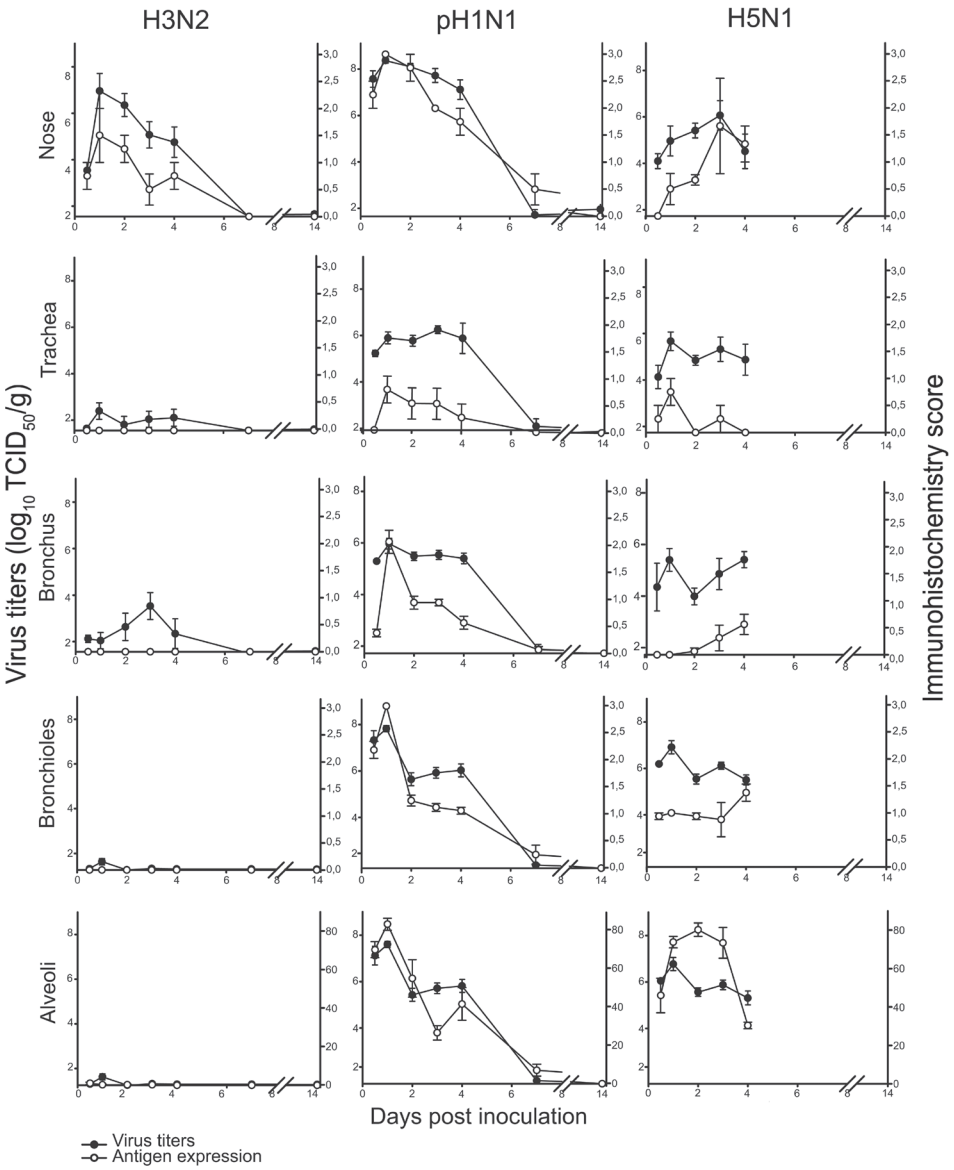

Figure 3. *Virus distribution in the respiratory tracts of ferrets inoculated with different influenza viruses. The data are depicted as median values and standard errors of the mean. Virus titers and antigen expression as demonstrated by immunohistochemistry scores are comparable for ferrets inoculated with H3N2 and pH1N1. Ferrets inoculated with H5N1 have highest antigen expression in the alveoli while virus titers are comparable for all parts of the respiratory tract, suggesting that most virus originated from the lower respiratory tract. The average cut-off values for the respiratory tissues are: nose 1.6 (range 1.3-1.8), trachea 1.6 (1.4-1.9), bronchus 1.6 (range 1.3-2.0) and lung 1.3 (range 0.9-1.4) log_{10} $TCID_{50}$. Immunohistochemistry scores in nose, trachea, bronchi, and bronchioles are scored from 0 to 3, and those in the alveoli are scored as a percentage.*

Histopathology and virus antigen expression

By histopathology, there was a mild to moderate multifocal rhinitis with necrosis of the epithelium and mild multifocal tracheitis. In the lungs, there was a moderate multifocal bronchitis and bronchiolitis, with intra-epithelial and intraluminal neutrophils, mild to moderate epithelial necrosis, and mild peribronchiolar and perivascular cuffing; a mild to severe broncho-adenitis; and a severe multifocal to diffuse alveolitis, with severe epithelial necrosis, intra-epithelial and intraluminal infiltration of neutrophils, severe intraluminal edema, and hypertrophy and hyperplasia of epithelial cells (Figures 4 to 8). The tracheo-bronchial lymph nodes and tonsils demonstrated lymphadenopathy. In the extra-respiratory tissues there was lymphadenopathy in a sternal lymph node and there was hyperplasia and necrosis in the gut associated lymphoid tissue (GALT) of the jejunum and in the spleen of few animals.

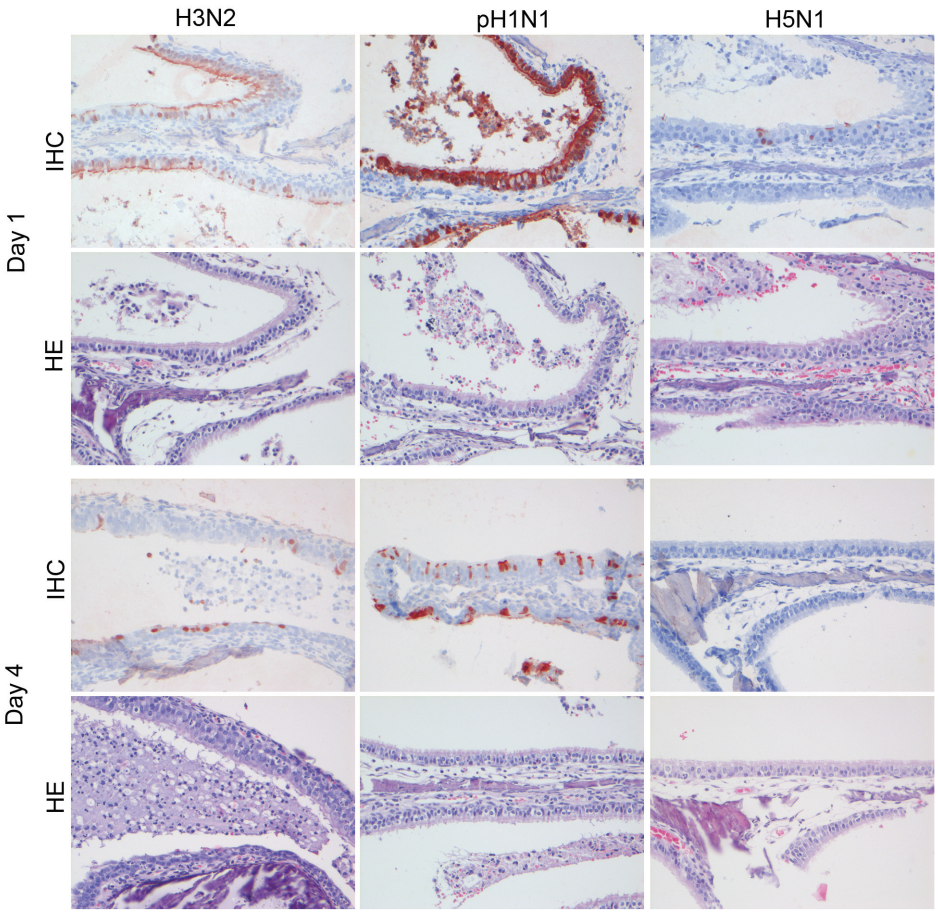

Figure 4. *Antigen expression and histopathology of nasal respiratory epithelium of ferrets inoculated with different influenza viruses. There is high antigen expression with associated lesions characterized by neutrophilic rhinitis in the nasal respiratory epithelium of ferrets inoculated with H3N2 and pH1N1 on 1 dpi and lower expression on 4 dpi, while for H5N1 there is only occasional expression on 1 dpi. HE and immunoperoxidase counterstained with hematoxylin.*

In the nose there was antigen expression from 1 to 4 dpi with highest values on 2 and 3 dpi. Antigen expression in the trachea was present from 0.5 to 3 dpi, predominantly on 1 dpi. The bronchi demonstrated antigen from 2 to 4 dpi, and in the bronchioles from 0.5 to 4 dpi. Antigen expression in the alveoli was present in type II pneumocytes (Figure 8), and less in type I pneumocytes and alveolar macrophages. It was seen from 0.5 to 4 dpi with large percentages from 1 to 3 dpi. In the tracheo-bronchial lymph nodes there was antigen expression from 1 to 3 dpi and in the tonsils on 2 and 3 dpi in mononuclear cells. One animal had virus antigen expression in squamous stratified epithelium in the tip of the nose and one animal showed expression in endothelial cells in the pharynx. In the extra-respiratory tissues there was virus antigen expression in mononuclear cells in the GALT of the jejunum on 2 and 3 dpi and in the spleen on 4 dpi. No antigen expression was seen

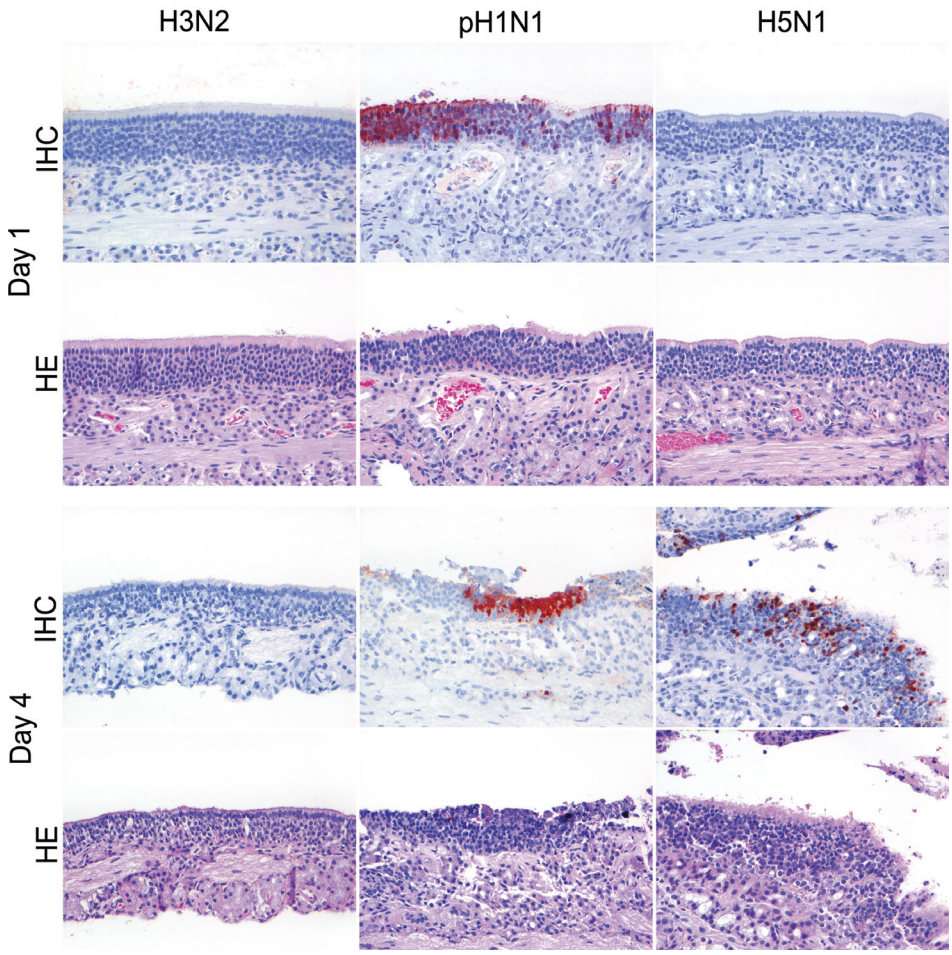

Figure 5. *Antigen expression and histopathology of nasal olfactory epithelium of ferrets inoculated with different influenza viruses. There is high antigen expression with associated lesions characterized by neutrophilic rhinitis in the olfactory epithelium of ferrets inoculated with pH1N1 on 1 and 4 dpi, and for H5N1 only on 4 dpi. There were no antigen expression and no lesions for H3N2. HE and immunoperoxidase counterstained with hematoxylin.*

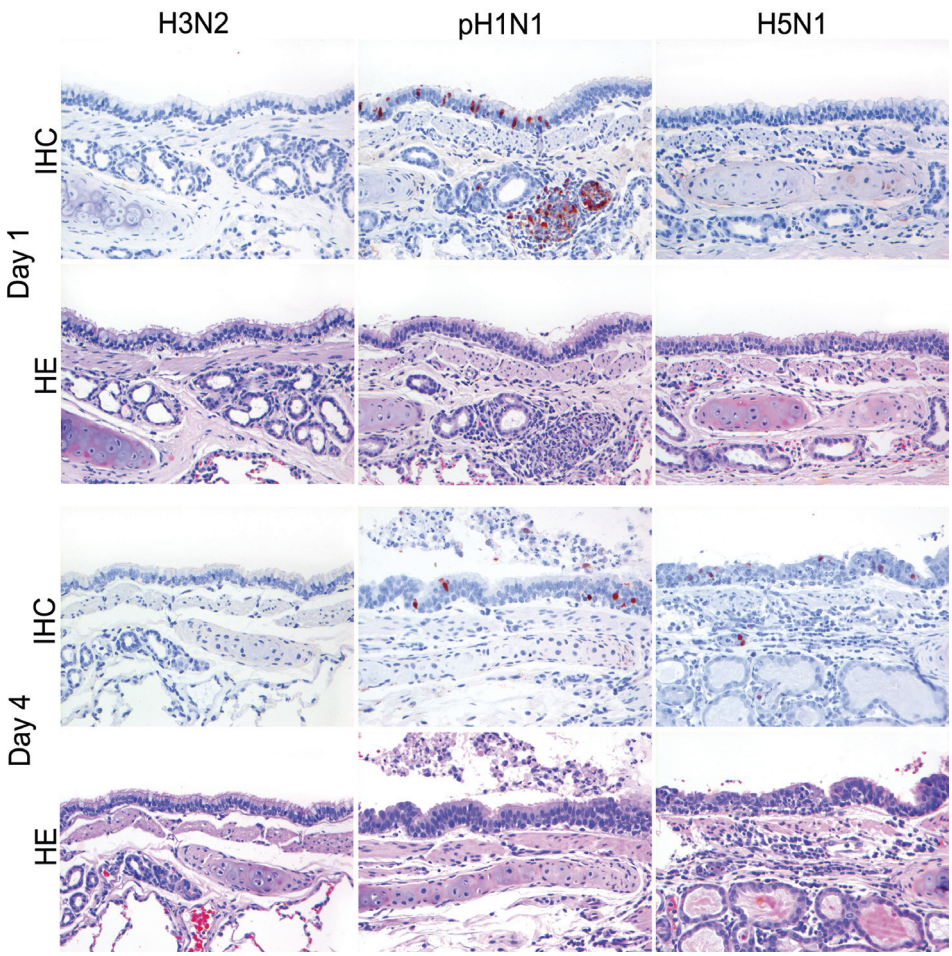

Figure 6. *Antigen expression and histopathology of bronchial epithelium of ferrets inoculated with different influenza viruses. There is moderate antigen expression with associated lesions characterized by bronchitis in bronchial and glandular epithelium of ferrets inoculated with pH1N1 on 1 and 4 dpi, and for H5N1 only on 4 dpi. There were no antigen expression and no lesions for H3N2. HE and immunoperoxidase counterstained with hematoxylin.*

in other extra-respiratory tissues. Changes in the histological lesions and antigen expression over time are described in the supporting information (Supporting information S1, p 155).

Digital scoring demonstrated that the amount of air-containing tissue was lower than in the other virus groups, and decreased over time (Table 3, p 164). Digital scoring for antigen expression showed positive values on all time points with highest values on 1 dpi, but with high variation (Table 3, p 164).

Virology of tissues

In the nose, the virus titers were higher than expected based on virus antigen expression in the nose, indicating a different origin of the virus (Figure 3). In the lungs, virus titers on 1 dpi were higher than on the other days. This could be due to slower replication on 0.5 dpi and necrosis of virus-

replicating cells on 4 dpi. In the extra-respiratory tissues, virus was isolated from the olfactory bulb, cerebrum, cerebellum, heart, spleen, liver, kidney, adrenal gland, pancreas, and jejunum in one or more animals from 0.5 to 4 dpi. The highest virus titers were seen on 2 dpi in olfactory bulb and jejunum, and on 3 and 4 dpi in the spleen (Table 4, p 166).

Hematology and comparison of leucocytes in blood and alveolar lumina

The total leucocyte counts were decreased from 1 to 4 dpi (Table 5, p 168). The number of neutrophils in the alveolar lumina was low on 0.5 dpi but increased strongly with a peak value on 1 dpi. However, in the blood, after a small peak on 1 dpi, there was a decrease of the number of neutrophils (Figure 9). The number of mononuclear cells in the alveolar lumina showed an

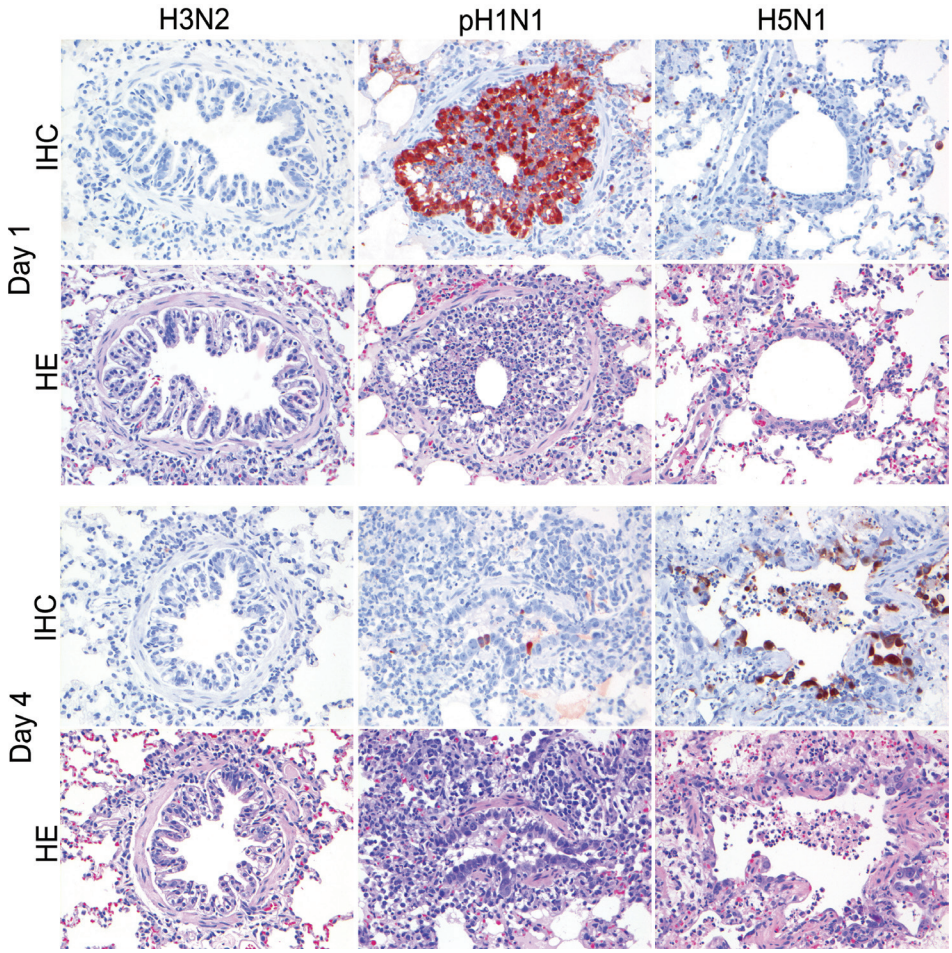

Figure 7. *Antigen expression and histopathology of bronchiolar epithelium of ferrets inoculated with different influenza viruses. There is high antigen expression with associated lesions characterized by bronchiolitis in bronchiolar epithelium of ferrets inoculated with pH1N1 on 1 dpi that was low on 4 dpi, consistent with severe loss of bronchiolar epithelium, and for H5N1 there was no expression on 1 dpi and moderate antigen expression with associated lesions on 4 dpi. There were no antigen expression and no lesions for H3N2. HE and immunoperoxidase counterstained with hematoxylin.*

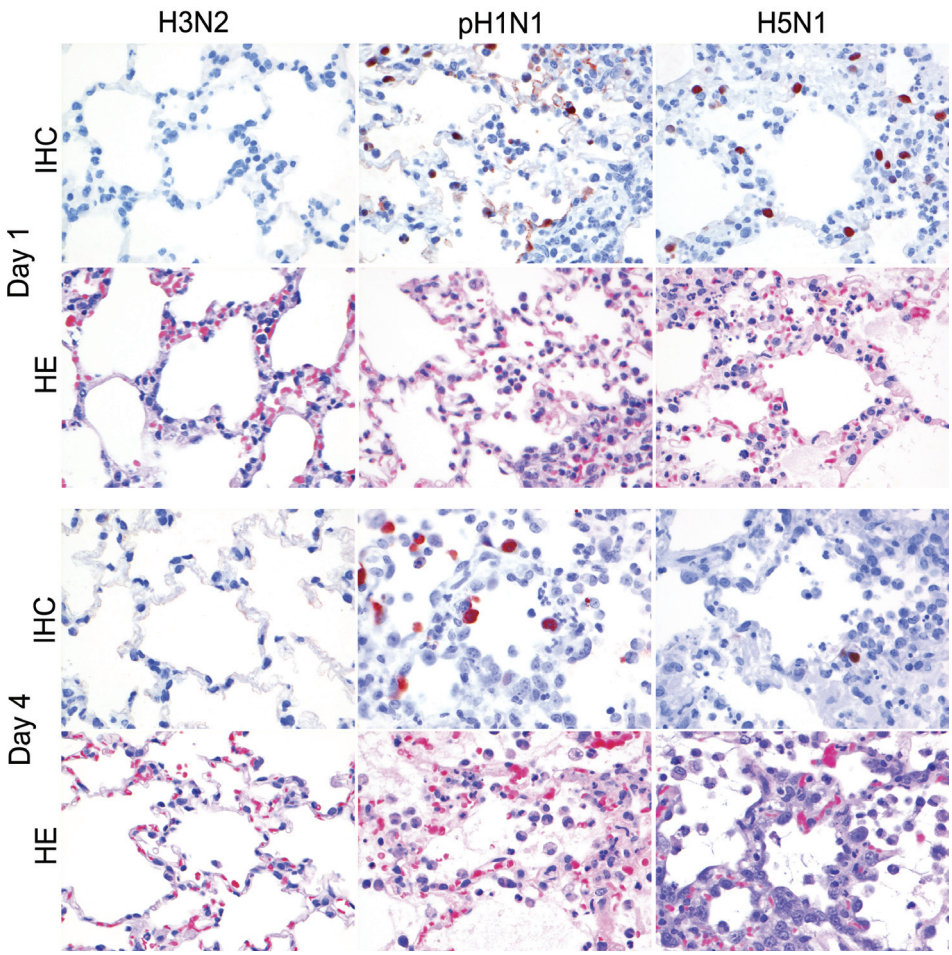

Figure 8. *Antigen expression and histopathology of alveolar epithelium of ferrets inoculated with different influenza viruses. There was moderate to high antigen expression for pH1N1 and H5N1 on 1 and 4 dpi with associated lesions characterized by severe DAD and no expression and lesions for H3N2. HE and immunoperoxidase counterstained with hematoxylin.*

increase on 4 dpi. This increase was later than in the pH1N1 group, while the number of mononuclear cells in the blood did not increase. The number of lymphocytes in the blood was decreased on all days (Table 5, p 168).

Generalized linear model of viral excretion

The final GLM predicting excretion of the H5N1 included 6 significant predictors (LR $\chi^2 = 14.1$, df = 6, $P = 0.029$): viral production and damage in the deeper regions of the respiratory tract (bronchi, bronchioles and alveoli; $P = 0.018$ and $P = 0.024$, respectively); their product ($P = 0.025$); damage in the upper regions of the respiratory tract (nose and trachea; $P = 0.001$); its product with viral production in these regions ($P = 0.002$); and its product with viral production in the deeper regions ($P = 0.031$). Excretion of H5N1 was a negative linear function of each of the three single predictors and a positive linear function of each of the three products. Coefficients are given in Table 6.

Control group with inoculum

Clinical signs and gross pathology

No clinical signs were seen and there was a survival rate of 100 %. The body weight loss in the control group increased slightly in time (Figure 1D). By gross pathology, the lungs had few dark red and slightly raised areas consistent with mild pulmonary consolidation. The area of affected lung tissue varied between 0 and 10 % of the lung area (Figure 2A). The relative lung weight remained constant at around 0.6 % on all time points (Figure 2B). Tracheo-bronchial lymph nodes were slightly enlarged (Table 1, p 160) and mild splenomegaly was present on all time points (data not shown).

Histopathology and virus antigen expression

By histopathology, there was mild multifocal rhinitis, tracheitis, bronchitis and bronchiolitis with few neutrophils, mild perivascular and peribronchiolar cuffing, mild broncho-adenitis, and mild focal alveolitis with infiltration of few neutrophils in the alveolar septa.

No virus antigen expression was seen in any of the tissues. Changes in the histological lesions over time are described in the supporting information (Supporting information S1, p 155). Digital scoring demonstrated that the amount of air-containing tissue was slightly lower on 3 and 4 dpi (Table 3, p 164).

Virology

All swabs and tissues were negative in virus titration for influenza virus.

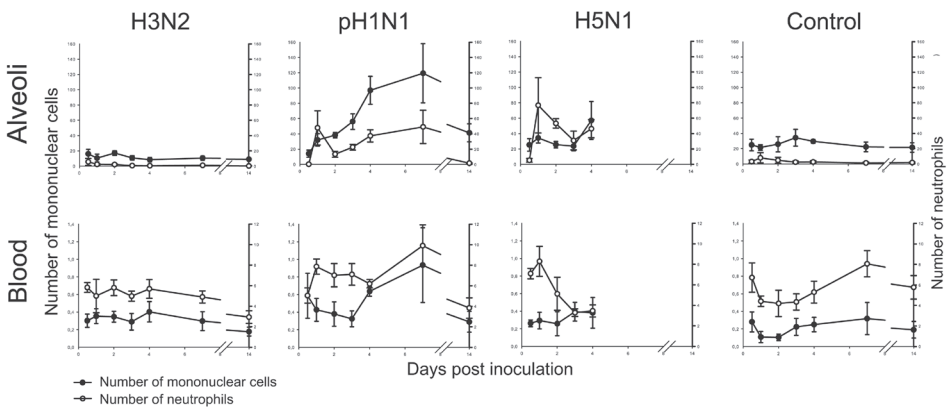

Figure 9. *Leucocyte counts in alveoli and blood of ferrets inoculated with different influenza viruses. The number of leucocytes in the alveolar lumina (scores) and blood (x10⁹/L) are depicted as median values and standard errors of the mean. The number of mononuclear cells and neutrophils in the alveolar lumina and blood follow the same pattern for H3N2 and pH1N1. The increase of the number of mononuclear cells in the alveoli and decrease in the blood for pH1N1 demonstrates the demand in the alveoli. For pH1N1 there is a peak of neutrophils in the alveoli on 0.5 dpi followed by a dip and a response of myelopoiesis in the blood. For H5N1 the number of mononuclear cells is not elevated in the alveoli and blood, and the high demand for neutrophils in the alveoli is not followed by higher release of neutrophils in the blood. In negative control animals (non-inoculated) the median number (range) of mononuclear cells is 0.30 10⁹/L (0.13-0.37) in the blood and 17 (5-22) in the alveolar lumina, for neutrophils 4.33 (3.07-7.28) in the blood and 0.5 (0-2) in the alveolar lumina.*

Hematology and comparison of leucocytes in blood and alveolar lumina
No trends were observed in total leucocyte, segmented neutrophil, mononuclear cell and lymphocyte counts in the blood, or in comparison of leucocyte counts between blood and alveolar lumina (Figure 9 and Table 5, p 168).

DISCUSSION

Our time course experiments show how strongly the spatial and temporal dynamics of infection and associated lesions in the ferret respiratory tract differ between a seasonal human influenza virus (H3N2), a pandemic human influenza virus (pH1N1), and a zoonotic avian influenza virus (H5N1): H3N2 infection was restricted to the nose and peaked at 1 dpi; pH1N1 infection also peaked at 1 dpi, but occurred at similar levels throughout the respiratory tract ; and H5N1 infection occurred predominantly in the alveoli, where it peaked for a longer period, from 1 to 3 dpi (Figure 3). The associated lesions followed the same spatial distribution as virus infection, but their severity peaked between 1 and 6 days later (Table 2, p 162): at 4 to 7 dpi for H3N2 and pH1N1, after which lesions decreased in severity by 14 dpi; and at 4 dpi for H5N1, when all H5N1-infected ferrets had either died or been euthanized on humane grounds. An important implication of these results is that location and timing of sample collection need to be chosen carefully in any comparative study of infection and pathology by different influenza viruses, otherwise the comparison will not be valid.

The main source of excreted virus likely differs between H3N2 and H5N1 infections, based on comparison of virus titers in nasal and pharyngeal swabs (Figure 1) with virus antigen expression in respiratory tract tissues (Figure 3). For H3N2, the temporal dynamics of nasal swab virus titers, pharyngeal swab virus titers, and virus antigen expression in the nose were comparable. Together with the lack of virus antigen expression in the lower respiratory tract, these results suggest that the nose is the main source of excreted H3N2. This is supported by the final GLM for H3N2 viral excretion, which included only viral production in the upper regions of the respiratory tract as significant predictor. In contrast, for H5N1, virus titers in both nasal swabs and pharyngeal swabs were already near peak levels at 1 dpi, while virus antigen expression in the nose remained relatively low until 3 dpi. Together with the higher levels of virus antigen expression in the trachea, bronchioles, and especially alveoli at 1 to 2 dpi, these results suggest that the lower respiratory tract is the main source of excreted H5N1, at least until 3 dpi. In fact, the final GLM for H5N1 viral excretion suggests that viral production and damage in the deeper regions of the respiratory tract (bronchi, bronchioles and alveoli) may have a strong negative impact on viral excretion. This may be due to physical obstruction of the deeper airways due to damage caused by H5N1 virus infection and immune responses. For pH1N1, it is more difficult to determine the main source of excreted virus, because virus antigen expression was high at all levels of the respiratory tract. However, the final GLM for pH1N1 viral excretion revealed that only the viral production in the nose and trachea was a significant predictor of viral excretion, suggesting that as for the H3N2 virus, the upper regions of the respiratory tract may be the main sources of excreted virus.

The pattern of H3N2 and H5N1 antigen expression in the ferret respiratory tract corresponded only in part with the pattern of attachment for these viruses (for the pH1N1 virus, the pattern of attachment in ferrets has not been determined). Attachment of an influenza virus to a host cell is the first step in the virus replication cycle and is considered to be necessary, but not sufficient, for subsequent infection of that cell. Previously, we found that H3N2 attached to many tracheal epithelial

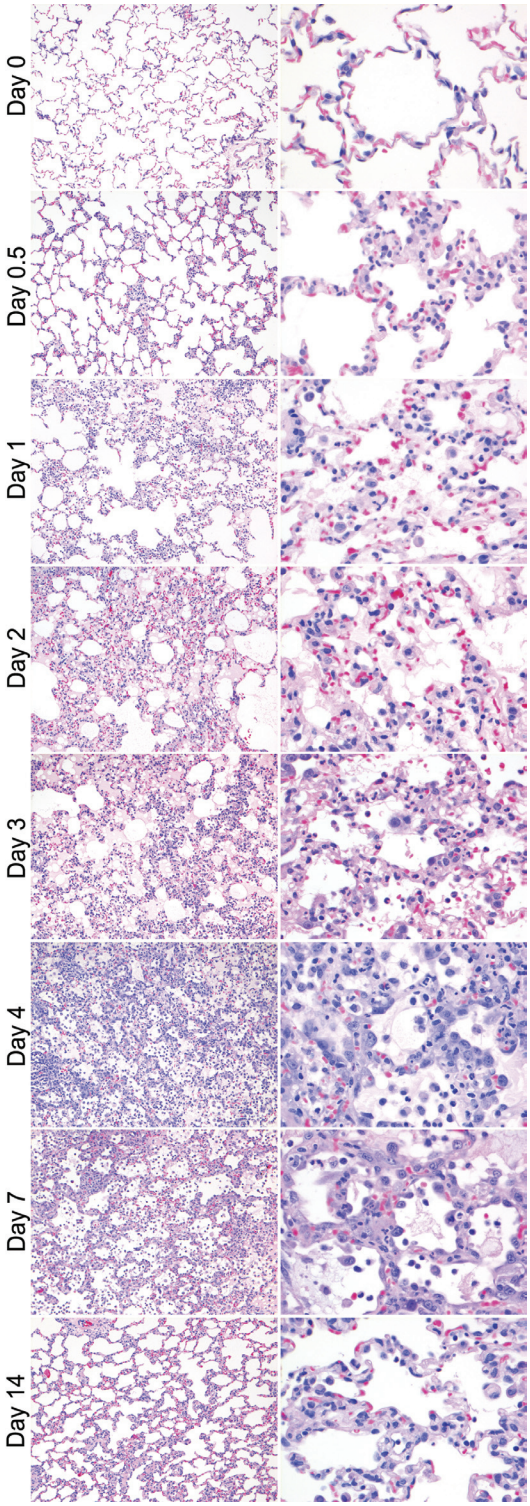

Figure 10. *Histopathologic changes in the alveoli during time in ferrets inoculated with pH1N1. On 0.5 dpi there was mild DAD that was characterized by neutrophils in the alveolar walls. On 1 dpi the alveolar walls were thickened with mild necrosis of the lining epithelium and increased number of neutrophils, in the lumina there were more mononuclear cells, little amount of edema fluid mixed with fibrin, hemorrhage and little cellular debris. On 2 dpi there was increased presence of necrosis, edema, hemorrhage and hyperplasia. On 3 dpi there were both new lesions with acute necrosis and old lesions with type II hyperplasia present, with increased amounts of edema and hemorrhage. On 4 dpi the type II hyperplasia and hypertrophy was more pronounced with increased amount of edema and high numbers of mononuclear cells. On 7 dpi there was severe epithelial hyperplasia and hypertrophy as well as intraluminal edema and hemorrhage. On 14 dpi the walls were mildly thickened. HE.*

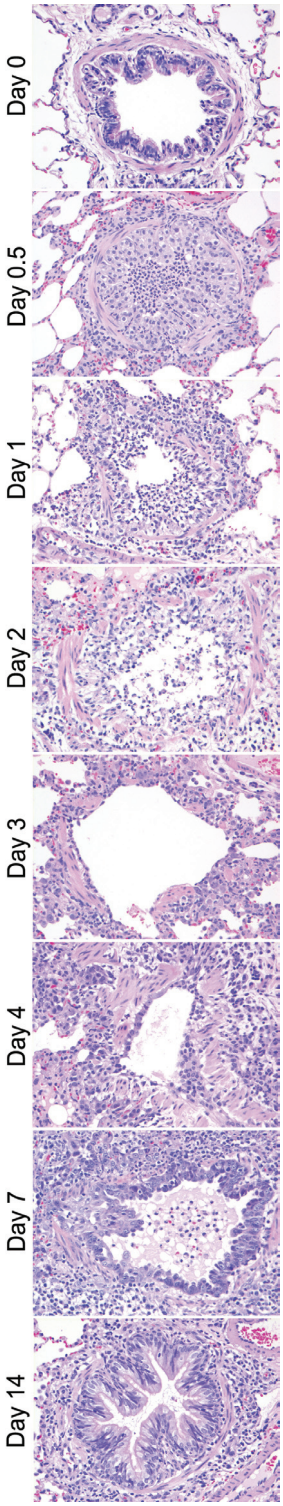

Figure 11. *Histopathologic changes in the bronchioles during time in ferrets inoculated with pH1N1. On 0.5 dpi there was infiltration of neutrophils in the bronchiolar epithelium and lumen with mild peribronchiolar cuffing. On 1 dpi the number of neutrophils increased with necrosis of the epithelium, intraluminal cellular debris and peribronchiolar cuffing. On 2 dpi the necrosis was more severe than on 1 dpi. On 3 dpi there was denudation of the basement membrane and little regeneration of the bronchiolar epithelium with hyperplasia, peribronchiolar cuffing and occasionally cellular debris in the lumen. On 4 dpi there was increased epithelial hyperplasia with moderate cuffing. On 7 dpi the epithelium covered the basement membrane of the bronchiole with hypertrophic cells and moderate cuffing. On 14 dpi the epithelium was slightly hypertrophic with little cuffing. HE.*

cells (predominantly ciliated cells), rare or few bronchial and bronchiolar epithelial cells, and a moderate number of alveolar epithelial cells (predominantly type I pneumocytes, which have a low metabolism) in the lower respiratory tract of the ferret.[125] However, in the current study, we found very little H3N2 infection (based on virus antigen expression) in any cell types of the ferret lower respiratory tract (Figure 3). This suggests that other factors were necessary for H3N2 to infect these cell types. These factors may be the virus load that may need to be higher for infection with H3N2 and the influence of surfactant that protect against influenza in humans and pigs.[311] We previously found that H5N1 did not attach to tracheal or bronchial epithelial cells, and attached to rare or few bronchiolar epithelial cells and a moderate number of alveolar epithelial cells (predominantly type II pneumocytes, which have a high metabolism) in the lower respiratory tract of the ferret.[125] In the current study, we found abundant H5N1 infection in alveolar and bronchiolar epithelial cells, which fits with the pattern of virus attachment (Figure 3).

However, we also found H5N1 infection in tracheal and bronchial epithelial cells, which does not. Next to the fact that this could be related to a different H5N1 strain (A/Vietnam/1194/04),[125] while in the present experiment we used A/Indonesia/5/05), the replication of H5N1 in alveolar and bronchiolar epithelial cells was so abundant that tracheal and bronchial epithelial cells became infected despite the relatively weak attachment of H5N1 to the latter cell types.

Different parameters were used to measure the severity of lower respiratory tract disease in our ferrets. Of these parameters, relative lung weight and affected lung tissue allowed the best quantitative distinction between the virus groups: they showed clear differences between virus groups from 2 dpi onwards (Table 7, p 171), with relatively little within-group variation (Figure 2). These parameters have been used with success before for studies on severe acute respiratory syndrome[172] and on influenza.[292] Immunohistochemistry score for virus antigen expression in the alveoli (Figure 3) (Table 7, p 171), alveolar edema score, and alveolar hemorrhage score (Table 2, p 162) also showed clear differences between the virus groups. However, between-group differences differed according to the dpi, and within-group variation was large. Comparing the histopathology scoring for extent and severity of alveolitis and alveolar damage with the digital scoring for air-containing space in pulmonary tissue showed that the latter demonstrated less statistically significant results, and therefore is less useful for discriminating between viruses (Table 7, p 171). Comparing the antigen expression scoring in the alveoli by hand with the digital scoring and the virus titers, the *P*-values are similar and allow distinction between the virus groups (Table 7, p 171). The other parameters did not allow a clear distinction between the three virus groups.

Besides quantitative differences in severity of lower respiratory tract disease, the three virus infections also showed clear differences in the qualitative character of lower respiratory tract disease, related to the tropism of the virus and the ability of the host to counter infection. This is particularly well illustrated in the alveoli. For the mildest disease, caused by H3N2 infection, there was rare evidence of virus infection in the alveolar epithelium (Figure 3). There was a mild acute inflammatory response with small numbers of neutrophils and macrophages, peaking at 2 dpi. Damage to the alveolar epithelium was so mild that there was no visible evidence of epithelial cell hypertrophy or hyperplasia to re-epithelialize the alveolar walls (Table 2, p 162).

For the intermediate disease, caused by pH1N1 infection, virus infection already was high at 0.5 dpi and peaked soon afterwards at 1 dpi (Figure 3). There was a moderate acute inflammatory response characterized by influx of neutrophils, peaking at 1 dpi (Figure 9). At the same time, there was evidence of damage to the alveolar wall, characterized by necrosis of the epithelium and edema

and hemorrhage in the alveolar lumina, which was maximal at 4 to 7 dpi (Table 2, p 162). After 1 dpi, the alveolar lesion progressed to a more chronic inflammatory response, with neutrophils being replaced by mononuclear cells, which peaked at 7 dpi (Figure 9). At the same time, repair of the alveolar epithelial damage was visible as hypertrophy and hyperplasia of type II pneumocytes, which was maximal at 7 dpi. During this period, the level of virus infection decreased to a low level. By 14 dpi the damage to and inflammation of the alveoli was completely resolved, except for a remnant of mononuclear cells in the alveolar lumina, and virus infection was no longer detectable. The resolution of edema and hemorrhage could be explained on the one hand by the action of alveolar macrophages,[312] and on the other hand by re-epithelialization of the alveolar walls.[313]

For the most severe disease, caused by H5N1 infection, the virus infection reached about the same level as that by pH1N1 infection at 1 dpi but remained high until death or euthanasia at 4 dpi, indicating that the host was not able to control virus infection. There was concurrent alveolar damage, which was so severe and extensive that all ferrets either died or had to be euthanized on humane grounds by 4 dpi. This was despite clear attempts at re-epithelialization, based on prominent type II pneumocyte hypertrophy and hyperplasia from 1 dpi onwards (Table 2, p 162). There was a marked acute inflammatory response characterized by neutrophil influx peaking at 1 dpi but much greater than in pH1N1 infection, with a neutrophil count that was nearly twice as high (Figure 9). This could be explained by a higher induction of pro-inflammatory cytokine production (e.g., IL-6 and IL-8) and NO production due to H5N1 infection.[314,315] Maines et al.[299] demonstrated a relatively high production of IL-6 and IL-8 in the lower respiratory tract of ferrets infected with H5N1, but not with pH1N1. Similarly, humans infected with H5N1 had high levels of IL-6 and IL-8 in the blood.[134] Another major difference with pH1N1 infection was the low influx of mononuclear cells, with a mononuclear cell count of less than half that in pH1N1 infection by 4 dpi, suggesting that the inflammatory response never progressed beyond the acute stage.

Comparison of the dynamics of neutrophil and mononuclear cell influx in the alveolar lumina with neutrophil and monocyte counts in peripheral blood helps to explain the differences in hematological dynamics among the three virus infections (Figure 9). For H3N2 infection, the slight and transient increase in the numbers of neutrophils and monocytes in the blood at 1 dpi correlates with the mild influx of these cell types into the alveolar lumina at that time. This corresponds with a low demand for neutrophils and monocytes during H3N2 infection. For pH1N1 infection, the marked increase in first the number of neutrophils and then of monocytes in the blood correlates with the moderate influx of first neutrophils and then mononuclear cells in the alveolar lumina. This corresponds with increased demand for both cell types, both of which can be met adequately by the myelopoietic compartment. Neutrophils and monocytes are back to normal levels in the blood by 14 dpi, indicating resolution of the respiratory tract inflammation. For H5N1 infection, the initial increase of neutrophils in the blood at 1 dpi correlates with a massive influx of neutrophils into the alveolar lumina. The steep decline in neutrophils in the blood on subsequent days, despite continued high influx in alveolar lumina, corresponds to a demand that has outstripped the available supply by the myelopoietic compartment. This is corroborated by the presence of immature neutrophils with rod-shaped nuclei in the blood from 1 dpi onwards (Table 5, p 168). The lack of increase in monocytes in the blood corresponds with the failure of the acute inflammatory response in the lungs to transform into a more chronic inflammatory response. In addition to changes in neutrophil and monocyte counts, there was an overall leucopenia from 2 dpi (Table 5, p 168). Such a leucopenia has been described previously for H5N1 infection in both humans and ferrets,[101,104,281,300]

whereas ferrets infected with pH1N1 showed higher leucocyte counts.[300] Together, this comparison between inflammatory cell dynamics in alveoli and blood provides insight into the interpretation of hematological analyses of influenza pneumonia.

Besides the respiratory tract, there was evidence, by virus isolation, of extra-respiratory spread for H5N1 and pH1N1, but not for H3N2 (Table 4, p 166). The failure to detect virus antigen in any of these virus-isolation-positive tissues except jejunum may be because virus isolation is more sensitive than immunohistochemistry, or because virus was present but not replicating in these tissues. Previously, H5N1 virus antigen expression in extra-respiratory tissue has been found in the central nervous system and liver of experimentally inoculated ferrets.[308,316,317] In our experiment, we additionally found virus antigen in other extra-respiratory tissues: for pH1N1 in sero-mucous glandular epithelial cells in the palatine roof, and for H5N1 in mononuclear cells in tracheo-bronchial lymph nodes, tonsils, sternal lymph node, spleen, and GALT of the jejunum, and in squamous stratified epithelium on the tip of the nose. The implication of these sites of replication for the pathogenesis and transmission of these viruses is yet to be elucidated.

The extensive H5N1 infection in extra-respiratory tissues known from previous studies[280,281,316,317] likely occurs by spread from the respiratory tract via the blood.[134,144,318] However, the expression of H5N1 antigen in olfactory mucosa (Figure 5) together with high virus titres in the olfactory bulb (Table 4, p 166) suggest that H5N1 may reach the central nervous system from the nasal cavity via the olfactory route, as demonstrated recently by Schrauwen et al.[319] This H5N1 infection of the central nervous system resulted in clinical disease, judging by the presentation of neurological signs (Table 1, p 160). In addition to extra-respiratory spread of H5N1, there also was evidence of pH1N1 in extra-respiratory tissues, especially the central nervous system (Table 4, p 166), and pH1N1 expression in olfactory mucosa (Figure 5). This suggests that pH1N1 also may be neurotropic and enter the central nervous system via the olfactory route.

Acknowledgments

We thank C. van Hagen, R. Boom, W. van Aert, R. van Lavieren, L. Leijten, P. van Run, E. Veldhuis Kroeze, D. van Riel, D. van de Vijver, and T. Bestebroer for technical assistance, A. Gomersbach and W. Vos for biotechnical assistance, F. van der Panne for figure preparation, A. Nigg for assistance with the digital scoring and M. van Leeuwen (UVDL, Utrecht) for reading the thin blood slides.

SUPPORTING INFORMATION S1

Detailed description per virus of histopathologic changes and antigen expression by immunohistochemistry.

Seasonal H3N2

On 0.5 dpi, no lesions were seen in the nasal concha and immunohistochemistry showed few cells (scored as < 25 % of the total nasal epithelium) expressing viral antigen in the respiratory nasal epithelium (Figure 3). In the trachea, bronchi and bronchioles there were few intra-epithelial neutrophils and focal mild peribronchiolar and perivascular infiltration (cuffing) of few lymphocytes and plasma cells of 1 to 2 cells thick. No antigen expression was seen in the tracheal, bronchial, bronchiolar, and tracheo-bronchial glandular epithelium at any time point. The alveoli showed mild multifocal alveolitis, characterized by mild infiltration of few neutrophils in the alveolar walls (Table 2) and few neutrophils, mononuclear cells (believed to be alveolar macrophages) (Figure 9) and a small amount of edema in the alveolar lumina. The extent of the alveolitis was between 0 and 50 % of the lung tissue present in the slides (Table 2, p 162). Semiquantitative scoring showed antigen expression in 0 to 2 % of the type II pneumocytes in the alveoli examined.

On 1 dpi, similar lesions were seen. Additionally, there was a mild rhinitis with infiltration of few neutrophils in the respiratory epithelium accompanied by a slight increase in antigen expressing cells (in between 25-50 %) and also virus antigen expression in a few cells of the olfactory epithelium (Figure 4 and 5). In the alveoli, there was focal mild necrosis of the lining epithelium but no edema (Figure 8). One animal had a severe multifocal chronic granulomatous pleuropneumonia that was not related to the influenza virus infection.

On 2 dpi, there was a slight decrease in the number of antigen expressing cells in the nose. There was a mild broncho-adenitis with infiltration of few neutrophils, macrophages and mild necrosis of glandular epithelial cells and a mild increase of the numbers of neutrophils in the alveolar walls (Table 2, p 162).

On 3 dpi, there were few to moderate numbers of neutrophils in the nasal respiratory epithelium and extending into the lamina propria, with mild interstitial edema and mild necrosis as well as regeneration of the epithelium. In the bronchi, there was no broncho-adenitis. In the alveoli, a small amount of edema was seen and there were no neutrophils in the alveolar lumina.

On 4 dpi, the severity of the rhinitis increased with moderate numbers of neutrophils, and antigen was seen in < 25 % of the epithelium. In the alveoli, the number of neutrophils in the walls slightly increased as compared to 3 dpi (Table 2, p 162).

On 7 dpi, there were many neutrophils but no antigen expression in the nose (Figure 3, 4 and 5). In the lungs, there was a mild broncho-adenitis.

On 14 dpi, the extent of the lesions in the alveoli was < 25 % with no neutrophils in the alveolar lumen and few neutrophils in the alveolar walls.

pH1N1

On 0.5 dpi the lesions were limited to the following sites. The nasal concha showed a mild rhinitis with few neutrophils in the nasal epithelium. By immunohistochemistry, there was antigen expression in 25 to 50 % of the single layered nasal respiratory epithelial cells (Figures 3 and 4). In the trachea, there was a mild multifocal tracheitis with mild infiltration of neutrophils in the wall and lumen (and occasionally in the tracheal glands) that lasted until 14 dpi. The bronchial and bronchiolar

epithelium had mild infiltration of few neutrophils. In peribronchiolar and to a lesser extent peribronchial and perivascular tissues, there was infiltration of few cells (1 to 2 cells thick), consisting predominantly of macrophages and lymphocytes, with few neutrophils and plasma cells. In the bronchi, there was antigen expression in < 25 % of the epithelium and in the bronchioles it was between 25 and 50 %. Bronchial glandular epithelial cells expressed virus antigen with often more expression in glandular cells than in bronchial epithelial cells. The alveoli showed diffuse alveolar damage (DAD) (Figure 8 and 10) that was characterized by an alveolitis with a moderate number of neutrophils in the alveolar walls (Table 2, p 162) and occasional neutrophils, few alveolar macrophages, and few eosinophils in the alveolar lumina (Figure 9). The extent of the alveolar lesions was between 25 and 50 % of the pulmonary tissue on the slides. Influenza virus antigen expression was closely associated with the presence of histological lesions and was seen predominantly in type II pneumocytes and less in type I pneumocytes and alveolar macrophages (Figure 8). Semi-quantitative scoring of the alveoli showed that the percentage of antigen expressing cells was high (Figure 3).

On 1 dpi, the numbers of neutrophils in the nose had increased and antigen expression was present in > 50 % of the respiratory epithelium and was also seen in the basal and olfactory cells of the olfactory epithelium (Figures 3 and 5). The inflammatory infiltrate in bronchial and bronchiolar epithelium was increased to many neutrophils, and necrosis of the epithelium that was more pronounced in the bronchioles when compared to the bronchi. There was cellular debris in the bronchiolar lumina. There were many inflammatory cells, predominantly macrophages and lymphocytes, with few neutrophils and plasma cells, in the bronchiolar epithelium. Peribronchial, peribronchiolar and perivascular cuffing was increased to 3 to 10 cells thick, and consisted predominantly of macrophages and lymphocytes, with few neutrophils and plasma cells. Broncho-adenitis was present. There was antigen expression in > 50 % of the bronchiolar epithelium and in 25 to 50 % of the bronchial epithelium. In the alveolar walls and lumina, there were more neutrophils, and in the alveolar lumina there were more mononuclear cells mixed with scant edema fluid, fibrin, erythrocytes, and cellular debris. The alveolar walls were thickened, had mild necrosis of the lining epithelium, and mild type II pneumocyte hypertrophy and hyperplasia. There was a mild to severe broncho-adenitis. Immunohistochemistry scores showed a peak in the number of antigen expressing cells in both upper and lower respiratory tract.

On 2 dpi in the bronchioles, necrosis was more severe, in some locations with complete absence of bronchiolar epithelial cells, clearly present denuded basement membranes and large amounts of cellular debris mixed with alveolar macrophages, neutrophils, erythrocytes, fibrin and edema fluid in the lumina. There was regeneration of bronchiolar epithelial cells with hyperplasia and hypertrophy, and moderate broncho-adenitis. Antigen expression in the bronchioles was decreased to between 25 and 50 %. In the alveoli, the severity of the lesions had increased, with more epithelial necrosis, edema, hemorrhage and type II pneumocyte hyperplasia. Semi-quantitative scoring of the alveoli showed that the percentage of antigen expressing cells had decreased (Figure 3), possibly due to necrosis of antigen-expressing epithelial cells.

On 3 dpi, there was regeneration of the nasal epithelium, characterized by hypertrophy and hyperplasia of epithelial cells. In the trachea, there was expression of antigen in epithelial cells. In the bronchi and bronchioles, there was more epithelial regeneration, and infiltration with many inflammatory cells. In the alveoli, it was remarkable that there were both new lesions with acute necrosis and old lesions with type II hyperplasia present; the amount of edema and hemorrhage as well as type II hyperplasia were increased. The number of neutrophils in the lumina was slightly

decreased but the number of mononuclear cells was increased (Figure 9). By semi-quantitative scoring, the percentage of antigen-expressing cells in the alveoli had decreased again (Figure 3).

On 4 dpi, the number of antigen expressing bronchial epithelial cells had decreased to < 25 %. In the alveoli, both old and new lesions were present with increased amount of edema, hemorrhage, hyperplasia and increased numbers of mononuclear cells (Table 2 p 162 and Figure 8). Antigen expression was less than on 3 dpi for all tissues except the alveoli were there were more antigen expressing cells (Figure 3).

On 7 dpi, antigen expression in the nose had decreased and was absent in the tracheal epithelium. Peribronchial, peribronchiolar and perivascular cuffing was increased to sometimes more than 10 cells thick. Antigen expression scoring was lower in bronchi and bronchioles, and there was severe broncho-adenitis. In the alveoli, there was more edema, hemorrhage, necrosis and type II hyperplasia, often around bronchi and bronchioles. The number of mononuclear cells and neutrophils in the lumina showed the highest values (Figure 9). Antigen expression decreased further with only few positive cells (Figure 3).

On 14 dpi, there were few inflammatory cells in the nose. In the bronchi and bronchioles, there were few inflammatory cells and peribronchial, peribronchiolar and perivascular cuffing was between 3 to 10 cells thick. The numbers of neutrophils in the alveolar walls and lumina were comparable to those on 0.5 dpi, and the number of mononuclear cells in the lumina was decreased (Figure 9). The extent of the lesions was between 25 and 50 %. No antigen expression was seen in any of the respiratory tissues (Figure 3).

In the tracheo-bronchial lymph nodes, there was mild lymphoid hyperplasia on 0.5 dpi. Additionally, on 4 dpi, there was multifocal accumulation of proteinaceous fluid, histiocytosis and infiltration of mononuclear cells in the surrounding tissue, and on 14 dpi there was also severe lymphocytolysis. In the tonsils, there was mild lymphoid hyperplasia with few intra-epithelial lymphocytes and neutrophils with mild lymphocytolysis on 1 dpi. On 2 and 3 dpi, there were slightly more inflammatory cells, which decreased in number on 4 dpi. On 14 dpi, the tonsillar tissue was again normal. Tracheo-bronchial lymph nodes and tonsils did not express virus antigen. In the palatine roof of two animals on 7 dpi, there was a severe adenitis of the sero-mucous glands with necrosis of glandular epithelial cells, infiltration by many neutrophils, dilatation of glands, and antigen expression in the glandular epithelial cells. There was no virus antigen expression in other extra-respiratory tissues.

H5N1

On 0.5 dpi, the nose showed a moderate rhinitis with necrosis of epithelial cells and infiltration of a moderate number of neutrophils in the lumen, epithelium, and lamina propria. There was no virus antigen expression. In the trachea, there was a mild multifocal tracheitis with infiltration of few neutrophils in the wall and lumen, and tracheal glands. By immunohistochemistry, few tracheal epithelial cells presented virus antigen (Figure 3). The bronchial and bronchiolar epithelium had multifocal infiltration with moderate numbers of neutrophils and mild epithelial necrosis. There were peribronchial, peribronchiolar, and perivascular infiltrates (cuffing), 3 to 10 cells thick, consisting of few macrophages, lymphocytes, neutrophils and plasma cells. Bronchial and bronchiolar lumina contained small amounts of cellular debris, fibrin, and edema fluid, mixed with few neutrophils. Overall, changes in the bronchi were milder than in the bronchioles. There was a focally mild broncho-adenitis. By immunohistochemistry, virus antigen expression was present in < 25 % of the bronchiolar epithelial cells and not in the bronchial epithelial cells. The alveoli showed DAD

(Figure 8) characterized by few neutrophils, eosinophils, and erythrocytes, and a moderate number of mononuclear cells, mixed with scant edema fluid in the alveolar lumina, and a moderate number of neutrophils in the alveolar walls (Table 2, p 162). The alveolar walls were mildly thickened and showed mild necrosis of epithelial cells and mild epithelial hypertrophy. The extent of the alveolar lesions was between 25 and 50 %. Semi-quantitative scoring showed that the extent and severity of the lesions was high (Table 2, p 162). Virus antigen expression was closely associated with the presence of histological lesions and was seen predominantly in type II pneumocytes (Figure 8), and less in type I pneumocytes and alveolar macrophages. Semiquantitative scoring for virus antigen expression in the alveoli was high (Figure 3).

On 1 dpi, the number of inflammatory cells in the nose was decreased. By immunohistochemistry, virus antigen expression occurred occasionally in the olfactory epithelium (with cytoplasmic staining towards the lumen), in respiratory epithelial cells and cells in the lamina propria (presumably glandular cells). The extent of the antigen expression was < 25 %. There were moderate to high numbers of neutrophils in the bronchiolar walls and lumina with increased epithelial necrosis. The number of neutrophils in the alveolar walls was increased with severe epithelial necrosis, and there were increased numbers of neutrophils and mononuclear cells with more edema fluid mixed with fibrin, necrotic neutrophils, cellular debris, and erythrocytes in the alveolar lumina. Semi-quantitative scoring for virus antigen expression was increased in the trachea and alveoli.

On 2 dpi, virus antigen expression in the nose was between 25 and 50 %. Bronchial epithelium showed < 25 % antigen expression. In the bronchioles, there was hypertrophy and hyperplasia of bronchiolar epithelium, as well as inflammation. In the alveoli, there was hypertrophy and hyperplasia of type II pneumocytes, and slightly fewer neutrophils and mononuclear cells (Table 2, p 162 and Figure 9). There were high scores for the presence of edema fluid, hemorrhage and type II hypertrophy and hyperplasia.

On 3 dpi the extent of the antigen expression was between 25 and 50 % in the nose and bronchioles and < 25 % in the bronchi. In the alveoli, there was severe necrosis, and slightly decreased numbers of neutrophils and mononuclear cells.

On 4 dpi the extent of the antigen expression in the nose was < 25 %. In the trachea, the scores for tracheitis were higher than on previous days. In the bronchioles, there was severe epithelial necrosis as well as epithelial hypertrophy and hyperplasia. There was broncho-adenitis with only rare antigen expression. In the alveoli, epithelial necrosis was very severe, the number of neutrophils in the walls was decreased, and the number of mononuclear cells in the lumina was increased. There was severe interstitial and pleural edema and hemorrhage and the extent of the lesions was > 50 %. Semiquantitative scoring for antigen expression in the alveoli was decreased. This severe drop in antigen expressing cells could be explained by the severe necrosis.

In the tracheo-bronchial lymph nodes, there was mild lymphoid hyperplasia on 0.5 dpi. On 1 dpi, there was moderate lymphoid hyperplasia and histiocytosis, multifocal accumulation of proteinaceous fluid, infiltration of neutrophils, lymphocytolysis and antigen expressing mononuclear cells in the perifollicular area. On 3 dpi additionally there was severe multifocal necrosis and associated antigen expression, and on 4 dpi there was lymphoid depletion with decreased numbers of follicles and no antigen expression. In the tonsils, there was mild lymphoid hyperplasia with few intra-epithelial neutrophils and few virus-antigen-expressing cells (macrophage-like) on 2 dpi. On 3 dpi, there was multifocal necrosis and many intra-epithelial neutrophils, and antigen expression in few mononuclear cells and on 4 dpi there was little necrosis and little antigen expression. In one animal,

there was virus antigen expression in squamous stratified epithelium in the tip of the nose on 2 dpi, with associated intraepithelial neutrophils and erosion of the epithelium. In the extra-respiratory tissues, one animal had few virus antigen expressing mononuclear cells in the sternal lymph node on 2 dpi, associated with mild lymphoid hyperplasia, and another animal had virus antigen expression in endothelial cells of the soft palate on 1 dpi associated with severe necrotizing and neutrophilic pharyngitis. Two animals had virus antigen expression in the gut associated lymphoid tissue (GALT) of the jejunum on 2 and 3 dpi, and associated lymphoid hyperplasia, mild necrosis, multifocal accumulation of proteinaceous material and neutrophils. One animal had few virus antigen expressing mononuclear cells in the spleen on 4 dpi, and associated necrosis, protein deposits and mild lymphoid depletion.

Control group with inoculum

On 0.5 dpi, there was a mild rhinitis and tracheitis with few inflammatory cells. Almost all animals had a mild bronchitis or bronchiolitis with few neutrophils. There was perivascular and peribronchiolar cuffing (1-2 cells thick) with few neutrophils, lymphocytes, plasma cells and macrophages. In the alveoli, there was a mild focal alveolitis with infiltration of few neutrophils and eosinophils in the alveolar septa and in the alveolar lumina occasionally few neutrophils, mononuclear cells and eosinophils with small amounts of edema fluid and few erythrocytes. In few animals, there was a mild broncho-adenitis with few neutrophils, lymphocytes and plasma cells in the bronchial glands.

On 1 dpi, there was a slight increase in the number of eosinophils and slightly more edema fluid in the alveoli.

On 2 dpi, perivascular and peribronchiolar cuffing was up to 10 cells thick. One ferret had multifocal moderate neutrophilic infiltrates mixed with edema fluid in the alveoli and associated terminal bronchioles. This was considered an incidental finding.

On 7 dpi, the number of neutrophils in the alveolar walls was higher than on other days.

No virus antigen expression was seen in any of the tissues.

Table 1. Survival and clinical signs in ferrets inoculated with different influenza viruses. Data also are provided for enlargement of the tracheo-bronchial lymph nodes, virus excretion from the rectum, and virus neutralization antibody titers in the serum

			Clinical signs per group: median (range)										
Virus	**Days post inoculation**	**Percentage of survival [a] (n of total)**	**Activity status (0-3)**	**Inappetence (0-1)**	**Sneezing (0-1)**	**Dyspnea (0-1)**	**Nasal discharge (0-1)**	**Conjunctival discharge (0-1)**	**Diarrhea (0-1)**	**Nervous symptoms (0-1) (n of total)[a]**	**Tracheo-bronchial lymph node scores (median and range)**	**Virus excretion rectal swab [number positive / total (log10 $TCID_{50}$ /ml)][b]**	**Homologous VN antibody titers (median and range)**
H3N2	0.5	100% (28/28)	0	0	0 (0-1)	0	0	0	0	0	0	0/4	<8
	1	100% (24/24)	0	0	0	0	0	0	0	0	1 (0-1)	0/4	<8
	2	100% (20/20)	0.2 (0-1)	0	1	0	0	0 (0-1)	0	0	1.5 (1-2)	0/4	<8
	3	100% (16/16)	0	0	1	0	0	0	0	0	0.5 (0-1)	0/4	<8
	4	100% (12/12)	0	0	1	0	0	0	0	0	0.5 (0-1)	0/4	<8
	7	100% (8/8)	0	0	1	0	0	0	0	0	0 (0-1)	1/4 (2.8)	397 (256-609)
	14	100% (4/4)	0	0	1	0	0	0	0	0	0	0/4	1 669 (1 024-3 444)
pH1N1													
	0.5	100% (28/28)	0	0	0	0	0	0	0	0	0	0/4	<8
	1	100% (24/24)	0	0	0	0	0	0	0	0	2 (1-2)	2/4 (2.8)	<8
	2	100% (20/20)	1	1	1	0	0	0	0	0	1.5 (0-2)	0/4	<8
	3	100% (16/16)	1	1	1	0	0	0	0	0	2 (0-2)	1/4 (1.0)	<8
	4	100% (12/12)	1	1	1	0	0	0	0	0	3	1/4 (1.0)	<8
	7	100% (8/8)	1	0	1	0	0	0	0	0	4	0/4	9 423 (4096-2 3170)
	14	100% (4/4)	0	0	1	0	0	0	0	0	3	0/4	2 1327 (1 3777-2 3912)

followw up table 1

H5N1												
	0.5	100% (20/20)	0	0	0	0	0	0	0	0	0	0/4	<8
	1	100% (16/16)	1	0.5 (0-1)	0	0	0	0	0.8 (0-1)	0	1 (0-3)	0/4	<8
	2	50% (6/12)	2 (2-3)	1	0	0	0	0	0.3 (0-1)	1 (1/12)	0 (0-2)	0/4	<8
	3	50% (3/6)	2 (2-3)	1	0	1	0	0	0	1 (2/6)	0	0/4	<8
	4	100% (3/3)	2 (2-3)	1	0	1	0	0	0	1 (2/3)	2 (0-2)	0/4	<8
Control													
	0.5	100% (28/28)	0	0	0 (0-1)	0	0	0	0	0	0	0/4	<8
	1	100% (24/24)	0	0	0	0	0	0	0	0	0	0/4	<8
	2	100% (20/20)	0	0	0	0	0	0	0	0	0 (0-1)	0/4	<8
	3	100% (16/16)	0	0	0	0	0	0	0	0	0	0/4	<8
	4	100% (12/12)	0	0	0	0	0	0	0	0	0 (0-2)	0/4	<8
	7	100% (8/8)	0	0	0	0	0	0	0	0	1 (0-2)	0/4	<8
	14	100% (4/4)	0	0	0	0	0	0	0	0	0 (0-2)	0/4	<8

[a] Scores are based on individual animals. [b] The cut off values are < 0.8 $\log_{10}$ $TCID_{50}$ /ml)

Table 2. Histopathology scores in ferrets inoculated with different influenza viruses

		Histopathology score: median (range)									
Virus	**Days post inoculation**	**Severity of alveolitis and alveolar damage (0-3)**	**Extent of alveolitis and alveolar damage (0-3)**	**Presence of alveolar edema (0-1)**	**Presence of alveolar hemorrhage (0-1)**	**Presence of hyperplasia and hypertrophy (0-1)**	**Presence of bronchitis and bronchiolitis (0-3)**	**Presence of perivascular and peribronchiolar cuffing (0-3)**	**Presence of tracheitis (0-3)**	**Presence of rhinitis (0-3)**	**Number of neutrophils in the alveolar wall in 20 hpf per animal (median and range)**
H3N2	0.5	1.0 (1-1.75)	1.4 (1.25-2.25)	0 (0-0.25)	0	0	0.6 (0.15-1.5)	0.9 (0.5-1.5)	1.0 (0-2)	0	70.0 (52-106)
	1	0.9 (0.75-1)	1.4 (1-1.75)	0	0	0	0.4 (0-0.75)	0.9 (0-1.75)	0.5 (0-2)	0 (0-1)	71.0 (28-148)
	2	1.0	1.8 (1-2.25)	0	0	0	0.1 (0-0.25)	0.8 (0-1.25)	0 (0-1)	0	102.5 (86-124)
	3	0.8 (0.75-1)	1.6 (1-2.25)	0 (0-0.25)	0	0	0.1 (0-0.25)	0.6 (0-0.75)	0	1.5 (0-3)	79.0 (53-99)
	4	1.0 (0.75-1.25)	2.3 (1.25-2.50)	0 (0-0.25)	0	0	0.1 (0-0.5)	0.6 (0.25-0.75)	0 (0-1)	2.5 (2-3)	102.0 (63-143)
	7	1.0 (0.75-1.25)	1.8 (1-2)	0	0	0	0.3 (0-1)	1.1 (1-1.5)	1.0 (0-2)	2.5 (1-3)	75.0 (51-82)
	14	0.8	0.9 (1-1.50)	0	0	0	0 (0-0.25)	0.1 (0.25-0.75)	0	1.0 (0-2)	55.0 (22-61)
pH1N1	0.5	1.3 (1.25-1.75)	1.9 (1.5-3)	0	0	0	0.5 (0.25-1.75)	0.5 (0.15-1.5)	0 (0-2)	0 (0-1)	57.5 (28-93)
	1	2.5 (1.5-2.75)	2.6 (2.50-3)	0.6 (0-1)	0.1 (0-0.25)	0.1 (0-0.25)	2.9 (2.75-3)	1.8 (1.5-2)	0 (0-1)	2.0 (1-3)	124.5 (98-256)
	2	2.5 (2-2.75)	2.4 (2.25-2.5)	0.6 (0.25-1)	0.3 (0.25-0.5)	0.3 (0.25-0.5)	3.0 (2.25-3)	1.8 (1.5-2)	1.0	1.0 (0-2)	104.5 (72-145)
	3	2.5 (2.25-2.75)	2.8 (2-3)	0.8 (0.5-1)	0.4 (0.25-0.5)	0.4 (0.25-0.5)	2.6 (2.25-2.75)	1.8 (1.5-2)	1.0 (0-2)	2.5 (1-3)	128.0 (104-142)
	4	2.8 (2-3)	2.6 (2.5-2.75)	1.0 (0.75-1)	0.6 (0.25-0.75)	0.6 (0.25-0.75)	2.6 (2-2.75)	2.0 (1.5-2)	0.5 (0-1)	2.5 (0-3)	99.0 (78-144)
	7	2.6 (2.25-3)	2.6 (2.25-3)	0.9 (0.75-1)	0.8	0.8	3.0 (2.75-3)	2.4 (2.25-2.75)	2.4 (2.25-2.75)	3.0 (2-3)	120.0 (104-149)
	14	1.8 (1.75-2)	2.1 (1.75-2.5)	0	0	0	0.8 (1-1.5)	1.5 (1.5-2)	1.0 (0-2)	1.0 (1-2)	56.0 (17-63)

follow up table 2

H5N1	0.5	2.1 (1.75-2.75)	2.4 (2-3)	0.1 (0-0.75)	0 (0.75-0)	0 (0-0.75)	2.1 (1.75-2.75)	2.0 (1.75-2.0)	1.5 (1-3)	1.5 (1-2)	70.5 (45-110)
	1	2.6 (2.25-2.75)	2.4 (2-2.5)	0.9 (0.5-1)	0.6 (0.25-1)	0.6 (0.25-1)	2.8 (2-2.75)	2.0 (1.75-2)	1.5 (0-3)	0.5 (0-2)	170.0 (88-211)
	2	2.8 (2.75-3)	2.8 (2.5-3)	1.0	0.8 (0.75-1)	0.8 (0.75-1)	2.9 (1.75-3)	1.9 (0-2)	2.0 (0-2)	0.5 (0-2)	132.5 (77-190)
	3	3.0 (2.5-3)	3.0 (2.25-3)	1.0 (0.75-1)	1.0 (0.75-1)	1.0 (0.75-1)	2.5 (2.25-3)	2.0 (1-2)	1.0	1.0	135.0 (46-190)
	4	3.0 (2.75-3)	3.0	1.0	1.0	1.0	2.8 (2.25-2.75)	1.3 (1.25-1.5)	3.0 (2-3)	1.0 (0-1)	105.0 (105-125)
Control	0.5	1.4 (1-1.75)	1.9 (1.75-2.5)	0.1 (0-0.25)	0.1 (0-0.25)	0.1 (0-0.25)	0.9 (0.25-1.25)	1.1 (1-2)	1.5 (0-2)	0.5 (0-2)	58.5 (42-82)
	1	1.0 (0.75-2.25)	1.4 (0.75-2.25)	0 (0-0.75)	0	0 (0-0.25)	1.3 (0.5-2)	1.4 (1.25-1.75)	1.5 (0-2)	1.0 (0-2)	51.0 (37-94)
	2	1.9 (1-2)	2.4 (1.25-3)	0.1 (0-0.25)	0	0 (0-0.25)	1.1 (0.25-1.75)	1.6 (0.75-2)	1.5 (0-2)	1.5 (0-2)	45.0 (24-91)
	3	1.4 (1.25-2)	2.0 (2-2.25)	0	0	0	1.1 (0.75-1.25)	1.9 (1.5-2)	1.0 (0-2)	1.0 (0-1)	41.0 (27-107)
	4	1.1 (0.75-1.5)	1.6 (1.25-2.25)	0	0	0	0.8 (0.5-1.25)	1.5 (0.75-1.75)	2.5 (2-3)	1.5 (1-2)	62.5 (47-97)
	7	1.1 (1-1.5)	2.0 (1-2.25)	0	0	0	0.8	1.1 (1-1.5)	2.5 (2-3)	1.5 (1-3)	123 (68-154)
	14	1.3 (1-1.5)	1.6 (1.25-2)	0	0	0	0.9 (0-1.25)	1.1 (0.75-1.75)	2.0 (2-3)	2.0 (0-2)	59.0 (32-81)
Negative control		0.25	0.25	0	0	0	0.25 (0-0.25)	0.25 (0-0.5)	0	0	23.5

Table 3. Digital histopathology scores in ferrets inoculated with different influenza viruses

		Digital score: median (range)		
Virus	**Days post inoculation**	**Percentage of air containing space in pulmonary tissue**	**Percentage of antigen expression**	**Number of antigen expression counts**
H3N2	0.5	66.6 (49.4-75.9)	0	1 (0-2)
	1	65.1 (61.1-69.2)	0	1 (0-1)
	2	62.7 (58.0-72.1)	0	0 (0-1)
	3	66.6 (63.4-73.7)	0	1 (0-2)
	4	67.4 (46.2-70.4)	0	0 (0-1)
	7	72.9 (68.9-86.7)	0	0.5 (0-4)
	14	66.5 (57.3-74.1)	0	0 (0-2)
pH1N1	0.5	64.7 (56.0-80.3)	0.63 (0.09-0.74)	87.5 (21-164)
	1	65.0 (48.4-69.0)	0.92 (0.557-1.49)	273.5 (115-522)
	2	63.0 (59.3-71.1)	0.10 (0.05-0.16)	30 (15-49)
	3	70.3 (63.8-78.0)	0.06 (0.01-0.08)	14 (1-19)
	4	77.1 (73.3-81.0)	0.03 (0-0.05)	5.5 (1-50)
	7	63.1 (45.4-78.0)	0 (0-0.01)	1 (1-2)
	14	65.4 (55.7-73.1)	0 (0-0.1)	0.5 (0-6)
H5N1	0.5	58.3 (56.5-72.7)	0.06 (0.12-0.78)	24 (4-264)
	1	48.9 (45.8-51.6)	0.50 (0.29-0.57)	265.5 (174-282)
	2	44.0 (38.8-58.3)	0.20 (0.04-0.31)	114 (24-148)
	3	44.2 (39.0-56.9)	0.11 (0.09-0.20)	59 (43-73)
	4	38.9 (27.0-51.2)	0.04 (0.02-0.08)	19 (13-39)
Control	0.5	63.3 (48.7-74.8)	0	0
	1	66.4 (56.4-74.8)	0	0 (0-2)
	2	64.1 (53.4-70.4)	0	0
	3	57.8 (46.4-71.2)	0	0
	4	53.7 (42.1-67.1)	0	0.5 (0-1)
	7	63.4 (56.1-67.9)	0	0.5 (0-1)
	14	68.4 (61.1-77.4)	0	0 (0-1)
Negative control		81.1 (78.6-82.8)	0 (0-0.01)*	1.5 (0-2)*

*Antigen expression counts in the negative control animals are considered false positive counts due to the incapacity of the program to determine artifact staining.

Table 4. Virus isolation from tissues in ferrets inoculated with different influenza viruses

		Presence of virus (number of animals positive / total number of animals) and virus titer (range log10 $TCID_{50}$/gram tissue)											
Virus	**Days post inoculation**	**Tracheo-bronchial lymph node**	**Tonsil**	**Olfactory bulb**	**Cerebrum**	**Cerebellum**	**Liver**	**Spleen**	**Heart**	**Kidney**	**Adrenal gland**	**Pancreas**	**Jejunum**
H3N2	0.5	0/4 (2.0-2.2)	0/4	1/4 (2.9)	0/4	0/4	0/4	0/4	0/4	0/4	0/4	0/4	0/4
	1	0/4 (2.0-2.4)	4/4 (2.7-3.8)	1/4 (1.7)	0/4	0/4	0/4	0/4	0/4	0/4	0/4	0/4	0/4
	2	0/4 (1.6-2.3)	2/4 (2.5-3.3)	1/4 (1.8)	0/4	0/4	0/4	0/4	0/4	0/4	0/4	0/4	0/4
	3	1/4 (1.8)	1/4 (2.8)	1/4 (1.8)	0/4	0/4	0/4	0/4	0/4	0/4	0/4	0/4	0/4
	4	0/4	1/4 (2.2)	0/4	0/4	0/4	0/4	0/4	0/4	0/4	0/4	0/4	0/4
	7	0/4	0/4	0/4	0/4	0/4	0/4	0/4	0/4	0/4	0/4	0/4	0/4
	14	0/4	0/4	0/4	0/4	0/4	0/4	0/4	0/4	0/4	0/4	0/4	0/4
pH1N1	0.5	2/4 (2.0-2.5)	4/4 (3.3-5.5)	3/4 (1.9-3.3)	3/4 (1.3-1.9)	1/4 (2.2)	0/4	0/4	0/4	0/4	0/4	0/4	0/4
	1	4/4 (3.8-4.5)	4/4 (4.8-6.2)	4/4 (1.6-5.4)	2/4 (2.0-3.2)	3/4 (1.6-2.9)	1/4 (1.4)	0/4	2/4 (1.6-2.6)	0/4	0/4	0/4	0/4
	2	4/4 (2.0-3.3)	4/4 (2.9-4.4)	4/4 (2.2-5.7)	3/4 (1.7-3.7)	2/4 (1.9-3.6)	0/4	0/4	1/4 (3.0)	0/4	0/4	0/4	0/4
	3	4/4 (2.0-2.8)	4/4 (3.7-5.3)	4/4 (2.0-4.5)	4/4 (1.2-3.8)	3/4 (1.3-4.1)	0/4	0/4	2/4 (1.7-2.4)	0/4	0/4	0/4	0/4
	4	4/4 (1.6-2.2)	3/4 (4.3-5.1)	4/4 (2.1-5.7)	3/4 (1.6-4.1)	3/4 (1.2-3.7)	0/4	0/4	2/4 (1.2-2.2)	0/4	0/4	0/4	0/4
	7	0/4	0/4	2/4 (1.7-1.8)	0/4	1/4 (1.3)	0/4	0/4	0/4	0/4	0/4	0/4	0/4
	14	0/4	0/4	0/4	0/4	0/4	0/4	0/4	0/4	0/4	0/4	0/4	0/4

follow up table 4

H5N1	0.5	4/4 (3.4-4.7)	3/4 (2.2-4.3)	1/4 (1.9)	1/4 (0.9)	0/4	0/3[a]	0/4	3/4 (0.9-1.2)	0/4	0/4	0/1[a]	0/1[a]
	1	4/4 (3.1-6.2)	4/4 (3.8-4.5)	2/4 (2.3-2.7)	2/4 (1.6-1.8)	2/4 (1.4-1.5)	2/4 (1.0-1.8)	4/4 (1.5-2.5)	2/4 (1.0-1.2)	3/4 (1.3-2.1)	1/4 (1.7)	nd	1/4 (1.6)
	2	6/6 (2.7-7.2)	6/6 (3.4-4.4)	5/6 (1.5-3.9)	4/6 (1.2-3.5)	0/6	3/6 (1.5-3.6)	5/6 (1.9-3.4)	3/6 (1.1-1.8)	3/6 (1.0-1.6)	3/6 (1.4-2.6)	nd	3/6 (4.2-5.2)
	3	3/3 (5.2-6.7)	3/3 (4.4-6.1)	2/3 (3.5-5.8)	1/4 (2.5)	2/3 (3.1-3.2)	3/3 (1.1-1.8)	3/3 (3.9-4.5)	2/3 (1.3-1.6)	1/3 (1.5)	2/3 (2.4-2.9)	nd	1/3 (4.5)
	4	3/3 (4.9-6.3)	3/3 (3.9-5.4)	2/3 (2.5-3.3)	3/4 (1.0-3.8)	2/3 (1.4-2.0)	3/3 (1.0-2.1)	3/3 (2.1-5.2)	3/3 (1.4-3.2)	2/3 (1.3-1.4)	2/3 (1.4-2.6)	nd	0/3
Cut off (Range)[b]		1.1-2.4	1.7-2.6	1.3-2.5	0.9-1.9	1.0-1.8	0.9-1.6	0.9-1.6	0.3-1.4	1.1-1.7	1.3-1.9	1.3-1.8	1.1-1.6

[a] Virus titers of the other animals in the group could not be determined. [b] The range of the cut off values is the range of the cut off values of the individual animals. nd, not determined.

Table 5. Leucocyte concentrations in the peripheral blood of ferrets inoculated with different influenza viruses

		Concentration of cells (10^9/L)						
Virus	**Days post inoculation**	**Total leucocytes**	**Lymphocytes**	**Blastocytes**	**Rod-shaped neutrophils**	**Eosinophils**	**Basophils**	**Normoblasts**
H3N2	0.5	9.6 (7.2-10.0)	2.59 (2.23-3.60)	0	0.04 (0-0.09)	0.19 (0-0.18)	0 (0-0.07)	0
	1	9.3 (4.2-14.1)	3.76 (2.14-4.51)	0	0	0.27 (0.08-0.55)	0 (0-0.08)	0
	2	8.3 (7.0-10.5)	2.18 (1.61-2.38)	0	0.04 (0-0.11)	0.27 (0-0.41)	0	0 (0-0.08)
	3	8.9 (7.6-9.3)	2.97 (1.95-3.59)	0	0 (0-0.09)	0.40 (0.09-0.53)	0.09 (0-0.34)	0
	4	9.1 (6.3-11.0)	2.23 (1.89-3.46)	0	0	0.30 (0.22-0.44)	0 (0-0.07)	0
	7	7.9 (5.8-9.5)	2.24 (2.03-2.61)	0	0 (0-0.09)	0.23 (0-0.17)	0.04 (0-0.10)	0
	14	5.8 (3.0-6.7)	1.95 (1.16-2.72)	0	0	0.26 (0-0.46)	0 (0-0.06)	0
pH1N1	0.5	9.9 (6.2-10.9)	2.95 (2.67-4.46)	0	0 (0-0.20)	0.30 (0.12-0.33)	0	0
	1	9.1 (8.6-12.1)	1.00 (0.73-1.29)	0	0.09 (0-0.36)	0.18 (0.17-0.46)	0 (0-0.12)	0
	2	9.4 (6.7-11.4)	1.66 (1.46-1.84)	0	0 (0-0.11)	0.03 (0-0.34)	0 (0-0.07)	0
	3	10.8 (7.9-11.2)	2.25 (1.56-4.31)	0	0 (0-0.11)	0.10 (0-0.21)	0 (0-0.11)	0
	4	8.5 (7.3-9.0)	1.31 (0.79-1.68)	0	0.04 (0-0.36)	0.04 (0-0.18)	0 (0-0.09)	0
	7	11.5 (10.7-20.7)	2.19 (1.44-4.17)	0	0	0 (0-0.62)	0.11 (0-0.22)	0
	14	9.0 (6.6-10.6)	4.57 (2.90-5.86)	0	0.05 (0-0.13)	0.15 (0-0.19)	0	0

follow up table 5

H5N1	0.5	10.5 (8.5-12.4)	2.46 (1.32-4.34)	0	0 (0-0.11)	0.25 (0.10-1.10)	0 (0-0.12)	0
	1	8.0 (6.6-14.1)	0.27 (0.07-0.99)	0	0.19 (0-0.34)	0 (0-0.07)	0	0
	2	5.4 (2.6-13.5)	0.47 (0.21-0.81)	0	0.06 (0.03-0.49)	0.03 (0-0.06)	0	0
	3	4.6 (4.1-5.0)	0.72 (0.70-0.74)	0	0.14 (0.12-0.15)	0.02 (0-0.04)	0	0
	4	5.8 (3.3-6.1)	0.73 (0.73-0.99)	0	0.46 (0.23-0.49)	0 (0-0.06)	0	0
Control	0.5	11.2 (9.0-19.0)	5.41 (2.97-6.84)	0	0 (0-0.19)	0.27 (0.09-0.42)	0.05 (0-0.12)	0
	1	9.1 (7.9-11.9)	3.97 (3.16-7.73)	0	0	0.16 (0.10-0.48)	0 (0-0.08)	0
	2	7.8 (5.9-11.8)	3.71 (2.89-5.09)	0	0 (0-0.12)	0.11 (0-0.24)	0	0
	3	10.1 (6.5-12.1)	4.07 (3.45-8.23)	0	0	0.11 (0-0.35)	0 (0-0.07)	0
	4	9.1 (5.3-15.2)	3.35 (2.06-6.38)	0	0 (0-0.05)	0.32 (0.20-0.46)	0	0
	7	13.6 (7.5-14.0)	3.15 (2.03-6.07)	0	0	0.18 (0.13-0.28)	0	0
	14	11.7 (6.1-15.6)	5.94 (2.20-6.71)	0	0 (0-0.16)	0.05 (0-0.16)	0	0
Negative control		7.6 (6.4-9.1)	2.86 (1.45-3.28)	0	0	0.03 (0-0.08)	0	0

Table 6. Parameter-estimates of generalized linear models predicting viral excretion of ferrets inoculated with different influenza viruses

Virus	Predictor	B coefficient	Standard error	Wald χ^2	P
H3N2	Intercept	1.605	0.34	22.3	<0.0001
	Viral production in URRT	0.383	0.08	22.3	<0.0001
pH1N1	Intercept	0.325	0.25	1.7	0.187
	Viral production in URRT	0.508	0.04	201.7	<0.0001
H5N1	Intercept	27.830	10.06	7.6	0.006
	Viral production in DRRT	-2.827	1.19	5.6	0.018
	Damage in DRRT	-3.887	1.72	5.1	0.024
	Viral production in DRRT x Damage in DRRT	0.456	0.20	5.0	0.025
	Damage in URRT	-0.687	0.20	11.8	0.001
	Damage in URRT x Viral production in URRT	0.046	0.01	9.2	0.002
	Damage in URRT x Viral production in DRRT	0.049	0.02	4.6	0.031

URRT: upper regions of the respiratory tract (nose and trachea); DRRT: deeper regions of the respiratory tract (bronchi, bronchioles and alveoli).

Table 7. Statistical analyses comparing pathology and virology scores among ferrets inoculated with different influenza viruses

		Significance of the difference (P-value)							
		Pathology scores				Virology scores			
Comparison	**Day**	**Percentage of affected lung tissue**	**Relative lung weight (%)**	**Extent and severity of alveolitis and alveolar damage (Score 0-3)**	**Percentage of air containing space in pulmonary tissue (Digital scoring)**	**Virus titers lung tissue (log10 TCID50 per gram)**	**Antigen expression in the alveoli by immunohistochemistry (%)**	**Percentage of antigen expression in the alveoli (Digital scoring)**	**Number of antigen expression counts in the alveoli (Digital scoring)**
H3N2 versus pH1N1	0.5	0.739	0.248	0.245	1.000	0.020*	0.019*	0.021*	0.020*
	1	0.017*	0.021*	0.019*	0.773	0.021*	0.018*	0.021*	0.018*
	2	0.018*	0.021*	0.019*	0.773	0.021*	0.018*	0.018*	0.017*
	3	0.013*	0.021*	0.021*	0.386	0.021*	0.017*	0.021*	0.076
	4	0.011*	0.021*	0.019*	0.021*	0.020*	0.014*	0.018*	0.026*
	7	0.014*	0.021*	0.019*	0.386	0.245	0.014*	0.772	0.439
	14	0.017*	0.021*	0.020*	0.564	0.309	1.000	0.508	0.508
H3N2 versus H5N1	0.5	0.036*	0.083	0.020*	0.386	0.020*	0.019*	0.021*	0.020*
	1	0.028*	0.083	0.019*	0.021*	0.021*	0.018*	0.021*	0.018*
	2	0.009**	0.011*	0.010*	0.019*	0.011*	0.009**	0.010*	0.010*
	3	0.019*	0.034*	0.032*	0.034*	0.034*	0.028*	0.034*	0.032*
	4	0.019*	0.034*	0.031*	0.077	0.032*	0.019*	0.028*	0.028*
pH1N1 versus H5N1	0.5	0.052	0.083	0.110	0.564	0.021*	0.083	0.386	0.386
	1	0.757	1.000	1.000	0.083	0.021*	0.083	0.043*	0.773
	2	0.009**	0.019*	0.010*	0.011*	0.831	0.054	0.201	0.032*
	3	0.048*	0.034*	0.285	0.034*	0.724	0.032*	0.034*	0.034*
	4	0.067	0.034*	0.064	0.034*	0.157	0.593	0.724	0.289

P-values were calculated by using the Mann-Whitney test. * P-value < 0.05. ** P-value < 0.01

CHAPTER 3

INFLUENZA VIRUS INFECTION IN ANIMAL MODELS

3.6

Efficacy of vaccination with different combinations of MF59-adjuvanted and non-adjuvanted seasonal and pandemic influenza vaccines against pandemic H1N1 (2009) influenza virus infection in ferrets

Journal of Virology (2011) 85(6): 2851-2858

JMA van den Brand,[1*] JHCM Kreijtz,[1*] R Bodewes,[1] KJ Stittelaar,[1,2]
G van Amerongen,[1] T Kuiken,[1] J Simon,[2] RAM Fouchier,[1] GD Giudice,[3]
R Rappuoli,[3] GF Rimmelzwaan,[1,2] ADME Osterhaus[1,2]

[*] *These authors contributed equally to this study*

Department of Virology, Erasmus Medical Centre, Rotterdam, The Netherlands [1]
Viroclinics Biosciences BV, Rotterdam, The Netherlands [2]
Novartis Vaccines and Diagnostics, Siena, Italy [3]

ABSTRACT

Serum antibodies induced by seasonal influenza or seasonal influenza vaccination exhibit limited or no cross-reactivity against the 2009 pandemic swine-origin influenza virus of the H1N1 subtype (pH1N1). Ferrets immunized once or twice with MF59-adjuvanted seasonal influenza vaccine exhibited significantly reduced lung virus titers but no substantial clinical protection against pH1N1 associated disease. However, priming with MF59-adjuvanted seasonal influenza vaccine significantly increased the efficacy of a pandemic MF59-adjuvanted influenza vaccine against pH1N1 challenge. Elucidating the mechanism involved in this priming principle will contribute to our understanding of vaccine- and infection-induced correlates of protection. Furthermore, a practical consequence of these findings is that during an emerging pandemic, the implementation of a priming strategy with an available adjuvanted seasonal vaccine to precede the eventual pandemic vaccination campaign may be useful and life-saving.

INTRODUCTION

The first influenza pandemic of the 21st century caused by the swine-origin influenza virus of the H1N1 subtype (pH1N1) emerged in Mexico in 2009 and caused an as-yet-unknown number of clinical and fatal cases.[320] Due to its rapid spread and the apparent absence of preexisting immunity in especially young people, there was an urgent need for a safe and effective vaccine.[321] Early in the pandemic phase it became clear that seasonal influenza infection or vaccination with seasonal influenza vaccines did not or only marginally induce antibodies that cross-reacted with pH1N1.[322,323] The vaccines used against seasonal influenza are so-called conventional non-adjuvanted vaccines that display suboptimal immunogenicity and reduced protection due to periodic antigenic drifts.[324,325] To enhance immunogenicity and/or broaden the immune response, there are several options: the use of alternative routes for antigen delivery, the administration of higher antigen doses, the selection of more conserved vaccine antigens, or the addition of an adjuvant to the vaccine.[326] There are several adjuvants under development, most of them based on oil-in-water emulsions.

MF59 is such an adjuvant that has been well characterized and is used in a seasonal influenza vaccine that has been registered in many European and other countries since 1997. The adjuvant is an oil-in-water emulsion that contains 9.75 mg squalene, 1.175 mg polysorbate 80, 1.175 mg sorbitan trioleate, sodium citrate dihydrate, and citric acid monohydrate.[327] MF59 has been shown to potentiate the immunogenicity of seasonal and pandemic vaccines at all ages.[328] It was the first adjuvant to be shown to successfully allow dose sparing with an H5-based vaccine and to widen the breadth of cross-clade neutralization by anti-HA antibodies.[327,329] In addition, more recently MF59 was shown to expand the repertoire of B-cell epitopes recognized by anti-HA cross-neutralizing antibodies.[330] MF59-adjuvanted swine origin H1N1 vaccine has been widely used in many European and other countries during the past pandemic[331] and is now utilized for the trivalent vaccine for the season 2010-2011 which contains the new H1N1 strain. For all of these reasons, it was relevant to ask what contribution MF59 could have given to a potential effect of vaccination of seasonal H1N1 on subsequent vaccination with the swine-origin H1N1 vaccine.[332]

In pre-clinical and clinical studies it thus has been demonstrated that the adjuvant MF59 has an antigen-sparing effect and broadens the intra-subtypic antibody response against influenza viruses upon vaccination.[330,333-335] Therefore, we investigated the potential of an MF59-adjuvanted trivalent seasonal influenza vaccine to elicit protection against pH1N1 infection in ferrets, since in this vac-

cine a virus strain is represented that shares an ancestor with pH1N1.[336] Recently, we have shown that immunization with an MF59-adjuvanted seasonal influenza vaccine did prime ferrets for the protective antibody response induced upon a second immunization with the MF59 adjuvanted pH1N1 vaccine.[332] To obtain a more detailed understanding of the impact of different vaccination strategies, we analyzed here to what extent thus-vaccinated ferrets would be protected from pH1N1 replication in the upper and lower respiratory tracts and from pH1N1 infection associated disease by evaluating the gross pathology and histopathological changes of their lungs.

MATERIALS AND METHODS

Vaccines

In the present study we used commercially available seasonal trivalent vaccine with (sVacMF59) and without (sVac) MF59 as an adjuvant. Both vaccines contained envelope subunits (hemagglutinin [HA] and neuraminidase [NA]) (15 μg HA) from the influenza viruses A/Brisbane/59/2007 (H1N1), A/Brisbane/10/2007 (H3N2), and B/Brisbane/60/2008. The subunit vaccine based on pandemic influenza virus A/California/4/2009 (H1N1) was used as a prototype pH1N1 vaccine (15 μg HA), which was also used with (pVacMF59) or without MF59 (pVac) as an adjuvant. The ferrets received 0.5 ml of vaccine containing 0.25 ml of antigen and 0.25 ml of MF59. The adjuvant MF59 and phosphate-buffered saline (PBS) were also used to immunize control animals.

Viruses

Influenza virus A/Netherlands/602/2009 (A/NL/602/09) (pH1N1) was isolated from a 3-year-old child that was the first laboratory-confirmed case of the pandemic influenza virus in the Netherlands.[152] The virus was isolated in embryonated chicken eggs and subsequently passaged once in Madin-Darby canine kidney (MDCK) cells. The infectious virus titer (50% tissue culture infective dose [$TCID_{50}$]) was determined as described previously.[279]

Ferret studies

Healthy outbred male and female ferrets (*Mustela putorius furo*) between 6 and 12 months of age and seronegative for antibodies against circulating influenza viruses H1N1, H3N2 and pH1N1 by hemagglutination inhibition (HI) assay were used. Two weeks prior to the start of the experiment, the animals were anesthetized by using a cocktail of ketamine (Alfasan, Woerden, The Netherlands) and domitor (Orion Pharma, Espoo, Finland), and a temperature logger (DST micro-T ultra small temperature logger; Star-Oddi, Reykjavik, Iceland) was placed in their peritoneal cavities. This device recorded body temperature of the animals every 15 min. The animals were maintained in standard housing and provided with commercial food pellets and water *ad libitum*. For the challenge inoculation, the animals were placed in BSL-3 isolator units. An independent animal ethics committee of the Erasmus Medical Center (DEC consult) approved the experimental protocol before the start of the experiments.

Immunizations and infection: experiment 1

Three groups of 6 ferrets each were immunized intramuscularly in a 3-week interval regimen. Animals received the following immunizations: two doses of MF59, one dose of sVacMF59, or two times sVacMF59 (Table 1). At 4 weeks after the last immunization the animals were challenged

intratracheally with pH1N1 at a dose of 10^6 $TCID_{50}$ in a volume of 3 ml. On days 0, 2 and 4 after infection, nose and throat swabs were taken from the animals under anesthesia. At 4 days after challenge, the ferrets were euthanized by exsanguination under anesthesia.

Table 1. Clinical parameters, percentage of lung tissue affected, and relative lung weights of ferrets 4 days after infection with pH1N1 in experiment 1

Immunization	% Wt loss (SD)	Presence of Fever	% Affected Lung area (SD)	% Relative Lung wt[a] (SD)
MF59	12.9 (4.2)	Yes	36.7 (10.3)	1.67 (0.22)
sVacMF59 (one dose)	14.0 (7.8)	Yes	28.3 (7.5)	1.59 (0.30)
sVacMF59 (two doses)	11.4 (2.6)	Yes	18.3 (13.3)	1.60 (0.38)

[a] The relative lung weight is expressed as a percentage of the total body weight.

Immunizations and infection: experiment 2

For the second experiment 7 groups of 6 animals each received two immunizations at an interval of 4 weeks with different combinations of vaccines (Table 2). Animals that were primed with adjuvanted seasonal vaccine (sVacMF59) were boosted with pandemic vaccine without (pVac) or with (pVacMF59) adjuvant (groups 1 and 2). Animals primed with unadjuvanted seasonal vaccine (sVac) were boosted with sVac, pVac, or pVacMF59 (groups 3, 4 and 5). The animals in groups 6 and 7 received a mock vaccination with PBS and subsequently an immunization with pVacMF59 or PBS, respectively. A group that would receive PBS and subsequently sVacMF59 was not included in experiment 2 since results similar as observed in groups 3 and 7 of experiment 2 could be expected by extrapolation of the results from experiment 1.

At 4 weeks after the second immunization the animals were challenged intratracheally with pH1N1 at a dose of 10^6 $TCID_{50}$. On days 0, 1, 2, 3 and 4 after infection, nose and throat swabs were taken from the animals, and on day 4 the animals were euthanized by exsanguination under total anesthesia.

Serology

Serum samples collected prior to the first and second immunizations and prior to infection were stored at –20°C. They were tested for the presence of anti-HA antibodies using an HI assay with 1% turkey erythrocytes.[289] Subsequently, the sera were tested for the presence of virus neutralizing antibodies by using a micro virus neutralization (VN) assay.[337] Sera were tested for the presence of antibodies reactive with influenza viruses A/NL/602/09 (pH1N1), A/Brisbane/59/2007

Table 2. Vaccination parameters in experiment 2[a]

Group	1st immunization		2nd immunization	
	Antigen	Adjuvant	Antigen	Adjuvant
1	sVac	MF59	pVac	
2	sVac	MF59	pVac	MF59
3	sVac		sVac	
4	sVac		pVac	
5	sVac		pVac	MF59
6	PBS		pVac	MF59
7	PBS	PBS	PBS	PBS

[a] Animals were immunized intramuscularly with an interval of 4 weeks. sVac, seasonal vaccine, subunits (0.25 ml antigen, 15 µg HA) from influenza viruses A/Brisbane/59/2007 (H1N1), A/Brisbane/10/2007 (H3N2) and B/Brisbane/60/2008; pVac, pandemic vaccine, subunits (0.25 ml antigen, 15 µg HA) from virus strain A/California/04/2009 (pH1N1); MF59, 0.25 ml.

(H1N1) and A/Uruguay/716/2007 (H3N2) in the HI assay and in the VN-assay (experiment 2 sera only). For this purpose, a reverse genetics virus was used with the HA and NA of the 2009 H1N1 virus and the remaining six gene segments of influenza virus A/Puerto Rico/8/34 (A/PR/8/34). The antibody titers obtained with this virus were comparable with those obtained with the wild-type pH1N1 virus (data not shown). The sera of ferrets infected with the homologous strain were used as control sera. These sera were also tested against other swine influenza H1N1 viruses: A/swine/Iowa/15/30, A/swine/Netherlands/25/80, A/Netherlands/386/86 (derived from a zoonotic infection),[338] and influenza H5N1 virus A/Vietnam/1194/04. Post-infection sera from ferrets infected with these viruses were used as positive controls.

Virus replication in the upper and lower respiratory tracts

Samples of all lobes of the right lung and the accessory lobe were collected and snap-frozen by using a dry ice-ethanol bath and stored at –70°C until further processing. Lung samples were weighed and subsequently homogenized with a FastPrep-24 (MP Biomedicals, Eindhoven, The Netherlands) in Hanks balanced salt solution containing 0.5% lactalbumin, 10% glycerol, 200 U of penicillin/ml, 200 μg of streptomycin/ml, 100 U of polymyxin B sulfate/ml, 250 μg of gentamycin/ml, and 50 U of nystatin/ml (ICN Pharmaceuticals, Zoetermeer, The Netherlands) and centrifuged briefly before dilution.

After collection, nose and throat swabs were stored at -70°C in the same medium used for the processing of the lung samples. Quadruplicate 10-fold serial dilutions of lung and swab supernatants were used to determine the virus titers in confluent layers of MDCK cells as described previously.[279]

Histopathology and immunohistochemistry

The animals were necropsied according to a standard protocol. The trachea was clamped off so that the lungs would not deflate upon opening the pleural cavity. This allowed an accurate visual quantification of the areas of affected lung parenchyma. Samples for histological examination of the left lung and trachea were taken and stored in 10% neutral-buffered formalin (lungs after inflation with formalin), embedded in paraffin, sectioned at 4 μm, and stained with hematoxylin and eosin (HE) for examination by light microscopy. Samples were taken in a standardized way and not guided by changes observed in the gross pathology. Histopathology was described, and semi-quantitative assessment of influenza virus-associated inflammation in the lung was performed as described previously (Table 4).[292] For the extent of alveolitis and alveolar damage we used the following scoring scale: 0, 0%; 1, 1 to 25%; 2, 25 to 50%; 3, > 50 %. The severity of alveolitis was scored as follows: 0, no inflammatory cells; 1, few inflammatory cells; 2, moderate numbers of inflammatory cells; 3, many inflammatory cells. We also scored for presence of: alveolar edema (no = 0, yes = 1), alveolar hemorrhage (no = 0, yes = 1), and type II pneumocyte hyperplasia (no = 0, yes = 1). For the severity of bronchiolitis, bronchitis and tracheitis we used the following scale: 0, no inflammatory cells; 1, few inflammatory cells; 2, moderate numbers of inflammatory cells; 3, many inflammatory cells. Finally, the extent of peribronchial, peribronchiolar and perivascular infiltrates we scored as follows: 0, none, 1, 1 to 2 cells thick, 2, 3 to 10 cells thick, 3, > 10 cells thick. Slides were examined without knowledge of the identity of the animals. The cumulative scores for size and severity of inflammation provided the total score per animal.

Immunohistochemistry

For the detection of influenza A virus antigen, sequential slides were stained with a monoclonal antibody (Clone HB65 IgG2a [American Type Culture Collection]) against the nucleoprotein of influenza A virus. Goat-anti-mouse IgG2a HRP (Southern Biotech, Birmingham, Alabama, USA) was used as secondary antibody. Peroxidase was revealed with a diaminobenzidine substrate, resulting in a deep red precipitate in the nuclei of infected cells and a less intense red staining of their cytoplasm. The sections were counterstained with hematoxylin. After determining the cell types expressing viral antigen, semiquantitative assessment of influenza virus antigen expression in the lungs was performed as reported previously.[292] For the alveoli, 25 arbitrarily chosen, x20 objective, fields of lung parenchyma in each lung section were examined by light microscopy for the presence of influenza virus nucleoprotein, without the knowledge of the identity of the animals. The cumulative scores for each animal were presented as number of positive fields per 100 fields. For the bronchi and bronchioles, the percentage of positively staining bronchial and bronchiolar epithelium was determined on every slide, and the average of the four slides was taken to provide the score per animal.

Statistical analysis

Differences between groups were analyzed statistically using the Student t test. Differences were considered significant at $P < 0.05$.

RESULTS

Experiment 1: efficacy of MF59-adjuvanted seasonal influenza vaccine

Ferrets immunized once or twice with sVac-MF59 developed HI antibodies against the seasonal H1N1 strain A/Brisbane/59/07 with a geometric mean titer (GMT) of 45 (standard deviation [SD] = 6) and 968 (SD = 3), respectively. After a single immunization four of six animals developed detectable antibody titers, whereas after two immunizations all animals tested positive. The A/Brisbane/59/07-specific antibodies did not cross-react with pH1N1 in the HI assay.

Upon infection with pH1N1 virus animals from both vaccinated and the control MF59 groups developed clinical signs such as lethargy, loss of appetite, and dyspnea from day 2 onward. All animals lost weight after infection ranging from 12.9 (SD = 4.2) to 14.0% (SD = 7.8) and 11.4% (SD = 2.6) for the animals immunized with MF59, sVac and sVacMF59 (two immunizations), respectively (Table 1). Virus was detected in the nose on 2 days post infection (dpi) in at least one of six animals and by day 4 all animals had detectable virus in the nose with GMTs of $10^{5.6}$ (SD = $10^{0.6}$), $10^{4.3}$ (SD = $10^{1.9}$) and $10^{4.6}$ (SD = $10^{0.4}$) for the three groups, respectively (Figure 1A). All animals had detectable virus titers in their throats on day 2 and 4 (Figure 1B). The differences in virus titers in the upper respiratory tract between the respective study groups were not statistically significant. On 4 dpi virus titers in the lungs of ferrets that had received two immunizations with sVac-MF59 were significantly lower ($P = 0.003$) than those in the MF59 immunized group (Figure 1C). The reduced virus replication correlated with a reduction in gross pathological changes of the lungs (Table 1).

Experiment 2: efficacy of pandemic vaccine and effects of priming and MF59 usage

Serology

After primary immunization with seasonal influenza vaccine or PBS, animals received a second

immunization with seasonal vaccine, pandemic vaccine or PBS. Both vaccines were used with or without MF59, and all groups that had received pVac in combination with MF59 developed antibody titers against the homologous strain, as detected in the HI and VN assays.

In the sVacMF59-pVac group and sVac-pVac animals (groups 1 and 4) the mean HI antibody titers against the pandemic virus were 48.8 (SD = 5.6) and 26.2 (SD = 4.8), and the animals had VN antibody titers of 46.5 (SD = 3.6) and 18.3 (SD = 4.0), respectively. Animals that had received pVac-MF59 as a second immunization appeared to have higher antibody titers, especially when they had first been immunized with sVac-MF59 (group 2). The mean antibody titers in this group were 565.2 (SD = 1.9) compared to 163.2 (SD = 2.3) and 231.6 (SD = 2.4) in the PBS-pVacMF59 (group 6) and sVac-pVacMF59 animals (group 5), respectively. The VN titers for these groups were 767.1 (SD = 1.6), 97.9 (SD = 4.8) and 229.0 (SD = 2.4), respectively. In the sVac-sVac animals (group 3), only a serological response against the seasonal influenza A/H1N1 virus was detected, whereas no virus-specific antibodies were detected in sera from the PBS-PBS animals (group 7).

Post-immunization sera were tested for cross-reactive antibody responses against multiple swine influenza viruses of the H1N1 subtype and H5N1 virus. Cross-reactive antibody titers were detected

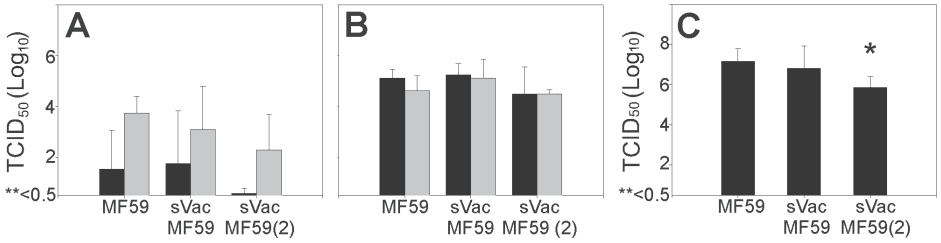

Figure 1. *Virus replication in the upper and lower respiratory tract of ferrets. Virus replication was determined in the nose (A) and throat (B) on 2 (black bars) and 4 (grey bars) dpi and expressed as TCID50/ml. (C) Lung virus titers were determined on 4 dpi and expressed as $TCID_{50}$/g lung. (An asterisk indicates that the mean titer is significantly lower than that in the MF59 immunized group; 0.5 $TCID_{50}$ is the limit of detection of the assay.)*

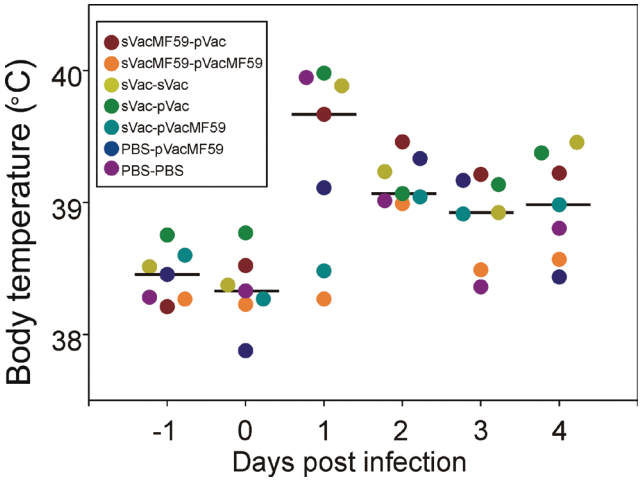

Figure 2. *Mean body temperature of ferrets. The mean body temperatures in ferrets (n = 6 per group) were measured by a temperature logger (DST micro-T ultra small temperature logger; Star-Oddi, Reykjavik, Iceland) placed in the peritoneal cavity. Black bars indicate the median. (In group 3, data from four temperature loggers could be retrieved and in groups 1, 6 and 7 data from five temperature loggers could be retrieved. The data from the other loggers could not be retrieved.)*

against two swine influenza H1N1 strains from the Netherlands: A/Netherlands/386/86 (derived from a zoonotic event) and A/swine/Netherlands/25/80 (Table 3). The ranking of GMTs in the HI assay for the different groups was identical to that of the GMTs against the homologous influenza virus. No cross-reactivity was seen with influenza virus A/Swine/Iowa/15/30 H1N1 or with A/Vietnam/1194/04 H5N1.

Clinical signs

From 1 dpi onward, all infected animals developed symptoms including lethargy, loss of appetite, and dyspnea. These symptoms were mild in the sVacMF59-pVacMF59 animals (group 2). To quantify clinical outcome, animals were weight before infection, and on 4 dpi and their body temperatures were recorded during the course of the experiment. The greatest weight loss was observed in animals from groups 3, 4, 6 and 7 (12 to 17%), whereas animals from groups 1, 2 and 5 had reduced weight loss with median percentages of 10.8 (range; 0 to 17), 7.5 (2 to 16), and 10.1 (1 to 22), respectively (Table 4). The weight losses in the sVacMF59-pVac or pVacMF59 animals (groups 1 and 2) were lower than those of the other groups. Body temperature rose during 1 dpi in all animals (Figure 2). The sVacMF59-pVacMF59 animals (group 2) displayed a reduced temperature rise and did not develop a sustained fever in contrast to the other groups.

Virus replication in the respiratory tract

Nose and pharyngeal swabs were collected daily to determine the kinetics of virus replication in the upper respiratory tract. Not all nasal swabs tested positive or animals became positive only after 3 or 4 dpi. However, those that were positive showed an increase in virus titers in time with maximum titers on 4 dpi of $10^{3.1}$ (SD = $10^{1.4}$), $10^{3.4}$ (SD = $10^{1.4}$), $10^{3.1}$ (SD = $10^{1.3}$) and $10^{3.3}$ (SD = $10^{1.1}$) for groups 1, 3, 4 and 7, respectively (Figure 3A). Lower virus titers – $10^{2.0}$ (SD = $10^{2.0}$) and $10^{1.7}$ (SD = $10^{1.3}$), respectively – were found in the ferrets that had been immunized with sVac or PBS and subsequently with pVacMF59 (groups 5 and 6). Except for one ferret with a low titer on 3 dpi, no virus was detectable in nasal swabs from animals that had been immunized with sVac-MF59, followed by pVacMF59 (group 2). In pharyngeal swabs of virtually all animals of groups 1, 3, 4, 5, 6 and 7 virus was detected from 1 dpi onward, with titers increasing until 4 dpi, resulting in mean titers of $10^{4.1}$ (SD = $10^{0.9}$), $10^{4.3}$ (SD = $10^{0.8}$), $10^{4.2}$ (SD = $10^{1.3}$), $10^{3.0}$ (SD = $10^{2.1}$), $10^{4.1}$ (SD = $10^{0.8}$) and $10^{3.8}$ (SD = $10^{0.4}$), respectively (Figure 3B). All of the sVacMF59-pVacMF59 animals (group 2) tested negative on 4 dpi, and most of them also tested negative on 2 dpi.

On 4 dpi the highest virus titers were found in the lungs of ferrets that had been immunized twice with sVac, $10^{6.0}$ (SD = $10^{0.6}$), or PBS, $10^{5.5}$ (SD = $10^{0.8}$) (groups 3 and 7; Table 4). Animals that had received sVacMF59 or sVac, followed by pVac (groups 1 and 4) showed lower virus titers of $10^{2.7}$ (SD = $10^{1.9}$) and $10^{3.1}$ (SD = $10^{1.8}$), respectively. The sVac-pVacMF59 immunized animals (group 6) had significantly lower virus titers – $10^{1.0}$ (SD=0) – in their lungs than those of the other groups. Moreover, no virus was detected in the lungs of animals that had been immunized with sVacMF59 or PBS, and subsequently received pVacMF59 (groups 2 and 6).

Pathology

In all ferrets, the primary macroscopic lesions were found in the lungs and consisted of pulmonary consolidation, characterized by reddening and slightly increased firmness of the lung parenchyma. The extent of pulmonary consolidation was assessed by visual quantification of the affected lung

Table 3. HI and VN antibody titers against swine origin influenza A/H1N1 viruses and H5N1 virus

Group	Immunization		GMT (SD) [a]									
			Swine-origin H1N1									
			A/NL/602/09[b]		A/NL/386/86		A/NL/25/80		A/Iowa/15/30		A/VN/1194/04	
	First	Second	HI	VN	HI	VN	HI	VN	HI	VN	HI	VN
1	sVacMF59	pVac	49 (6)	47 (4)	9 (3)	6 (1)	8 (2)	<10	<10	<10	<10	<10
2	sVacMF59	pVacMF59	565 (2)	767 (2)	181 (2)	18 (3)	80 (2)	16 (2)	<10	<10	<10	<10
3	sVac	sVac	<10	<10	<10	6 (1)	<10	<10	<10	<10	<10	<10
4	sVac	pVac	26 (5)	18 (4)	<10	10 (3)	<10	6 (1)	<10	<10	<10	<10
5	sVac	pVacMF59	232 (2)	229 (2)	45 (4)	<10	33 (3)	7 (2)	<10	<10	<10	<10
6	PBS	pVacMF59	163 (2)	98 (5)	28 (3)	<10	27 (3)	<10	<10	<10	<10	<10
7	PBS	PBS	<10	<10	<10	<10	<10	<10	<10	<10	<10	<10

[a] Antibody titers are expressed as geometric mean titer (GMT) with the standard deviation in parentheses. A/NL/602/09, A/Netherlands/602/2009; A/NL/386/86, A/Netherlands/386/1986; A/NL/25/80, A/Netherlands/25/1980; A/Iowa/15/30, A/Swine/Iowa/15/30; A/VN/1194/04, A/Vietnam/1194/04.
[b] Data were obtained as described by Del Giudice et al.332

Table 4. Weight loss, percentage of lung tissue affected, relative lung weights, and virus titers in the lungs of ferrets 4 days after infection with pH1N1

Group	Immunization		Wt loss (%)		Affected lung tissue (%)		Relative lung Weight (%)		Lung virus titers ($TCID_{50}$/gr of lung)[a]	
	First	Second	Median	Range	Median	Range	Median	Range	Mean (SD)	nb
1	sVacMF59	pVac	10.8	<0 - 17	5.0	0-20	0.9	0.8-1.3	2.7 (1.9)	4
2	sVacMF59	pVacMF59	7.5	2-16	5.0	0-5	0.8	0.7-0.9	Neg[d]	0
3	sVac	sVac	15.1	7-33	15.0	5-30	1.2	0.8-2.0	6.0 (0.6)	6
4	sVac	pVac	15.6	8-23	7.5	0-20	1.0	0.7-1.3	3.1 (1.8)	4
5	sVac	pVacMF59	10.1	1-22	5.0	0-20	0.9	0.6-1.3	1.0 (0.0)	1
6	PBS	pVacMF59	13.0	6-17	5.0	0-5	1.0	0.7-1.3	Neg	0
7	PBS	PBS	14.3	9-30	40.0	40-80	1.2	0.8-1.9	5.5 (0.8)	6

[a] Data were obtained in the study as described by Del Giudice et al.332 and are given as log10 values. [b] n, The number of animals positive for virus isolation from the lungs of six animals per group. [c] Weight loss data were available for 5 of 6 animals. [d] Neg, negative (i.e., all animals tested negative for virus replication in the lungs).

area and the relative lung weight. The average percentage of affected lung tissue was lowest in ferrets first vaccinated with sVac with or without MF59 or with PBS and subsequently with pVac with or without MF59 (groups 1, 2, 4, 5 and 6). The ferrets vaccinated twice with sVac (group 3) and the sham-vaccinated animals (group 7) had the highest percentages of affected lung tissue (Table 4). However, a slightly different pattern was found for the relative lung weights: only animals that had first received sVac with or without MF59 and subsequently pVac with MF59 (groups 2 and 5) had low relative lung weights. Other macroscopic lesions related to challenge with influenza virus were enlargement of the tracheo-bronchial lymph nodes (lymphadenopathy) and splenomegaly. This was considered to be an effect of the immune response following influenza virus infection of the respiratory tract. No notable lesions were found in other tissues.

The macroscopically observed pulmonary consolidation corresponded with necrotizing broncho-interstitial pneumonia at microscopic examination (Figure 4). This broncho-interstitial pneumonia was characterized by the presence of inflammatory cells in alveolar and bronchiolar lumina and walls and necrosis of alveolar and bronchiolar epithelium. The inflammatory cells consisted mainly of neutrophils and macrophages with variable amounts of intraluminal edema fluid, fibrin, and erythrocytes. Type II pneumocyte hyperplasia was observed as a reaction to alveolar epithelial cell damage. Mild to severe interstitial edema was seen in perivascular and peribronchiolar areas. The tracheo-bronchial submucosal glands in many animals exhibited infiltration of neutrophils and fewer macrophages and lymphocytes with associated epithelial cell necrosis. Less severe inflammation and epithelial necrosis were observed in bronchi and trachea. There were no indications for concurrent infections.

The histological parameters that were scored are summarized in Table 5. For all parameters but one, the sVacMF59-pVacMF59 animals (group 2) had the lowest scores for alveolar lesions. The most severe lesions were found in the sham-vaccinated animals (group 7). Again, the sVacMF59-pVacMF59 animals (group 2) had the lowest scores for bronchiolitis and bronchitis. These scores were lower in the PBS-pVacMF59 and control animals (groups 6 and 7) than in the other groups (group 1, 3, 4 and 5). The colocalization of perivascular and peribronchiolar cuffing with lymphocytes at areas of alveolar inflammation in lung sections suggests that the lymphocytic infiltration was a response to the alveolar inflammation.

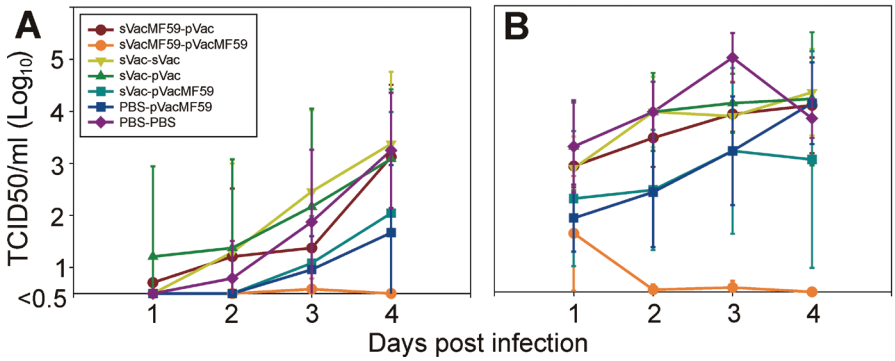

Figure 3. *Virus titer kinetics in the upper respiratory tracts of ferrets. Virus titers were determined daily in the noses (A) and throats (B) of the infected animals (n = 6 per group). Nasal and pharyngeal swabs that tested negative were assigned a value of 0.5. (0.5 is the limit of detection of the assay)*

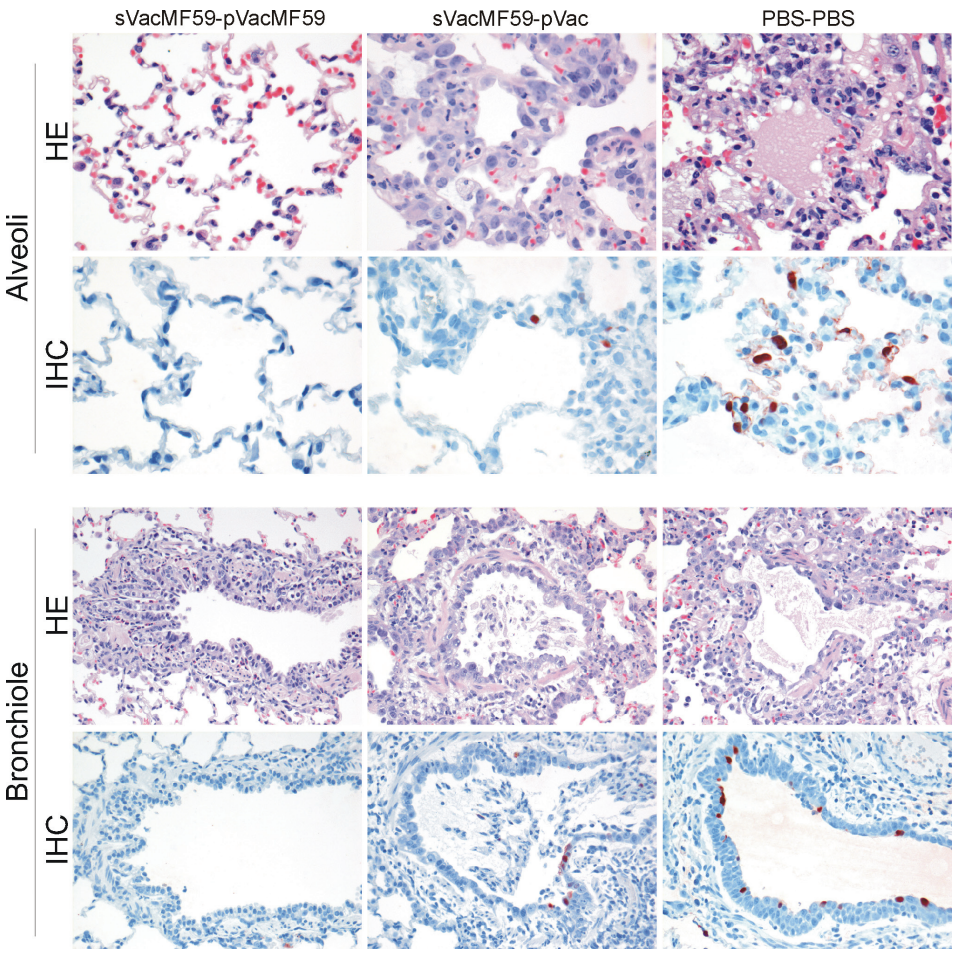

Figure 4. *Lung pathology and virus replication on 4 dpi. Histopathology and immunohistochemistry analyses were performed 4 dpi with pH1N1. Representative slides were selected for the protected animals from group 2 (immunized with sVacMF59 and pVacMF59). For intermediate protection representative slides were chosen from group 1 (immunized with sVacMF59 and pVac) and represent group 1 and groups 3 to 6. The unprotected animals were from group 7; these were immunized twice with PBS and developed severe pneumonia upon challenge infection. Based on the histopathology of the alveoli (first row, HE stained) there was only mild inflammation in the sVacMF59-pVacMF59 immunized animals (group 2) with few inflammatory cells. The inflammation was intermediate in animals of group 1 and groups 3 to 6, with thickening of the septa with moderate infiltration of neutrophils, pneumocyte type II hyperplasia, and mild necrosis, and a severe pneumonia was seen in the PBS control group with severe necrosis and intra-alveolar flooding with edema fluid and inflammatory cells. Based on immunohistochemistry of the alveoli (second row, IHC) there was no antigen expression in sVacMF59-pVacMF59 immunized animals, intermediate expression of predominantly pneumocytes type II in group 1 and groups 3 to 6, and abundant expression in the PBS control group. In the bronchioles (third row) there was a mild to moderate bronchiolitis with neutrophils and macrophages and necrosis in sVacMF59-pVacMF59 immunized animals (group 2) and the animals in group 1 and groups 3 to 6, and there was severe bronchiolitis with severe necrosis in the animals in group 7. Based upon immunohistochemistry (fourth row), there was no antigen expression in sVacMF59-pVacMF59 immunized animals, mild expression in bronchiolar epithelial cells in groups 1 and 3-6, and moderate expression in the PBS control group.*

Table 5. Semiquantitative scoring for histopathology in lungs of ferrets 4 days after infection with pH1N1

Group	Immunization		Average[a]							
			Score (0 to 3)		% positive slides			Score (0 to 3)		
	First	Second	Extent of alveolitis/ alveolar damage	Severity of alveolitis	Alveolar oedema	Alveolar hemorrhage	Type II pneumocyte hyperplasia	Severity of bronchitis/ bronchiolitis	Degree of perivascular/ peribronchial cuffing	Severity of tracheitis
1	sVacMF59	pVac	1.92	1.13	17	0	100	2.21	2.13	1.17
2	sVacMF59	pVacMF59	1.58	0.96	4	0	100	1.13	1.58	1.17
3	sVac	sVac	2.85	1.55	65	35	95	2.00	2.05	0.17
4	sVac	pVac	2.29	1.33	50	8	100	2.04	2.08	0.50
5	sVac	pVacMF59	1.92	1.25	17	0	100	2.00	1.79	0.80
6	PBS	pVacMF59	2.50	1.29	13	0	100	1.96	2.04	1.30
7	PBS	PBS	2.75	1.79	88	17	100	1.67	1.63	0.50

[a] Scores and values were determined as follows. Extent of alveolitis and alveolar damage: 0, 0%; 1, 25%; 2, 25-50%; 3, > 50 %. Severity of alveolitis: 0, no inflammatory cells; 1, few inflammatory cells; 2, moderate numbers of inflammatory cells; 3, many inflammatory cells. Alveolar edema: 0, no; 1, yes. Alveolar hemorrhage: 0, no; 1, yes. Type II pneumocyte hyperplasia: 0, no; 1, yes. Severity of bronchiolitis, bronchitis and tracheitis: 0, no inflammatory cells; 1, few inflammatory cells; 2, moderate numbers of inflammatory cells; 3, many inflammatory cells. Extent of peribronchial, peribronchiolar, and perivascular infiltrates: 0, none; 1, 1 to 2 cells thick; 2, 3 to 10 cells thick; 3, more than 10 cells thick.

Table 6. Semiquantitative assessment of influenza virus antigen expression in the lungs of ferrets 4 days after infection with pH1N1

Group	Immunization		Score[a]					
			Alveoli		Bronchioles		Bronchi	
	First	Second	Median	Range	Median	Range	Median	Range
1	sVacMF59	pVac	4.5	0-8	4.5	0.5-6.3	0.5	0-2.8
2	sVacMF59	pVacMF59	0	n.a.	0	0-1.3	0	n.a.
3	sVac	sVac	10.5	5-84	4.5	1.8-6.3	4.5	1.3-8.8
4	sVac	pVac	7	1-56	2.13	1.5-7.5	1.75	0-2.8
5	sVac	pVacMF59	2.5	0-5	2.5	0-5	0.25	0-0.3
6	PBS	pVacMF59	4.5	1-10	8.75	2.5-20	1.88	0-15
7	PBS	PBS	66	14-96	5.63	5-6.3	5.75	5-16.3

[a] For the alveoli, 25 arbitrarily chosen, 20x objective fields of lung parenchyma in each lung section were examined by light microscopy for the presence of influenza viral nucleoprotein, without the knowledge of the identity of the animals. The cumulative scores for each animal are presented as number of positive fields per 100 fields. For the bronchi and bronchioles, the percentages of positively staining bronchial and bronchiolar epithelium were estimated on every slide, and the average of the four slides was taken to provide the score per animal.

Immunohistochemistry

By immunohistochemistry, influenza virus antigen expression was visible as diffuse to granular red staining, most often stronger in the nucleus than in the cytoplasm (Figure 4). Influenza virus antigen expression was closely associated with the presence of histological lesions at different levels of the lower respiratory tract. Antigen expression was seen predominantly in type I and II pneumocytes, alveolar macrophages, bronchiolar epithelial cells, bronchial epithelial cells and tracheal and bronchial epithelial cells of submucosal glands. Semiquantitative scoring showed that there was no influenza virus antigen expression in the alveoli and bronchi, and expression in only few cells in the bronchioles of the sVacMF59-pVacMF59 animals (group 2; Table 6). The highest expression at all levels of the respiratory tract was seen in the control animals (group 7), followed by the PBS-pVacMF59 animals (group 6), as well as the sVac-sVac and sVac-pVac animals (groups 3 and 4).

DISCUSSION

The primary aim of vaccination against pH1N1 influenza is the reduction of virus replication and the associated spread of the virus, as well as prevention of the disease and pathological changes in the respiratory tract. In the present paper we have carefully described these parameters in ferrets after different vaccination regimes using combinations of MF59-adjuvanted and nonadjuvanted seasonal and pandemic influenza vaccines. The most striking finding was that pre-vaccination with sVacMF59 not only induced a strong priming effect on the antibody response elicited by pVacMF59 vaccination but also a strong priming effect on the protection induced with this vaccine against virus replication, associated disease, and pathological changes in the respiratory tract.

First, we showed that immunization with sVacMF59 alone, administered either once or twice, failed to induce pH1N1 influenza virus-specific antibodies and, at best, afforded modest protection. These findings are in agreement with the failure to induce antibodies cross-reactive with pH1N1 influenza virus in humans with adjuvanted and nonadjuvanted seasonal influenza vaccines.[323] Apparently, the HAs of the seasonal and pandemic H1N1 strains are antigenically quite distinct, as had already been shown by using post infection ferret serum against both strains.[96]

Although sVacMF59 failed to induce cross-reactive antibodies, it did have a significant priming effect on the induction of both specific antibodies and protective responses induced by pVacMF59 against pH1N1 influenza virus. It may be speculated that this priming effect, which apparently should be attributed to the adjuvant, is caused by eliciting cross-reactive T-cell and memory B-cell responses.[330,339] Such responses may indeed contribute to protective and cross-reactive immunological memory, which may be an additional correlate of protection against influenza besides specific HI or VN antibodies.

Cross-reactive antibody titers against two swine influenza viruses of the H1N1 subtype indicate broadening of the antibody response by MF59 adjuvanted vaccines when used for prime and boost immunizations. This, as well as the absence of intersubtypic cross-reactive antibodies upon vaccination with adjuvanted influenza vaccines, is in line with previous data from studies using different adjuvant systems.[330,340]

In the control ferrets (group 7) and those not protected after vaccination, the character of the macroscopic and microscopic lung lesions with associated antigen expression was consistent with that described previously in pH1N1 influenza virus infected ferrets and humans.[292,341] Immunization

with sVacMF59, followed by administration of pVacMF59 (group 2), resulted in the strongest reduction of alveolar, bronchiolar and bronchial lesions, as well as the extent of inflammation. Leaving out the adjuvant in the priming seasonal or the boosting pandemic vaccine strongly reduced the protective efficacy of vaccination against the development of alveolar lesions (groups 1 and 5). Omitting the priming vaccination reduced this protective efficacy of pVacMF59 vaccination even further (group 6). The substantial alveolar damage observed in these animals was apparently not paralleled by the levels of weight loss and increased lung weight. This could probably be explained by the delay between viral clearance and the resolution of histopathological changes. The extent of lymphocytic cuffing and the severity of bronchitis and bronchiolitis were more pronounced in the ferrets of group 1 (sVacMF59 - pVac) and in those primed with sVac regardless the vaccine used for boosting (groups 3, 4 and 5) than in the ferrets of groups 2, 6 and 7. It may be speculated that this finding is related to a phenomenon recently described in Canada suggesting that subjects vaccinated with seasonal vaccine would be more at risk to develop severe pH1N1 influenza.[342] However, the mechanism underlying this phenomenon is poorly understood, and more research is required to elucidate its postulated immunological basis.

Collectively it may be concluded that the MF59-adjuvanted pandemic influenza vaccine used afforded strong protection against the development of severe pH1N1 influenza-associated lesions and disease in the ferret model. This vaccine-induced protective immunity could further be enhanced by prior vaccination with a MF59-adjuvanted seasonal vaccine. Further studies into the mechanism involved in this priming immune response will yield understanding of novel correlates of infection and vaccine-induced protection. This understanding will especially be important for future quality assessment of novel generations of adjuvanted, vectored, and live influenza vaccines that are expected to induce broader protection than the currently used classical seasonal vaccines. Finally, a practical consequence of these findings is that during an emerging pandemic, the implementation of a priming strategy with an available adjuvanted seasonal vaccine that precedes the eventual pandemic vaccination campaign, may be useful and life saving.

Acknowledgments

We thank P. van Run, L. Leijten, R. van Lavieren, C. Verhagen, W. van Aert and R. Boom for technical assistance and S. van Trierum and W. Vos for biotechnical assistance.

CHAPTER 4

SUMMARIZING DISCUSSION

Animal models are needed to study the pathogenesis of SARS-CoV and influenza virus infections and to develop therapeutic measures and vaccines against them. Such animal models should replicate most features of the infections and associated disease in humans and provide discriminating, sensitive, and reproducible results. The differences and similarities between the pathology of SARS-CoV infection and that of influenza virus infection are related to their distinctive pathogeneses (Tables 1-4). Therefore, in the present thesis the pathology and pathogenesis of SARS-CoV and influenza virus infections in different laboratory animal species have been investigated and compared with those in humans.

SARS CORONAVIRUS INFECTION IN ANIMAL MODELS

The pathology of SARS-CoV infection

Previous experiments have demonstrated that SARS-CoV infection causes disease in many different animal species, including non-human primates, carnivores and rodents.[63,68-72] In the present thesis, SARS-CoV infection is described in non-human primates (cynomolgus macaques and African green monkeys [AGM]) and carnivores (ferrets and cats).[6,7,69,75] In these species, the pathological changes from SARS-CoV infection are variable and resemble those in human fatal cases to a greater or lesser extent.

Non-human primates

Although they are both non-human primates, young-adult AGMs suffer more severe lesions from SARS-CoV infection than young-adult cynomolgus macaques.[6,7,75,343] By gross pathology, the percentage of affected lung tissue is higher in AGMs than in cynomolgus macaques. By histopathology, pulmonary lesions are significantly more severe in AGMs than in cynomolgus macaques. However, the character of the pulmonary lesions is similar, except that AGMs show hyaline membranes and cynomolgus macaques do not (Table 1).

Carnivores

Cats and ferrets infected with SARS-CoV develop similar lesions in the respiratory tract as humans and AGMs (Table 1). However, the resultant DAD is more extensive and severe in ferrets than in cats, and includes alveolar edema. Another difference is that cats develop tracheo-bronchoadenitis, while ferrets do not.

Comparative pathology

When the pathological features of SARS in humans and in the above-mentioned laboratory animal species are compared, there are both similarities and differences in localization, character, and severity (Table 1).[32,34,36,37] First, the localization of the lesions is similar among all species: lesions are centered on alveoli and bronchioles. Additionally, AGMs, young-adult macaques, and cats have lesions in the submucosal glands of trachea and bronchi that are not seen in humans. Second, the character of the lesions is similar among all species; these characteristics are epithelial necrosis, infiltration of inflammatory cells, and type II pneumocyte hyperplasia. Additionally, syncytia and hyaline membranes are present in lesions of humans, macaques, and AGMs. Third, the severity of the lesions among species can be divided into two groups. Humans, aged macaques, and AGMs have severe DAD, characterized

by edema, fibrin, and hyaline membranes. Young-adult macaques, cats, and ferrets have milder DAD demonstrating a more multifocal distribution and lacking above-named features.

The development of fibrosis in the late stages of human cases of SARS may be related to several factors. First, irreversible damage to the pneumocytes that therefore fail to re-epithelialize the alveolar walls. Instead, the denuded basement membrane is repaired by fibrosis. Second, specific epithelial sensitivity to IFN-gamma: lung epithelial cells are more responsive to IFN-gamma-induced damage than fibroblasts. Third, Th1-dominant immune-mediated cell death, which may favor the damage to alveolar epithelial cells over damage to fibroblasts, leaving the latter relatively intact. This would mean destruction to the epithelial parenchyma; a basis for stimulation of fibroblasts for repair.[344] Fourth, Fas-mediated apoptosis of human epithelial cells, while lung fibroblasts are protected and are also not infected by SARS-CoV.[345,346] The importance of above-mentioned factors for fibrosis in SARS is not clear. Unfortunately, fibrosis is not a prominent feature of SARS-CoV infection in laboratory animals. This may be explained in part by the less severe lesions and the early time point of euthanasia. Therefore, this phenomenon is difficult to study in animal models.

There are several differences that one has to take into account when comparing the lesions of SARS in humans with those in experimentally infected laboratory animals (Table 1). These include differences in the: route of entry of the virus, dose of the virus upon entry, physiology of the respiratory tract, susceptibility to SARS-CoV infection, tropism of the virus, and immune response. Furthermore, one needs to realize that most pathological descriptions of human SARS involve people who have been hospitalized for an extended period and have undergone multiple interventions; there are only a limited number of descriptions of human acute fatal cases without intervention. In contrast, animals that have been infected experimentally with SARS-CoV usually do not undergo intervention and are euthanized before the endpoint of severe disease. Finally, one needs to consider that only about 10% of people with confirmed SARS-CoV infection died[14] and it is likely that many people who recovered from SARS had less severe respiratory tract lesions.

The pathogenesis of SARS-CoV infection

The pathological changes induced by SARS-CoV infection and the similarities and differences in these pathological changes among humans and experimental animals can be related to several factors: 1) virus-specific factors, 2) factors related to host-virus interaction, and 3) host-specific factors (Tables 3 and 4).

Virus-specific factors:

Receptor specificity

The cell type tropism of SARS-CoV is at least in part related to the presence of receptors such as ACE2 on the host cell surface. ACE2 is the most important receptor for SARS-CoV. The presence of ACE2 on type I and type II pneumocytes of human lungs corresponds to SARS-CoV infection of those cell types. Similarly, the localization of ACE2 can explain the tropism of SARS-CoV for small intestine in humans.[52,53] In laboratory animals, cell type tropism of SARS-CoV is also related to ACE2 expression (Table 1). Similar to human ACE2, both ferret and feline ACE2 bind the attaching S-protein of SARS-CoV efficiently.[222,223]

However, cell type tropism and ACE2 expression do not always correspond. For example, ferret bronchiolar epithelial cells express ACE2 but are apparently not infected by SARS-CoV (Table 1). This discrepancy may be explained by the necessity for other receptors besides ACE2 for virus

attachment or for other factors (such as cathepsin L) for SARS-CoV replication in the host cell.[46,47,49,224,226,227] The low expression of cathepsin L in human endothelial cells might explain the low infection rate of these cells despite their high expression of ACE2.[227] On the other hand, virus replication was observed in colonic epithelial cells and in hepatocytes without ACE2 expression, which may be explained by the presence of other receptors and co-receptors like dendritic cell-specific DC-SIGN and human CD209L.[347] DC-SIGN (or CD209) is expressed by macrophages and dendritic cells. Binding of SARS-CoV to this receptor did not lead to entry of virus into dendritic cells, but facilitated transfer of viruses to other susceptible cells.[46] L-SIGN (CD209L or DC-SIGNR) acted in conjunction with LSECtin to enhance SARS-CoV infection.[47]

Another discrepancy between cell type tropism and ACE2 expression was observed in tracheo-bronchial submucosal glands. While the submucosal glands of both and cats and ferrets expressed ACE2, only the submucosal glands of cats became infected and inflamed. As indicated above, this discrepancy may be due to species differences in expression of other co-factors necessary for viral replication. Alternatively, this discrepancy may also be due to species differences in the histological architecture of the tracheo-bronchial submucosal glands, which contain both serous and mucous cells. Ferrets have relatively more mucous cells than cats. This may have inhibited the attachment of SARS-CoV to serous cells, which was the main cell type infected in cats.

Direct cytopathic effect

The epithelial damage in the respiratory tract of patients with SARS can partly be explained by the direct cytopathic effect and apoptotic mechanisms due to viral infection and replication, resulting in lysis of the infected cells and necrosis as well as subsequent inflammation in the infected tissue.[348,349] High titers of virus have been found in severely damaged organs,[34,53] with necrosis at the sites of virus particles.[31] Additionally, SARS-CoV caused cytopathic changes in Vero E6 (African green monkey kidney) cells after inoculation.[19,350] Fas-mediated apoptosis was demonstrated in human epithelial cells.[346] However, most likely direct cytopathic damage due to virus replication in SARS is not the most important factor for cellular and tissue damage, since differences in the severity of the pulmonary lesions between young-adult and aged macaques were observed, despite having similar virus loads.

Factors related to host-virus interaction

Immune- and inflammatory cells

Immune- and inflammatory cells such as lymphocytes, monocytes, and neutrophils may play a role in the lesions caused by SARS-CoV infection. Lymphopenia with a rapid decrease of CD4 and CD8 T-cells was seen in the blood of human patients in the acute phase of SARS-CoV infection, and was associated with an adverse outcome.[22] This lymphopenia may be caused by apoptosis via the caspase-dependent pathway induced by protein 7a[54] or by direct cytolysis of lymphocytes due to virus replication, although ACE2 was not detected on T-lymphocytes or macrophages.[213] In experimentally infected ferrets, decreased numbers of lymphocytes also were observed in the blood of animals infected with SARS-CoV.[351] Additionally, a high neutrophil count in the blood of patients with SARS-CoV infection, that was associated with a poor prognosis, was also seen in the blood of ferrets infected with SARS-CoV.[351] These findings show that changes in the immune cell population are present in humans and animals infected with SARS-CoV and may influence the host response to infection with SARS-CoV.

Table 1. Histopathology, virus antigen expression and ACE2 antigen expression in different species infected with SARS-CoV

Species	Age	Histological lesions												Virus antigen expression												ACE2 antigen expression											
		Alveoli					Bronchioles		Bronchi		Interstitium		Trachea																									
		Epithelial necrosis	Edema	Hyaline membranes	Inflammation	Syncytial cells	Type II pneumocyte hyperplasia	Epithelial necrosis	Inflammation	Epithelial necrosis	Inflammation	Perivascular /peribronchiolar cuffing	Tracheo-bronchoadenitis	Epithelial necrosis	Inflammation	Type I pneumocytes	Type II pneumocytes	Alveolar macrophages	Bronchiolar epithelial cells	Bronchial epithelial cells	Tracheal epithelial cells	Serous cells of submucosal glands	Type I pneumocytes	Type II pneumocytes	Alveolar macrophages	Bronchiolar epithelial cells	Bronchial epithelial cells	Pulmonary goblet cells	Tracheal epithelial cells	Serous cells of submucosal glands	Type I pneumocytes	Type II pneumocytes	Alveolar macrophages	Bronchiolar epithelial cells	Bronchial epithelial cells	Pulmonary goblet cells	Tracheal epithelial cells	Serous cells of submucosal glands
Human		+	+	+	+	+	+	+	-	-		+	-	-	-	+	+	+	+	+	+	+	-	+	+	+	+	+	+	+	+	+	+	+	+	+	+
Macaque[a]	Young adult	+	+	-	+	-	+	+	-	-	+	+	-	-	-	+	+	+	+	+	+	-	-	+	+	+	+	n	n	+	+	+	+	+	n	n	+
	Aged	+	+	+	+	+	+	+	-	-	+	+	-	-	-	+	+	+	+	+	+	-	-	+	+	+	+	n	n	+	+	+	+	+	n	n	+
AGM[b]	Young adult	+	+	+	+	+	+	+	-	-	+	+	+	-	-	+	+	+	+	-	+	+	-	+	+	+	+	n	n	+	+	+	+	+	n	n	+
Ferret	Young adult	+	+	-	+	-	+	+	-	-	+	+	-	-	-	+	+	+	+	+	-	-	-	+	+	+	+	-	+	+	+	+	+	+	+	+	+
Cat	Young adult	+	-	-	+	-	+	+	-	-	-	+	+	-	-	+	+	+	+	+	+	+	+	+	+	+	+	+	+	+	+	+	+	+	+	+	+

n = not done. [a] Macaque = Cynomolgus macaque. [b] AGM = African green monkey

Induction of cytokines

One remarkable feature of SARS is the relatively strong induction of inflammatory cytokines like IP-10, MCP-1, IL-6, IL-8, IL-12, and IL-1beta in infected patients.[56-59,165,344] Increased expression of chemokines and cytokines such as IP-10, MCP-1, IL-6, and IL-8 are important for chemotaxis and activation of neutrophils and monocytes.[133,160,181] Infiltration of these inflammatory cells corresponds with the severe pulmonary lesions observed in human cases.[58,59,165,174] SARS-CoV-infected young-adult and aged macaques demonstrated expression of various cytokines and chemokines such as IP-10, MCP-1, IL-6, and IL-8 in a similar pattern as was seen in humans.[173] The cytokine response in SARS is probably host-specific since aged macaques had a stronger upregulation of those chemokines and cytokines than young-adult macaques, despite similar virus replication.[174] When upregulated chemokines and cytokines of macaques and AGMs were compared, IP-10, MCP-1, IL-6, and IL-8 were upregulated in macaques but not in AGMs. The AGMs showed more severe pathology with hyaline membranes when compared to the young-adult macaques despite similar virus replication levels. Comparative gene expression analyses revealed induction of proinflammatory and antiviral pathways in both species. Cytokines important for ARDS or neutrophils attracting activity, such as CXCL-1, CXCL2, IL-6 and IL-8, were upregulated in the macaques but not in the AGMs. Other proinflammatory chemokines and cytokines such as SPP1 (osteopontin), CCL20 and CCL3 were upregulated more in AGMs than in macaques. Additionally, osteopontin and CCL20 were significantly more upregulated in AGMs and aged macaques than in young-adult macaques. CCL3 was upregulated in human patients with H5N1 infection and was related to lung inflammation and fibrosis in mice infected with H5N1.[134,187] Osteopontin is predominantly expressed by macrophages and is important in type 1 (Th1) cytokine expression and plays a role in development of lung fibrosis.[184,195] In AGMs, many macrophages, presumed to express osteopontin, were seen histologically, whereas in macaques there were both macrophages and neutrophils. The above-mentioned differences in the gene expression profile as well as the difference in the tropism, which also involves bronchiolar and tracheal epithelial cells in AGMs (Table 1), may not fully explain the more severe lesions in the AGMs. Therefore, other species differences may be involved.

The production of type I interferons (IFN) by the host upon infection with a virus is an essential part of the antiviral innate immune system. SARS-CoV is suggested to cause inhibition of IFN production.[352] In humans with SARS, treatment with type I IFNs was associated with reduced disease-associated hypoxia and a more rapid resolution of radiographic lung abnormalities.[353] When macaques, experimentally infected with SARS-CoV, were directly treated with IFN, there also was a protective effect, suggesting that supplementing IFN as a therapy can be beneficial.[172] These results demonstrate that the inhibition of IFN production caused by the virus plays an important role in the induction of virus replication and associated severe lesions after SARS-CoV infection.

Host-specific factors

The most important host specific risk factors in humans for increased SARS-related disease and deaths due to acute respiratory distress syndrome (ARDS) are advanced age, sex, co-morbidities and genetic factors.[18,26-30,354,355] In addition, the difference between species is another important host-specific factor. As discussed above, aged cynomolgus macaques (10 to 19 years old) infected with SARS-CoV had more severe lesions than young-adult animals, even though viral replication levels were similar.[174,159,356] Additionally, aged mice showed more severe lesions than young adult mice upon infection with SARS-CoV and the transcription profile in aged mice generally indicated a

stronger proinflammatory response than in young mice.[61,63] It is suggested that age-related accumulated oxidative damage and a weakened antioxidative defense system cause a disturbance in the redox balance, resulting in increased reacting oxygen species.[174] Subsequently, redox-sensitive transcription factors, such as NF-κB, can be activated which is followed by the induction of proinflammatory genes such as IL-1β, IL-6, TNF-α and adhesion molecules.[357] Therefore, aging is not only associated with alterations in the adaptive immune responses, but also with a proinflammatory state in the host.[174] Oxidative stress and Toll-like signaling via NF-κB triggered by viral pathogens like SARS-CoV, may further amplify the host response, ultimately leading to acute lung injury.[159]

Other host-specific factors are the differences between the species as is demonstrated in the species differences in cell type tropism of SARS-CoV (Table 1) and the differences between cynomolgus macaques and AGMs in induction of cytokines.[174] Co-morbidities and genetic factors that are associated with severe disease in humans have not been investigated in laboratory animals and thus an insight on those factors from SARS animal models has not been obtained.

Intervention strategies against SARS-CoV infection

Intervention strategies consist of a combination of societal interventions sparked by early warning systems based on virus detection and discovery, and of more specific and targeted interventions such as the use of antivirals (e.g. IFN) and vaccines. In the present thesis, animal models were used in assessing one of the intervention strategies by evaluating the efficacy of different vaccines against SARS-CoV in ferrets and macaques. Ferrets vaccinated against SARS-CoV with MF59 adjuvanted recombinant spike protein or inactivated whole virus were protected against severe disease from SARS-CoV infection. This protection was demonstrated by less or absent clinical signs, reduced virus levels excreted in the throat, and no infectious virus in the lungs, which was correlated with the presence of circulating antibodies. In histopathology, lung lesions consistent with SARS-CoV infection were present and negatively correlated in severity with the level of circulating antibodies. Additionally, in the vaccinated animals there were perivascular mononuclear infiltrates and proliferation of BALT, predominantly consisting of CD3 positive staining T-cells. These increased perivascular infiltrates are in line with lymphocyte recall responses and correspond to higher antibody titers and high lymphocyte responses against SARS-CoV, but not to the presence or absence of virus in the lungs or throat swabs. Other experiments with mice vaccinated against SARS-CoV demonstrated similar strong T-cell responses against nucleoprotein that may contribute to the observed perivascular cuffing and BALT proliferation.[240,241] The presence of virus, albeit in reduced levels, in the throat swabs without signs for virus replication in the lungs, suggests other sites of virus replication, such as the nose, trachea, or salivary gland as was seen in macaques;[239] another suggestion may be that the virus is still present without replication. This vaccination study demonstrates protection against severe disease of SARS-CoV in ferrets. However, this study also shows vaccination-related histological changes possibly associated to a recall response, and virus excretion in the throat after vaccination. Therefore, this vaccine needs improvement.

Ferrets and macaques vaccinated against SARS-CoV with an aluminium-adjuvanted whole virus vaccine and infected with SARS-CoV, had similar but less severe lesions with more perivascular and peribronchiolar cuffing consisting of lymphocytes and plasma cells, when compared to non-vaccinated animals infected with SARS-CoV. In all macaques immunized with the aluminium adjuvanted vaccine there was an increase of the number of eosinophils in the peribronchial interstitium and in one animal also in the bronchial lumen. This increase of eosinophils was not seen in the

other animals. SARS-CoV infection causes induction of proinflammatory cytokines such as IL-1beta, IL-8, CXCL2 and IL-8, but also CCL11 (eotaxin), involved in eosinophil migration, and CCR3 (eotaxin receptor) are involved.[174,358] However, the vaccination likely played a more important role in the infiltration of eosinophils, since the increase in eosinophils upon SARS-CoV challenge was limited to vaccinated macaques. The absence of this phenomenon in ferrets suggests a difference in host response involving eosinophil migration. The immunized ferrets demonstrated fewer lesions in the lungs. However, not all ferrets had neutralizing antibodies and all ferrets did not reduce virus excretion on 2 dpi. Nevertheless, the virus was cleared more rapidly than in the control animals. The cuffing can be caused by the recall-response; however, further investigations into the cytokine profile of vaccinated compared to non-vaccinated animals can be helpful. Also, the vaccinations demonstrate no full protection against either SARS-CoV-associated disease or virus excretion.

The occurrence of pathological changes caused by the immune response has been a concern in the development of an effective vaccine against SARS[221] while disease-enhancing antibodies may be induced after natural virus infections as was seen in e.g. dengue virus infection and feline coronavirus infection.[359-362] Additionally, the results of vaccination experiments against SARS are ambiguous. Ferrets vaccinated with MF59 adjuvanted vaccine were less protected against disease when compared to vaccinated mice[229] while showing reduced virus replication but no sterile immunity.

INFLUENZA VIRUS INFECTIONS IN ANIMAL MODELS

The pathology of influenza virus infection

Both pathogenesis and vaccination studies for influenza viruses use many different experimental animal species: non-human primates such as macaques, carnivores such as ferrets and cats, and rodents such as mice and guinea pigs.[138,144,147-150] All these laboratory animal species are susceptible to influenza virus infection, but they demonstrate differences in clinical disease, virus replication, and pathological changes when compared to influenza in humans. Influenza viral pneumonia in human fatal cases shows similar pathological changes in the alveoli and bronchioles, regardless whether it is caused by seasonal human influenza virus, pH1N1, or H5N1. In macaques and ferrets, pH1N1 and H5N1 cause more severe lesions in the alveoli and bronchioles than seasonal influenza virus. This difference may be related to the virus strain used. Cats infected with H5N1 show systemic disease, while in humans the disease is predominantly confined to the respiratory tract. In this thesis the pathological changes of different influenza virus infections in macaques, ferrets, and cats are compared with those of human fatal cases, and the similarities and differences are related to the pathogenesis of the respective influenza virus infections.

Non-human primates

The cynomolgus macaque is a non-human primate that is often used in animal models for human disease caused by influenza virus infection.[148] Experimental H5N1 infection in cynomolgus macaques caused both morbidity and mortality, as reviewed by Kuiken et al.[297] Histological lesions were centered in the alveoli and bronchioles and consisted of DAD that was more severe than for human influenza viruses (Table 2).[148,151,259] Extra-respiratory tissues did not show histological lesions,[148,149,258,259] although suppurative tonsillitis, lymphocytic necrosis in lymphoid organs, hepatic necrosis, and renal tubular necrosis were rarely seen.[148,259] Experimental pH1N1 infection in cynomolgus macaques

caused morbidity but no mortality. Histological lesions consisted of multifocal moderate DAD (Table 2). In addition, there was moderate bronchiolitis and mild bronchitis, tracheitis, and rhinitis. The severity of pH1N1-induced pulmonary lesions was higher than those induced by seasonal influenza H1N1, but lower than those induced by H5N1. Experimental seasonal influenza virus infection in cynomolgus macaques also caused morbidity but no mortality. Histological lesions consisted of focal-to-multifocal mild DAD with mild necrosis and no edema, hyaline membranes, or lesions in the other parts of the respiratory tract.

Carnivores

A more frequently used animal species in influenza research is the ferret. Intratracheal inoculation of influenza virus into ferrets caused high morbidity and mortality for H5N1, moderate morbidity and low mortality for pH1N1, and neither obvious morbidity nor mortality for seasonal influenza virus.[281,363-365] This corresponded to differences in severity of pulmonary lesions (consisting of DAD), which was high for H5N1, intermediate for pH1N1, and low for seasonal H1N1. The extent and distribution of the lesions throughout the respiratory tract also differed per virus (Table 2). Extra-respiratory lesions were limited to H5N1 infection, and consisted of: non-suppurative necrotizing encephalitis,[281,363,364 316,366,367] multifocal hepatitis and necrosis, and hyperplasia of bile duct epithelium, as reviewed by Kuiken et al.[297,364,366,367]

When pH1N1 was inoculated intranasally into ferrets instead of intratracheally, lesions occurred higher in the respiratory tract and consisted of a mild-to-moderate necrotizing bronchiolitis, bronchitis, tracheitis, and rhinitis.[152] This illustrates the effect of route of inoculation on the pathogenesis of experimental influenza virus infection.[308]

Temporal and spatial dynamics after combined intranasal and intratracheal inoculation of influenza in ferrets differed per virus. H5N1 infection caused predominantly moderate DAD and bronchiolitis, starting on 12 hours post infection (pi), developing into severe DAD with edema from 1 to 4 dpi, and necrosis and inflammation in the bronchus, trachea and nose. pH1N1 infection caused mild lesions on 12 hours pi, developing in moderate-to-severe lesions from 1 to 7 dpi, with more involvement of the nose when compared to ferrets infected with H5N1. On 14 dpi the lesions were mild again. Human seasonal influenza virus infection did not consistently cause viral pneumonia but was limited mainly to bronchiolitis, bronchitis, tracheitis, and rhinitis.[152,291]

To develop a more useful model for viral pneumonia in humans caused by seasonal influenza virus, the previously used ferret model was modified by use of the intratracheal route and higher doses of up to 10^9 $TCID_{50}$. Both old and recent strains of seasonal H1N1 and H3N2 consistently caused viral pneumonia in ferrets. This viral pneumonia consisted of severe DAD, similar to that caused by pH1N1 infection. This modified animal model for severe human influenza caused by seasonal influenza virus is suitable to test vaccines and antiviral agents against pneumonia from these influenza virus infections.

Several felid species are susceptible to severe or fatal disease from influenza virus infection, as suggested by natural cases of H5N1 and/or pH1N1 infection in cats, tigers, and leopards.[284-286] Intratracheal inoculation of influenza virus into cats caused morbidity and mortality for H5N1,[144] morbidity but no mortality for pH1N1, and lack of infection for seasonal H3N2.[144] This corresponded to more severe DAD for H5N1 than for pH1N1, as seen in ferrets (Table 2). Extra-respiratory lesions, characterized by inflammation and necrosis in brain, heart, kidney, liver, and adrenal gland, were limited to H5N1 infection,[144] and much more extensive than in ferrets.

Comparative pathology

The pathological changes of influenza virus infection in fatal human cases and in above-described laboratory animals show both differences and similarities (Table 2). These can be compared according to localization, character, severity, and temporal changes of the lesions; and degree of extra-respiratory spread. First, the localization of the lesions in the respiratory tract, per virus, is similar for humans and laboratory animals: in seasonal influenza infection, the upper respiratory tract is mostly affected; in pH1N1 infection, all parts of the respiratory tract are affected; and in H5N1 infection, the lower respiratory tract is mostly affected.[108,132] There are few differences in localization as well, since H5N1 infection in laboratory animals involves more of the air-conducting parts of the respiratory tract than in humans, and vice versa for pH1N1 and seasonal influenza virus infections. Second, the character of the respiratory tract lesions is similar for humans and laboratory animals. This includes the alveolar lesions after infection with H5N1 and pH1N1. These alveolar lesions result in DAD, characterized by necrosis of epithelial cells, edema, infiltration of inflammatory cells, and epithelial regeneration. Third, the severity of the respiratory tract lesions appears greater in humans than in laboratory animals. For example, human fatal cases often show alveolar edema and hyaline membranes, which are less common in laboratory animals. One factor may be the euthanasia of laboratory animals before severe disease or death occur. Fourth, the temporal dynamics of influenza virus infection in ferrets may reflect the differences in the age of pathological changes in fatal human cases due to the duration of their illness before dying. Fifth, the degree of extra-respiratory involvement of H5N1 infection in humans is difficult to compare with that in laboratory animals, because it is so poorly described in humans. The involvement of the CNS in some human H5N1 cases[100] appears similar to that in ferrets, where extra-respiratory spread often is limited to the CNS. In contrast, extra-respiratory spread of H5N1 in humans is likely not as common or widespread as in cats.[144] Overall, many features of the pathological changes in humans and above-described laboratory animals are similar; the choice of animal model—including laboratory animal species, route of virus inoculation, and dose of inoculum—will depend on the specific feature of influenza in humans that one wishes to study.

The pathogenesis of influenza virus infection

Like in SARS, the pathology of influenza in all species and the similarities and differences between the pathology in human fatal cases and animal models can be related to several factors that have been proven important in influenza virus infection: 1) virus-specific factors, 2) factors related to host-virus interaction, and 3) host-specific factors (Tables 3 and 4).

Virus-specific factors

Receptor specificity

The greater severity of disease caused by H5N1 infection than by human seasonal influenza virus infection can be related in part to the cell type tropism of H5N1, which in turn is partly dependent on its receptor specificity. In general, human and avian viruses bind preferentially to different receptors; avian influenza viruses prefer sialic acids linked to galactose by α-2,3 linkage (avian-type receptors), while human influenza viruses prefer α-2,6 linked sialic acids (human-type receptors).[117,368] In humans, human-type receptors are predominantly expressed in the epithelium of the upper part of the respiratory tract (nose, trachea, bronchi), whereas avian-type receptors are mainly expressed in the epithelium of the lower part of the respiratory tract (bronchi, bronchioles, type II pneumocytes).[118,369] The receptor distribution differs between humans and different animal

Table 2. Histopathology, virus antigen expression and virus attachment in different species infected with different influenza viruses

Virus and species	Histological lesions												Virus antigen expression												Virus attachment											
	Alveoli				Bronchioles		Bronchi		Interstitium	Trachea		Nose																								
	Epithelial necrosis	Edema	Hyaline membranes	Inflammation	Type II pneumocyte hyperplasia	Epithelial necrosis	Inflammation	Epithelial necrosis	Inflammation	Tracheo-bronchoadenitis	Perivascular/peribronchiolar cuffing	Inflammation	Epithelial necrosis	Inflammation	Epithelial necrosis	Inflammation	Type I pneumocytes	Type II pneumocytes	Alveolar macrophages	Bronchiolar epithelial cells	Bronchial epithelial cells	Tracheal epithelial cells	Submucosal glandular epithelial cells	Nasal epithelial cells	Type I pneumocytes	Type II pneumocytes	Alveolar macrophages	Bronchiolar epithelial cells	Bronchial epithelial cells	Pulmonary goblet cells	Tracheal epithelial cells	Submucosal glandular epithelial cells	Nasal epithelial cells
H5N1																																				
Human	+	+	+	+	+	+	-	-	-	-	-	-	-	+	-	-	-	+	+	+	+	+	+	-	-	+	+	+	+	+	+	+	+	+	+	-
Macaque[a]	+	+	+	+	+	+	-	-	-	+	-	-	-	-	-	-	+	+	+	+	+	-	-	+	+	-	-	-	-	-	-	-	n	n	n	n
Ferret	+	+	-	+	+	+	+	+	+	+	+	+	+	+	+	+	+	+	+	+	+	-	-	+	-	+	+	+	+	+	+	+	n	n	n	n
Cat	+	+	-	+	+	+	-	-	+	-	-	-	-	+	+	+	+	+	+	+	+	-	-	+	-	+	+	+	+	+	+	+	n	n	n	n
pH1N1																																				
Human	+	+	+	+	+	+	+	+	+	+	+	+	+	+	+	+	+	+	+	+	+	+	+	+	n	+	+	+	+	+	+	+	+	+	+	+
Macaque	+	+	-	+	+	+	+	+	+	+	+	+	+	+	+	+	+	+	+	+	+	+	+	+	n	n	n	n	n	n	n	n	n	n	n	n
Ferret	+	+	-	+	+	+	+	+	+	+	+	+	+	+	+	+	+	+	+	+	+	+	+	+	n	n	n	n	n	n	n	n	n	n	n	n
Cat	+	+	-	+	+	+	+	-	+	-	+	-	-	+	+	+	+	+	+	+	+	+	+	+	n	n	n	n	n	n	n	n	n	n	n	n
Seasonal[b]																																				
Human	+	+	+	+	+	+	+	+	-	+	+	+	+	-	-	-	-	-	-	+	+	-	-	+	+	-	-	-	-	+	+	+	+	-	-	+
Macaque	+	-	-	+	-	-	-	-	-	-	-	-	-	-	-	-	-	-	-	-	-	-	-	-	-	-	-	-	n	n	-	-	-	-	-	n
Ferret	+	-	-	+	+	-	+	-	+	-	+	+	+	-	-	-	-	+	-	-	-	-	-	+	+	-	n	+	+	-	+	+	+	+	+	n
Cat	n	n	n	n	n	n	n	n	n	n	n	n	n	n	n	n	n	n	n	n	n	n	n	n	-	-	n	-	-	-	-	-	-	-	-	n

n = not done. [a] Macaque = Cynomolgus macaque. [b] Seasonal = seasonal human influenza virus H1N1 and H3N2

species as is determined by virus attachment studies (Table 2).[124] Those studies reveal that for H5N1, the virus attachment pattern in respiratory tissues of cats resembles that of humans best. For seasonal influenza virus, the virus attachment pattern in respiratory tissues of ferrets resembles that of humans best. For pH1N1, there are no data about virus attachment in animals.

While virus attachment studies show to which cells influenza viruses bind, virus antigen expression studies (using IHC) show in which cells influenza viruses actually replicate. Both pattern of virus attachment and pattern of virus antigen expression are linked to the severity of disease and pattern of lesions in the respiratory tract in humans and animals infected with influenza viruses (Table 2). Overall, pattern of virus attachment and pattern of virus antigen expression correspond with each other, but not always. A first reason for this discrepancy may be that, like SARS-CoV, influenza viruses also require other co-receptors or other factors for attachment and/or replication. A second reason may be the influence of surfactant proteins that protect against influenza in humans and pigs and possibly in other animal species, explaining virus attachment without virus antigen expression.[311]

To choose the most appropriate laboratory animal species for animal models of influenza in humans, it is useful to compare the pattern of virus antigen expression among species. For H5N1, there is more virus antigen expression in pulmonary epithelial cells of laboratory animals than of humans. For pH1N1, the pattern of virus antigen expression in ferrets most closely resembles that in humans. For seasonal influenza viruses, the pattern of virus antigen expression differs between humans, cynomolgus macaques, and ferrets. When comparing the results of virus antigen expression studies in experimentally infected animals and fatal human cases, the following factors need to be taken into account: route of virus entry, dose of virus inoculum, stage of disease at which tissue samples are taken, and immune status. The route of entry in animal models is mostly by intranasal or intratracheal inoculation, while in humans it is by air through small or large droplets. The dose of the virus inoculum in animal experiments is usually much higher than in human infection. Tissue samples are often taken at an earlier, less severe, stage of disease in laboratory animals than in humans. Tissue sampling in laboratory animals is usually from non-fatal cases, because the animals are euthanized before they succumb to the infection. In contrast, tissue sampling in humans is usually from fatal cases, where patients have died after protracted disease and multiple therapeutic interventions. Finally, the immune status is different: laboratory animals are usually naïve to influenza virus, while many humans have specific immunity, which may alter the course of subsequent influenza virus infections.

Direct cytopathic effect

Replication of influenza virus causes cellular damage due to cytopathic and apoptotic mechanisms. Direct cytopathic damage is suggested by high virus titers that were isolated from severely damaged lung tissue as well as throat or nose swabs[110,370] while virus antigen expression in epithelial cells was associated with severe DAD.[113,297 135] In animal models high virus titers in the lungs strongly suggest active viral replication in those tissues with subsequently more damage.[144,281,316,364] Apoptotic damage is suggested by experiments with TRAIL-expressing macrophages that induced epithelial cell apoptosis in influenza virus pneumonia.[371-373] These findings suggest that direct damage of the virus by cytopathic and apoptotic mechanisms are important in the development of pathological changes in influenza virus infections. However, damage due to other mechanisms, such as indirect damage of the host response, cannot be excluded.

Factors related to host-virus interaction

Immune- and inflammatory cells

Like in SARS, immune cells such as lymphocytes, monocytes, and neutrophils play a role in the lesions caused by influenza virus infection. In fatal human cases of H5N1 and pH1N1 infections, lymphopenia was associated with the severity of disease.[374,375] This depletion of lymphocytes was also seen in ferrets and can be related to apoptosis and bone marrow suppression.[318] After H5N1 inoculation, the number of monocytes in the blood and alveoli of ferrets decreased and remained low, which is suggestive for exhaustion of the bone marrow; after pH1N1 inoculation there was an increase again a few days later. Additionally, the neutrophil count in the blood of ferrets was lower with H5N1 infection than with pH1N1 infection, as was also seen in human cases.[376] This decreased neutrophil count may be attributed to a higher demand of neutrophils than can be met by myelopoiesis. This is corroborated by the high number of immature neutrophils in the blood, again suggesting exhaustion of the myelopoietic component. For macaques and cats, there are limited data.

Cytokines

In human cases of H5N1 infection, there are indications that a high production of proinflammatory cytokines and chemokines play an important role in the pathogenesis, as was seen in SARS. In fatal cases of H5N1 infection, high virus loads correlated with high cytokine and chemokine levels and severe inflammatory response in humans.[134] The high viral load accompanied with high cytokine response may suggest a balanced response. However, signaling pathways involved in inflammation showed an imbalance of proinflammatory responses and an impaired antiviral gene program after H5N1 infection of endothelial cells, compared to low pathogenic influenza virus infection of endothelial cells.[377] Similar features are seen in animal models. Macaques infected with H5N1 displayed severe disease and activation of proinflammatory cytokine and chemokine responses.[258] Also in ferrets, H5N1 infection induced severe disease associated with strong expression of interferon response genes, including IFN-gamma-induced cytokine CXCL10. When those ferrets were treated with an antagonist of the CXCL10 receptor (CXCR3), the severity of H5N1–related disease and the viral titers were reduced when compared to the controls.[365] For pH1N1, the abundance of neutrophils and macrophages in pulmonary lesions corresponded with up-regulation of CCL2, CCL3, CCL8, CXC10, IL-8, and CXCL1, which are known chemoattractants for neutrophils and monocytes, as is seen in macaques. Compared to lungs of cynomolgus macaques infected with seasonal human H1N1 virus, concentrations of MCP-1, MIP-1α, IL-6 and IL-18 were higher. This is in line with the more severe pulmonary lesions in cynomolgus macaques infected with pH1N1 than with seasonal human influenza H1N1 virus.[264] On the contrary, alveolar macrophages infected with H5N1 did not induce excessive TNF-alpha. However, alveolar macrophages were more abundantly infected by H5N1 than by seasonal or pH1N1.[378] Therefore, the imbalance in the level of virus infection and resultant cytokine and chemokines production may at least in part contribute to the development of lesions after infection with H5N1 and pH1N1.

Host specific factors

Important host specific risk factors for severe disease from human seasonal influenza virus infection are advanced age, co-morbidities like pulmonary disease and cardiovascular disease, and pregnancy.[106,379] Risk factors for severe disease from pH1N1 infection are similar as those for human

Table 3. Similarities and differences between SARS and H5N1 influenza related to the pathology (based in part on Ng et al. The comparative pathology of severe acute respiratory syndrome and avian influenza A subtype H5N1—a review. Human Pathology, 37:381-390, 2006)[107]

Similarities	Differences	
	SARS	**H5N1 Influenza**
1. Pneumocytes main target: resulting in DAD	*1. Acute alveolar lesions:*	
	DAD less fulminant with an acute and regenerative pattern	DAD more fulminant and necrotizing with marked hemorrhage
2. Hyaline membranes in human cases	*2. Typical histopathologic features:*	
	Multinucleated cells	No multinucelated cells
3. Hemophagocytic syndrome and lymphoid depletion	*3. Organizing phase:*	
	Fibrocellular intra-alveolar organization with a BOOPa- like pattern	Patchy and interstitial paucicellular fibrosis without BOOP-like pattern
4. Hypoxia-related skeletal muscle and renal tubular necrosis	*4. Development of severe disease:*	
	Less rapid, 2nd week of illness	More rapid, end of 1st week
5. Pathology centered around the bronchioles for SARS and pH1N1	*5. Dissemination:*	
	Respiratory tract, intestinal tract, liver, blood, urine, and feces	Respiratory tract, intestinal tract, brain, cerebrospinal fluid, and blood

[a] BOOP = bronchiolitis obliterans organizing pneumonia

seasonal influenza virus. In addition, they include diabetes, hypertension and obesity. Interestingly, advanced age does not appear to be a risk factor for severe disease from pH1N1 or H5N1 infections. Most pH1N1 patients were (young) adults with a median age of 36 years old,[132] while most severe human cases of H5N1 were previously healthy with a median age of 18 years.[94] In addition, the difference between species is another important host-specific factor.

Advanced age as a risk factor for severe disease from seasonal influenza virus infection may be related to increased host responses and decreased defense mechanisms against redox-induced damage as is seen in SARS-CoV infection. The different age distribution of disease and fatality from H5N1 infection may reflect age-related patterns of exposure or risk behavior such as close contact with sick poultry, or age-related host resistance.[380] The different age distribution of fatality from pH1N1 infection is probably related to the presence of immunity from previous infections with influenza viruses in older people. Because these viruses were antigenically related to pH1N1, the antibodies were cross-reactive and therefore protected from severe disease from pH1N1 infection.[323]

Other host specific factors such as pre-existing morbidities and pregnancies, which are risk factors for seasonal and pH1N1 infection, may be related to a compromised immune system in chronically ill patients and pregnant women as well as aerodynamic ventilation problems in advanced pregnancy and obesity. In animal models there are no reports on the effect of such factors. Differences in histopathological changes, antigen expression and receptor specificity among humans and laboratory animal species are species-related, as was seen in SARS-CoV infection.

Table 4. Similarities and differences between SARS and influenza related to the pathogenesis

Factors important for pathogenesis	Similarities	Differences
Virus specific factors		
Receptor specificity	-	Receptors: SARS: ACE2, DC-SIGN, L-SIGN Influenza: sialic acids
Direct cytopathic effect	-	SARS: not so important Influenza: important
Virus-host interaction		
Immune cells	Lymphopenia High neutrophil count	-
Imbalanced cytokines	-	SARS: host specific Influenza: virus specific
Host-specific factors		
Age	Old age is associated with fatal cases (SARS and seasonal influenza)	Not for pH1N1 and H5N1
Co-morbid disease	Co-morbid disease is associated with fatal cases (SARS, seasonal influenza and pH1N1)	Not for H5N1
Genetic factors	-	SARS: certain genetic factors are associated with severity of disease Influenza: not described
Species differences	Differences in pathologic changes and disease outcome among humans and non-human animal are species-related	-

Intervention strategies against pH1N1 infection

Intervention strategies for influenza, like those for SARS, consist of a combination of societal interventions sparked by early warning systems based on virus detection and discovery, and of more specific and targeted interventions such as the use of antivirals and vaccines. In the present thesis vaccination as one of the intervention strategies was evaluated by testing the efficacy of seasonal human influenza virus and pH1N1 vaccines against pH1N1 infection in ferrets. Ferrets vaccinated with MF59 adjuvanted or seasonal or pH1N1 vaccines all developed clinical signs upon infection with pH1N1, as well as weight loss, raised temperature, pulmonary consolidation, and increased relative lung weight. The severity of the pathological changes in the respiratory tract of vaccinated ferrets upon infection with pH1N1 was more severe when a non-adjuvanted or a seasonal vaccine alone was used. Animals vaccinated with the combination of adjuvanted seasonal vaccine followed by adjuvanted pandemic vaccine, raised the highest antibody titers and showed fewer lesions than the other animals. Although the type of antigen expressing cells was not changed, the number of cells expressing viral antigen was strongly reduced and even absent in effectively vaccinated animals. The priming of the adjuvanted seasonal vaccine that was followed by an adjuvanted pandemic vaccine may be attributed to protective and cross-reactive T-cell and memory B-cell responses.[330,381] Another

interesting finding was the perivascular and peribronchial lymphocytic cuffing that was more prominent in vaccinated ferrets than in non-vaccinated ferrets. This co-localization of the cuffing with the virus-associated histological lesions in alveoli may be a response to the alveolar infection, since lymphocytes are important contributors to clearance of challenge virus from the lungs.[382] The vaccination may therefore prime the combined innate and adaptive immune reaction that induces a lymphocyte response. Such a response may be associated to the finding that young subjects vaccinated with seasonal vaccine may be at risk to more severe pathologic changes from pH1N1.[342] However, although vaccinated ferrets had increased lymphocytic infiltrates, the other pulmonary lesions were less severe.

COMPARING THE PATHOLOGY AND PATHOGENESIS OF SARS AND INFLUENZA

Although SARS-CoV and influenza viruses use different receptors, the role of the receptors in the development of disease is crucial in both infections. For infections with SARS-CoV and influenza viruses, there is a correlation between the distribution of the receptor, the tropism of the virus, and the associated lesions (Tables 1 and 2). However, not all differences in the pathology between various animal species can be explained by the differences in receptor distribution (Tables 3 and 4). This implies that other receptors and factors also play a role in the attachment, replication, and infectiousness of both viruses.[347,369]

The location of the lesions in SARS-CoV and influenza virus infection is related to the receptors, while the character of the lesions is characterized by necrosis and inflammation. First, the necrosis that is seen in the lungs with both SARS and influenza can be explained by a direct cytopathic effect or apoptotic mechanisms. These mechanisms lead to damage of epithelial cells, increased permeability of the alveolar epithelium, endothelial damage, and subsequent edema and hemorrhage, followed by formation of hyaline membranes.[312] Second, the inflammation can additionally be attributed to the imbalanced cytokine and chemokine production. Dysregulation of cytokines and chemokines in SARS-CoV and H5N1 virus infection correlates with high viral loads in pharyngeal swabs and more severe pathological changes in severe or fatal cases.[134,165,173] Proinflammatory cytokines like IL-6 and IL-8, IP-10 and MCP-1 attract immune cells that constitute the inflammatory infiltrate, which leads to even more production of cytokines and chemokines.[312,344,383] Together with the activation of oxidative stress mechanisms that are induced by the up-regulated cytokines, there is further cellular damage and inflammation resulting in DAD.[160]

Not only the cytopathic effect, cell type tropism and cytokine induction, but also the biology of the viruses may influence the outcome of the disease (Tables 3 and 4). SARS-CoV-specific changes in the S-protein seem to trigger an aberrant host response. Similarly, changes in HA and NA also may affect virulence of influenza virus infection, as has been shown with seasonal influenza virus, pH1N1 and H5N1 infections in ferrets. These changes in virulence were linked with up-regulation of genes associated with apoptosis and tissue injury.[63,384,385]

Aging is associated with increased morbidity and mortality from infections with SARS-CoV and human seasonal influenza virus.[161,386] This phenomenon is also seen in a variety of other viral infections, such as West Nile virus and norovirus infections, probably because the elderly respond poorly to new antigens compared to younger persons due to immunoscenescence.[387-391]

Immunosenescence is a multifactorial process that is associated with thymic involution, chronic antigen stimulation due to persistent infections, signal transduction changes in immune cells, and protein-energy malnutrition.[392] Although all components of immunity are affected with aging, the T-cells are the most susceptible and the increased susceptibility to lower respiratory tract viral infections is particularly related to defective T-cell responses in the innate immunity.[392-394] Additionally, advanced age causes a general increase in the levels proinflammatory cytokines in plasma, resulting in an age-related increase of inflammation.[391] Increased amounts of proinflammatory cytokines, such as IL-1β and IL-8, were produced upon stimulation of leukocytes of the elderly, whereas induction of antiviral type I IFNs was decreased compared to young adults.[395-397] Also, aging results in less protection against oxidative stress that is induced by virus infections and overreacting proinflammatory responses.[357]

Other factors related to the severity of disease in SARS, seasonal influenza and pH1N1 are pre-existing co-morbidities (such as diabetes mellitus and cardiopulmonary disease), pregnancy, and sex. Pre-existing co-morbidities and pregnancy are predominantly associated with suppression of the immune response, as is seen in older patients. In SARS, male sex is correlated with more severe disease, while in H5N1, females seem to have a worse outcome than males, although not significantly (Table 4).[27,94,103] Interestingly, a sex difference in the pathology of immune responses after viral infection is suggested, since influenza virus infection of mice results in greater neutrophil influx and more severe lesions in females than in males.[398]

In humans, H5N1 appears more likely to spread to extra-respiratory tissues than seasonal influenza virus.[134] In patients infected with H5N1, diarrhea was associated with the detection of H5N1 RNA in feces; it was suggested that the virus may infect the gastrointestinal tract directly or after subsequent dissemination via blood, since H5N1 RNA was also isolated in plasma.[113,134,138,399] The hypothesis that H5N1 could enter the human host via blood vessels in the gastrointestinal tract is supported by the results of experimental H5N1 infections in cats. Intestinal H5N1 inoculation resulted in viral replication in capillary endothelium of the intestinal mucosa, which was not seen in cats intratracheally.[144,400] Like H5N1 influenza, SARS in humans is a respiratory disease with extra-respiratory virus dissemination, as is demonstrated by antigen expression in several organs and excretion of virus via respiratory secretions, stool, urine, and possibly sweat.[52,53] Also, diarrhea was seen in SARS with active viral replication in enterocytes, but minimal disruption of the intestinal architecture or cellular infiltrate. Upregulation of the potent immunosuppressive cytokine TGF-β[401] and an anti-apoptotic host cellular response in the intestinal epithelial cells[161] may be a cause for the diarrhea. Spread to other extra-respiratory tissues, such as the central nervous system, has been noted in H5N1 infection of mammals such as mice, ferrets, and felids,[286,402,403] but has rarely been recorded in human H5N1 infections.[100,404,405] For SARS in humans, no involvement of the central nervous system has been seen.

In our experiments, ferrets and macaques vaccinated against SARS-CoV and pH1N1 had increased infiltration of lymphocytes in the lungs, and macaques vaccinated against SARS-CoV with an aluminium adjuvanted vaccine had increased infiltration eosinophils after challenging. Infiltration of lymphocytes may be beneficial, but infiltration of eosinophils may be potentially damaging or be associated with more severe disease. This raises concerns that vaccination against SARS-CoV may fail to effectively protect against viral replication and may result in vaccine-enhanced pulmonary disease.[406-408] Immune enhancement has been demonstrated with a vaccine against feline infectious peritonitis coronavirus, a modified vaccinia vector expressing SARS-S, and a vaccine with inacti-

vated respiratory syncytial virus.[81,358,360,362,409] This finding has particular significance for inactivated SARS-CoV vaccines that also induce T-cell responses,[228,410-412] since they may lead to adverse effects.[240] Cellular immune responses, especially cytotoxic T-cell responses, play an important role in antiviral immunity.[410,411,413] Previously, it is suggested that the activity of specific T- cells in the absence of effective neutralizing antibody mediates the adverse response.[414] The perivascular appearance of the lymphocyte infiltrate can be explained by this recall principle: strong T-cell responses are raised against the viral nucleoproteins that occur around blood vessels and bronchioles.[240,241]

Finally, there are two pathologic features that are remarkable in both SARS-CoV and influenza virus infections: pulmonary fibrosis and tracheo-bronchoadenitis. First, in human severe cases of both SARS and influenza there is severe loss of alveolar epithelial lining, which may lead to re-epithelialisation and recovery, to death, or to pulmonary fibrosis. Late stages of fatal human cases of SARS were characterized by intra-alveolar and intrabronchiolar fibrosis and in approximately 62% of non-fatal SARS cases there was evidence for fibrosis in thin section computed tomography (CT) on 1 month of follow-up.[37,415] In contrast, interstitial fibrosis has been described in only a few fatal cases of H5N1 influenza. Exceptions are two case descriptions, with radiological follow-up showing fibrosis-related changes.[111] For pH1N1 influenza, pulmonary fibrosis also was seen in only a few cases by follow-up CT, and the fibrosis often disappeared after 1 month.[416,417] Pulmonary fibrosis is not described in any animal models for SARS-CoV, pH1N1, or seasonal influenza virus infections. However, there is a mouse model of H5N1 infection that shows pulmonary fibrosis.[418] The reason for the severe fibrosis in fatal human cases of SARS remains unclear and needs further investigation. Second, tracheo-bronchoadenitis was demonstrated in SARS-CoV infection in cats and young macaques and in pH1N1 virus infection in ferrets and was clearly associated with expression of virus antigen. This finding has potentially important implications for the excretion of those viruses. Excretion of virus might increase due to infection of the tracheo-bronchial submucosal glands and a diminished efficient defense by the mucociliary system; and virus secreted by these glands into the trachea and bronchi is more likely to be expectorated than virus produced lower in the respiratory tract.

CONCLUDING REMARKS

Points to consider for using animal models

SARS-CoV and influenza virus infections in experimental animals demonstrate different pathways that finally result in similar disease overall, which can be compared to the situation in human fatal cases (Tables 3 and 4). Samples taken from human fatal cases of SARS-CoV and influenza virus infections often do not represent the full range of the different temporal stages of a disease. Instead, they are more likely to represent late-stage disease. In addition, the lesions caused by the viral infection may be mixed up with lesions caused by clinical treatments and lesions from concurrent pre-existing disease. Therefore, to be able to study the course of the disease caused by these viruses good animal models are necessary for SARS-CoV and influenza virus infections in humans. The choice and design of an animal model used in an experiment is crucial for the outcome of the investigation and should be considered carefully. Time course experiments such as the one described in chapter 3.5 provide information about the temporal and spatial dynamics that help to design such

animal models, including which time points and which samples are best to gain the most useful information. Not only the best time points and analyses of the most informative samples should be considered carefully, also the animal species, the inoculation route and the age of the animals are important, as is shown by studies of H5N1 influenza in ferrets and of SARS in aged mice and macaques.[63,174,308]

To improve our knowledge of fatal SARS in humans, animal models should ideally show virus replication dynamics, clinical illness and pathological changes that resemble those of fatal human SARS cases. Although current animal models do not fully mimic the disease in fatal human cases of SARS, they can be useful in pathogenesis and vaccination studies. For pathogenesis studies, SARS-CoV need not cause mortality in the animal model, since the vast majority of human SARS cases also were non-fatal. For vaccination studies, virus replication, virus excretion, antibody titers and pathology scores are useful parameters to assess the level of protection against infection and disease.

An important factor in designing an animal model for SARS is the species of laboratory animal used. Non-human primates, especially aged cynomolgus macaques and AGMs, most closely reflect the pathology in fatal human SARS by demonstrating typical pathological features such as hyaline membranes and syncytial cells upon SARS-CoV infection. However, the severity of the clinical signs and lesions, level of mortality, and degree of antigen expression in non-human primates is less (Table 1).[419] The variation in pathological changes and cytokine profiles among different non-human primate species, as well as among age groups within each species, may reflect the variation in severity of disease among humans. For example, the mild degree of pneumonia in SARS-CoV-infected young-adult cynomolgus macaques may resemble the milder cases of SARS in humans.[257,420,421] While aged cynomolgus macaques are good animal models for pathogenesis studies, vaccination studies, and intervention studies of fatal SARS in humans, large disadvantages are the ethical, cost-related and housing problems. Ferrets infected with SARS-CoV only partly resemble fatal human SARS in terms of clinical illness, mortality and typical histopathologic features (Table 1). Also, methods for measuring gene expression profiles of ferrets are not fully developed yet. Nevertheless, ferrets can be used for pathogenesis and vaccination studies, because they show SARS-CoV-associated pulmonary lesions and develop humoral immunity associated with reduced virus replication upon vaccination. Cats infected with SARS-CoV show fewer similarities with the human situation and have greater ethical, cost-related and housing problems. Therefore they are used less in animal models for human SARS. Although not discussed in this thesis, the use of old BALB/c mice in an animal model for human fatal SARS may be an alternative since there are many difficulties in the use of aged macaques.[169] Recombinant zoonotic and early phase SARS-CoV infection of these mice results in clinical signs, virus replication, pulmonary lesions, and associated virus antigen expression in type II-resembling pneumocytes, bronchiolar and bronchial epithelial cells, that partly resemble the features seen in fatal human SARS cases.[63] Therefore, aged BALB/c mice may be used for pathogenesis, antiviral, and vaccination studies. A disadvantage may be age-related disease or mortality not related to SARS-CoV infection, which may influence the results.

To improve our knowledge of fatal influenza in humans, like in SARS, animal models should ideally show similar virus replication dynamics, clinical illness and pathological changes as in fatal human influenza cases. An important factor in designing an animal model for influenza is route of inoculation, because it can markedly affect the outcome of infection. Therefore, route of inoculation often depends on the purpose of the experiment. Transmission studies (at least in ferrets) may well

use intranasal inoculation, which favors replication in the nose rather than in the lungs. This may correlate with virus excretion from the nose and minor pulmonary lesions. In contrast, intratracheal inoculation favors replication in the lungs and is more likely to result in severe pneumonia, which makes this route of inoculation useful for pathogenesis and vaccination studies for viral pneumonia.

Another important factor in designing an animal model for influenza is the species of laboratory animal used. In cynomolgus macaques, the outcome of infection differs markedly according to the influenza virus used (Table 2). Therefore, cynomolgus macaques are probably not the best species to use for pathogenesis studies of fatal human disease from pH1N1 or seasonal influenza virus infections. However, because these viruses do replicate and cause virus-associated lesions, cynomolgus macaques may be useful for vaccination studies against these viruses. In contrast, cynomolgus macaques infected with H5N1 show similar features as fatal human H5N1 infection and therefore can be used for pathogenesis, vaccination or therapeutics studies of H5N1 infection. Ferrets infected with different influenza viruses show similar virus replication dynamics, clinical illness, virus associated pathological changes, and virus attachment pattern as in humans (Table 2), and therefore are often used in animal models for various purposes. Cats infected with H5N1 show similar pathology of the respiratory tract, but additionally demonstrate a more widespread systemic infection than is seen in human cases. The virus antigen expression and virus attachment patterns in cats show differences and similarities such as the ferrets. The systemic dissemination makes the cat less useful for animal models of fatal human H5N1 pneumonia or vaccination-studies, since extra-respiratory replication and inflammation can influence the results. Taken together, ferrets are good animal species to model fatal human influenza. However, one needs to keep in mind that there are species differences between humans and ferrets, as well as differences between laboratory and field conditions. Therefore, the conclusions from these ferret-studies need thorough assessment to be able to make full use of the results without over-interpreting them.

The use of animals in experiments is necessary in the development of new medicines and vaccines. However, for ethical reasons, scientists use the principle of the three Rs: reduction, refinement and replacement. Reduction of the number of animals can be done by improving experimental techniques and data analysis, and by sharing materials and information. Refinement of the research can be done by improving living conditions and medical care of the animals, and by using less invasive methods. Replacement can be done by using alternative techniques such as cell cultures, *ex vivo* tissue cultures, computerized models, epidemiological studies, and human volunteers. In this thesis, although animals were part of many studies, the results contribute strongly to the refinement of the animal models for viral pneumonia caused by SARS-CoV and influenza virus infections in humans. For both virus infections the best possible animal species and inoculation route have been evaluated in this thesis. For influenza virus infection, the time course study provides an extensive overview of the inflammation process during time and space that elucidates the best time point for taking samples and which samples to take to gain the best information about the factors studied. Additionally, a good animal model for viral pneumonia caused by seasonal influenza was developed for vaccination studies. By collaborating with other researchers, the samples and data from these studies are being used as thoroughly as possible. By using the results of the experiments in this thesis future researchers can reduce and refine their animal experiments. However, complete replacement of experimental animals is definitely not possible to date. Medicines and vaccines will only be approved by authorities after testing thoroughly in animals or humans since the full scope of a virus infection, the host response

against a virus infection, and the safety and efficacy of vaccination and therapeutic intervention can only be assessed in a whole organism (i.e. a human being or a non-human animal). Therefore, to meet the principle of replacement of experimental animals would imply an increase of using human volunteers, which for obvious reasons is also largely hampered by ethical considerations.

Lessons learnt

The lessons learnt from the SARS-CoV outbreak and pH1N1 pandemic may help us in coping with future outbreaks of respiratory viruses in humans. For SARS, the risk-communication in the SARS outbreak in Singapore showed that an efficient communication with the public was able to help contain the disease while the more withdrawn reaction of the government in the Toronto outbreak caused more panic and anxiety among the public. The development of medicines and vaccines against disease from SARS-CoV required the rapid development and use of animal models, which was largely accomplished in a record time span. However, until now there is still no good and useful animal model for fatal viral pneumonia caused by SARS-CoV in humans. For pH1N1, at the beginning of the pandemic there was lack of information about the situation in Mexico. Soon after the information became known, the manner of communication by the media and other authorities, and particularly the comparison of pH1N1 with the 1918 H1N1 influenza virus, caused great fear among the public, health authorities and government. The results of animal experiments with pH1N1 also suggested a higher severity of disease than seasonal influenza. A time course experiment such as is described in Chapter 3.5 would have been very useful if it could have been conducted at the beginning of the pandemic to provide information on the best time points and samples to focus on in vaccination studies. Also, the extrapolation of the disease caused by pH1N1 in ferrets should have been taken with precaution as is described above. Thus, lessons learnt from the SARS-CoV and pH1N1 situation involve good risk communication with the public supported by the interdisciplinary collaboration connecting all aspects of health care for humans, animals and the environment, as proscribed by the approach, and immediate and in-depth research to the cause, course of disease, and the development of good animal models.

Future perspectives

Many steps in the development of severe and fatal disease after SARS-CoV and influenza virus infection remain unknown. For the future, new or improved techniques such as genomics, proteomics, and stem cell research may improve our knowledge of disease and recovery after disease and may be helpful in the development of effective interventions like treatment and prevention of severe disease. For seasonal influenza, aged animals may be an alternative for the inoculation of high doses of virus in ferrets as is seen in SARS-CoV infection in aged macaques and mice and recently for pH1N1 in aged macaques.[63,174,422] For all respiratory viruses that cause severe damage of alveolar and bronchiolar epithelium, treatment with stem cells that cover the denuded basement membrane and later cause re-epithelialisation may prevent severely ill patients from dying.[423] For both SARS and influenza, experiments with immunosuppressed animals (e.g. by using methods that are also used in organ transplantation) may help finding better animal models for answering specific disease related questions.

Animal models are not only important for the known virus strains and subtypes of SARS-CoV and influenza A viruses. All kinds of viruses are ubiquitous among (wild) animals:[424,425] bats harbor viruses that are similar to the epidemic strain of SARS-CoV.[10] Such viruses may be the source of

future emerging infections. The travelling behavior of humans (and their domestic animals), can result in easy spread of such infections as was seen in the recent SARS and pH1N1 pandemics. Influenza viruses in humans evolve due to antigenic drift and shift, and small changes of the virus in animal species such as birds or pigs could change their virulence and transmissibility. This change could make the virus to cross the species barrier and spread among the human population, causing epidemics or even a pandemic, as was seen with pH1N1. If such a fast spreading virus would have the same morbidity and mortality as H5N1, this could have disastrous consequences for the human population worldwide. SARS-CoV emerged from bats, through civet cats, albeit with less fast changing properties than influenza viruses. However, there is a need to address the evolving diversity of SARS-CoV for vaccine development, since late cases of SARS show less ACE2 dependent virus entry and more resistance to antibody neutralization.[426]

In case of a future outbreak of a respiratory disease, presumable caused by a virus, that causes many fatal cases in humans, several steps should be made. First, thorough pathological evaluation of fatal cases should be performed with the appropriate tissues sampled for histopathology and random virus discovery, followed by PCR and virus isolation. Second, those samples should immediately be used for virus isolation and identification, also allowing the rapid inoculation of experimental animals as a pilot study. Cynomolgus macaques or other non-human primates may be the first animal species of choice due to the evolutionary proximity to humans, followed by ferrets and mice, to provide information about the pathogen by causing similar disease as in humans upon infection with this virus or, if not present yet, with tissue. Next, pathogenesis studies may be performed to study the effects of the pathogen more closely. Third, at the same time a good animal model for human disease caused by the pathogen should be established to start studies for therapeutic and preventive measures. Establishing such a model requires time course experiments in the animal species with an inoculation route and inoculation dose that best resembles the human situation in order to rapidly gain insight in the best time point of sampling and the best samples to take. Finally, it should be remembered to carry out an interdisciplinary study to identify and address the factors underlying the emergence of the pathogen into the human population in order to deal with the problem at its source.

In summary, at the time of an outbreak of severe fatal disease in humans, all steps from the discovery of the cause of the disease to the development and testing of appropriate therapeutic and preventive strategies should be carefully considered and pursued, by taking into account all the lessons learned from previous outbreaks and by working together with all relevant disciplines to reach the same goal.

CHAPTER 5

NEDERLANDSE SAMENVATTING

INLEIDING

Al sinds lange tijd bestaan er virale luchtweginfecties, waardoor er veel mensen ziek worden en soms sterven aan een ernstige longontsteking. In de afgelopen decennia zijn de H1N1 (2009) influenzavirus ('Mexicaanse griep') en 'Severe Acute Respiratory Syndrome' (SARS) pandemieën (epidemieën die zich over de gehele wereld uitbreiden) de belangrijkste geweest. Beide virusinfecties zijn zoönosen, wat betekent dat ze overgedragen worden van dier op mens: in SARS door o.a. civetkatten en wasbeerhonden en in Mexicaanse griep door varkens. Dit proefschrift beschrijft de pathogenese (het ontstaan van een ziekte) van infecties met verschillende influenzavirussen en het SARS-coronavirus (SARS-CoV) in laboratoriumdieren als model voor deze ziekten bij de mens. In het bijzonder wordt de pathologie van SARS en influenza in proefdieren vergeleken met die van de mens. Daarnaast worden de factoren die van invloed zijn op het ontstaan van een (ernstige) ziekte door deze virusinfecties vergeleken tussen proefdier en mens.

Een van de manieren om mensen tegen virale ziekten te beschermen, is het toedienen van vaccins. Deze zorgen ervoor dat mensen deels of geheel beschermd zijn tegen een ernstige ziekte door het virus. Voordat een vaccin gebruikt kan worden bij mensen, zal het eerst getest moeten worden op werkzaamheid en eventuele bijwerkingen, wat vooralsnog grotendeels met dierexperimenten gedaan moet worden. Voor zulke experimenten gebruiken we een 'proefdiermodel'; dit is een experimentele virusinfectie van een proefdiersoort op een zodanige wijze dat het dier een vergelijkbaar ziekteverloop heeft als bij de mens. Java-apen, groene meerkatten, fretten en katten zijn de proefdiersoorten die in dit proefschrift als model voor ernstige ziekte in de mens door influenzavirus of SARS-CoV werden gebruikt. De keuze van deze diersoorten werd geleid door een fysiologie van de luchtwegen en een ziekteverloop die sterk overeenkomen met die van de mens.

SARS-CORONAVIRUSINFECTIE IN LABORATORIUMDIEREN

In 2002 was er een uitbraak van SARS in China, waarbij mensen last hadden van koorts, keelpijn, hoesten, spierpijn en soms ook ernstige longontsteking. Om de pathogenese van SARS-CoV infectie beter te kunnen onderzoeken en om medicijnen en vaccins tegen SARS te kunnen ontwikkelen, werden proefdieren geïnfecteerd met het virus. Hiervoor kwamen verschillende proefdiersoorten in aanmerking. In hoofdstuk 2 beschrijven we SARS-CoV-infecties bij verschillende diersoorten, die allemaal een iets ander ziektebeeld lieten zien. In hoofdstuk 2.1 is de pathologie van SARS-CoV-infectie in groene meerkatten vergeleken met die in Java-apen waarbij opviel dat de longen een ernstigere longontsteking lieten zien met meer vloeistof in de luchtblaasjes over een groter oppervlak van de long. Het verschil in de uitkomst van SARS-CoV-infectie bij deze apensoorten kan verklaard worden door een verschillende manier van reageren van het lichaam op de infectie. In hoofdstuk 2.2 vergelijken we SARS-CoV-infecties in katten en fretten, waaruit bleek dat het celtype dat geïnfecteerd werd in de long, verschilt tussen deze twee soorten. De longblaasjes (waar de zuurstofuitwisseling tussen lucht en bloed plaatsvindt) bestaan uit twee types epitheelcellen: type I cellen, belangrijk voor de zuurstofuitwisseling en type II cellen, belangrijk voor o.a. de aanmaak van longvloeistof en herstel bij beschadigingen van de long. Bij katten werden, net als bij mensen, zowel type I als type II cellen geïnfecteerd, terwijl bij fretten dit voornamelijk type II cellen waren. Een receptor waar het SARS-CoV aan bindt om cellen te infecteren is 'angiotensine converting enzyme 2' (ACE2). Uit ons onderzoek bij fretten en katten bleek dat de celtypes die ACE2 droegen overeenkwamen met de celtypes die met SARS-CoV geïnfecteerd werden. Dit kan betekenen dat verschillende diersoorten,

door het wel of niet hebben van bepaalde receptoren, verschillend kunnen reageren op SARS-CoV-infectie. Dit geeft ook het belang van de juiste keuze van de proefdiersoort aan in diermodellen voor SARS bij de mens. Voor vaccins en therapeutische middelen tegen ernstige ziekte in SARS zal nog veel onderzoek gedaan moeten worden.

Interventiestrategieën tegen SARS-coronavirus

Als een lichaam geïnfecteerd wordt met een virus zoals het SARS-CoV, zal het antistoffen aanmaken om het virus uit te schakelen. Bij de SARS-CoV uitbraak waren er nog geen preventieve en therapeutische middelen aanwezig. De enige mogelijkheid om de uitbraak in te perken was het in quarantaine brengen van de personen, beperken van het reisgedrag, uitgebreide hygiënemaatregelen en het ondersteunen van de zieken. Omdat er altijd een mogelijkheid is dat een dergelijk virus opnieuw mensen kan infecteren, is het belangrijk om preventieve maatregelen te nemen zoals het ontwikkelen van vaccins. In hoofdstukken 2.3 en 2.4 zijn verschillende soorten vaccins geëvalueerd in fretten en Java-apen. Ondanks dat er na vaccinatie voldoende antistoffen in de dieren aangemaakt werden, was er geen volledige bescherming tegen het uitscheiden van virus maar wel tegen ziekte.

Helaas is er tot nu toe geen diermodel waarbij SARS-CoV-infectie een in ernst vergelijkbare longontsteking als bij de mens veroorzaakt. Het enige diermodel dat de menselijke situatie redelijk nabootst is de oude Java-aap, die vanwege ethische, huisvestings- en financiële problemen niet gemakkelijk gebruikt kan worden. Een goed diermodel voor longontsteking veroorzaakt door het SARS-CoV moet nog ontwikkeld worden.

INFLUENZAVIRUSINFECTIE IN LABORATORIUMDIEREN

Een influenzavirus bestaat uit viraal RNA dat omgeven wordt door een kapsel (nucleocapside) en daaromheen een enveloppe, een membraan met daarin twee verschillende receptoreiwitten: het hemagglutinine (H) en het neuraminidase (N). Van deze receptoreiwitten zijn er veel verschillende subtypes; van de H zijn er 17 en van de N zijn er 9. Op deze manier worden influenzavirussen gecategoriseerd.

In maart 2009 ontstond er in Mexico en de Verenigde Staten een uitbraak van een ziekte die gekenmerkt werd door ‘griep’verschijnselen zoals hoesten, koorts, keelpijn en spierpijn. De ziekte verspreidde zich snel en zorgde voor meerdere doden. De mensen die stierven waren voornamelijk jongvolwassenen die binnen korte tijd een ernstige longontsteking hadden ontwikkeld. Onderzoek wees uit dat de oorzaak van de ziekte een nieuw influenzavirus was van het H1N1 subtype, dat zorgde voor een pandemie. In het begin van de pandemie was het belangrijk om zo snel mogelijk onderzoek te doen naar de ernst van de ziekte die door dit virus veroorzaakt werd om zo snel mogelijk adequate maatregelen te kunnen nemen en om therapeutische en preventieve middelen zoals vaccins te ontwikkelen. In hoofdstukken 3.1 tot en met 3.3 vergelijken we infecties met verschillende influenzavirussen in proefdieren. Daaruit bleek dat het Mexicaanse griepvirus ernstiger was dan het seizoensgriepvirus in deze dieren, en dus ook potentieel ernstiger voor de mens.

Seizoensgriep (veroorzaakt door infecties met influenzavirussen van de subtypes H1N1 of H3N2) komt jaarlijks in de winter voor, voornamelijk als een ontsteking in de neus of keel. Veel mensen worden ziek en knappen snel weer op, terwijl heel jonge mensen, heel oude mensen of mensen met een chronische aandoening meer kans hebben om een ernstige longontsteking te ontwikkelen, waaraan ze soms overlijden. Tot nu toe bestond er geen diermodel waarin een seizoensgriepvirusinfec-

tie consistent een ernstige longontsteking veroorzaakt, zoals dat bij mensen uit de risicogroepen gezien wordt. In hoofdstuk 3.4 wordt een diermodel beschreven dat wel consistent ernstige longontsteking laat zien door fretten met een hoge dosis virus te infecteren. Dit diermodel kan goed gebruikt worden voor o.a. vaccinatie-experimenten tegen seizoensgriep.

Sommige subtypen van influenzavirussen zijn ongevaarlijk voor mensen en dieren, terwijl andere varianten ernstige ziekten en dood onder mensen kunnen veroorzaken. Hoogpathogene aviaire influenza H5N1 wordt ook wel de 'vogelgriep' genoemd. Oorspronkelijk gaf dit virus alleen ernstige ziekte en sterfte bij pluimvee, maar bij een ernstige uitbraak onder pluimvee in Hong Kong in 1997 werden ook mensen besmet met deze variant. Er is slechts zelden verspreiding van de kip naar de mens en tussen mensen, waardoor er maar weinig gevallen zijn geweest, maar na infectie overlijdt bijna 60% van de patiënten aan een ernstige longontsteking. Om een beter inzicht te krijgen in de verschillen tussen de genoemde influenzavirussen zijn in hoofdstuk 3.5 fretten geïnfecteerd met seizoensgriepvirus, Mexicaanse griepvirus en vogelgriepvirus en op diverse tijdstippen na infectie onderzocht. De resultaten laten zien dat er een grote variatie is tussen de virussen wat betreft de temporele (wat er gedurende de tijd gebeurt) en de spatiële (wat er op verschillende locaties in de luchtweg gebeurt) dynamiek. Dit impliceert dat het heel belangrijk is om bij het doen van een experiment een weloverwogen beslissing te nemen over de tijdstippen en plaats van de te gebruiken materialen, omdat de resultaten hierdoor erg kunnen verschillen.

Interventiestrategieën tegen de Mexicaanse griep

Na infectie met een influenzavirus zal het lichaam antistoffen aanmaken tegen de infectie. Als het virus weinig zou veranderen, dan zou je, nadat je eenmaal griep hebt gehad, vrijwel immuun zijn voor dat virus. Influenzavirus verandert echter van jaar tot jaar, waardoor de afweer die je op hebt gedaan door een eerdere besmetting na een paar jaar niet meer toereikend kan zijn. In het geval van de Mexicaanse griep was het een virus dat gevormd was door een combinatie van een humaan, vogel en varkens subtype (triple reassortment). Aan het begin van de pandemie had niemand antilichamen tegen dit virus, daardoor kon het virus zich ook zeer snel verspreiden. De groepen met de meeste kans om ernstig ziek te worden waren jongvolwassenen, kinderen en mensen met chronische hart- of longaandoeningen, obesitas, suikerziekte of zwangerschap. De mensen boven de 60 bleven verbazend genoeg relatief gespaard. Dit was in tegenstelling tot de gewone seizoensgriep, die ernstigere ziekte veroorzaakt bij minder adolescenten en meer ouderen. Uit onderzoek bleek dat het Mexicaanse griepvirus enigszins verwant was aan het 'Spaanse griep'-virus uit 1918. Door een dergelijke 'kruisimmuniteit' of door herhaaldelijke vaccinaties met een seizoensgriepvaccin gedurende langere tijd zou de oudere bevolking meer antistoffen kunnen bezitten en immuun kunnen zijn voor het Mexicaanse griepvirus. Door de snelle verspreiding van het virus, de afwijkende leeftijd van de ernstig zieken en het toegenomen sterftecijfer, moest er snel een vaccin komen om mensen preventief te behandelen en zo de verspreiding te doen afnemen. Een vaccin dat voldoende werkzaam is en het juiste effect heeft, is niet zomaar gemaakt en zeker niet op een dusdanig grote schaal. Daarom werd er eerst geëxperimenteerd met de seizoensgriepvaccins die al aanwezig waren, om te kijken of er een kruisreactiviteit was met het Mexicaanse griepvirus of om tijd te rekken door eerst een seizoensgriepvaccin toe te dienen, gevolgd door het Mexicaanse griepvaccin. Uit het onderzoek beschreven in hoofdstuk 3.6 bleek dat deze laatste mogelijkheid goed werkbaar was, mits er een geschikt adjuvans (dat de immuunrespons versterkt) aan de vaccins was toegevoegd.

CONCLUSIE

Influenzavirus en SARS-CoV blijven een gevaar, de eerste omdat dat telkens verandert en omdat zo nu en dan een volledige nieuwe variant opduikt, de tweede omdat er altijd een risico is dat een vergelijkbaar virus overspringt van dier naar mens. Bij het influenzavirus maken we ons vooral zorgen over het ontstaan van een variant die zowel efficiënt overdraagbaar is als hoge sterfte veroorzaakt. Daarom is het van belang om goede surveillance te blijven doen bij dier en mens en beter te begrijpen waardoor virussen van dier naar mens overspringen door samenwerking tussen geneeskunde, diergeneeskunde en geassocieerde disciplines ('One Health'). Dit proefschrift heeft daaraan bijgedragen door toegenomen kennis over de pathogenese van zowel SARS als influenza en door de ontwikkeling van betere diermodellen voor deze virusinfecties, die nodig zijn om preventieve en therapeutische maatregelen te testen.

CHAPTER 6

REFERENCES

1 Xu RH, He JF, Evans MR, Peng GW, Field HE, Yu DW et al.: Epidemiologic clues to SARS origin in China. Emerg Infect Dis 10:1030-1037, 2004.
2 WHO: Summary of probable SARS cases with onset of illness from 1 November 2002 to 31 July 2003. 31 December 2003. http://www.who.int/csr/sars/country/table2004_04_21/en/index.html.Assessed; 27-7-2012.
3 Wang LF, Shi Z, Zhang S, Field H, Daszak P, Eaton BT: Review of bats and SARS. Emerg Infect Dis 12:1834-1840, 2006.
4 Liang G, Chen Q, Xu J, Liu Y, Lim W, Peiris JS et al.: Laboratory diagnosis of four recent sporadic cases of community-acquired SARS, Guangdong Province, China. Emerg Infect Dis 10:1774-1781, 2004.
5 Drosten C, Günther S, Preiser W, van der Werf S, Brodt HR, Becker S et al.: Identification of a novel coronavirus in patients with severe acute respiratory syndrome. N Engl J Med 348:1967-1976, 2003.
6 Fouchier RA, Kuiken T, Schutten M, van Amerongen G, Van Doornum GJ, van den Hoogen BG et al.: Aetiology: Koch's postulates fulfilled for SARS virus. Nature 423:240, 2003.
7 Kuiken T, Fouchier RA, Schutten M, Rimmelzwaan GF, van Amerongen G, van Riel D et al.: Newly discovered coronavirus as the primary cause of severe acute respiratory syndrome. Lancet 362:263-270, 2003.
8 Weiss SR, Navas-Martin S: Coronavirus pathogenesis and the emerging pathogen severe acute respiratory syndrome coronavirus. Microbiol Mol Biol Rev 69:635-664, 2005.
9 Simmons G, Reeves JD, Rennekamp AJ, Amberg SM, Piefer AJ, Bates P: Characterization of severe acute respiratory syndrome-associated coronavirus (SARS-CoV) spike glycoprotein-mediated viral entry. Proc Natl Acad Sci U S A 101:4240-4245, 2004.
10 Li W, Shi Z, Yu M, Ren W, Smith C, Epstein JH et al.: Bats are natural reservoirs of SARS-like coronaviruses. Science 310:676-679, 2005.
11 Guan Y, Zheng BJ, He YQ, Liu XL, Zhuang ZX, Cheung CL et al.: Isolation and characterization of viruses related to the SARS coronavirus from animals in southern China. Science 302:276-278, 2003.
12 Webster RG: Wet markets--a continuing source of severe acute respiratory syndrome and influenza? Lancet 363:234-236, 2004.
13 Lau SK, Woo PC, Li KS, Huang Y, Tsoi HW, Wong BH et al.: Severe acute respiratory syndrome coronavirus-like virus in Chinese horseshoe bats. Proc Natl Acad Sci U S A 102:14040-14045, 2005.
14 Peiris JS, Yuen KY, Osterhaus AD, Stöhr K: The severe acute respiratory syndrome. N Engl J Med 349:2431-2441, 2003.
15 Wong T, Wallington T, McDonald LC, Abbas Z, Christian M, Low DE et al.: Late recognition of SARS in nosocomial outbreak, Toronto. Emerg Infect Dis 11:322-325, 2005.
16 Yu IT, Wong TW, Chiu YL, Lee N, Li Y: Temporal-spatial analysis of severe acute respiratory syndrome among hospital inpatients. Clin Infect Dis 40:1237-1243, 2005.
17 Peiris JS, Chu CM, Cheng VCC, Chan KS, Hung IFN, Poon LLM et al.: Clinical progression and viral load in a community outbreak of coronavirus-associated SARS pneumonia: a prospective study. Lancet 361:1767-1772, 2003.
18 Leung GM, Hedley AJ, Ho LM, Chau P, Wong IO, Thach TQ et al.: The epidemiology of severe acute respiratory syndrome in the 2003 Hong Kong epidemic: an analysis of all 1755 patients. Ann Intern Med 141:662-673, 2004.
19 Peiris JS, Lai ST, Poon LL, Guan Y, Yam LY, Lim W et al.: Coronavirus as a possible cause of severe acute respiratory syndrome. Lancet 361:1319-1325, 2003.
20 Leung WK, To KF, Chan PK, Chan HL, Wu AK, Lee N et al.: Enteric involvement of severe acute respiratory syndrome-associated coronavirus infection. Gastroenterology 125:1011-1017, 2003.
21 Hui DS, Chan PK: Clinical features, pathogenesis and immunobiology of severe acute respiratory syndrome. Curr Opin Pulm Med 14:241-247, 2008.
22 Wong RS, Wu A, To KF, Lee N, Lam CW, Wong CK et al.: Haematological manifestations in patients with severe acute respiratory syndrome: retrospective analysis. BMJ 326:1358-1362, 2003.
23 Muller MP, Tomlinson G, Marrie TJ, Tang P, McGeer A, Low DE et al.: Can routine laboratory tests discriminate between severe acute respiratory syndrome and other causes of community-acquired pneumonia? Clin Infect Dis 40:1079-1086, 2005.
24 Lee N, Rainer TH, Ip M, Zee B, Ng MH, Antonio GE et al.: Role of laboratory variables in differentiating SARS-coronavirus from other causes of community-acquired pneumonia within the first 72 h of hospitalization. Eur J Clin Microbiol Infect Dis 25:765-772, 2006.

25 Li T, Qiu Z, Zhang L, Han Y, He W, Liu Z et al.: Significant changes of peripheral T lymphocyte subsets in patients with severe acute respiratory syndrome. J Infect Dis 189:648-651, 2004.
26 Donnelly CA, Ghani AC, Leung GM, Hedley AJ, Fraser C, Riley S et al.: Epidemiological determinants of spread of causal agent of severe acute respiratory syndrome in Hong Kong. Lancet 361:1761-1766, 2003.
27 Karlberg J, Chong DS, Lai WY: Do men have a higher case fatality rate of severe acute respiratory syndrome than women do? Am J Epidemiol 159:229-231, 2004.
28 Lau EH, Hsiung CA, Cowling BJ, Chen CH, Ho LM, Tsang T et al.: A comparative epidemiologic analysis of SARS in Hong Kong, Beijing and Taiwan. BMC Infect Dis 10:50, 2010.
29 Lee N, Hui D, Wu A, Chan P, Cameron P, Joynt GM et al.: A major outbreak of severe acute respiratory syndrome in Hong Kong. N Engl J Med 348:1986-1994, 2003.
30 Manocha S, Walley KR, Russell JA: Severe acute respiratory distress syndrome (SARS): a critical care perspective. Crit Care Med 31:2684-2692, 2003.
31 Nicholls JM, Poon LLM, Lee KC, Ng WF, Lai ST, Leung CY et al.: Lung pathology of fatal severe acute respiratory syndrome. Lancet 361:1773-1778, 2003.
32 Ding Y, Wang H, Shen H, Li Z, Geng J, Han H et al.: The clinical pathology of severe acute respiratory syndrome (SARS): a report from China. J Pathol 200:282-289, 2003.
33 Tse GM, To KF, Chan PK, Lo AW, Ng KC, Wu A et al.: Pulmonary pathological features in coronavirus associated severe acute respiratory syndrome (SARS). J Clin Pathol 57:260-265, 2004.
34 Gu J, Gong E, Zhang B, Zheng J, Gao Z, Zhong Y et al.: Multiple organ infection and the pathogenesis of SARS. J Exp Med 202:415-424, 2005.
35 Hsueh PR, Chen PJ, Hsiao CH, Yeh SH, Cheng WC, Wang JL et al.: Patient data, early SARS epidemic, Taiwan. Emerg Infect Dis 10:489-493, 2004.
36 Shieh WJ, Hsiao CH, Paddock CD, Guarner J, Goldsmith CS, Tatti K et al.: Immunohistochemical, in situ hybridization, and ultrastructural localization of SARS-associated coronavirus in lung of a fatal case of severe acute respiratory syndrome in Taiwan. Hum Pathol 36:303-309, 2005.
37 Franks TJ, Chong PY, Chui P, Galvin JR, Lourens RM, Reid AH et al.: Lung pathology of severe acute respiratory syndrome (SARS): a study of 8 autopsy cases from Singapore. Hum Pathol 34:743-748, 2003.
38 Cheung OY, Chan JW, Ng CK, Koo CK: The spectrum of pathological changes in severe acute respiratory syndrome (SARS). Histopathology 45:119-124, 2004.
39 He L, Ding Y, Zhang Q, Che X, He Y, Shen H et al.: Expression of elevated levels of pro-inflammatory cytokines in SARS-CoV-infected ACE2+ cells in SARS patients: relation to the acute lung injury and pathogenesis of SARS. J Pathol 210:288-297, 2006.
40 Fisman DN: Hemophagocytic syndromes and infection. Emerg Infect Dis 6:601-608, 2000.
41 Lang ZW, Zhang LJ, Zhang SJ, Meng X, Li JQ, Song CZ et al.: A clinicopathological study of three cases of severe acute respiratory syndrome (SARS). Pathology 35:526-531, 2003.
42 Chong PY, Chui P, Ling AE, Franks TJ, Tai DY, Leo YS et al.: Analysis of deaths during the severe acute respiratory syndrome (SARS) epidemic in Singapore: challenges in determining a SARS diagnosis. Arch Pathol Lab Med 128:195-204, 2004.
43 Wu VC, Hsueh PR, Lin WC, Huang JW, Tsai HB, Chen YM et al.: Acute renal failure in SARS patients: more than rhabdomyolysis. Nephrol Dial Transplant 19:3180-3182, 2004.
44 Wei L, Sun S, Xu CH, Zhang J, Xu Y, Zhu H et al.: Pathology of the thyroid in severe acute respiratory syndrome. Hum Pathol 38:95-102, 2007.
45 Li W, Moore MJ, Vasilieva N, Sui J, Wong SK, Berne MA et al.: Angiotensin-converting enzyme 2 is a functional receptor for the SARS coronavirus. Nature 426:450-454, 2003.
46 Yang ZY, Huang Y, Ganesh L, Leung K, Kong WP, Schwartz O et al.: pH-dependent entry of severe acute respiratory syndrome coronavirus is mediated by the spike glycoprotein and enhanced by dendritic cell transfer through DC-SIGN. J Virol 78:5642-5650, 2004.
47 Jeffers SA, Tusell SM, Gillim-Ross L, Hemmila EM, Achenbach JE, Babcock GJ et al.: CD209L (L-SIGN) is a receptor for severe acute respiratory syndrome coronavirus. Proc Natl Acad Sci U S A 101:15748-15753, 2004.
48 Huang IC, Bosch BJ, Li W, Farzan M, Rottier PM, Choe H: SARS-CoV, but not HCoV-NL63, utilizes cathepsins to infect cells: viral entry. Adv Exp Med Biol 581:335-338, 2006.
49 Simmons G, Gosalia DN, Rennekamp AJ, Reeves JD, Diamond SL, Bates P: Inhibitors of cathepsin L prevent severe acute respiratory syndrome coronavirus entry. Proc Natl Acad Sci U S A 102:11876-11881, 2005.

50 Hamming I, Timens W, Bulthuis ML, Lely AT, Navis GJ, van Goor H: Tissue distribution of ACE2 protein, the functional receptor for SARS coronavirus. A first step in understanding SARS pathogenesis. J Pathol 203:631-637, 2004.

51 To KF, Lo AW: Exploring the pathogenesis of severe acute respiratory syndrome (SARS): the tissue distribution of the coronavirus (SARS-CoV) and its putative receptor, angiotensin-converting enzyme 2 (ACE2). J Pathol 203:740-743, 2004.

52 Ding Y, He L, Zhang Q, Huang Z, Che X, Hou J et al.: Organ distribution of severe acute respiratory syndrome (SARS) associated coronavirus (SARS-CoV) in SARS patients: implications for pathogenesis and virus transmission pathways. J Pathol 203:622-630, 2004.

53 Farcas GA, Poutanen SM, Mazzulli T, Willey BM, Butany J, Asa SL et al.: Fatal severe acute respiratory syndrome is associated with multiorgan involvement by coronavirus. J Infect Dis 191:193-197, 2005.

54 Tan YJ, Fielding BC, Goh PY, Shen S, Tan TH, Lim SG et al.: Overexpression of 7a, a protein specifically encoded by the severe acute respiratory syndrome coronavirus, induces apoptosis via a caspase-dependent pathway. J Virol 78:14043-14047, 2004.

55 Yen YT, Liao F, Hsiao CH, Kao CL, Chen YC, Wu-Hsieh BA: Modeling the early events of severe acute respiratory syndrome coronavirus infection in vitro. J Virol 80:2684-2693, 2006.

56 Wong CK, Lam CW, Wu AK, Ip WK, Lee NL, Chan IH et al.: Plasma inflammatory cytokines and chemokines in severe acute respiratory syndrome. Clin Exp Immunol 136:95-103, 2004.

57 Zhang Y, Li J, Zhan Y, Wu L, Yu X, Zhang W et al.: Analysis of serum cytokines in patients with severe acute respiratory syndrome. Infect Immun 72:4410-4415, 2004.

58 Jiang Y, Xu J, Zhou C, Wu Z, Zhong S, Liu J et al.: Characterization of cytokine/chemokine profiles of severe acute respiratory syndrome. Am J Respir Crit Care Med 171:850-857, 2005.

59 Huang JL, Lin HT, Wang YM, Yeh YC, Peck K, Lin BL et al.: Rapid and sensitive detection of multiple genes from the SARS-coronavirus using quantitative RT-PCR with dual systems. J Med Virol 77:151-158, 2005.

60 Tang NL, Chan PK, Wong CK, To KF, Wu AK, Sung YM et al.: Early enhanced expression of interferon-inducible protein-10 (CXCL-10) and other chemokines predicts adverse outcome in severe acute respiratory syndrome. Clin Chem 51:2333-2340, 2005.

61 Baas T, Roberts A, Teal TH, Vogel L, Chen J, Tumpey TM et al.: Genomic analysis reveals age-dependent innate immune responses to severe acute respiratory syndrome coronavirus. J Virol 82:9465-9476, 2008.

62 Tang XC, Zhang JX, Zhang SY, Wang P, Fan XH, Li LF et al.: Prevalence and genetic diversity of coronaviruses in bats from China. J Virol 80:7481-7490, 2006.

63 Rockx B, Baas T, Zornetzer GA, Haagmans B, Sheahan T, Frieman M et al.: Early upregulation of acute respiratory distress syndrome-associated cytokines promotes lethal disease in an aged-mouse model of severe acute respiratory syndrome coronavirus infection. J Virol 83:7062-7074, 2009.

64 Li W, Zhang C, Sui J, Kuhn JH, Moore MJ, Luo S et al.: Receptor and viral determinants of SARS-coronavirus adaptation to human ACE2. EMBO J 24:1634-1643, 2005.

65 Ip WK, Chan KH, Law HK, Tso GH, Kong EK, Wong WH et al.: Mannose-binding lectin in severe acute respiratory syndrome coronavirus infection. J Infect Dis 191:1697-1704, 2005.

66 Ng MH, Lau KM, Li L, Cheng SH, Chan WY, Hui PK et al.: Association of human-leukocyte-antigen class I (B*0703) and class II (DRB1*0301) genotypes with susceptibility and resistance to the development of severe acute respiratory syndrome. J Infect Dis 190:515-518, 2004.

67 Chan VS, Chan KY, Chen Y, Poon LL, Cheung AN, Zheng B et al.: Homozygous L-SIGN (CLEC4M) plays a protective role in SARS coronavirus infection. Nat Genet 38:38-46, 2006.

68 Liang L, He C, Lei M, Li S, Hao Y, Zhu H et al.: Pathology of guinea pigs experimentally infected with a novel reovirus and coronavirus isolated from SARS patients. DNA Cell Biol 24:485-490, 2005.

69 Martina BE, Haagmans BL, Kuiken T, Fouchier RA, Rimmelzwaan GF, van Amerongen G et al.: Virology: SARS virus infection of cats and ferrets. Nature 425:915, 2003.

70 Roberts A, Thomas WD, Guarner J, Lamirande EW, Babcock GJ, Greenough TC et al.: Therapy with a severe acute respiratory syndrome-associated coronavirus-neutralizing human monoclonal antibody reduces disease severity and viral burden in golden Syrian hamsters. J Infect Dis 193:685-692, 2006.

71 Weingartl HM, Copps J, Drebot MA, Marszal P, Smith G, Gren J et al.: Susceptibility of pigs and chickens to SARS coronavirus. Emerg Infect Dis 10:179-184, 2004.

72 Wentworth DE, Gillim-Ross L, Espina N, Bernard KA: Mice susceptible to SARS coronavirus. Emerg Infect Dis 10:1293-1296, 2004.

73 Yang ZY, Kong WP, Huang Y, Roberts A, Murphy BR, Subbarao K et al.: A DNA vaccine induces SARS coronavirus neutralization and protective immunity in mice. Nature 428:561-564, 2004.
74 Roberts A, Paddock C, Vogel L, Butler E, Zaki S, Subbarao K: Aged BALB/c mice as a model for increased severity of severe acute respiratory syndrome in elderly humans. J Virol 79:5833-5838, 2005.
75 McAuliffe J, Vogel L, Roberts A, Fahle G, Fischer S, Shieh WJ et al.: Replication of SARS coronavirus administered into the respiratory tract of African Green, rhesus and cynomolgus monkeys. Virol 330:8-15, 2004.
76 Rowe T, Gao G, Hogan RJ, Crystal RG, Voss TG, Grant RL et al.: Macaque model for severe acute respiratory syndrome. J Virol 78:11401-11404, 2004.
77 Bukreyev A, Lamirande EW, Buchholz UJ, Vogel LN, Elkins WR, St Claire M et al.: Mucosal immunisation of African green monkeys (Cercopithecus aethiops) with an attenuated parainfluenza virus expressing the SARS coronavirus spike protein for the prevention of SARS. Lancet 363:2122-2127, 2004.
78 Gao W, Tamin A, Soloff A, D'Aiuto L, Nwanegbo E, Robbins PD et al.: Effects of a SARS-associated coronavirus vaccine in monkeys. Lancet 362:1895-1896, 2003.
79 Li BJ, Tang Q, Cheng D, Qin C, Xie FY, Wei Q et al.: Using siRNA in prophylactic and therapeutic regimens against SARS coronavirus in Rhesus macaque. Nat Med 11:944-951, 2005.
80 Qin E, Shi H, Tang L, Wang C, Chang G, Ding Z et al.: Immunogenicity and protective efficacy in monkeys of purified inactivated Vero-cell SARS vaccine. Vaccine 24:1028-1034, 2006.
81 Weingartl H, Czub M, Czub S, Neufeld J, Marszal P, Gren J et al.: Immunization with modified vaccinia virus Ankara-based recombinant vaccine against severe acute respiratory syndrome is associated with enhanced hepatitis in ferrets. J Virol 78:12672-12676, 2004.
82 Beveridge WIB: Influenza: The last great plague. Prodist, New York, 1978.
83 Cox NJ, Subbarao K: Global epidemiology of influenza: past and present. Annu Rev Med 51:407-421, 2000.
84 Morens DM, Taubenberger JK, Fauci AS: The persistent legacy of the 1918 influenza virus. N Engl J Med 361:225-229, 2009.
85 Parker NR, Caywood DD: surgical diseases of the Esophagus. Veterinary Clinics of North America 17:333-358, 1987.
86 Jepson PD, Brew S, MacMillan AP, Baker JR, Barnett J, Kirkwood JK et al.: Antibodies to Brucella in marine mammals around the coast of England and Wales. Vet Rec 141:513-515, 1997.
87 Osterhaus ADME: Catastrophes after crossing species barriers. Phil Trans R Soc Lond 356:1-3, 2001.
88 Swayne DE, Halvorson DA: Influenza. In: Diseases of poultry, ed. Saif YM, Barnes HJ, Glisson JR, Fadly AM, McDougald LR, Swayne DE, 11th ed., pp. 135-160. Iowa State University Press, Ames, Iowa, 2003.
89 Tong S, Li Y, Rivailler P, Conrardy C, Castillo DA, Chen LM et al.: A distinct lineage of influenza A virus from bats. Proc Natl Acad Sci U S A 109:4269-4274, 2012.
90 Webster RG, Yakhno M, Hinshaw VS, Bean WJ, Murti KG: Intestinal influenza: replication and characterization of influenza viruses in ducks. Virol 84:268-278, 1978.
91 WHO: Manual on animal influenza diagnosis and surveillance. pp. 62-63. Geneva, 2004.
92 Horimoto T, Kawaoka Y: Pandemic threat posed by avian influenza A viruses. Clin Microbiol Rev 14:129-149, 2001.
93 Claas ECJ, Osterhaus ADME, van Beek R, de Jong JC, Rimmelzwaan GF, Senne DA et al.: Human influenza A H5N1 virus related to a highly pathogenic avian influenza virus. Lancet 351:472-477, 1998.
94 WHO: Cumulative number of confirmed human cases for avian influenza A(H5N1) reported to WHO, 2003-2012. http://www.who.int/influenza/human_animal_interface/EN_GIP_20120529CumulativeNumberH5N1cases.pdf. Assessed 27-6-2012.
95 Webby RJ, Webster RG: Are we ready for pandemic influenza? Science 302:1519-1522, 2003.
96 Garten RJ, Davis CT, Russell CA, Shu B, Lindstrom S, Balish A et al.: Antigenic and Genetic Characteristics of Swine-Origin 2009 A(H1N1) Influenza Viruses Circulating in Humans. Science 325:197-201, 2009.
97 Pandemic (H1N1) 2009 - update 112. http://www.who.int/csr/don/2010_08_06/en/index.html. Assessed 27-6-2012.
98 Monto AS, Gravenstein S, Elliott M, Colopy M, Schweinle J: Clinical signs and symptoms predicting influenza infection. Arch Intern Med 160:3243-3247, 2000.
99 Rothberg MB, Haessler SD, Brown RB: Complications of viral influenza. Am J Med 121:258-264, 2008.
100 de Jong MD, Bach VC, Phan TQ, Vo MH, Tran TT, Nguyen BH et al.: Fatal avian influenza A (H5N1) in a child presenting with diarrhea followed by coma. N Engl J Med 352:686-691, 2005.

101 Oner AF, Bay A, Arslan S, Akdeniz H, Sahin HA, Cesur Y et al.: Avian influenza A (H5N1) infection in eastern Turkey in 2006. N Engl J Med 355:2179-2185, 2006.
102 Kandun IN, Tresnaningsih E, Purba WH, Lee V, Samaan G, Harun S et al.: Factors associated with case fatality of human H5N1 virus infections in Indonesia: a case series. Lancet 372:744-749, 2008.
103 Louie JK, Jean C, Acosta M, Samuel MC, Matyas BT, Schechter R: A review of adult mortality due to 2009 pandemic (H1N1) influenza A in California. PLoS ONE 6:e182212011.
104 Abdel-Ghafar AN, Chotpitayasunondh T, Gao Z, Hayden FG, Nguyen DH, de Jong MD et al.: Update on avian influenza A (H5N1) virus infection in humans. N Engl J Med 358:261-273, 2008.
105 Walsh JJ, Dietlein LF, Low FN, Burch GE, Mogabgab WJ: Bronchotracheal response in human influenza: Type A, Asian strain, as studied by light and electron microscopic examination of bronchoscopic biopsies. Arch Intern Med 108:376-388, 1961.
106 Taubenberger JK, Morens DM: The pathology of influenza virus infections. Annu Rev Pathol 3:499-522, 2008.
107 Ng WF, To KF, Lam WW, Ng TK, Lee KC: The comparative pathology of severe acute respiratory syndrome and avian influenza A subtype H5N1--a review. Hum Pathol 37:381-390, 2006.
108 Guarner J, Paddock CD, Shieh WJ, Packard MM, Patel M, Montague JL et al.: Histopathologic and immunohistochemical features of fatal influenza virus infection in children during the 2003-2004 season. Clin Infect Dis 43:132-140, 2006.
109 Guarner J, Falcon-Escobedo R: Comparison of the pathology caused by H1N1, H5N1, and H3N2 influenza viruses. Arch Med Res 40:655-661, 2009.
110 Peiris JS, Yu WC, Leung CW, Cheung CY, Ng WF, Nicholls JM et al.: Re-emergence of fatal human influenza A subtype H5N1 disease. Lancet 363:617-619, 2004.
111 To KF, Chan PKS, Chan KF, Lee WK, Lam WY, Wong KF et al.: Pathology of fatal human infection associated with avian influenza A H5N1 virus. J Med Virol 63:242-246, 2001.
112 Chokephaibulkit K, Uiprasertkul M, Puthavathana P, Chearskul P, Auewarakul P, Dowell SF et al.: A child with avian influenza A (H5N1) infection. Pediatr Infect Dis J 24:162-166, 2005.
113 Uiprasertkul M, Puthavathana P, Sangsiriwut K, Pooruk P, Srisook K, Peiris M et al.: Influenza A H5N1 replication sites in humans. Emerg Infect Dis 11:1036-1041, 2005.
114 Studahl M: Influenza virus and CNS manifestations. J Clin Virol 28:225-232, 2003.
115 Ray CG, Icenogle TB, Minnich LL, Copeland JG, Grogan TM: The use of intravenous ribavirin to treat influenza virus-associated acute myocarditis. J Infect Dis 159:829-836, 1989.
116 Agyeman P, Duppenthaler A, Heininger U, Aebi C: Influenza-associated myositis in children. Infection 32:199-203, 2004.
117 Connor RJ, Kawaoka Y, Webster RG, Paulson JC: Receptor specificity in human, avian, and equine H2 and H3 influenza virus isolates. Virol 205:17-23, 1994.
118 Shinya K, Ebina M, Yamada S, Ono M, Kasai N, Kawaoka Y: Influenza virus receptors in the human airway. Nature 440:435-436, 2006.
119 Kuiken T, Taubenberger JK: Pathology of human influenza revisited. Vaccine 26 Suppl 4:D59-D662008.
120 Likos AM, Kelvin DJ, Cameron CM, Rowe T, Kuehnert MJ, Norris PJ: Influenza viremia and the potential for blood-borne transmission. Transfusion 47:1080-1088, 2007.
121 Gu J, Xie Z, Gao Z, Liu J, Korteweg C, Ye J et al.: H5N1 infection of the respiratory tract and beyond: a molecular pathology study. Lancet 370:1137-1145, 2007.
122 Mok CK, Lee DC, Cheung CY, Peiris M, Lau AS: Differential onset of apoptosis in influenza A virus. J Gen Virol 88:1275-1280, 2007.
123 Beal AL, Cerra FB: Multiple organ failure syndrome in the 1990s: systemic inflammatory response and organ dysfunction. JAMA 271:226-233, 1994.
124 van Riel D, Munster VJ, de Wit E, Rimmelzwaan GF, Fouchier RAM, Osterhaus ADME et al.: H5N1 virus attachment to lower respiratory tract. Science 311:399, 2006.
125 van Riel D, Munster VJ, de Wit E, Rimmelzwaan GF, Fouchier RA, Osterhaus AD et al.: Human and avian influenza viruses target different cells in the lower respiratory tract of humans and other mammals. Am J Pathol 171:1215-1223, 2007.
126 van Riel D, den Bakker MA, Leijten LM, Chutinimitkul S, Munster VJ, de Wit E et al.: Seasonal and pandemic human influenza viruses attach better to human upper respiratory tract epithelium than avian influenza viruses. Am J Pathol 176:1614-1618, 2010.
127 Hers JFP, Mulder J: Broad aspects of the pathology and pathogenesis of human influenza. Am Rev Respir Dis 83:84-97, 1961.

128 Mulder J, Hers JFP: Influenza. Wolters-Noordhoff Publishing, Groningen, The Netherlands, 1972.
129 Martin CM, Kunin CM, Gottlieb LS, Barnes MW, Liu C, Finland M: Asian influenza A in Boston, 1957-1958. I. Observations in thirty-two influenza-associated fatal cases. AMA Arch Intern Med 103:515-531, 1959.
130 Gill JR, Sheng ZM, Ely SF, Guinee DG, Beasley MB, Suh J et al.: Pulmonary pathologic findings of fatal 2009 pandemic influenza A/H1N1 viral infections. Arch Pathol Lab Med 134:235-243, 2010.
131 Korteweg C, Gu J: Pathology, molecular biology, and pathogenesis of avian influenza A (H5N1) infection in humans. Am J Pathol 172:1155-1170, 2008.
132 Shieh WJ, Blau DM, Denison AM, Deleon-Carnes M, Adem P, Bhatnagar J et al.: 2009 pandemic influenza A (H1N1): pathology and pathogenesis of 100 fatal cases in the United States. Am J Pathol 177:166-175, 2010.
133 Ware LB, Matthay MA: The acute respiratory distress syndrome. N Engl J Med 342:1334-1349, 2000.
134 de Jong MD, Simmons CP, Tran TT, Hien VM, Smith GJ, Chau TN et al.: Fatal outcome of human influenza A (H5N1) is associated with high viral load and hypercytokinemia. Nat Med 12:1203-1207, 2006.
135 Uiprasertkul M, Kitphati R, Puthavathana P, Kriwong R, Kongchanagul A, Ungchusak K et al.: Apoptosis and pathogenesis of avian influenza A (H5N1) virus in humans. Emerg Infect Dis 13:708-712, 2007.
136 Barnard DL: Animal models for the study of influenza pathogenesis and therapy. Antiviral Res 82:A110-A1222009.
137 Mizgerd JP, Skerrett SJ: Animal models of human pneumonia. Am J Physiol Lung Cell Mol Physiol 294:L387-L398, 2008.
138 Beigel JH, Farrar J, Han AM, Hayden FG, Hyer R, de Jong MD et al.: Avian influenza A (H5N1) infection in humans. N Engl J Med 353:1374-1385, 2005.
139 Friedewald WF, Hook EW, Jr.: Influenza virus infection in the hamster; a study of inapparent virus infection and virus adaptation. J Exp Med 88:343-353, 1948.
140 Giebink GS, Berzins IK, Marker SC, Schiffman G: Experimental otitis media after nasal inoculation of Streptococcus pneumoniae and influenza A virus in chinchillas. Infect Immun 30:445-450, 1980.
141 Wattrang E, Jessett DM, Yates P, Fuxler L, Hannant D: Experimental infection of ponies with equine influenza A2 (H3N8) virus strains of different pathogenicity elicits varying interferon and interleukin-6 responses. Viral Immunol 16:57-67, 2003.
142 Rubin S, Liu D, Pletnikov M, McCullers J, Ye Z, Levandowski R et al.: Wild-type and attenuated influenza virus infection of the neonatal rat brain. J Neurovirol 10:305-314, 2004.
143 Giese M, Harder TC, Teifke JP, Klopfleisch R, Breithaupt A, Mettenleiter TC et al.: Experimental infection and natural contact exposure of dogs with avian influenza virus (H5N1). Emerg Infect Dis 14:308-310, 2008.
144 Rimmelzwaan G, van Riel D, Baars M, Bestebroer TM, van Amerongen G, Fouchier RAM et al.: Influenza A virus (H5N1) infection in cats causes systemic disease with potential novel routes of virus spread within and between hosts. Am J Pathol 168:176-183, 2006.
145 Boukhvalova MS, Prince GA, Blanco JC: The cotton rat model of respiratory viral infections. Biologicals 37:152-159, 2009.
146 Lipatov AS, Kwon YK, Sarmento LV, Lager KM, Spackman E, Suarez DL et al.: Domestic pigs have low susceptibility to H5N1 highly pathogenic avian influenza viruses. PLoS Pathog 4:e1000102 2008.
147 Kwon YK, Lipatov AS, Swayne DE: Bronchointerstitial pneumonia in guinea pigs following inoculation with H5N1 high pathogenicity avian influenza virus. Vet Pathol 46:138-141, 2009.
148 Kuiken T, Rimmelzwaan GF, van Amerongen G, Osterhaus AD: Pathology of human influenza A (H5N1) virus disease in cynomolgus macaques (Macaca fascicularis). Vet Pathol 40:304-310, 2003.
149 Chen Y, Deng W, Jia C, Dai X, Zhu H, Kong Q et al.: Pathological lesions and viral localization of influenza A (H5N1) virus in experimentally infected Chinese rhesus macaques: implications for pathogenesis and viral transmission. Arch Virol 154:227-233, 2009.
150 Murphy BR, Hinshaw VS, Sly DL, London WT, Hosier NT, Wood FT et al.: Virulence of avian influenza A viruses for squirrel monkeys. Infect Immun 37:1119-1126, 1982.
151 Kreijtz JH, Suezer Y, de Mutsert G, van den Brand JM, van Amerongen G, Schnierle BS et al.: Recombinant modified vaccinia virus Ankara expressing the hemagglutinin gene confers protection against homologous and heterologous H5N1 influenza virus infections in macaques. J Infect Dis 199:405-413, 2009.
152 Munster VJ, de Wit E, van den Brand JM, Herfst S, Schrauwen EJ, Bestebroer TM et al.: Pathogenesis and transmission of swine-origin 2009 A(H1N1) influenza virus in ferrets. Science 325:481-483, 2009.

153 Baker JR, Hall A, Hiby L, Munro R, Robinson I, Ross HM et al.: Isolation of salmonellae from seals from UK waters. Veterinary record 136:471-472, 1995.
154 van den Brand JMA, Stittelaar KJ, van Amerongen G, Rimmelzwaan GP, Simon J, de Wit E et al.: Severity of New H1N1 Influenza Pneumonia in Ferrets Intermediate between that of Seasonal H1N1 Virus and Highly Pathogenic Avian Influenza H5N1 Virus. J Infect Dis 201(7):993-9, 2010.
155 Muller MA, Paweska JT, Leman PA, Drosten C, Grywna K, Kemp A et al.: Coronavirus antibodies in African bat species. Emerg Infect Dis 13:1367-1370, 2007.
156 Gloza-Rausch F, Ipsen A, Seebens A, Gottsche M, Panning M, Felix DJ et al.: Detection and prevalence patterns of group I coronaviruses in bats, northern Germany. Emerg Infect Dis 14:626-631, 2008.
157 Reusken CB, Lina PH, Pielaat A, de Vries A, Dam-Deisz C, Adema J et al.: Circulation of group 2 coronaviruses in a bat species common to urban areas in Western Europe. Vector Borne Zoonotic Dis 10:785-791, 2010.
158 Kreijtz JH, Osterhaus AD, Rimmelzwaan GF: Vaccination strategies and vaccine formulations for epidemic and pandemic influenza control. Hum Vaccin 5:126-135, 2009.
159 Imai Y, Kuba K, Neely GG, Yaghubian-Malhami R, Perkmann T, van Loo G et al.: Identification of oxidative stress and Toll-like receptor 4 signaling as a key pathway of acute lung injury. Cell 133:235-249, 2008.
160 Tsushima K, King LS, Aggarwal NR, De Gorordo A, D'Alessio FR, Kubo K: Acute lung injury review. Intern Med 48:621-630, 2009.
161 Peiris JS, Guan Y, Yuen KY: Severe acute respiratory syndrome. Nat Med 10:S88-S97, 2004.
162 Hon KL, Leung CW, Cheng WT, Chan PK, Chu WC, Kwan YW et al.: Clinical presentations and outcome of severe acute respiratory syndrome in children. Lancet 361:1701-1703, 2003.
163 Leung CW, Chiu WK: Clinical picture, diagnosis, treatment and outcome of severe acute respiratory syndrome (SARS) in children. Paediatr Respir Rev 5:275-288, 2004.
164 Wong GW, Li AM, Ng PC, Fok TF: Severe acute respiratory syndrome in children. Pediatr Pulmonol 36:261-266, 2003.
165 Cameron MJ, Ran L, Xu L, Danesh A, Bermejo-Martin JF, Cameron CM et al.: Interferon-mediated immunopathological events are associated with atypical innate and adaptive immune responses in patients with severe acute respiratory syndrome. J Virol 81:8692-8706, 2007.
166 Huang KJ, Su IJ, Theron M, Wu YC, Lai SK, Liu CC et al.: An interferon-gamma-related cytokine storm in SARS patients. J Med Virol 75:185-194, 2005.
167 Reghunathan R, Jayapal M, Hsu LY, Chng HH, Tai D, Leung BP et al.: Expression profile of immune response genes in patients with Severe Acute Respiratory Syndrome. BMC Immunol 6:2, 2005.
168 Haagmans BL, Osterhaus AD: Nonhuman primate models for SARS. PLoS Med 3:e194, 2006.
169 Subbarao K, Roberts A: Is there an ideal animal model for SARS? Trends Microbiol 14:299-303, 2006.
170 Roberts A, Deming D, Paddock CD, Cheng A, Yount B, Vogel L et al.: A mouse-adapted SARS-coronavirus causes disease and mortality in BALB/c mice. PLoS Pathog 3:e5, 2007.
171 Roberts A, Paddock C, Vogel L, Butler E, Zaki S, Subbarao K: Aged BALB/c mice as a model for increased severity of severe acute respiratory syndrome in elderly humans. J Virol 79:5833-5838, 2005.
172 Haagmans BL, Kuiken T, Martina BE, Fouchier RA, Rimmelzwaan GF, van Amerongen G et al.: Pegylated interferon-alpha protects type 1 pneumocytes against SARS coronavirus infection in macaques. Nat Med 10:290-293, 2004.
173 de Lang A, Baas T, Teal T, Leijten LM, Rain B, Osterhaus AD et al.: Functional genomics highlights differential induction of antiviral pathways in the lungs of SARS-CoV-infected macaques. PLoS Pathog 3:e112, 2007.
174 Smits SL, de Lang A, van den Brand JM, Leijten LM, van Ijcken WF, Eijkemans MJ et al.: Exacerbated innate host response to SARS-CoV in aged non-human primates. PLoS Pathog 6:e1000756, 2010.
175 Deng R, Lu M, Korteweg C, Gao Z, McNutt MA, Ye J et al.: Distinctly different expression of cytokines and chemokines in the lungs of two H5N1 avian influenza patients. J Pathol 216:328-336, 2008.
176 Livak KJ, Schmittgen TD: Analysis of relative gene expression data using real-time quantitative PCR and the 2(-Delta Delta C(T)) Method. Methods 25:402-408, 2001.
177 Huber W, von Heydebreck A, Sultmann H, Poustka A, Vingron M: Variance stabilization applied to microarray data calibration and to the quantification of differential expression. Bioinformatics 18 Suppl 1:S96-104, 2002.
178 Tukey JW: Some thoughts on clinical trials, especially problems of multiplicity. Science 198:679-684, 1977.

179 Smyth GK: Linear models and empirical bayes methods for assessing differential expression in microarray experiments. Stat Appl Genet Mol Biol 3:Article3, 2004.
180 Benjamini Y, Hochberg Y: Controlling the false discovery rate: a practical and powerful approach to multiple testing. Journal of the Royal Statistical Society: Series B (Statistical Methodology) 57:289-300, 1995.
181 Fan J, Ye RD, Malik AB: Transcriptional mechanisms of acute lung injury. Am J Physiol Lung Cell Mol Physiol 281:L1037-L1050, 2001.
182 Haddad JJ: Science review: Redox and oxygen-sensitive transcription factors in the regulation of oxidant-mediated lung injury: role for nuclear factor-kappaB. Crit Care 6:481-490, 2002.
183 Kobayashi Y: Neutrophil infiltration and chemokines. Crit Rev Immunol 26:307-316, 2006.
184 O'Regan A: The role of osteopontin in lung disease. Cytokine Growth Factor Rev 14:479-488, 2003.
185 Wang KX, Denhardt DT: Osteopontin: role in immune regulation and stress responses. Cytokine Growth Factor Rev 19:333-345, 2008.
186 Perrone LA, Plowden JK, Garcia-Sastre A, Katz JM, Tumpey TM: H5N1 and 1918 pandemic influenza virus infection results in early and excessive infiltration of macrophages and neutrophils in the lungs of mice. PLoS Pathog 4:e1000115, 2008.
187 Quintero PA, Knolle MD, Cala LF, Zhuang Y, Owen CA: Matrix metalloproteinase-8 inactivates macrophage inflammatory protein-1 alpha to reduce acute lung inflammation and injury in mice. J Immunol 184:1575-1588, 2010.
188 Smith RE, Strieter RM, Zhang K, Phan SH, Standiford TJ, Lukacs NW et al.: A role for C-C chemokines in fibrotic lung disease. J Leukoc Biol 57:782-787, 1995.
189 Chabas D, Baranzini SE, Mitchell D, Bernard CC, Rittling SR, Denhardt DT et al.: The influence of the proinflammatory cytokine, osteopontin, on autoimmune demyelinating disease. Science 294:1731-1735, 2001.
190 Gravallese EM: Osteopontin: a bridge between bone and the immune system. J Clin Invest 112:147-149, 2003.
191 Morimoto J, Kon S, Matsui Y, Uede T: Osteopontin; as a target molecule for the treatment of inflammatory diseases. Curr Drug Targets 11:494-505, 2010.
192 Petrow PK, Hummel KM, Schedel J, Franz JK, Klein CL, Muller-Ladner U et al.: Expression of osteopontin messenger RNA and protein in rheumatoid arthritis: effects of osteopontin on the release of collagenase 1 from articular chondrocytes and synovial fibroblasts. Arthritis Rheum 43:1597-1605, 2000.
193 Berman JS, Serlin D, Li X, Whitley G, Hayes J, Rishikof DC et al.: Altered bleomycin-induced lung fibrosis in osteopontin-deficient mice. Am J Physiol Lung Cell Mol Physiol 286:L1311-L1318, 2004.
194 Eferl R, Hasselblatt P, Rath M, Popper H, Zenz R, Komnenovic V et al.: Development of pulmonary fibrosis through a pathway involving the transcription factor Fra-2/AP-1. Proc Natl Acad Sci U S A 105:10525-10530, 2008.
195 Pardo A, Gibson K, Cisneros J, Richards TJ, Yang Y, Becerril C et al.: Up-regulation and profibrotic role of osteopontin in human idiopathic pulmonary fibrosis. PLoS Med 2:e251, 2005.
196 Takahashi F, Takahashi K, Shimizu K, Cui R, Tada N, Takahashi H et al.: Osteopontin is strongly expressed by alveolar macrophages in the lungs of acute respiratory distress syndrome. Lung 182:173-185, 2004.
197 Lorenzen JM, Neunhoffer H, David S, Kielstein JT, Haller H, Fliser D: Angiotensin II receptor blocker and statins lower elevated levels of osteopontin in essential hypertension--results from the EUTOPIA trial. Atherosclerosis 209:184-188, 2010.
198 Imai Y, Kuba K, Rao S, Huan Y, Guo F, Guan B et al.: Angiotensin-converting enzyme 2 protects from severe acute lung failure. Nature 436:112-116, 2005.
199 Kuba K, Imai Y, Rao S, Gao H, Guo F, Guan B et al.: A crucial role of angiotensin converting enzyme 2 (ACE2) in SARS coronavirus-induced lung injury. Nat Med 11:875-879, 2005.
200 Zhao J, Zhao J, Perlman S: T cell responses are required for protection from clinical disease and for virus clearance in severe acute respiratory syndrome coronavirus-infected mice. J Virol 84:9318-9325, 2010.
201 Zhao J, Zhao J, Van Rooijen N, Perlman S: Evasion by stealth: inefficient immune activation underlies poor T cell response and severe disease in SARS-CoV-infected mice. PLoS Pathog 5:e1000636, 2009.
202 Zornetzer GA, Frieman MB, Rosenzweig E, Korth MJ, Page C, Baric RS et al.: Transcriptomic analysis reveals a mechanism for a prefibrotic phenotype in STAT1 knockout mice during severe acute respiratory syndrome coronavirus infection. J Virol 84:11297-11309, 2010.
203 Favre D, Lederer S, Kanwar B, Ma ZM, Proll S, Kasakow Z et al.: Critical loss of the balance between Th17 and T regulatory cell populations in pathogenic SIV infection. PLoS Pathog 5:e1000295, 2009.

204 Jacquelin B, Mayau V, Targat B, Liovat AS, Kunkel D, Petitjean G et al.: Nonpathogenic SIV infection of African green monkeys induces a strong but rapidly controlled type I IFN response. J Clin Invest 119:3544-3555, 2009.
205 Mandl JN, Barry AP, Vanderford TH, Kozyr N, Chavan R, Klucking S et al.: Divergent TLR7 and TLR9 signaling and type I interferon production distinguish pathogenic and nonpathogenic AIDS virus infections. Nat Med 14:1077-1087, 2008.
206 Sodora DL, Allan JS, Apetrei C, Brenchley JM, Douek DC, Else JG et al.: Toward an AIDS vaccine: lessons from natural simian immunodeficiency virus infections of African nonhuman primate hosts. Nat Med 15:861-865, 2009.
207 Haagmans BL, Andeweg AC, Osterhaus AD: The application of genomics to emerging zoonotic viral diseases. PLoS Pathog 5:e1000557, 2009.
208 Chen M, Chen G, Nie H, Zhang X, Niu X, Zang YC et al.: Regulatory effects of IFN-beta on production of osteopontin and IL-17 by CD4+ T Cells in MS. Eur J Immunol 39:2525-2536, 2009.
209 Gu J, Korteweg C: Pathology and pathogenesis of severe acute respiratory syndrome. Am J Pathol 170:1136-1147, 2007.
210 Pei F, Zheng J, Gao ZF, Zhong YF, Fang WG, Gong EC et al.: Lung pathology and pathogenesis of severe acute respiratory syndrome: a report of six full autopsies. Zhonghua Bing Li Xue Za Zhi 34:656-660, 2005.
211 To KF, Tong JH, Chan PK, Au FW, Chim SS, Chan KC et al.: Tissue and cellular tropism of the coronavirus associated with severe acute respiratory syndrome: an in-situ hybridization study of fatal cases. J Pathol 202:157-163, 2004.
212 Ye J, Zhang B, Xu J, Chang Q, McNutt MA, Korteweg C et al.: Molecular pathology in the lungs of severe acute respiratory syndrome patients. Am J Pathol 170:538-545, 2007.
213 Hamming I, Timens W, Bulthuis ML, Lely AT, Navis GJ, van Goor H: Tissue distribution of ACE2 protein, the functional receptor for SARS coronavirus. A first step in understanding SARS pathogenesis. J Pathol 203:631-637, 2004.
214 Greenough TC, Carville A, Coderre J, Somasundaran M, Sullivan JL, Luzuriaga K et al.: Pneumonitis and multi-organ system disease in common marmosets (Callithrix jacchus) infected with the severe acute respiratory syndrome-associated coronavirus. Am J Pathol 167:455-463, 2005.
215 Glass WG, Subbarao K, Murphy B, Murphy PM: Mechanisms of host defense following severe acute respiratory syndrome-coronavirus (SARS-CoV) pulmonary infection of mice. J Immunol 173:4030-4039, 2004.
216 Roberts A, Vogel L, Guarner J, Hayes N, Murphy B, Zaki S et al.: Severe acute respiratory syndrome coronavirus infection of golden Syrian hamsters. J Virol 79:503-511, 2005.
217 Nagata N, Iwata N, Hasegawa H, Fukushi S, Yokoyama M, Harashima A et al.: Participation of both host and virus factors in induction of severe acute respiratory syndrome (SARS) in F344 rats infected with SARS coronavirus. J Virol 81:1848-1857, 2007.
218 Nikitin AY, Alcaraz A, Anver MR, Bronson RT, Cardiff RD, Dixon D et al.: Classification of proliferative pulmonary lesions of the mouse: recommendations of the mouse models of human cancers consortium. Cancer Res 64:2307-2316, 2004.
219 ter Meulen J, Bakker AB, van den Brink EN, Weverling GJ, Martina BE, Haagmans BL et al.: Human monoclonal antibody as prophylaxis for SARS coronavirus infection in ferrets. Lancet 363:2139-2141, 2004.
220 Darnell ME, Plant EP, Watanabe H, Byrum R, St Claire M, Ward JM et al.: Severe acute respiratory syndrome coronavirus infection in vaccinated ferrets. J Infect Dis 196:1329-1338, 2007.
221 Czub M, Weingartl H, Czub S, He R, Cao J: Evaluation of modified vaccinia virus Ankara based recombinant SARS vaccine in ferrets. Vaccine 23:2273-2279, 2005.
222 Guo H, Guo A, Wang C, Yan B, Lu H, Chen H: Expression of feline angiotensin converting enzyme 2 and its interaction with SARS-CoV S1 protein. Res Vet Sci 84:494-496, 2008.
223 Zamoto A, Taguchi F, Fukushi S, Morikawa S, Yamada YK: Identification of ferret ACE2 and its receptor function for SARS-coronavirus. Adv Exp Med Biol 581:519-522, 2006.
224 Gramberg T, Hofmann H, Moller P, Lalor PF, Marzi A, Geier M et al.: LSECtin interacts with filovirus glycoproteins and the spike protein of SARS coronavirus. Virol 340:224-236, 2005.
225 Jeffers SA, Tusell SM, Gillim-Ross L, Hemmila EM, Achenbach JE, Babcock GJ et al.: CD209L (L-SIGN) is a receptor for severe acute respiratory syndrome coronavirus. Proc Natl Acad Sci U S A 101:15748-15753, 2004.

226 Marzi A, Gramberg T, Simmons G, Moller P, Rennekamp AJ, Krumbiegel M et al.: DC-SIGN and DC-SIGNR interact with the glycoprotein of Marburg virus and the S protein of severe acute respiratory syndrome coronavirus. J Virol 78:12090-12095, 2004.
227 Huang IC, Bosch BJ, Li F, Li W, Lee KH, Ghiran S et al.: SARS coronavirus, but not human coronavirus NL63, utilizes cathepsin L to infect ACE2-expressing cells. J Biol Chem 281:3198-3203, 2006.
228 Spruth M, Kistner O, Savidis-Dacho H, Hitter E, Crowe B, Gerencer M et al.: A double-inactivated whole virus candidate SARS coronavirus vaccine stimulates neutralising and protective antibody responses. Vaccine 24:652-661, 2006.
229 Stadler K, Roberts A, Becker S, Vogel L, Eickmann M, Kolesnikova L et al.: SARS vaccine protective in mice. Emerg Infect Dis 11:1312-1314, 2005.
230 Zhou J, Wang W, Zhong Q, Hou W, Yang Z, Xiao SY et al.: Immunogenicity, safety, and protective efficacy of an inactivated SARS-associated coronavirus vaccine in rhesus monkeys. Vaccine 23:3202-3209, 2005.
231 Song HC, Seo MY, Stadler K, Yoo BJ, Choo QL, Coates SR et al.: Synthesis and characterization of a native, oligomeric form of recombinant severe acute respiratory syndrome coronavirus spike glycoprotein. J Virol 78:10328-10335, 2004.
232 Pogrebnyak N, Golovkin M, Andrianov V, Spitsin S, Smirnov Y, Egolf R et al.: Severe acute respiratory syndrome (SARS) S protein production in plants: development of recombinant vaccine. Proc Natl Acad Sci U S A 102:9062-9067, 2005.
233 Bisht H, Roberts A, Vogel L, Subbarao K, Moss B: Neutralizing antibody and protective immunity to SARS coronavirus infection of mice induced by a soluble recombinant polypeptide containing an N-terminal segment of the spike glycoprotein. Virol 334:160-165, 2005.
234 Kam YW, Kien F, Roberts A, Cheung YC, Lamirande EW, Vogel L et al.: Antibodies against trimeric S glycoprotein protect hamsters against SARS-CoV challenge despite their capacity to mediate FcgammaRII-dependent entry into B cells in vitro. Vaccine 25:729-740, 2007.
235 Hu MC, Jones T, Kenney RT, Barnard DL, Burt DS, Lowell GH: Intranasal Protollin-formulated recombinant SARS S-protein elicits respiratory and serum neutralizing antibodies and protection in mice. Vaccine 25:6334-6340, 2007.
236 Kong WP, Xu L, Stadler K, Ulmer JB, Abrignani S, Rappuoli R et al.: Modulation of the immune response to the severe acute respiratory syndrome spike glycoprotein by gene-based and inactivated virus immunization. J Virol 79:13915-13923, 2005.
237 Finney DJ: The Spearman-Karber method. In: Statistical Methods in Biological Assay, ed. Finney DJ, pp. 524-530. Charles Griffin, London, 1964.
238 van den Brand JM, Haagmans BL, Leijten L, van Riel D, Martina BE, Osterhaus AD et al.: Pathology of experimental SARS coronavirus infection in cats and ferrets. Vet Pathol 45:551-562, 2008.
239 Liu L, Wei Q, Alvarez X, Wang H, Du Y, Zhu H et al.: Epithelial cells lining salivary gland ducts are early target cells of severe acute respiratory syndrome coronavirus infection in the upper respiratory tracts of rhesus macaques. J Virol 85:4025-4030, 2011.
240 Deming D, Sheahan T, Heise M, Yount B, Davis N, Sims A et al.: Vaccine efficacy in senescent mice challenged with recombinant SARS-CoV bearing epidemic and zoonotic spike variants. PLoS Med 3:e525, 2006.
241 Du L, Zhao G, Lin Y, Sui H, Chan C, Ma S et al.: Intranasal vaccination of recombinant adeno-associated virus encoding receptor-binding domain of severe acute respiratory syndrome coronavirus (SARS-CoV) spike protein induces strong mucosal immune responses and provides long-term protection against SARS-CoV infection. J Immunol 180:948-956, 2008.
242 Selin LK, Cornberg M, Brehm MA, Kim SK, Calcagno C, Ghersi D et al.: CD8 memory T cells: cross-reactivity and heterologous immunity. Semin Immunol 16:335-347, 2004.
243 Subbarao K, McAuliffe J, Vogel L, Fahle G, Fischer S, Tatti K et al.: Prior infection and passive transfer of neutralizing antibody prevent replication of severe acute respiratory syndrome coronavirus in the respiratory tract of mice. J Virol 78:3572-3577, 2004.
244 Sui J, Li W, Roberts A, Matthews LJ, Murakami A, Vogel L et al.: Evaluation of human monoclonal antibody 80R for immunoprophylaxis of severe acute respiratory syndrome by an animal study, epitope mapping, and analysis of spike variants. J Virol 79:5900-5906, 2005.
245 Traggiai E, Becker S, Subbarao K, Kolesnikova L, Uematsu Y, Gismondo MR et al.: An efficient method to make human monoclonal antibodies from memory B cells: potent neutralization of SARS coronavirus. Nat Med 10:871-875, 2004.

246 Sui J, Li W, Murakami A, Tamin A, Matthews LJ, Wong SK et al.: Potent neutralization of severe acute respiratory syndrome (SARS) coronavirus by a human mAb to S1 protein that blocks receptor association. Proc Natl Acad Sci U S A 101:2536-2541, 2004.
247 Zhong NS, Zheng BJ, Li YM, Poon, Xie ZH, Chan KH et al.: Epidemiology and cause of severe acute respiratory syndrome (SARS) in Guangdong, People's Republic of China, in February, 2003. Lancet 362:1353-1358, 2003.
248 Lip KM, Shen S, Yang X, Keng CT, Zhang A, Oh HL et al.: Monoclonal antibodies targeting the HR2 domain and the region immediately upstream of the HR2 of the S protein neutralize in vitro infection of severe acute respiratory syndrome coronavirus. J Virol 80:941-950, 2006.
249 Keng CT, Zhang A, Shen S, Lip KM, Fielding BC, Tan TH et al.: Amino acids 1055 to 1192 in the S2 region of severe acute respiratory syndrome coronavirus S protein induce neutralizing antibodies: implications for the development of vaccines and antiviral agents. J Virol 79:3289-3296, 2005.
250 Zhang GQ, Gu CD, Zhu YQ, Wang LY, Liu P: [Comparison between two methods of acute physiology and chronic health evaluation III and acute lung injury scale to evaluate the severity and prognosis of severe acute respiratory syndrome.]. Zhonghua Liu Xing Bing Xue Za Zhi 25:802-804, 2004.
251 Yasui F, Kai C, Kitabatake M, Inoue S, Yoneda M, Yokochi S et al.: Prior immunization with severe acute respiratory syndrome (SARS)-associated coronavirus (SARS-CoV) nucleocapsid protein causes severe pneumonia in mice infected with SARS-CoV. J Immunol 181:6337-6348, 2008.
252 Lin JT, Zhang JS, Su N, Xu JG, Wang N, Chen JT et al.: Safety and immunogenicity from a phase I trial of inactivated severe acute respiratory syndrome coronavirus vaccine. Antivir Ther 12:1107-1113, 2007.
253 He Y, Li J, Du L, Yan X, Hu G, Zhou Y et al.: Identification and characterization of novel neutralizing epitopes in the receptor-binding domain of SARS-CoV spike protein: revealing the critical antigenic determinants in inactivated SARS-CoV vaccine. Vaccine 24:5498-5508, 2006.
254 Lien SP, Shih YP, Chen HW, Tsai JP, Leng CH, Lin MH et al.: Identification of synthetic vaccine candidates against SARS CoV infection. Biochem Biophys Res Commun 358:716-721, 2007.
255 Rockx B, Donaldson E, Frieman M, Sheahan T, Corti D, Lanzavecchia A et al.: Escape from human monoclonal antibody neutralization affects in vitro and in vivo fitness of severe acute respiratory syndrome coronavirus. J Infect Dis 201:946-955, 2010.
256 World Health Organization: Influenza A(H1N1) - update 43. www.who.int/csr/don/2009_06_03/en/print.html. Assessed 3-6-2009.
257 Kuiken T, van den Hoogen BG, van Riel DA, Laman JD, van Amerongen G, Sprong L et al.: Experimental human metapneumovirus infection of cynomolgus macaques (Macaca fascicularis) results in virus replication in ciliated epithelial cells and pneumocytes with associated lesions throughout the respiratory tract. Am J Pathol 164:1893-1900, 2004.
258 Baskin CR, Bielefeldt-Ohmann H, Tumpey TM, Sabourin PJ, Long JP, Garcia-Sastre A et al.: Early and sustained innate immune response defines pathology and death in nonhuman primates infected by highly pathogenic influenza virus. Proc Natl Acad Sci U S A 106:3455-3460, 2009.
259 Rimmelzwaan GF, Kuiken T, van Amerongen G, Bestebroer TM, Fouchier RAM, Osterhaus ADME: Pathogenesis of influenza A (H5N1) virus infection in a primate model. J Virol 75:6687-6691, 2001.
260 Kobasa D, Takada A, Shinya K, Hatta M, Halfmann P, Theriault S et al.: Enhanced virulence of influenza A viruses with the haemagglutinin of the 1918 pandemic virus. Nature 431:703-707, 2004.
261 Fouchier RA, Bestebroer TM, Herfst S, Van Der Kemp L, Rimmelzwaan GF, Osterhaus AD: Detection of influenza A viruses from different species by PCR amplification of conserved sequences in the matrix gene. J Clin Microbiol 38:4096-4101, 2000.
262 Karber G: Beitrag zur kollektiven behandlung pharmakologischer reihenversuche. Exp Pathol pharmakol 162:480-483, 1931.
263 Fornek JL, Korth MJ, Katze MG: Use of functional genomics to understand influenza-host interactions. Adv Virus Res 70:81-100, 2007.
264 Itoh Y, Shinya K, Kiso M, Watanabe T, Sakoda Y, Hatta M et al.: In vitro and in vivo characterization of new swine-origin H1N1 influenza viruses. Nature 460:1021-1025, 2009.
265 Pham I, Uchida T, Planes C, Ware LB, Kaner R, Matthay MA et al.: Hypoxia upregulates VEGF expression in alveolar epithelial cells in vitro and in vivo. Am J Physiol Lung Cell Mol Physiol 283:L1133-L1142, 2002.
266 Childs RA, Palma AS, Wharton S, Matrosovich T, Liu Y, Chai W et al.: Receptor-binding specificity of pandemic influenza A (H1N1) 2009 virus determined by carbohydrate microarray. Nat Biotechnol 27:797-799, 2009.

267 Kobasa D, Jones SM, Shinya K, Kash JC, Copps J, Ebihara H et al.: Aberrant innate immune response in lethal infection of macaques with the 1918 influenza virus. Nature 445:319-323, 2007.
268 Dawood FS, Jain S, Finelli L, Shaw MW, Lindstrom S, Garten RJ et al.: Emergence of a novel swine-origin influenza A (H1N1) virus in humans. N Engl J Med 360:2605-2615, 2009.
269 Outbreak of swine-origin influenza A (H1N1) virus infection - Mexico, March-April 2009 MMWR Morb Mortal Wkly Rep 58:467-470, 2009.
270 Olson DR, Simonsen L, Edelson PJ, Morse SS: Epidemiological evidence of an early wave of the 1918 influenza pandemic in New York City. Proc Natl Acad Sci U S A 102:11059-11063, 2005.
271 Trifonov V, Khiabanian H, Rabadan R: Geographic Dependence, Surveillance, and Origins of the 2009 Influenza A (H1N1) Virus. N Engl J Med 361:115-119, 2009.
272 Chan, M.: Influenza A (H1N1). www.who.int/mediacentre/news/statements/2009/h1n1_20090429/en/print.html. Assessed 3-6-0009.
273 Morens DM, Taubenberger JK, Fauci AS: The predominant role of bacterial pneumonia as a cause of death in influenza pandemics: Implications for pandemic influenza preparedness. J Infect Dis 198:962-970, 2008.
274 Comision Nacional de Arbitraje Medico: Preliminary findings of clinical characterization of dead patients with confirmed diagnosis by the new influenza A (H1N1) occurred in Mexico. http://new.paho.org/hq/index.php?option=com_frontpage&Itemid=1&lang=en. Assessed 3-6-2009.
275 Fraser C, Donnelly CA, Cauchemez S, Hanage WP, Van Kerkhove MD, Hollingsworth TD et al.: Pandemic Potential of a Strain of Influenza A (H1N1) : Early Findings. Science 324:1557-1561, 2009.
276 Hayden F, Croisier A: Transmission of avian influenza viruses to and between humans. J Infect Dis 192:1311-1314, 2005.
277 Baras B, Stittelaar KJ, Simon JH, Thoolen RJ, Mossman SP, Pistoor FH et al.: Cross-protection against lethal H5N1 challenge in ferrets with an adjuvanted pandemic influenza vaccine. PLoS ONE 3:e1401-doi:10.1371/journal.pone.0001401, 2008.
278 Stittelaar KJ, Tisdale M, van Amerongen G, van Lavieren RF, Pistoor F, Simon J et al.: Evaluation of intravenous zanamivir against experimental influenza A (H5N1) virus infection in cynomolgus macaques. Antiviral Res 80:225-228, 2008.
279 Rimmelzwaan GF, Baars M, Claas ECJ, Osterhaus ADME: Comparison of RNA hybridization, hemagglutination assay, titration of infectious virus and immunofluorescence as methods for monitoring influenza virus replication in vitro. Journal of Virological Methods 74:57-66, 1998.
280 Govorkova EA, Rehg JE, Krauss S, Yen HL, Guan Y, Peiris M et al.: Lethality to ferrets of H5N1 influenza viruses isolated from humans and poultry in 2004. J Virol 79:2191-2198, 2005.
281 Zitzow LA, Rowe T, Morken T, Shieh WJ, Zaki S, Katz JM: Pathogenesis of avian influenza A (H5N1) viruses in ferrets. J Virol 76:4420-4429, 2002.
282 Maines TR, Jayaraman A, Belser JA, Wadford DA, Pappas C, Zeng H et al.: Transmission and pathogenesis of swine-origin 2009 A(H1N1) influenza viruses in ferrets and mice. Science 325:484-487, 2009.
283 Maher JA, DeStefano J: The ferret: an animal model to study influenza virus. Lab Anim (NY) 33:50-53, 2004.
284 Sponseller BA, Strait E, Jergens A, Trujillo J, Harmon K, Koster L et al.: Influenza A pandemic (H1N1) 2009 virus infection in domestic cat. Emerg Infect Dis 16:534-537, 2010.
285 Lohr CV, DeBess EE, Baker RJ, Hiett SL, Hoffman KA, Murdoch VJ et al.: Pathology and viral antigen distribution of lethal pneumonia in domestic cats due to pandemic (H1N1) 2009 influenza A virus. Vet Pathol 47:378-386, 2010.
286 Keawcharoen J, Oraveerakul K, Kuiken T, Fouchier RA, Amonsin A, Payungporn S et al.: Avian influenza H5N1 in tigers and leopards. Emerg Infect Dis 10:2189-2191, 2004.
287 Desvaux S, Marx N, Ong S, Gaidet N, Hunt M, Manuguerra JC et al.: Highly pathogenic avian influenza virus (H5N1) outbreak in captive wild birds and cats, Cambodia. Emerg Infect Dis 15:475-478, 2009.
288 Kuiken T, Rimmelzwaan G, van Riel D, van Amerongen G, Baars M, Fouchier R et al.: Avian H5N1 influenza in cats. Science 306:241, 2004.
289 Palmer DF, Dowdle WR, Coleman MT, Schild GC: Haemagglutination inhibition test. In: Advanced laboratory techniques for influenza diagnosis. Procedural guide, pp. 25-62. Department of Health and Welfare, Atlanta, 1975.
290 World Health Organization: Influenza (Seasonal). Fact sheet No 211. http://www.who.int/mediacentre/factsheets/fs211/en/index.html.
291 Svitek N, Rudd PA, Obojes K, Pillet S, von M, V: Severe seasonal influenza in ferrets correlates with reduced

interferon and increased IL-6 induction. Virol 376:53-59, 2008.
292 van den Brand JM, Stittelaar KJ, van Amerongen G, Rimmelzwaan GF, Simon J, de Wit E et al.: Severity of pneumonia due to new H1N1 influenza virus in ferrets is intermediate between that due to seasonal H1N1 virus and highly pathogenic avian influenza H5N1 virus. J Infect Dis 201:993-999, 2010.
293 Herfst S, van den Brand JM, Schrauwen EJ, de Wit E, Munster VJ, van Amerongen G et al.: Pandemic 2009 H1N1 influenza virus causes diffuse alveolar damage in Cynomolgus Macaques. Vet Pathol 47:1040-1047, 2010.
294 Bodewes R: Pathogenesis of Influenza A/H5N1 virus infection in ferrets differs between intranasal and intratracheal routes of inoculation. Am J Pathol 179:30-36, 2011.
295 van den Brand JM, Kreijtz JH, Bodewes R, Stittelaar KJ, van Amerongen G, Kuiken T et al.: Efficacy of vaccination with different combinations of MF59-adjuvanted and non-adjuvanted seasonal and pandemic influenza vaccines against pandemic H1N1 (2009) influenza in ferrets. J Virol 85:2851-2858, 2011.
296 Guarner J, Shieh WJ, Dawson J, Subbarao K, Shaw M, Ferebee T et al.: Immunohistochemical and in situ hybridization studies of influenza A virus infection in human lungs. Am J Clin Pathol 114:227-233, 2000.
297 Kuiken T, van den Brand JM, van Riel D, Pantin-Jackwood M, Swayne DE: Comparative pathology of select agent influenza a virus infections. Vet Pathol 47:893-914, 2010.
298 WHO: Number of human H5N1 cases. http://www.who.int/influenza/human_animal_interface/EN_GIP_20120405CumulativeNumberH5N1cases.pdf. Assessed 6-4-2012.
299 Maines TR, Belser JA, Gustin KM, Van Hoeven N, Zeng H, Svitek N et al.: Local innate immune responses and influenza virus transmission and virulence in ferrets. J Infect Dis 205:474-485, 2012.
300 Belser JA, Gustin KM, Maines TR, Blau DM, Zaki SR, Katz JM et al.: Pathogenesis and transmission of triple-reassortant swine H1N1 influenza viruses isolated before the 2009 H1N1 pandemic. J Virol 85:1563-1572, 2011.
301 Rowe T, Leon AJ, Crevar CJ, Carter DM, Xu L, Ran L et al.: Modeling host responses in ferrets during A/California/07/2009 influenza infection. Virol 401:257-265, 2010.
302 McBrayer A, Camp JV, Tapp R, Yamshchikov V, Grimes S, Noah DL et al.: Course of seasonal influenza A/Brisbane/59/07 H1N1 infection in the ferret. Virol J 7:149-doi: 10.1186/1743-422X-7-1492010.
303 Smith JH, Nagy T, Driskell E, Brooks P, Tompkins SM, Tripp RA: Comparative pathology in ferrets infected with H1N1 influenza A viruses isolated from different hosts. J Virol 85:7572-7581, 2011.
304 Meunier I, Embury-Hyatt C, Stebner S, Gray M, Bastien N, Li Y et al.: Virulence differences of closely related pandemic 2009 H1N1 isolates correlate with increased inflammatory responses in ferrets. Virol 422:125-131, 2012.
305 van den Brand JM, Stittelaar KJ, Leijten LM, van Amerongen G, Simon JH, Osterhaus AD et al.: Modification of the Ferret Model for Pneumonia From Seasonal Human Influenza a Virus Infection. Vet Pathol 49:562-568, 2012.
306 Lin YP, Gregory V, Collins P, Kloess J, Wharton S, Cattle N et al.: Neuraminidase receptor binding variants of human influenza A(H3N2) viruses resulting from substitution of aspartic acid 151 in the catalytic site: a role in virus attachment? J Virol 84:6769-6781, 2010.
307 Baras B, de Waal L, Stittelaar KJ, Jacob V, Giannini S, Kroeze EJ et al.: Pandemic H1N1 vaccine requires the use of an adjuvant to protect against challenge in naive ferrets. Vaccine 29:2120-2126, 2011.
308 Bodewes R, Kreijtz JH, van Amerongen G, Fouchier RA, Osterhaus AD, Rimmelzwaan GF et al.: Pathogenesis of Influenza A/H5N1 virus infection in ferrets differs between intranasal and intratracheal routes of inoculation. Am J Pathol 179:30-36, 2011.
309 Dellmann HD: Textbook of veterinary histology. 4 ed., pp. 56-149. Lea & Febiger, Philadelphia, 1993.
310 Kuiken T, Rimmelzwaan G, van Riel D, van Amerongen G, Baars M, Fouchier R et al.: Avian H5N1 influenza in cats. Science 306:241, 2004.
311 Benne CA, Kraaijeveld CA, van Strijp JA, Brouwer E, Harmsen M, Verhoef J et al.: Interactions of surfactant protein A with influenza A viruses: binding and neutralization. J Infect Dis 171:335-341, 1995.
312 Berthiaume Y, Matthay MA: Alveolar edema fluid clearance and acute lung injury. Respir Physiol Neurobiol 159:350-359, 2007.
313 Folkesson HG, Nitenberg G, Oliver BL, Jayr C, Albertine KH, Matthay MA: Upregulation of alveolar epithelial fluid transport after subacute lung injury in rats from bleomycin. Am J Physiol 275:L478-L490, 1998.
314 Karpuzoglu E, Ahmed SA: Estrogen regulation of nitric oxide and inducible nitric oxide synthase (iNOS) in immune cells: implications for immunity, autoimmune diseases, and apoptosis. Nitric Oxide 15:177-186, 2006.

315 Teijaro JR, Walsh KB, Cahalan S, Fremgen DM, Roberts E, Scott F et al.: Endothelial cells are central orchestrators of cytokine amplification during influenza virus infection. Cell 146:980-991, 2011.
316 Maines TR, Lu XH, Erb SM, Edwards L, Guarner J, Greer PW et al.: Avian influenza (H5N1) viruses isolated from humans in Asia in 2004 exhibit increased virulence in mammals. J Virol 79:11788-11800, 2005.
317 Yen HL, Lipatov AS, Ilyushina NA, Govorkova EA, Franks J, Yilmaz N et al.: Inefficient transmission of H5N1 influenza viruses in a ferret contact model. J Virol 81:6890-6898, 2007.
318 Tumpey TM, Lu X, Morken T, Zaki SR, Katz JM: Depletion of lymphocytes and diminished cytokine production in mice infected with a highly virulent influenza A (H5N1) virus isolated from humans. J Virol 74:6105-6116, 2000.
319 Schrauwen EJ, Herfst S, Leijten LM, van Run P, Bestebroer TM, Linster M et al.: The Multibasic Cleavage Site in H5N1 Virus Is Critical for Systemic Spread along the Olfactory and Hematogenous Routes in Ferrets. J Virol 86:3975-3984, 2012.
320 Pandemic (H1N1) 2009 - update 97. http://www.who.int/csr/don/2010_04_23a/en/index.html. Assessed 28-4-2010.
321 Fiore AE, Shay DK, Broder K, Iskander JK, Uyeki TM, Mootrey G et al.: Prevention and control of seasonal influenza with vaccines: recommendations of the Advisory Committee on Immunization Practices (ACIP), 2009. MMWR Recomm Rep 58:1-52, 2009.
322 Serum cross-reactive antibody response to a novel influenza A (H1N1) virus after vaccination with seasonal influenza vaccine MMWR Morb Mortal Wkly Rep 58:521-524, 2009.
323 Hancock K, Veguilla V, Lu X, Zhong W, Butler EN, Sun H et al.: Cross-reactive antibody responses to the 2009 pandemic H1N1 influenza virus. N Engl J Med 361:1945-1952, 2009.
324 Carrat F, Flahault A: Influenza vaccine: the challenge of antigenic drift. Vaccine 25:6852-6862, 2007.
325 Nichol KL: The efficacy, effectiveness and cost-effectiveness of inactivated influenza virus vaccines. Vaccine 21:1769-1775, 2003.
326 Durando P, Icardi G, Ansaldi F: MF59-adjuvanted vaccine: a safe and useful tool to enhance and broaden protection against seasonal influenza viruses in subjects at risk. Expert Opin Biol Ther 10:639-651, 2010.
327 Nicholson KG, Colegate AE, Podda A, Stephenson I, Wood J, Ypma E et al.: Safety and antigenicity of non-adjuvanted and MF59-adjuvanted influenza A/Duck/Singapore/97 (H5N3) vaccine: a randomised trial of two potential vaccines against H5N1 influenza. Lancet 357:1937-1943, 2001.
328 O'Hagan DT, Wack A, Podda A: MF59 is a safe and potent vaccine adjuvant for flu vaccines in humans: what did we learn during its development? Clin Pharmacol Ther 82:740-744, 2007.
329 Stephenson I, Bugarini R, Nicholson KG, Podda A, Wood JM, Zambon MC et al.: Cross-reactivity to highly pathogenic avian influenza H5N1 viruses after vaccination with nonadjuvanted and MF59-adjuvanted influenza A/Duck/Singapore/97 (H5N3) vaccine: a potential priming strategy. J Infect Dis 191:1210-1215, 2005.
330 Khurana S, Chearwae W, Castellino F, Manischewitz J, King LR, Honorkiewicz A et al.: Vaccines with MF59 adjuvant expand the antibody repertoire to target protective sites of pandemic avian H5N1 influenza virus. Sci Transl Med 2:15ra5, 2010.
331 Clark TW, Pareek M, Hoschler K, Dillon H, Nicholson KG, Groth N et al.: Trial of 2009 influenza A (H1N1) monovalent MF59-adjuvanted vaccine. N Engl J Med 361:2424-2435, 2009.
332 Del Giudice G, Stittelaar KJ, van Amerongen G, Simon J, Osterhaus AD, Stohr K et al.: Seasonal influenza vaccine provides priming for A/H1N1 immunization. Sci Transl Med 1:12re1, 2009.
333 Ansaldi F, Bacilieri S, Durando P, Sticchi L, Valle L, Montomoli E et al.: Cross-protection by MF59-adjuvanted influenza vaccine: neutralizing and haemagglutination-inhibiting antibody activity against A(H3N2) drifted influenza viruses. Vaccine 26:1525-1529, 2008.
334 Ansaldi F, Zancolli M, Durando P, Montomoli E, Sticchi L, Del Giudice G et al.: Antibody response against heterogeneous circulating influenza virus strains elicited by. Vaccine 28:4123-4129, 2010.
335 Forrest HL, Khalenkov AM, Govorkova EA, Kim JK, Del Giudice G, Webster RG: Single- and multiple-clade influenza A H5N1 vaccines induce cross protection in ferrets. Vaccine 27:4187-4195, 2009.
336 Igarashi M, Ito K, Yoshida R, Tomabechi D, Kida H, Takada A: Predicting the antigenic structure of the pandemic (H1N1) 2009 influenza virus hemagglutinin. PLoS ONE 5:e8553, 2010.
337 Frank AL, Puck J, Hughes BJ, Cate TR: Microneutralization test for influenza A and B and parainfluenza 1 and 2 viruses that uses continuous cell lines and fresh serum enhancement. J Clin Microbiol 12:426-432, 1980.

338 Rimmelzwaan GF, de Jong JC, Bestebroer TM, van Loon AM, Claas EC, Fouchier RA et al.: Antigenic and genetic characterization of swine influenza A (H1N1) viruses isolated from pneumonia patients in The Netherlands. Virol 282:301-306, 2001.
339 Galli G, Hancock K, Hoschler K, DeVos J, Praus M, Bardelli M et al.: Fast rise of broadly cross-reactive antibodies after boosting long-lived human memory B cells primed by an MF59 adjuvanted prepandemic vaccine. Proc Natl Acad Sci U S A 106:7962-7967, 2009.
340 Bosch BJ, Bodewes R, de Vries RP, Kreijtz JH, Bartelink W, van Amerongen G et al.: Recombinant soluble, multimeric HA and NA exhibit distinctive types of protection against pandemic swine-origin 2009 A(H1N1) influenza virus infection in ferrets. J Virol 84:10366-10374, 2010.
341 Webb SA, Seppelt IM: Pandemic (H1N1) 2009 influenza ("swine flu") in Australian and New Zealand intensive care. Crit Care Resusc 11:170-172, 2009.
342 Skowronski DM, De Serres G, Crowcroft NS, Janjua NZ, Boulianne N, Hottes TS et al.: Association between the 2008-09 seasonal influenza vaccine and pandemic H1N1 illness during Spring-Summer 2009: four observational studies from Canada. PLoS Med 7:e1000258, 2010.
343 Smits SL, van den Brand JM, de Lang A, Leijten LM, van Ijcken WF, van Amerongen G et al.: Distinct severe acute respiratory syndrome coronavirus-induced acute lung injury pathways in two different nonhuman primate species. J Virol 85:4234-4245, 2011.
344 Theron M, Huang KJ, Chen YW, Liu CC, Lei HY: A probable role for IFN-gamma in the development of a lung immunopathology in SARS. Cytokine 32:30-38, 2005.
345 Coulter KR, Doseff A, Sweeney P, Wang Y, Marsh CB, Wewers MD et al.: Opposing effect by cytokines on Fas-mediated apoptosis in A549 lung epithelial cells. Am J Respir Cell Mol Biol 26:58-66, 2002.
346 Tanaka T, Yoshimi M, Maeyama T, Hagimoto N, Kuwano K, Hara N: Resistance to Fas-mediated apoptosis in human lung fibroblast. Eur Respir J 20:359-368, 2002.
347 Lau YL, Peiris JS: Pathogenesis of severe acute respiratory syndrome. Curr Opin Immunol 17:404-410, 2005.
348 Ng ML, Tan SH, See EE, Ooi EE, Ling AE: Proliferative growth of SARS coronavirus in Vero E6 cells. J Gen Virol 84:3291-3303, 2003.
349 Zhou J, Law HK, Cheung CY, Ng IH, Peiris JS, Lau YL: Functional tumor necrosis factor-related apoptosis-inducing ligand production by avian influenza virus-infected macrophages. J Infect Dis 193:945-953, 2006.
350 Ksiazek TG, Erdman D, Goldsmith CS, Zaki SR, Peret T, Emery S et al.: A novel coronavirus associated with severe acute respiratory syndrome. N Engl J Med 348:1953-1966, 2003.
351 Chu YK, Ali GD, Jia F, Li Q, Kelvin D, Couch RC et al.: The SARS-CoV ferret model in an infection-challenge study. Virol 374:151-163, 2008.
352 Weber F, Kochs G, Haller O: Inverse interference: how viruses fight the interferon system. Viral Immunol 17:498-515, 2004.
353 Loutfy MR, Blatt LM, Siminovitch KA, Ward S, Wolff B, Lho H et al.: Interferon alfacon-1 plus corticosteroids in severe acute respiratory syndrome: a preliminary study. JAMA 290:3222-3228, 2003.
354 Chan-Yeung M, Xu RH: SARS: epidemiology. Respirology 8 Suppl:S9-14, 2003.
355 Liu M, Liang WN, Chen Q, Xie XQ, Wu J, He X et al.: Risk factors for SARS-related deaths in 2003, Beijing. Biomed Environ Sci 19:336-339, 2006.
356 Rockx B, Feldmann F, Brining D, Gardner D, LaCasse R, Kercher L et al.: Comparative pathogenesis of three human and zoonotic SARS-CoV strains in cynomolgus macaques. PLoS ONE 6:e18558, 2011.
357 Chung HY, Sung B, Jung KJ, Zou Y, Yu BP: The molecular inflammatory process in aging. Antioxid Redox Signal 8:572-581, 2006.
358 De Swart RL, Kuiken T, Timmerman HH, van Amerongen G, van den Hoogen BG, Vos HW et al.: Immunization of macaques with formalin-inactivated respiratory syncytial virus (RSV) induces interleukin-13-associated hypersensitivity to subsequent RSV infection. J Virol 76:11561-11569, 2002.
359 Green S, Rothman A: Immunopathological mechanisms in dengue and dengue hemorrhagic fever. Curr Opin Infect Dis 19:429-436, 2006.
360 Huisman W, Martina BE, Rimmelzwaan GF, Gruters RA, Osterhaus AD: Vaccine-induced enhancement of viral infections. Vaccine 27:505-512, 2009.
361 Smith H, Sweet C: Lessons for human influenza from pathogenicity studies with ferrets. Rev Infect Dis 10:56-75, 1988.
362 Olsen CW, Corapi WV, Ngichabe CK, Baines JD, Scott FW: Monoclonal antibodies to the spike protein of feline infectious peritonitis virus mediate antibody-dependent enhancement of infection of feline

macrophages. J Virol 66:956-965, 1992.
363 Rowe T, Cho DS, Bright RA, Zitzow LA, Katz JM: Neurological manifestations of avian influenza viruses in mammals. Avian Dis 47:1122-1126, 2003.
364 Govorkova EA, Rehg JE, Krauss S, Yen HL, Guan Y, Peiris M et al.: Lethality to ferrets of H5N1 influenza viruses isolated from humans and poultry in 2004. J Virol 79:2191-2198, 2005.
365 Cameron CM, Cameron MJ, Bermejo-Martin JF, Ran L, Xu L, Turner PV et al.: Gene expression analysis of host innate immune responses during lethal H5N1 infection in ferrets. J Virol 82:11308-11317, 2008.
366 Yen HL, Lipatov AS, Ilyushina NA, Govorkova EA, Franks J, Yilmaz N et al.: Inefficient transmission of H5N1 influenza viruses in a ferret contact model. J Virol 81:6890-6898, 2007.
367 Boltz DA, Rehg JE, McClaren J, Webster RG, Govorkova EA: Oseltamivir prophylactic regimens prevent H5N1 influenza morbidity and mortality in a ferret model. J Infect Dis 197:1315-1323, 2008.
368 Rogers GN, Paulson JC, Daniels RS, Skehel JJ, Wilson IA, Wiley DC: Single amino acid substitutions in influenza haemagglutinin change receptor binding specificity. Nature 304:76-78, 1983.
369 Nicholls JM, Chan MCW, Chan WY, Wong HK, Cheung CY, Kwong DL et al.: Tropism of avian influenza A (H5N1) in the upper and lower respiratory tract. Nat Med 13:147-149, 2007.
370 Hien TT, de Jong M, Farrar J: Avian influenza--a challenge to global health care structures. N Engl J Med 351:2363-2365, 2004.
371 Lowy RJ: Influenza virus induction of apoptosis by intrinsic and extrinsic mechanisms. Int Rev Immunol 22:425-449, 2003.
372 Herold S, Steinmueller M, von Wulffen W, Cakarova L, Pinto R, Pleschka S et al.: Lung epithelial apoptosis in influenza virus pneumonia: the role of macrophage-expressed TNF-related apoptosis-inducing ligand. J Exp Med 205:3065-3077, 2008.
373 Takizawa T, Matsukawa S, Higuchi Y, Nakamura S, Nakanishi Y, Fukuda R: Induction of programmed cell death (apoptosis) by influenza virus infection in tissue culture cells. J Gen Virol 74 (Pt 11):2347-2355, 1993.
374 Yuen KY, Chan PK, Peiris M, Tsang DN, Que TL, Shortridge KF et al.: Clinical features and rapid viral diagnosis of human disease associated with avian influenza A H5N1 virus. Lancet 351:467-471, 1998.
375 Perez-Padilla R, Rosa-Zamboni D, Ponce dL, Hernandez M, Quinones-Falconi F, Bautista E et al.: Pneumonia and respiratory failure from swine-origin influenza A (H1N1) in Mexico. N Engl J Med 361:680-689, 2009.
376 Hien ND, Ha NH, Van NT, Ha NT, Lien TT, Thai NQ et al.: Human infection with highly pathogenic avian influenza virus (H5N1) in northern Vietnam, 2004-2005. Emerg Infect Dis 15:19-23, 2009.
377 Viemann D, Schmolke M, Lueken A, Boergeling Y, Friesenhagen J, Wittkowski H et al.: H5N1 virus activates signaling pathways in human endothelial cells resulting in a specific imbalanced inflammatory response. J Immunol 186:164-173, 2011.
378 van Riel D, Leijten LM, van der EM, Hoogsteden HC, Boven LA, Lambrecht BN et al.: Highly pathogenic avian influenza virus H5N1 infects alveolar macrophages without virus production or excessive TNF-alpha induction. PLoS Pathog 7:e1002099, 2011.
379 Morens DM, Fauci AS: The 1918 influenza pandemic: insights for the 21st century. J Infect Dis 195:1018-1028, 2007.
380 Peiris JS, de Jong MD, Guan Y: Avian influenza virus (H5N1): a threat to human health. Clin Microbiol Rev 20:243-267, 2007.
381 Galli G, Medini D, Borgogni E, Zedda L, Bardelli M, Malzone C et al.: Adjuvanted H5N1 vaccine induces early CD4+ T cell response that predicts long-term persistence of protective antibody levels. Proc Natl Acad Sci U S A 106:3877-3882, 2009.
382 Lau YF, Wright AR, Subbarao K: The contribution of systemic and pulmonary immune effectors to vaccine-induced protection from H5N1 influenza virus infection. J Virol 86:5089-5098, 2012.
383 Thiel V, Weber F: Interferon and cytokine responses to SARS-coronavirus infection. Cytokine Growth Factor Rev 19:121-132, 2008.
384 Kash JC, Basler CF, Garcia-Sastre A, Carter V, Billharz R, Swayne DE et al.: Global host immune response: pathogenesis and transcriptional profiling of type A influenza viruses expressing the hemagglutinin and neuraminidase genes from the 1918 pandemic virus. J Virol 78:9499-9511, 2004.
385 Kash JC, Tumpey TM, Proll SC, Carter V, Perwitasari O, Thomas MJ et al.: Genomic analysis of increased host immune and cell death responses induced by 1918 influenza virus. Nature 443:578-581, 2006.
386 Meyer KC: The role of immunity in susceptibility to respiratory infection in the aging lung. Respir Physiol 128:23-31, 2001.

387 Licastro F, Candore G, Lio D, Porcellini E, Colonna-Romano G, Franceschi C et al.: Innate immunity and inflammation in ageing: a key for understanding age-related diseases. Immun Ageing 2:8, 2005.
388 Meyer KC: Aging. Proc Am Thorac Soc 2:433-439, 2005.
389 Plackett TP, Boehmer ED, Faunce DE, Kovacs EJ: Aging and innate immune cells. J Leukoc Biol 76:291-299, 2004.
390 Murasko DM, Jiang J: Response of aged mice to primary virus infections. Immunol Rev 205:285-296, 2005.
391 Salvioli S, Capri M, Valensin S, Tieri P, Monti D, Ottaviani E et al.: Inflamm-aging, cytokines and aging: state of the art, new hypotheses on the role of mitochondria and new perspectives from systems biology. Curr Pharm Des 12:3161-3171, 2006.
392 Fulop T, Larbi A, Wikby A, Mocchegiani E, Hirokawa K, Pawelec G: Dysregulation of T-cell function in the elderly : scientific basis and clinical implications. Drugs Aging 22:589-603, 2005.
393 Johnston SL: Innate immunity in the pathogenesis of virus-induced asthma exacerbations. Proc Am Thorac Soc 4:267-270, 2007.
394 Holt PG, Upham JW, Sly PD: Contemporaneous maturation of immunologic and respiratory functions during early childhood: implications for development of asthma prevention strategies. J Allergy Clin Immunol 116:16-24, 2005.
395 Kong KF, Delroux K, Wang X, Qian F, Arjona A, Malawista SE et al.: Dysregulation of TLR3 impairs the innate immune response to West Nile virus in the elderly. J Virol 82:7613-7623, 2008.
396 Rink L, Cakman I, Kirchner H: Altered cytokine production in the elderly. Mech Ageing Dev 102:199-209, 1998.
397 Yoon P, Keylock KT, Hartman ME, Freund GG, Woods JA: Macrophage hypo-responsiveness to interferon-gamma in aged mice is associated with impaired signaling through Jak-STAT. Mech Ageing Dev 125:137-143, 2004.
398 Karnam G, Rygiel TP, Raaben M, Grinwis GC, Coenjaerts FE, Ressing ME et al.: CD200 Receptor Controls Sex-Specific TLR7 Responses to Viral Infection. PLoS Pathog 8:e1002710 2012.
399 Chutinimitkul S, Bhattarakosol P, Srisuratanon S, Eiamudomkan A, Kongsomboon K, Damrongwatanapokin S et al.: H5N1 influenza A virus and infected human plasma. Emerg Infect Dis 12:1041-1043, 2006.
400 Reperant LA, van de Bildt MW, van Amerongen G, Leijten LM, Watson S, Palser A et al.: Marked endotheliotropism of highly pathogenic avian influenza virus H5N1 following intestinal inoculation in cats. J Virol 86:1158-1165, 2012.
401 Cheng VC, Hung IF, Tang BS, Chu CM, Wong MM, Chan KH et al.: Viral replication in the nasopharynx is associated with diarrhea in patients with severe acute respiratory syndrome. Clin Infect Dis 38:467-475, 2004.
402 Lipatov AS, Krauss S, Guan Y, Peiris M, Rehg JE, Perez DR et al.: Neurovirulence in mice of H5N1 influenza virus genotypes isolated from Hong Kong poultry in 2001. J Virol 77:3816-3823, 2003.
403 Tanaka H, Park CH, Ninomiya A, Ozaki H, Takada A, Umemura T et al.: Neurotropism of the 1997 Hong Kong H5N1 influenza virus in mice. Vet Microbiol 95:1-13, 2003.
404 Morishima T, Togashi T, Yokota S, Okuno Y, Miyazaki C, Tashiro M et al.: Encephalitis and encephalopathy associated with an influenza epidemic in Japan. Clin Infect Dis 35:512-517, 2002.
405 Sugaya N: Influenza-associated encephalopathy in Japan. Semin Pediatr Infect Dis 13:79-84, 2002.
406 Hung IF, Cheng VC, Wu AK, Tang BS, Chan KH, Chu CM et al.: Viral loads in clinical specimens and SARS manifestations. Emerg Infect Dis 10:1550-1557, 2004.
407 Chu CM, Poon LL, Cheng VC, Chan KS, Hung IF, Wong MM et al.: Initial viral load and the outcomes of SARS. CMAJ 171:1349-1352, 2004.
408 Kim HW, Canchola JG, Brandt CD, Pyles G, Chanock RM, Jensen K et al.: Respiratory syncytial virus disease in infants despite prior administration of antigenic inactivated vaccine. Am J Epidemiol 89:422-434, 1969.
409 Hancock GE, Speelman DJ, Heers K, Bortell E, Smith J, Cosco C: Generation of atypical pulmonary inflammatory responses in BALB/c mice after immunization with the native attachment (G) glycoprotein of respiratory syncytial virus. J Virol 70:7783-7791, 1996.
410 Xiong S, Wang YF, Zhang MY, Liu XJ, Zhang CH, Liu SS et al.: Immunogenicity of SARS inactivated vaccine in BALB/c mice. Immunol Lett 95:139-143, 2004.
411 Zakhartchouk AN, Liu Q, Petric M, Babiuk LA: Augmentation of immune responses to SARS coronavirus by a combination of DNA and whole killed virus vaccines. Vaccine 23:4385-4391, 2005.

412 Takasuka N, Fujii H, Takahashi Y, Kasai M, Morikawa S, Itamura S et al.: A subcutaneously injected UV-inactivated SARS coronavirus vaccine elicits systemic humoral immunity in mice. Int Immunol 16:1423-1430, 2004.
413 Kim TW, Lee JH, Hung CF, Peng S, Roden R, Wang MC et al.: Generation and characterization of DNA vaccines targeting the nucleocapsid protein of severe acute respiratory syndrome coronavirus. J Virol 78:4638-4645, 2004.
414 Johnson TR, Varga SM, Braciale TJ, Graham BS: Vbeta14(+) T cells mediate the vaccine-enhanced disease induced by immunization with respiratory syncytial virus (RSV) G glycoprotein but not with formalin-inactivated RSV. J Virol 78:8753-8760, 2004.
415 Antonio GE, Wong KT, Chu WC, Hui DS, Cheng FW, Yuen EH et al.: Imaging in severe acute respiratory syndrome (SARS). Clin Radiol 58:825-832, 2003.
416 Bai L, Gu L, Cao B, Zhai XL, Lu M, Lu Y et al.: Clinical features of pneumonia caused by 2009 influenza A(H1N1) virus in Beijing, China. Chest 139:1156-1164, 2011.
417 Mineo G, Ciccarese F, Modolon C, Landini MP, Valentino M, Zompatori M: Post-ARDS pulmonary fibrosis in patients with H1N1 pneumonia: role of follow-up CT. Radiol Med 117:185-200, 2012.
418 Qiao J, Zhang M, Bi J, Wang X, Deng G, He G et al.: Pulmonary fibrosis induced by H5N1 viral infection in mice. Respir Res 10:107, 2009.
419 Nicholls JM, Butany J, Poon LL, Chan KH, Beh SL, Poutanen S et al.: Time course and cellular localization of SARS-CoV nucleoprotein and RNA in lungs from fatal cases of SARS. PLoS Med 3:e27, 2006.
420 Lawler JV, Endy TP, Hensley LE, Garrison A, Fritz EA, Lesar M et al.: Cynomolgus macaque as an animal model for severe acute respiratory syndrome. PLoS Med 3:e149, 2006.
421 Qin C, Wang J, Wei Q, She M, Marasco WA, Jiang H et al.: An animal model of SARS produced by infection of Macaca mulatta with SARS coronavirus. J Pathol 206:251-259, 2005.
422 Josset L, Engelmann F, Haberthur K, Kelly S, Park B, Kawoaka Y et al.: Increased viral loads and exacerbated innate host response in aged macaques infected with 2009 pandemic H1N1 influenza A virus. J Virol 86:11115-111127, 2012.
423 Kumar PA, Hu Y, Yamamoto Y, Hoe NB, Wei TS, Mu D et al.: Distal airway stem cells yield alveoli in vitro and during lung regeneration following H1N1 influenza infection. Cell 147:525-538, 2011.
424 Kuiken T, Leighton FA, Fouchier RA, LeDuc JW, Peiris JS, Schudel A et al.: Public health. Pathogen surveillance in animals. Science 309:1680-1681, 2005.
425 van den Brand JM, van Leeuwen M, Schapendonk CM, Simon JH, Haagmans BL, Osterhaus AD et al.: Metagenomic analysis of the viral flora of pine marten and European badger feces. J Virol 86:2360-2365, 2012.
426 Yang ZY, Werner HC, Kong WP, Leung K, Traggiai E, Lanzavecchia A et al.: Evasion of antibody neutralization in emerging severe acute respiratory syndrome coronaviruses. Proc Natl Acad Sci U S A 102:797-801, 2005.

CHAPTER 7

APPENDICES

ABBREVIATIONS

ACE2	Angiotensin-converting enzyme 2
AEC	3-Amino-9-ethylcarbazole
AGM	African green monkey
AI	Avian influenza
ALI	Acute lung injury
ARDS	Acute respiratory distress syndrome
BALT	Bronchus-associated lymphoid tissue
BOOP	Bronchiolitis obliterans organizing pneumonia
BPL	Beta-propiolactone
BSA	Bovine serum albumin
BSL-3	Biosafety level 3
CPE	Cytopathologic effect
CT	Computed tomography
DAB	3,3'-Diaminobenzidine-tetrachlorhydrate
DAD	Diffuse alveolar damage
DAPI	4,6-Diamidino-2-phenylindole
DC	Dentritic cells
DEC	Dierexperimentencommissie
dNTPs	Deoxynucleoside triphosphates
dpi	Days post inoculation/infection
FDR	False discovery rate
GAPDH	Glyceraldehydes-3-phosphate dehydrogenase
GLM	Generalized linear models
GMT	Geometric mean titer
H5N1	A/Indonesia/5/2005
HA	Hemagglutinin
HE	Hematoxylin and eosin
HI assay	Hemagglutination inhibition assay
HPAI	Highly pathogenic avian influenza virus
IFN	Interferon
IHC	Immunohistochemistry
IL	Interleukin
im	Intramuscular
IMDM	Iscove's Modified Dulbecco's Medium
in	Intranasal
IP-10	Interferon gamma-induced protein 10
ISH	In situ hybridization
it	Intratracheal
iv	Intravenous
LPAI	Low pathogenic avian influenza
LST	Lymphocyte stimulation test

MCP-1	Monocyte chemotractant protein
MDCK	Madin-Darby Canine Kidney
MIG	Monokine induced by IFN gamma
mRNA	Messenger RNA
NA	Neuraminidase
NF-κB	Nuclear factor kappa B
NP	Nucleoprotein
PAS	Periodic acid-Schiff
PBMC	Peripheral blood monocytes
PBS	Phosphate-buffered saline (PBS)
PCA	Principal component analysis
PCR	Polymerase chain reaction
pH1N1	Pandemic influenza virus A(H1N1)pdm09 (A/ Netherlands/602/09)
pVac	Pandemic influenza virus vaccine
pVacMF59	Pandemic influenza virus vaccine with MF59 adjuvant
RNA	Ribo Nucleic Acid
RT-PCR	Reverse transcriptase PCR
SA	Sialic acid
SARS	Severe acute respiratory syndrome
SARS-CoV	SARS coronavirus (HKU-39849 strain)
sc	Subcutaneous
SD	Standard deviation
Seasonal H1N1	A/Netherlands/26/07 (Old strain: A/Bilthoven/3075/1978)
Seasonal H3N2	A/Netherlands/177/2008 (Old strain: A/Bilthoven/16190/1968)
SEM	Standard error of the mean
SIV	Simian immunodeficiency virus
S-protein	Spike protein
sVac	Seasonal influenza virus vaccine
sVacMF59	Seasonal influenza virus vaccine with MF59 adjuvant
$TCID_{50}$	Median tissue culture infective doses
TGF-β	Transforming growth factor beta
Th1	T helper 1
TNF-α	Tumor necrosis factor-α
WHO	World Health Organization

CURRICULUM VITAE

Judith van den Brand was born on 12 August 1973 in Den Haag, the Netherlands. After she finished high school at Gymnasium Bernrode in Heeswijk-Dinther in 1991, she worked as an au-pair in Great Britain for one year. In 1992 she started studying veterinary medicine in Ghent, Belgium, and in 1993 she continued her veterinary medicine studies in Utrecht. She graduated in 2000 with a focus on companion animal medicine. After graduation she worked as a lecturer at the Exotics and Wildlife Group of the Pathology Department and at the Anatomy Department of the Faculty of Veterinary Medicine in Utrecht. In 2001 and 2002 she worked as a veterinarian in several veterinary practices. From 2002 to 2006 she trained as a veterinary pathology resident at the Pathology Department of the Veterinary Faculty in Utrecht in the Exotics and Wildlife Group and received her Basic Teaching Qualification. In 2006 she started her PhD at the Department of Viroscience of the Erasmus MC. In 2007 she passed her European veterinary pathology board exam and became an ECVP diplomate. In 2007 she married Jochem Garritsen and in 2008 and 2011 she had two children: Karlijn and Michiel.

PHD PORTFOLIO

Judith M.A. van den Brand - Garritsen
DVM, Dipl ECVP
Erasmus MC : Department of Viroscience
Research School : Post-graduate Molecular Medicine
PhD period : 2006 - 2012
Promotors : Prof.dr. T. Kuiken
Prof.dr. A.D.M.E. Osterhaus
Co-promotor : Dr. B.L. Haagmans

PhD training

In-depth courses

2012 One Health course (Antigone)
2012 Cursus promoveren en presenteren
2010 Photoshop CS3 workshop
2009 Basic introduction course on SPSS
2009 Biomedical English Writing and Communication
2007 Rosai session; Infectious diseases

International scientific presentations

2012 30th European Society of Veterinary Pathology meeting, Leon, Spain (oral, presentation award)
2012 Joint 61st World Wildlife Health Association and 10th European Wildlife Health Association conference, Lyon, France (poster)
2010 9th European Wildlife Health Association conference, Vlieland, the Netherlands (oral)
2010 28th European Society of Veterinary Pathology meeting, Belgrade, Serbia (oral)
2009 5th Orthomyxovirus Research Conference, Freiburg, Germany (poster)
2007 25th European Society of Veterinary Pathology meeting, Munich, Germany (oral)

National scientific presentations

2010 14th Molecular Medicine Day, Rotterdam (poster)
2009 Comparative pathology meeting, Rotterdam (oral)
2008 Dutch Society of Wildlife Health wet lab, Utrecht (oral and workshop presentation)
2008 12th Molecular Medicine Day, Rotterdam (poster)
2008 Pathologen dagen: Nederlandse Vereniging Voor Pathologen, Zeist (poster)

International scientific meetings

2007 European Respiratory Society annual meeting, Stockholm, Sweden

National scientific meetings

2012 9th Dutch Society of Wildlife Health symposium, Utrecht

2011 8th Dutch Society of Wildlife Health symposium, Utrecht
2010 Pathologen dagen: Nederlandse Vereniging Voor Pathologen, Zeist
2009 6th Dutch Society of Wildlife Health symposium, Lelystad
2009 Pathologen dagen: Nederlandse Vereniging Voor Pathologen, Zeist
2008 5th Dutch Society of Wildlife Health symposium, Utrecht
2007 Dutch Annual Virology Symposium, Amsterdam
2007 4th Dutch Society of Wildlife Health symposium, de Bilt

Teaching

Lecturing
2012 Masters course ”Infection and Immunity” (lecture), Rotterdam
2010 Course in virology (lecture), Rotterdam
2009 Masters course ”Infection and Immunity” (lecture), Rotterdam
2009 Exam preparation veterinary pathology residents, Gent, Belgium
2007-2012 Exam preparation veterinary pathology residents, Utrecht

Tutoring
2009-2012 Tutor of three veterinary pathology residents, Utrecht

Other
2009 Preparation for Academieprijs 2009
2009 Preparation teaching material for Natuur Historisch Museum, Rotterdam

PUBLICATIONS

Comparison of temporal and spatial dynamics of seasonal H3N2, pandemic H1N1 and highly pathogenic avian influenza H5N1 virus infections in ferrets. **JMA van den Brand**, KJ Stittelaar, G van Amerongen, L Reperant, L de Waal, ADME Osterhaus, T Kuiken. *PloS ONE* (2012) 7(8): e42343.

Modification of the ferrets model for pneumonia from seasonal human influenza A virus infection. **JMA van den Brand**, KJ Stittelaar, L Leijten, G van Amerongen, J Simon, ADME Osterhaus, T Kuiken. *Vet Pathol* (2012) 49(3): 562-568.

Metagenomic analysis of the viral flora of pine marten and European badger feces. **JMA van den Brand**, M van Leeuwen, CM Schapendonk, J Simon, BL Haagmans, ADME Osterhaus, SL Smits. *J Virol* (2012) 86(4):2360-5.

Efficacy of vaccination with different combinations of MF59-adjuvanted and non-adjuvanted seasonal and pandemic influenza vaccines against pandemic H1N1 (2009) influenza virus infection in ferrets. **JMA van den Brand**, JHCM Kreijtz, R Bodewes, KJ Stittelaar, G van Amerongen, T Kuiken, J Simon, RAM Fouchier, G Del Giudice, R Rappuoli, GF Rimmelzwaan, ADME Osterhaus. *J Virol* (2011) 85(6):2851-58.

Distinct SARS-Coronavirus Induced Acute Lung Injury Pathways in Two Different Non-Human Primate Species. SL Smits, **JMA van den Brand**, A de Lang, LME Leijten, WF van IJcken, G van Amerongen, ADME Osterhaus, A Andeweg, BL Haagmans. *J Virol* (2011) 85(9):4234-45.

Pandemic H1N1 Vaccine Requires the Use of an Adjuvant to Protect against challenge in Naïve Ferrets. B Baras, L de Waal, KJ Stittelaar, V Jacob, S Giannini, EJB Veldhuis Kroeze, **JMA van den Brand**, G van Amerongen, J Simon, E Hanon, SP Mossman, ADME Osterhaus. *Vaccine* (2011) 29(11):2120-6.

Pigs, Poultry, and Pandemic Influenza: How Zoonotic Pathogens Threaten Human Health. In: Hot Topics in Infection and Immunity in Children VIII. T Kuiken, RAM Fouchier, GF Rimmelzwaan, **JMA van den Brand**, D van Riel, ADME Osterhaus. *Adv Exp Med Biol* (2011) 719:59-66.

Severity of New H1N1 Influenza Pneumonia in Ferrets Intermediate between that of Seasonal H1N1 Virus and Highly Pathogenic Avian Influenza H5N1 Virus. **JMA van den Brand**, KJ Stittelaar, G van Amerongen, GF Rimmelzwaan, J Simon, E de Wit, V Munster, T Bestebroer, RAM Fouchier, T Kuiken, ADME Osterhaus. *J Infect Dis* (2010) 201(7):993-9.

Pandemic 2009 H1N1 influenza virus causes diffuse alveolar damage in cynomolgus macaques. S Herfst, **JMA van den Brand**, EJA Schrauwen, E de Wit, VJ Munster, G van Amerongen, M Linster, F Zaaraoui, WFJ van Ijcken, GF Rimmelzwaan, ADME Osterhaus, RAM Fouchier, AC Andeweg, T Kuiken. *Vet Pathol* (2010) 47(6):1040-1047.

Comparative Pathology of Select Agent Influenza A Virus Infections (Review). T Kuiken, **JMA van den Brand**, D van Riel, M Pantin-Jackwood, DE Swayne. *Vet Pathol* (2010) 47(5):893-914.

Experimental Pandemic (H1N1) 2009 Influenza Virus Infection in Cats. **JMA van den Brand**, KJ Stittelaar, G van Amerongen, M van de Bildt, LME Leijten, T Kuiken, ADME Osterhaus. *Emerg Infect Dis* (2010) 16(11):1745-7.

Exacerbated innate host response to SARS-CoV in aged non-human primates. SL Smits, A de Lang, **JMA van den Brand**, LME Leijten, WF van IJcken, MJ Eijkemans, G van Amerongen, T Kuiken, AC Andeweg, ADME Osterhaus, BL Haagmans. *PLoS Pathog* (2010) 6(2):e1000756.

In vitro assessment of attachment pattern and replication efficiency of H5N1 influenza A viruses with altered receptor specificity. S Chutinimitkul, D van Riel, VJ Munster, **JMA van den Brand**, GF Rimmelzwaan, T Kuiken, ADME Osterhaus, RAM Fouchier, E de Wit. *J Virol* (2010) 84(13):6825-33.

Insertion of a multi basic cleavage motif in low pathogenic avian influenza H6N1 virus induces a highly pathogenic phenotype. VJ Munster, EJA Schrauwen, E de Wit, **JMA van den Brand**, TM Bestebroer, S Herfst, GF Rimmelzwaan, ADME Osterhaus, RAM Fouchier. *J Virol* (2010) 84(16):7953-60.

A single immunization with CoVaccine HT™-adjuvanted H5N1 influenza vaccine induces protective cellular and humoral immune responses in ferrets. R Bodewes, JHCM Kreijtz, G van Amerongen, MM Geelhoed-Mieras, RJ Verburgh, JGM Heldens, J Bedwell, **JMA van den Brand**, T Kuiken, CA van Baalen, RAM Fouchier, ADME Osterhaus, GF Rimmelzwaan. *J Virol* (2010) 84:7943-7952.

Evaluation of an MVA-based candidate pandemic influenza A/H1N1 vaccine in the ferret model. JHCM Kreijtz, Y Süzer, R Bodewes, A Schwantes, G van Amerongen, RJ Verburgh, G de Mutsert, **JMA van den Brand**, S van Trierum, T Kuiken, RAM Fouchier, ADME Osterhaus, G Sutter, GF Rimmelzwaan. *J Gen Virol* (2010) 91:2745-2752.

Recombinant modified vaccinia virus Ankara expressing the hemagglutinin gene confers protection against homologous and heterologous H5N1 influenza virus infections in macaques. JH Kreijtz, Y Suezer, G de Mutsert, **JMA van den Brand**, G van Amerongen, BS Schnierle, T Kuiken, RA Fouchier, J Löwer, ADME Osterhaus, G Sutter, GF Rimmelzwaan. *J Infect Dis* (2009) 199(3):405-13.

Pathogenesis and Transmission of Swine-Origin 2009 A(H1N1) Influenza Virus in Ferrets. VJ Munster, E de Wit, **JMA van den Brand**, S Herfst, EJ Schrauwen, TM Bestebroer, D van de Vijver, CA Boucher, M Koopmans, GF Rimmelzwaan, T Kuiken, ADME Osterhaus, RA Fouchier. *Science* (2009) 325(5939):481-3.

Vaccination against human influenza A/H3N2 virus prevents the induction of heterosubtypic immunity against lethal infection with avian influenza A/H5N1 virus. R Bodewes, JH Kreijtz, C Baas, MM Geelhoed-Mieras, G de Mutsert, G van Amerongen, **JMA van den Brand**, RA Fouchier, ADME Osterhaus, GF Rimmelzwaan. *PLoS ONE* (2009) 4(5):e5538.

Early upregulation of acute respiratory distress syndrome-associated cytokines promotes lethal disease in an aged-mouse model of severe acute respiratory syndrome coronavirus infection. B Rockx, T Baas, GA Zornetzer, B Haagmans, T Sheahan, M Frieman, MD Dyer, TH Teal, S Proll, **JMA van den Brand**, R Baric, MG Katze. *J Virol* (2009) 83(14):7062-74.

Infection of mice with a human influenza A/H3N2 virus induces protective immunity against lethal infection with influenza A/H5N1 virus. JH Kreijtz, R Bodewes, **JMA van den Brand**, G de Mutsert, C Baas, G van Amerongen, RA Fouchier, ADME Osterhaus, GF Rimmelzwaan. *Vaccine* (2009) 27(36):4983-9.

Pathology and virus distribution in chickens naturally infected with highly pathogenic avian influenza A virus (H7N7) during the 2003 outbreak in the Netherlands. D van Riel, **JMA van den Brand**, VJ Munster, TM Besteboer, RA Fouchier, ADME Osterhaus, T Kuiken. *Vet Pathol* (2009) 46(5):971-6.

Preclinical evaluation of a modified vaccinia virus Ankara (MVA)-based vaccine against influenza A/H5N1 viruses. JH Kreijtz, Y Suezer, G de Mutsert, **JMA van den Brand**, G van Amerongen, BS Schnierle, T Kuiken, RA Fouchier, J Löwer, ADME Osterhaus, G Sutter, GF Rimmelzwaan. *Vaccine* (2009) 27(45):6296-9.

MVA-based H5N1 vaccine affords cross-clade protection in mice against influenza A/H5N1 viruses at low doses and after single immunization. JH Kreijtz, Y Suezer, G de Mutsert, G van Amerongen, A Schwantes, **JMA van den Brand**, RA Fouchier, J Löwer, ADME Osterhaus, G Sutter, GF Rimmelzwaan. *PLoS ONE* (2009) 4(11):e7790.

Pathology of experimental SARS coronavirus infection in cats and ferrets. **JMA van den Brand**, BL Haagmans, LME Leijten, D van Riel, BE Martina, ADME Osterhaus, T Kuiken. *Vet Pathol* (2008) 45(4):551-62.

Reovirus infections associated with high mortality in psittaciformes in The Netherlands. **JMA van den Brand**, R Manvell, G Paul, MJ Kik, GM Dorrestein. *Avian Pathol* (2007) 36(4):293-9.

A clinicopathological study of 52 feline epulides. ND de Bruijn, J Kirpensteijn, IJ Neyens, **JMA van den Brand**, TS van den Ingh. *Vet Pathol* (2007) 44(2):161-9.

Renal cysts, nephrolithiasis, and ovarian cysts in a donkey suspected of having been sexually abused. **JMA van den Brand**, WK Hendriks-Onstein, MJ Kik, A Gröne, MM Sloet vam Oldruitenborgh-Oosterbaan. *Tijdschr Diergeneeskd* (2006) 131(20):730-5.

DANKWOORD

Dit proefschrift heb ik niet alleen gemaakt en zonder alle mensen die me geholpen hebben op wat voor manier dan ook, had dit boek(je) – en het vele werk dat erachter zit – nooit tot stand kunnen komen. Ik wil iedereen bedanken die hieraan meegewerkt heeft! Mocht ik iemand vergeten, dan wil ik die bij voorbaat ook hartelijk bedanken!

Thijs, bedankt dat je me deze kans hebt gegeven om bij jou de fijne kneepjes van de pathologie en het wetenschappelijk onderzoek te mogen leren. Zoals ik al eerder zei: het is niet zomaar een promotieplaats! Je bent voor mij een motiverend en inspirerend voorbeeld!

Ab, bedankt voor deze promotieplek en de mogelijkheid om van dichtbij een kijkje te nemen in het Lab van Ab; een ongeloofelijk wervelende afdeling. Ab en Thijs, daarnaast wil ik jullie bedanken voor de studietijd die ik gekregen heb om mijn board examen te doen en diplomate ECVP te worden. (Toch onverwachts in één keer gehaald!) Als laatste bedankt voor de switch naar influenza op het juiste moment, waardoor ik het geluk heb gehad om met mijn neus in de pandemie te vallen. Geweldig om mee te mogen maken hoe het was om op hoog niveau als een van de eerste labs heel spannend onderzoek te doen naar het nieuwe pandemie virus. Vooral de avonden en weekenden schrijven voor Nature waren heel spannend.

Bart, mijn SARS-goeroe, bedankt voor je nuchtere kijk op de zaken en je enthousiasme als je weer iets uitgevogeld had om te onderzoeken. Het is altijd stimulerend en verhelderend om met je over SARS te praten.

Lonneke en Debby, mijn paranimfen, bedankt voor jullie steun en gezelligheid. Lonneke, al dat werk met de immunokleuringen… hoe kan ik je bedanken! Je hebt een enorm aandeel in dit proefschrift. Debby, bedankt voor je fijne gesprekken over werk, promotie en het gewone leven. Peter, als ik nog denk aan al die coupes, stapels, ik was altijd blij als je weer wat op mijn bureau legde, maar ik keek ook wel op tegen dat werk. Marco, bedankt voor de virologische kennis die je me geeft en je nuchtere kijk op dingen. Edwin, eerst samen bij Pathologie UU, nu weer collega's in Rotterdam, bedankt voor de goede gesprekken, de pathologie uitwisseling en de toekomstplaatjes die we delen. Leslie, bedankt voor de gesprekken over werk en privé, 'hoe je toch die modellen maakt'? Niels, de keren dat ik je zag was het altijd erg gezellig, bedankt. Joost Phillipa, Jolianne en Fiona, bedankt voor de gezellige tijd, al is het lang geleden. Pierre-Yves, Ursula, Caroline en Toni, thanks for the good time and hopefully we'll meet again.

Anna, bedankt voor de SARS oppepgesprekken; Saskia, bedankt voor de hulp met SARS-werk en wildlife; Joost en Rogier, bedankt voor al jullie hulp met de pandemie-fretten papers en voor de gezelligheid; Sander, we hebben vooral samen gewacht en vet path issues opgelost, wel gezellig; Emmie en Vincent, jullie hebben er mede voor gezorgd dat ik hier ben komen werken, bedankt voor de steun en leuke tijd; Eefje, jammer dat ik niet vaker met je heb kunnen samenwerken; Robert, bedankt voor de hulp met de dieren; David, bedankt voor het delen van je statistische kennis; Arno, bedankt voor de genomic input, vooal in tijden van Mexicaanse griep; Stella, bedankt voor de terugkoppeling na mijn colleges, dat waardeer ik enorm; Simone, Loubna en Carola, bedankt voor de secretariële hulp met allerlei zaken, zoals faxen en scannen; Guus en Ron, zonder jullie input waren mijn experimenten niet zo mooi geweest, bedankt! Mede-flufighters, het was

een leuk en interessant initiatief! Bedankt!

Alle anderen van de influenzagroep, hepatitisgroep, HIV-groep, mazelengroep en de overige virologiemensen ook enorm bedankt voor de gezelligheid tijdens de borrels en de hulp op wat voor gebied dan ook.

Frank, bedankt voor het zo prachtig maken van mijn foto's; elke keer ben ik weer verwonderd over hoe mooi je ze kan maken. Alex, bedankt voor je hulp met de digitale scoring en voor het tijdelijk 'in beslag nemen' van je computer.

De medewerkers van Viroclinics Biosciences waren erg belangrijk voor mijn proefschrift. Zonder hen was het zeker niet van de grond gekomen. Koert, je was mijn grote steun en toeverlaat als ik weer eens opzag tegen de grote experimenten. Cindy, toch gezellig om een vrouwelijke lotgenoot te hebben tijdens de experimenten op het NVI. Leon en Rob, bedankt voor het meeverzamelen van alle materialen en het uitlezen van de temperatuurdata. Ronald, Willem en de andere werknemers van Viroclinics die zich hebben ingezet om alle virologische data van de grote experimenten te verwerken: heel erg bedankt.

Geert, bedankt voor je gezelligheid tijdens de secties - het is altijd lekker en vlot werken - en voor de gastvrijheid bij het NVI. Je koeien smaken heerlijk! Dan de heren (en enkele dames) van het NVI onder wie Wim, Stephane, Nico, Jan (†), Hans, Mieke en Jasper; door jullie heeft het woord 'treintje' een nieuw begrip gekregen. Bedankt voor al jullie humor en gezelligheid op soms nachtelijke uurtjes op het NVI, waarbij mij een kijkje in de mannenwereld gegund werd!

Rob, bedankt voor je inzicht in de humane pathologie. Collega's van de pathologie, bedankt voor de hulp en dat ik aanwezig mocht zijn bij 3 pH1N1 obducties ten behoeve van het onderzoek. Alle personen die betrokken waren bij het onderzoek hiervan in het ziekenhuis, bedankt. Jammer dat het paper uiteindelijk te mager bleek.

Dierverzorgers van het EDC, bedankt voor de goede zorgen voor mijn dieren. Graag zou ik ook mijn proefdieren vernoemen. Zonder hen had ik niet de vragen kunnen beantwoorden over de ziekte veroorzaakt door influenza en SARS. Jullie hebben de mensheid weer een stukje verder geholpen in deze grote vraagstukken.

Ondanks dat mijn onderzoek een heel andere kant is opgegaan door het overstappen op influenza, zodat er geen plaats meer was voor coronavirusen en wildlife in mijn boekje, wil ik toch de volgende personen bedanken: van de vleermuizen: Chantal, Peter, Bart, en van de boommarters: Jasja, Chris, Sim, Maurice, en natuurlijk alle vrijwilligers voor het verzamelen en helpen met de vleermuizen en boommarters. Mensen van de Pathobiologie op de faculteit Diergeneeskunde en van de DSWH en DWHC, bedankt voor de betrokkenheid en de steun bij de eerste stappen binnen de veterinaire pathologie en de wildlife diseases. Ruby, bedankt voor de lunch dates en de papers die je tevoorschijn weet te toveren! Mentorkindjes (Lidewij, Lineke en Sandra) en SIO's, fijn om mee te mogen denken over het leven als een patholoog-in-wording en de voorbereiding op het ECVP-examen!

Lieve vrienden en vriendinnen, wat heb ik jullie weinig gezien de afgelopen tijd! De spaarzame ontmoetingen waren wel heel belangrijk voor me. Sjannie, de ups en down van het leven delen we en altijd schijnt die zon achter de wolken! Bedankt voor de taalaanpassingen. Wout, Jantien en kleine Jop, de Brabantse gezelligheid bij jullie zouden we graag van dichterbij willen beleven. Linda, bedankt voor het nakijken van de tekst. Krista, Ingeborg, Suzan, Maartje en Imke, hopelijk weer wat vaker afspreken? Jaarclub L'ego en Fortissimo met partners, en CV 'Dus' met aanhang: eindelijk tijd voor een feestje!

Marianne en Wim, jullie natuurlijk bedankt voor het oppassen op Karlijn en Michiel. Het was soms moeilijk om tussen onze drukke werkzaamheden door in Son langs te komen. Meike, Claire en Viktor, Fleur, Henk-Jan, en kleine Mats, hopelijk kunnen we elkaar nu weer wat vaker zien.

Lieve Paul en Karina, wat hebben we uitgekeken naar jullie huwelijk in Mexico! Misschien mogen we de reis nog eens overdoen! Kleine Lisa, lief klein half-Mexicaantje, ik hoop je nu veel vaker te zien!

Lieve mama en papa, de afgelopen tijd hebben we samen heel fijne tijden beleefd, maar ook heel zware. Toch ben ik heel blij dat we ze samen hebben mogen beleven. Jullie onvoorwaardelijke steun en warmte zijn mijn drijfveer. Jullie zijn de liefste en beste ouders die ik me maar kan wensen. Bedankt voor het vaak oppassen op Karlijn en Michiel, zeker tijdens de pandemie, toen Karlijn nog maar zo klein was. Heerlijk te weten dat ze met veel liefde en plezier in goede handen zijn.

Lieve Jochem, jij bent mijn enorme rots in de branding. Vaak heb je mijn verhalen moeten aanhoren en heb je mijn traantjes gedroogd als ik het even niet meer zag zitten. Als ik weer eens vragen had over computerprogramma's, kon ik je altijd bellen. Ook ben je, zeker net na de geboorte van Karlijn, tijdens de pandemie een jaar lang heel vaak thuis geweest voor haar. Sorry dat je me de avonden en weekenden amper zag. Jij bent mijn 'thuiskomen' en relativerend rustpunt; degene bij wie ik altijd terecht kan.

Lieve Karlijn, jouw kinderlijke wijsheid en lieve zorgzaamheid verbazen me elke dag weer. Je voelt me feilloos aan en maakt me altijd aan het lachen!

Lieve Michiel, jouw ontwapenende lach, enthousiasme en verwondering doen me smelten en alle zorgen vergeten.

Ik heb jullie vaak moeten missen de afgelopen tijd, maar de momenten die ik samen met jullie ben, geniet ik 200% en meer!